



GH5 crosslinked onto DNA with dithiobis (succinimidyl propionate), then cleaved with chymotrypsin, displayed highly uniform contacts that appeared to involve the C-terminal four amino acids, and suggests protein-protein interactions are important for binding. This finding may be relevant since GH5 (and H5) were observed to self-associate free in solution in an arguably specific manner. Finally, the exposure of Phe 93 to chymotrypsin was used to identify the surface of the globular domain that contacts DNA for the binding of intact H5. Results suggests that the side of the protein opposite to the recognition helix preferentially binds to DNA, supporting a novel winged-helix protein DNA-binding mechanism.

Furthermore, parallel studies with octamers reconstituted onto a DNA fragment with twelve copies of the 208 b.p. rDNA 5s gene from *Lytechinus variegatus*, shows that H5 had a high binding affinity with all detectable protein binding to the reconstituted complex. H5 binding conferred protection to a site located near the dyad axis from endonuclease digestion, supporting the contention that H5 binds near or at the nucleosome dyad axis. H5 binding also was observed to condense fibers as observed from agarose gel electrophoresis, although velocity analytical sedimentation studies indicate that H5 in itself was not sufficient to fully compact chromatin fibers; rather H5 and 30 mM NaCl, in combination, were required. Results indicate that the chromatin-reconstituted "208-12 DNA" makes an excellent model for analyzing the effect of linker proteins on chromatin morphology.

**Binding and Assembly of H5 (and the Globular Domain of H5)  
onto DNA**

by

George John Carter

A Thesis Submitted

to

Oregon State University

In Partial Fulfillment of  
the requirements for the  
degree of

Doctor of Philosophy

Completed January 07, 1998  
Commencement June 1998

Doctor of Philosophy thesis of George John Carter presented on January 07, 1997

Approved:

*Redacted for Privacy*

---

Major Professor, representing Molecular and Cellular Biology

*Redacted for Privacy*

---

Chair of Department, Molecular and Cellular Biology

*Redacted for Privacy*

---

Dean of Graduate School

I understand that my thesis will become part of the permanent collection of Oregon State University libraries. My signature below authorizes release of my thesis to any reader upon request.

*Redacted for Privacy*

---

George John Carter, Author

## Acknowledgements

I would like to thank those who generously devoted time and materials towards completion of my degree and include: Woojin An, Dr. Karen Miller, Emily Ray and Tom Ellen from Dr. Kensal van Holde's laboratory for the gifts of DNAs, and in providing useful suggestions and advice. I would also like to especially thank Dr. van Holde's technician, Valerie Stanik, for help in purifying the "208-12 *Lytechnius variegatus* DNA", and technical support related to the chromatin reconstitution work. Recognition is further given to others in the Biochemistry and Biophysics Department at Oregon State University. Jeannine Lawrence for expert technical support with the circular dichroism studies, Dr. Dean Malencik for advice and help regarding protein purification and analytical ultracentrifugation, and Drs. Gary Schroth and Shing Ho for advice related to biochemical methods. From my graduate committee I would like to express gratitude towards Dr. Isaac Wong and Dr. Victor Hsu, whose excellent advice helped make my thesis an all-around better work. During the course of my Ph.D., I was given the opportunity to work at the University of Texas Health Science Center in San Antonio, TX in the laboratory of Dr. Jeffrey Hansen for purposes related to chromatin reconstitutions. I am indebted to Dr. Hansen, and his research staff including Patricia Schwarz and Isabelle Kreider for helping me developing important skills pertaining to chromatin reconstitutions. Finally, I wish to express my appreciation to my advisor, Dr. Kensal van Holde, for his help in seeing the thesis through, and for providing the necessary guidance in converting the research work into a finished thesis.

# TABLE OF CONTENTS

|  | <u>Page</u> |
|--|-------------|
| Chapter 1: Introduction.....   | 1           |
| 1.1 Chromatin and linker histones.....   | 1           |
| 1.2 Linker histone-DNA interactions from a molecular perspective.....  | 5           |
| 1.3 Linker histone self-association and cooperativity in binding to DNA.....   | 11          |
| 1.4 DNA-linker histone complexes from a macromolecular perspective.....  | 18          |
| 1.5 Interaction of linker histones with chromatin .....  | 24          |
| 1.6 Organization of thesis.....  | 29          |
| <br>Chapter 2: Self-Association and Complexing of H5-Related Proteins in<br>Solution and Bound to DNA: Evidence for Specific Contacts..... | <br>32      |
| 2.0 Summary.....   | 32          |
| 2.1 Introduction .....   | 33          |
| 2.2 Methods and materials .....  | 36          |
| 2.3 Results .....  | 47          |
| 2.4 Discussion .....   | 100         |
| <br>Chapter 3: Linker Histone H5 (and the Globular Domain of H5) Binding to DNA and<br>Chromatin.....                                      | <br>108     |
| 3.0 Summary.....   | 108         |
| 3.1 Introduction.....  | 109         |
| 3.2 Methods and materials.....   | 114         |
| 3.3 Result of model H5 (and GH5) DNAbinding studies.....   | 125         |
| 3.4 Results of small chromatin fiber reconstitution with H5.....   | 178         |
| 3.5 Discussion .....   | 195         |

## TABLE OF CONTENTS (Continued)

|  | <u>Page</u> |
|--|-------------|
| Chapter 4: Analysis of Linker Histone-DNA Complexes Using SDS-PAGE.....  | 204         |
| 4.0 Summary .....  | 204         |
| 4.1 Introduction.....  | 205         |
| 4.2 Methods and materials.....   | 208         |
| 4.3 Results .....  | 213         |
| 4.5 Discussion .....   | 239         |
| <br>Chapter 5: Conclusion.....   | <br>248     |
| 5.0 Summary.....   | 248         |
| 5.1 Molecular aspects of linker histone binding.....   | 248         |
| 5.2 Model DNA and solution studies.....  | 250         |
| 5.3 Chromatin-related analysis.....  | 252         |
| 5.4 Concluding remarks.....  | 253         |
| <br>Bibliography.....  | <br>255     |
| <br>Appendices.....  | <br>268     |
| Appendix A1: Sequences of Relevant DNA and Proteins.....   | 269         |
| Appendix A2: Using the Sedimentation Coefficient to Estimate the Number<br>of Octamers Bound to the "208-12" DNA Fragment..... | 274         |
| Appendix A3: Alternative Methods for Determining the Number of Octamer<br>Histones Bound to the "208-12" DNA.....              | 277         |

## LIST OF FIGURES

| <u>Figure</u>  | <u>Page</u> |
|--|-------------|
| 1.1 Schematic illustration of the chromosome.....  | 2           |
| 1.2 Illustration of GH5 docked to DNA.....   | 8           |
| 1.3 Simplified schematic of two models for chromatin compaction.....   | 27          |
| 2.1 Purification of recombinant GH1° and GH5 .....   | 49          |
| 2.2 Absorbance spectra for purified GH1°, GH5, and H5, and the effect of 6 M guanidine HCl on the UV absorbance profile..... | 53          |
| 2.3 Circular dichroism of linker histone proteins, and the effect of PO <sub>4</sub> <sup>-3</sup> .....                     | 55          |
| 2.4 Salt-dependent turbidity analysis of linker histone proteins .....   | 58          |
| 2.5 Crosslinking GH5 free in solution with DSP .....   | 62          |
| 2.6 Crosslinking H5 free in solution with DSP .....  | 68          |
| 2.7 Equilibrium analytical ultracentrifugation of GH5 free in solution.....  | 74          |
| 2.8 Equilibrium analytical ultracentrifugation of H5 free in solution.....   | 76          |
| 2.9 Effect of GH5:DNA ratio and ionic strength on the polymer distribution of GH5 crosslinked onto DNA.....                  | 80          |
| 2.10 Influence of the type of DNA substrate (or lack of substrate) on GH5 self-interaction.....                              | 84          |
| 2.11 Effect of DNA substrate on the distribution of DSP crosslinked polymers.....  | 89          |
| 2.12 Examples of indefinite protein filaments and the expected results of quantitative proteolysis.....                      | 92          |
| 2.13 Determining DSP-crosslinked GH5 complex organization by quantitative proteolysis.....                                   | 94          |

## LIST OF FIGURES (Continued)

| <u>Figure</u>   | <u>Page</u> |
|---|-------------|
| 2.14 Models for potential contacts of adjacent GH5 molecules bound to a 22 b.p. DNA.....  | 97          |
| 3.1 Competitive binding between a 22 b.p. and 42 b.p. oligonucleotides by GH5 and H5.....   | 126         |
| 3.2 Binding curves of GH5 or H5 titrated onto a 22 b.p. oligonucleotide....   | 130         |
| 3.3 Estimating the number of GH5 molecules bound to 22 b.p. and 42 b.p. oligonucleotides.....                                       | 135         |
| 3.4 The effect of NaCl concentration and DNA topology on GH5 and H5 binding to long DNA.....  | 139         |
| 3.5 Solubility of GH5 and H5 complexed to HhaI cut pPol208-12 in 2% SDS.....  | 146         |
| 3.6 The solubility of H5 in 2% SDS as a function of DNA topology as detected by SDS-PAGE.....                                       | 148         |
| 3.7 Salt-dependent release of GH5 and the 22 b.p. oligonucleotide from the nucleoprotein aggregate.....                             | 152         |
| 3.8 Urea-dependent disruption of linker histone-DNA complexes.....  | 158         |
| 3.9 Plot of H5-related peptides as a result of chymotrypsin digestion of free protein at room temperature.....                      | 162         |
| 3.10 Plot of H5-related peptides as a result of chymotrypsin digestion of DNA-bound protein at 37°C.....                            | 166         |
| 3.11 GH5 filament based on crystalized GH5 lattice.....   | 172         |
| 3.12 Computer generated picture of putative minor groove binding GH5-DNA model and the prototypical major groove binding model..... | 175         |

## LIST OF FIGURES (Continued)

| <u>Figure</u>   | <u>Page</u> |
|---|-------------|
| 3.13 Schematic representation of the 208-12 DNA used in the small fiber chromatin reconstitution studies.....                                     | 179         |
| 3.14 Use of large-pore dialysis membrane to detect binding and dissociation of H5 from reconstituted 208-12 DNA.....                              | 181         |
| 3.15 EcoR I endonuclease digestion of reconstituted 208-12 DNA chromatin fibers.....  | 186         |
| 3.16 Histogram of electrophoretic mobilities for samples chromatin fibers reconstituted in the presence of H5.....                                | 191         |
| 4.1 Modification of amine groups upon reaction with glutaraldehyde.....   | 207         |
| 4.2 Effect of glutaraldehyde on GH5 binding to a 42 b.p. oligonucleotide....  | 215         |
| 4.3 Sensitivity of DNA imaging by silver staining, and stability of DNA duplex in SDS.....  | 219         |
| 4.4 Comparison of the electrophoretic mobility of chemically-crosslinked GH5 homopolymer complexes, a 42 b.p. oligonucleotide and marker DNA..... | 222         |
| 4.5 Demonstrating the efficiency of specific staining of H5 and DNA using diamine silver staining and non-diamine silver staining protocols.....  | 226         |
| 4.6 Differential staining SDS-PAGE (DS-SDS-PAGE) analysis of GH5-DNA complexes.....   | 230         |
| 4.7 GH5 and H5 crosslinking to Hha I cut pPol208-12 as a function of NaCl concentration.....  | 236         |
| 4.8 GH5 and H5 binding to DNA as a function of NaCl concentration in terms of an isolated binding motif model.....                                | 245         |

## LIST OF TABLES

| <u>Table</u>  | <u>Page</u> |
|---|-------------|
| 1.1 The effect of protein concentration and salt concentration on linker histone cooperativity.....   | 12          |
| 1.2 Linker histone protein-association studies.....   | 13          |
| 2.1 List of calculated extinction coefficient for H5 and related proteins.....  | 51          |
| 2.2 Previously reported extinction coefficients for GH5 and H5.....   | 52          |
| 2.3 Results of equilibrium analytical sedimentation.....  | 73          |
| 3.1 The effect of H5 binding and NaCl on the sedimentation coefficient of octamer-supersaturated reconstituted 208-12 DNA.....                                | 194         |
| 4.1 A comparison of the theoretical and experimental values of pPol208-12 cut with Hha I as measured with an SDS polyacrylamide gel (18% polyacrylamide)..... | 224         |

## LIST OF APPENDIX FIGURES

| <u>Figure</u>  | <u>Page</u> |
|--|-------------|
| A2.1 Relationship between reconstituted 208-12 DNA and the nucleoprotein complex sedimentation coefficient.....                              | 275         |
| A3.1 Analyzing reconstituted 208-12 DNA chromatin fibers using agarose gel electrophoresis.....  | 284         |
| A3.2 EcoR I endonuclease digestion of reconstituted 208-12 chromatin fibers.....   | 291         |
| A3.3 Effect of temperature, and 50 mM NaCl on EcoR I endonuclease digestion of octamer histone subsaturated 208-12 DNA chromatin fibers..... | 294         |
| A3.4 Effect of digestion time on the stability of mononucleosomes produced by digesting reconstituted 208-12 DNA with EcoR I .....           | 297         |

# Binding and Assembly of H5 (and the Globular Domain of H5) onto DNA

## CHAPTER 1

### Introduction

#### 1.1 Chromatin and linker histones

Chromatin is a DNA-protein assembly that packages the genome of eukaryotes. As an analogy, chromatin can be thought of as string and spools. DNA, like string, is literally wrapped around a multiple-subunit "protein spool", known as the histone octamer. The *octamer* is composed of four different histone subunits: H2A, H2B, H3 and H4 with each protein subunit represented twice in the octamer complex (Arents et al., 1991; Klug et al., 1980). The wedge-shaped octamer and DNA (wrapped about 1.65 times around the octamer) (Luger et al., 1997) in turn comprise the basis for the repeating chromatin element unit known as the *nucleosome* (reviewed in van Holde, 1989). Linker histones constitute a separate protein family that binds to the octamer-DNA complex to form what is known as a *chromatosome* (Figure 1.1). Because linker histones are particularly sensitive to dissociation, this protein class is believed to bind externally to the nucleosome. Although the chromatosome contains approximately 166 b.p., the amount of DNA associated with the nucleosome repeat can be quite heterogeneous with lengths ranging from less than 200 b.p. up to 240 b.p (reviewed in van Holde, 1989). Despite this

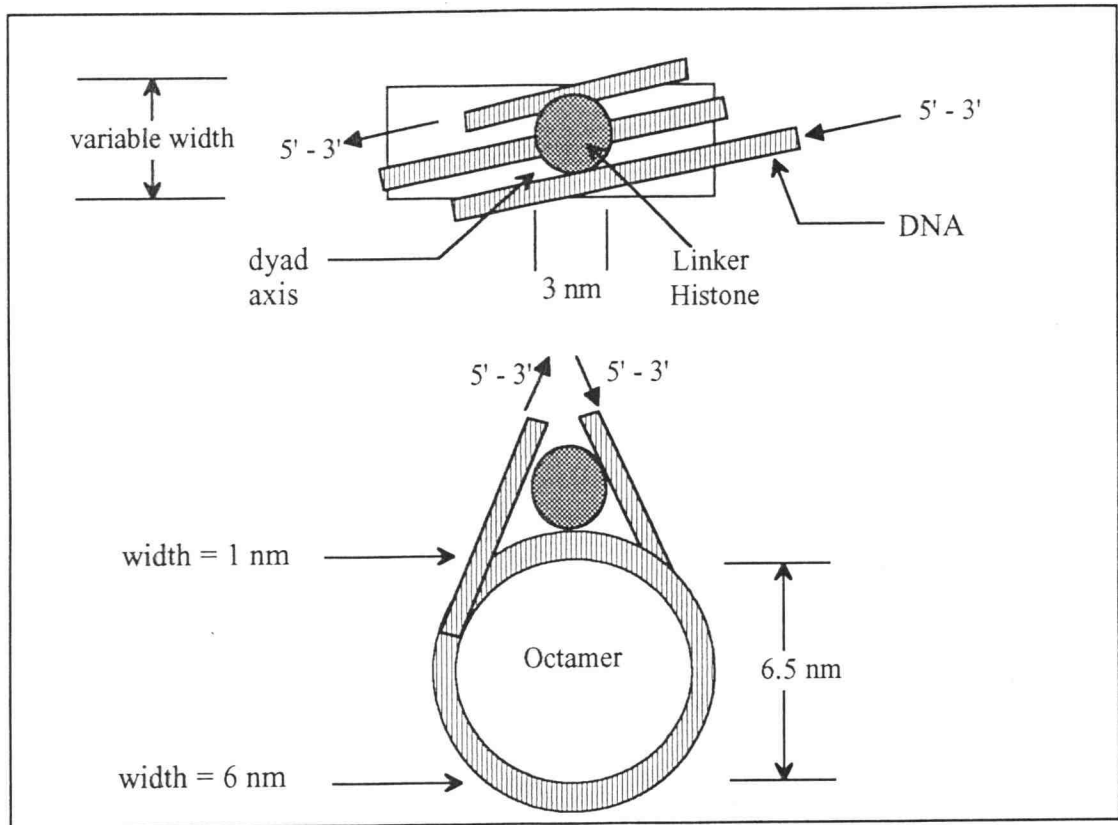


Figure 1.1. Schematic illustration of the nucleosome. As shown, the nucleosome consists of an octamer, linker histone, and 166 b.p. DNA. The octamer (H2A, H2B, H3, H4) actually forms a wedge-shaped protein complex. As viewed from the dyad, the octamer "wedge" has its smallest dimensions, and at the point opposite of the dyad axis, the octamer dimensions are largest. This is partially due to the association of the H2A-H2B dimer onto the H3-H4 tetramer at the point opposite the dyad axis. In this depiction the linker histone is placed at the dyad axis, though the exact location of the linker histone remains unelucidated. Dimensions are based on the crystal structure of the octamer histone (Pruss et al., 1996), and the model is based on Allan et al. (1980).

variation in linker DNA, micrococcal digestion of the nucleosome leads to two "stops" with invariant DNA sizes (Noll and Kornberg, 1977). The *chromatosome stop* includes the linker protein and octamer histone along with about 166 b.p. of protected DNA. The *core particle stop* includes the octamer complex along with 146 b.p. of protected DNA (reviewed in van Holde, 1989).

The types of proteins associated with nucleosomes generally fall into two classes. *Linker histones* are the most common nucleosome binding protein, and include ubiquitous H1 and its associated subtypes, including the avian erythrocyte-specific linker histone H5. Linker histones in isolated nuclei have been found to bind to the nucleosome at a molar stoichiometry of between 0.8 to 1.3 (Bates and Thomas, 1981), though up to two linker histones bound per nucleosome have been observed both *in situ* (Nelson et al., 1979) and *in vitro* (Seger et al., 1991). Evidence suggests that the primary role of linker histones is to stabilize condensed isoforms of chromatin (Thoma and Koller, 1977; Losa et al., 1984; Leuba et al., 1994). HMG ("*high mobility group*") proteins comprise the second most common group of nucleosome-binding proteins. Included in this group are a rather diverse assortment of proteins including HMG 1, HMG 2, HMG 14, and HMG 17. In contrast to linker histones, HMG proteins appear to "open" or decondense chromatin, and may have transcriptional, or replicative-related functions (reviewed in van Holde and Zlatanova, 1996).

Chromatin is highly dynamic, and displays three-dimensional, higher-order structure through an interplay between nucleosomes (reviewed in van Holde, 1989). Chromatin morphology is usually described in terms of compaction or condensations of

the fiber. Compaction or condensation essentially refers to octamer density, with values ranging between extended and compacted endpoints. Originally, these endpoints were believed to be an extended 10 nm-sized form where octamers appeared as "beads on a string" at low ionic strength, and a condensed, uniform 30-nm diameter isoform found at higher salt concentrations, and requiring the presence of linker histones (Klug and Finch, 1976; Thoma et al., 1979; Widom, 1989). However, this view has recently been challenged as a result of images of chromatin obtained by scanning force microscopy (SFM) under less extreme conditions. Results suggest that the low ionic strength fiber is three dimensional though still somewhat "flattened" in appearance, and that fiber morphology shows considerable heterogeneity with no clear indication of a homogenous 30-nm fiber (Leuba et al., 1994; reviewed in van Holde and Zlatanova, 1995).

Historically, the analysis of the role of linker histones has relied largely on model studies. In its simplest form, purified H1 can be analyzed free in solution, and in the most complicated assays, chromatin can be completely reconstituted from individual protein components, and further analyzed using functional-based assays with enzymes like RNA polymerase. Research presented in this thesis exploits a variety of these experimental systems to explore topics that are both related yet quite diverse. In order to effectively describe relevant topics of linker histone binding to DNA and chromatin, the introduction has been further divided into four sections: (a) linker histone-DNA interactions from a molecular perspective, (b) linker histone self-association and cooperativity, (c) linker histone-DNA complexes from a macromolecular perspective, and (d) interaction of linker histones with chromatin.

## 1.2 Linker histone-DNA interactions from a molecular perspective

Most of the studies described in this thesis will utilize the avian erythrocyte linker histone H5. This protein has a tripartite structure consisting of an N-terminal basic domain from amino acids 1-21, a well-structured, trypsin-resistant globular domain (called GH5) from amino acids 22-97, and very basic C-terminal domain from amino acids 98-189 (Aviles et al., 1978). While the tails are generally regarded as having relatively little defined secondary structure when free in solution (Aviles et al., 1978; Liao and Cole, 1981; Clark et al., 1988), the globular domain folds into a stable winged-helix motif as indicated from NMR analysis of the trypsin resistant globular domain of linker histone H1 (called GH1) (Cerf et al., 1994), and X-diffraction studies of crystals of the globular domain of linker histone H5 (called GH5) (Ramakrishnan et al., 1993). Winged-helix motif proteins are characterized by a core three- $\alpha$ -helix bundle, and large, solvent-accessible loops (stabilized by  $\beta$ -sheets) that likely interact with DNA (Brennan, 1993; Overdier et al., 1994). The molecular structures of a number of winged-helix motif proteins have also been solved and include: (a) HNF-3 $\gamma$  (Clark et al., 1993), (b) the transcription regulator ETS (Werner et al., 1995), (c) Mu internal activation sequence (IAS) binding domain (Clubb et al., 1994), and (d) yeast heat shock transcription factor (HSF) (Harrison et al., 1994).

Linker histones bind to DNA, though it remains a matter of debate to what extent binding can be sequence specific (Yaneva et al., 1995; Yaneva and Zlatanova, 1992; reviewed in Zlatanova and van Holde, 1996). However, certainly there is nonspecific

binding. All domains bind to DNA, but the affinity of the C-terminal domain for DNA is greatest. For example, based on fluorescence polarization of dansylated H1, it has been reported that the H1 linker histone globular domain dissociated from DNA by 600 mM NaCl while the C-terminal domain dissociates from DNA only at 800 mM NaCl (Glotov et al., 1978b). However, it has also been published that H1 and H5 dissociates at about 400 mM NaCl and 600 mM NaCl, respectively, for both DNA (Matthews and Bradbury, 1978; Watanabe, 1986; Clark and Thomas, 1988; Segers et al., 1991) and chromatin models (Kumar and Walker, 1980). Thus, there is an unresolved discrepancy (Glotov et al., 1978b). Furthermore, the isolated globular domains have been reported to dissociate at considerably lower salt concentrations: GH1 dissociates at a little less than 200 mM NaCl (Thoma et al., 1983), and GH5 dissociates at slightly over 200 mM NaCl (Thoma et al., 1983; Segers et al., 1991).

Linker histone binding to DNA is moderately strong with a reported  $K_d$  of  $3 \times 10^{-9}$  M (Watanabe, 1986) for H1 binding to linear DNA, and virtually all detectable protein is reported to be bound to DNA under common experimental conditions (1-1000  $\mu\text{g/ml}$  DNA, comparable levels of histones) (Singer and Singer, 1978; Clark and Thomas, 1986; De Bernadin et al., 1986). The globular domain and terminal tails both contain putative DNA-binding motifs. Specifically, the globular domain contains three regions that display a high density of basic residues, one of which lies in the vicinity of the putative recognition helix ( $\alpha$ -helix three) (Cerf et al., 1994). The C-terminal tail contains numerous SPKK minor-groove binding motifs (Hill et al., 1991; Churchill, 1989; Bailly et al., 1993) and possibly other DNA binding elements (Turnell et al., 1988). The C-terminal tail appears

to be particularly important in binding DNA as illustrated by: (a) its role in chromatin folding (Allan et al., 1986), (b) its relatively high binding affinity to DNA (Glotov, 1978b) and chromatin (Thoma et al., 1983) (both based on salt dissociation studies), and (c) induced folding of the C-terminal domain upon binding to DNA (Hill et al., 1989; Clark et al., 1988; Bohm and Creemers, 1993). In addition to domains that may fold into defined DNA-binding structures, the C-terminal tail may also contain regions that bind to DNA in a rather "unstructured" fashion (Subirana, 1990).

Both CAP (a helix-turn-helix motif protein) (Schultz et al., 1991) and HNF-3 $\gamma$  (Clark et al., 1993) have been crystallized bound to DNA, and thereby constitute potential models for GH1 or GH5 binding to DNA. All winged-helix proteins so studied to date bind the major groove primarily through the interaction of a particular  $\alpha$ -helix, the recognition helix, and small loops located near the recognition helix (Brennan, 1993; see [Figure 1.2](#)). It should be noted that, all the other winged-helix proteins differ from GH5 and GH1 in that their binding to DNA is strongly sequence specific. These differences cast some doubt as to whether the way in which these other winged-helix proteins bind to DNA is, in fact, representative of the GH5-DNA complex. Certainly, without x-ray diffraction or NMR studies of the GH5-DNA complex, the exact details of GH5 binding remain a matter of some speculation.

Biochemical-related studies have provided an important, independent means of elucidating how GH5 binds to DNA, and partially support a model in which the recognition helix is inserted into the major groove as with CAP and HNF-3 $\gamma$ . Of particular significance: this "major groove binding model" predicts that the third  $\alpha$ -helix

Figure 1.2. Illustration of GH5 dock to DNA. Here, the recognition  $\alpha$ -helix (helix 3) is inserted into the DNA major groove based upon the crystal structure coordinates and speculated binding structure by Ramakrishnan et al. (1993). Indicated are residues believed to be important in DNA binding (Goytisolo et al., 1996). One cluster of residues located in the "primary" binding site relies on the interaction of the recognition  $\alpha$ -helix,  $\beta$ -hairpin, small looping domains in the very N-terminal part of the globular domain, as well as parts of the  $\alpha$ -helix 2 and  $\alpha$ -helix 3. Important residues in the "primary" DNA-binding site include: His 25, His 62, Lys 69, Arg 73, and Lys 85 (Goytisolo et al., 1996). Another cluster of residues located in the "secondary" binding site mainly interacts with DNA via the loop between  $\alpha$ -helix 1 and  $\alpha$ -helix 2, and includes residues Lys 40, Arg 42, Lys 52, and Arg 94 (Goytisolo et al., 1996). Also pictured is Phe 93, a residue that is predicted to lie in the DNA-GH5 interaction surface based on homologous interactions of HNF-3 $\gamma$  with DNA (Clark and Thomas, 1993). The terms "primary" and "secondary" are used as a means to reference the binding domains, and not intended to imply relative binding affinities. Note: bracketed residues are located on the other side of GH5, and are not easily seen in the illustration. Modeling was performed with Insight II (Biosyms, San Diego).

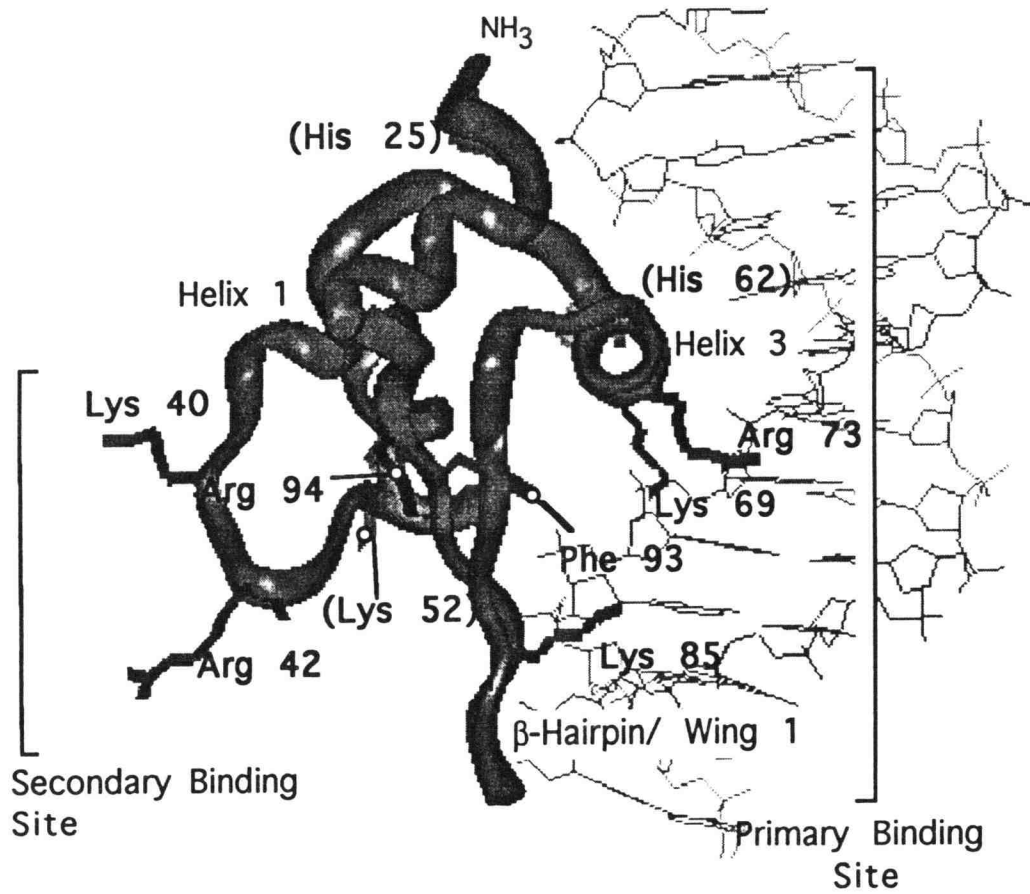


Figure 1.2

and the  $\beta$ -hairpin of GH5 lie in the GH5-DNA interface, with Lys 69 of  $\alpha$ -helix 3 and Lys 85 of the  $\beta$ -hairpin interacting with phosphates on opposite DNA strands (Figure 1.2) (Ramakrishnan et al., 1993). In support of this model, Lys 85 was found to be particularly important for DNA binding: (a) its homologue was protected three times more than any other lysine from reductive methylation upon H1 binding to DNA (Thomas and Wilson, 1986) and (b) replacement of Lys 85 with glutamate eliminates the chromatosome stop (Buckle et al., 1992). Second, Phe 93 of H5 (and Phe 71 of GH1) is positioned at an important point between the third  $\alpha$ -helix and the  $\beta$ -hairpin, and thus would be expected to be protected at the GH5-DNA interface. Chymotrypsin proteolysis protection assays indicate that the residue is hidden for both H5 bound to nucleosomes (Leuba et al., 1993) and linker histones in folded chromatin as compared to extended chromatin (Losa et al., 1984; Leuba et al., 1993). However, this may be a result specific for chromatin binding (see Chapter 3). Third, elimination of basic residues that are predicted to lie in the GH5-DNA interface (Lys 69, Arg 73, and Lys 85) dramatically reduce binding to four-way junction DNA (Goytisolo et al., 1996)- though, in the same study, elimination of residues on the "other side" of GH5 (Lys 40, Arg 42, Lys 52, and Arg 94) also reduced binding by an almost equivalent extent.

Evidence strongly suggests that the trypsin-resistant globular domain is capable of binding to more than one DNA duplex giving rise to the notion of a "primary" and "secondary" binding site on the protein. This is supported by: (a) the presence of three regions on the protein that contain an unusually high density of basic residues (Cerf et al., 1994), (b) preferred binding of linker histones to nucleosomes and four-way junctions,

implying the availability of more than one DNA strand for binding (Varga-Weisz et al., 1993; Varga-Weisz et al., 1994), (c) EM micrographs showing that GH5-DNA complexes form "tramline" structures in which GH5 appears to sandwich itself between two parallel DNA strands (Draves et al., 1992; Thomas et al., 1992; Clark and Thomas, 1988), and (d) recent mutagenesis studies of GH5 which support two DNA binding sites (Goytisolo et al., 1996). Both binding sites appear to consist of basic residues: the "primary" and "secondary" binding sites (as referenced in [Figure 1.2](#)) reportedly consist of Lys 69, Arg 73, Lys 85, His 25, His 62, and Lys 40, Arg 42, Lys 52, Arg 94, respectively. Interestingly, His 25 and His 62 were previously implicated in H1 binding to DNA in chromatin (Mirzabekov et al., 1989). The "primary" and "secondary" binding sites are located on opposite sides of GH5 ([Figure 1.2](#)), and provide a reasonable explanation for simultaneously GH5 binding to two DNA strands. Taken together, these data indicate that a number of residues on both sides of the globular domain are likely to be involved in binding, and the term "primary" and "secondary" binding site may not be reflective of relative DNA-binding affinity; indeed, four-way junction DNA binding studies by (Goytisolo et al., 1996) indicate almost identical affinities.

### **1.3 Linker histone self-association and cooperativity in binding to DNA**

It is well established that linker histones are cooperative, DNA-binding proteins that form crosslinkable ([Table 1.2](#)), closely associated nucleoprotein complexes in which the DNA appears to be "braided" or intertwined much like a cable—as seen by EM (Clark

**Table 1.1.** The effects of protein concentration and salt concentration on linker histone cooperativity .

| AUTHOR                      | TECHNIQUE                             | OBSERVATION   |
|-----------------------------|---------------------------------------|---|
| Clark and Thomas., (1988)   | sucrose gradients                     | <b>H5 (linear DNA):</b> cooperative even at low salt - 15% H5:DNA (w/w), 5 mM NaCl<br><b>H1(linear DNA) :</b> non-cooperative at 5 mM NaCl -tested up to 35% H1:DNA (w/w); <b>cooperative</b> at 35 mM NaCl, 35% H1:DNA (w/w) |
|                             | chemical crosslinking                 | <b>H5 (linear DNA):</b> extensive crosslinks from 9% H5:DNA (w/w) 5 mM up to 35% H5:DNA (w/w) 35 mM NaCl- cooperative under all conditions  |
| Yaneva et al., (1991)       | gel electrophoresis                   | <b>H1 (supercoiled DNA):</b> noncooperative up to 50 mM NaCl  |
| Clark and Thomas., (1986)   | sucrose gradients                     | <b>H1 (linear DNA):</b> for 60% H1:DNA ( w/w) transition from noncooperative to cooperative: 20-40 mM NaCl  |
|                             | chemical crosslinking                 | <b>H1 (linear DNA):</b> minimal crosslinking at 40% H1:DNA (w/w), 15 mM NaCl and extensive crosslinking at 40% H1/DNA (w/w), 35 mM NaCl- salt-dependent cooperativity   |
| Thomas et al., (1992)       | sucrose gradients                     | <b>GH1/ GH5(linear DNA):</b> bind cooperatively even in 10% w/w, 5 mM NaCl  |
| De Bernardin et al., (1986) | gel electrophoresis                   | <b>H1 (supercoiled DNA):</b> aggregation point* reached at 70% w/w, 10 mM sodium phosphate; 60% w/w, 40 mM sodium phosphate; 20% w/w, 100 mM sodium phosphate   |
| Draves et al.,(1992)        | sucrose gradients                     | <b>GH5 (linear DNA):</b> binds cooperatively to DNA under all conditions analyzed   |
| Singer and Singer, (1978)   | metrizamide gradients, filter binding | <b>H1 (linear DNA):</b> transition from noncooperative to cooperative: 20- 4<br><b>H1 (supercoiled DNA):</b> transition from noncooperative to cooperative: 40-100 mM NaCl  |
| Renz and Day, (1976)        | sucrose gradient, filter binding      | <b>H1 (linear DNA):</b> transition from noncooperative to cooperative: 20-40 NaCl   |
| Watanabe (1985)             | fluorescence anisotropy               | <b>H1:linear DNA:</b> cooperative at all salt concentration   |

\*Aggregation point: conditions where adding more H1 leads to no mobility shift of supercoiled DNA, only aggregation.

Table 1.2. Linker histone protein-association studies.

| Author                    | Sample                             | Method or Crosslinking Reagent | Result   |
|---------------------------|------------------------------------|--------------------------------|--|
| Glotov et al. (1985)      | mouse liver nuclei                 | dithiobispropionimidate        | H1 oligomerization with head-to-head, head-to-tail, and tail-to-tail contact between all linker histones |
|                           | H1 (1 mg/ml) free in solution      | dithiobispropionimidate        | oligomerization  |
| Thomas and Khabaza (1980) | rat liver chromatin                | DS                             | salt-dependent increase in H1 oligomerization  |
|                           | rat liver nucleosomes              | DS                             | salt-dependent increase in H1 oligomerization  |
|                           | rat liver oligonucleosomes         | DS                             | salt-dependent increase in H1 oligomerization  |
|                           | H1 (.04 mg/ml)                     | DS                             | no crosslinking  |
| Clark and Thomas (1986)   | H1-DNA (600 b.p.)                  | DSP                            | salt-dependent and protein concentration dependent increase in H1 oligomerization                        |
| Butler and Thomas (1980)  | rat liver long chromatin           | DTBP                           | H1 oligomerization   |
| Russo et al. (1983)       | H5 (4 mg/ml) free in solution      | 1% formaldehyde                | oligomerization  |
|                           | H1 (4 mg/ml) free in solution      | 1% formaldehyde                | oligomerization  |
|                           | N-GH1 in solution                  | 1% formaldehyde                | little crosslinking  |
|                           | N-GH5 in solution                  | 1% formaldehyde                | no crosslinking  |
|                           | trypsinized H5                     | 1% formaldehyde                | oligomerization up to trimers  |
| Ring and Cole (1979)      | H1 (4 mg/ml) free in solution      | DTP                            | oligomerization  |
|                           | steer kidney nuclei                | DTP, DMSI, CMTD                | H1 oligomerization   |
|                           | steer kidney nuclei                | DTP                            | H1 oligomerization up to dimers  |
|                           | steer kidney nuclei                | DTP                            | H1 contacts to octamers and HMG proteins   |
| Thomas et al. (1992)      | GH5 (.0125 mg/ml) free in solution | DSP                            | no crosslinking  |
|                           | GH1 (.0125 mg/ml) free in solution | DSP                            | no crosslinking  |
|                           | GH1 / GH5 on 146 b.p. DNA          | DSP                            | oligomerization up to pentamers  |

Table 1.2 (Continued)

|                             |                                   |                           |  |
|-----------------------------|-----------------------------------|---------------------------|--|
| Lennard and Thomas (1985)   | chicken erythrocyte (C.E.) Nuclei | DSP                       | salt -dependent increase in multiple H1/H5 oligomerization                                   |
|                             | C. E. chromatin                   | DSP                       | salt-dependent increase in multiple H1/H5 oligomerization                                    |
|                             | C. E. oligonucleosomes            | DSP                       | H1/H5 oligomerization with head-to-head, head-to-tail, and tail-to-tail contact <sup>1</sup> |
|                             | C. E. dinucleosomes               | DSP                       | H1/H5 oligomerization largely head-to-tail contacts <sup>1</sup>                             |
| Maman et al. (1994)         | GH1 (.2 mg/ml) free in solution   | DSP                       | oligomerization up to trimer   |
|                             | GH5 (.1-3 mg/ml) in solution      | DTBP, DSP, DTSSP          | oligomerization up to pentamer   |
|                             | GH5 (.2 mg/ml) / GH1 (.2 mg/ml)   | DST                       | no crosslinking  |
| Boulikas et al. (1980)      | bovine thymus chromatin           | EDAC                      | H1A oligomerization; possible GH1 contacts   |
| De Bernardin et al. (1986)  | H1 on supercoiled DNA             | EDAC                      | oligomerization  |
| Nikolaev et al. (1983a)     | calf thymus nuclei/ chromatin     | MMB                       | GH1 oligomerization up to dimers   |
| Olins and Wright (1973)     | C. E. nuclei                      | glutaraldehyde            | H1 /H5 oligomerization.  |
| Bonner and Pollard (1975)   | rat liver nuclei                  | EDAC                      | H1 (and GH1) oligomerization   |
| Chalkley and Hunter (1975)  | calf thymus (C.T.) chromatin      | formaldehyde              | no H1 crosslinking   |
|                             | C.T. chromatin                    | glutaraldehyde            | H1 oligomerization   |
| Ring and Cole, (1983)       | steer kidney nuclei               | EDAC                      | H1 oligomerization; primarily tail-tail and head-tail contacts                               |
| Itkes et al. (1980)         | C.T. nuclei                       | MMB, DS                   | H1 oligomerization (in groups of 12)   |
|                             | C.T. chromatin                    | MMB, DS                   | H1 oligomerization (in groups of 12)   |
| Glotov et al. (1978b)       | N-GH1                             | fluorescence polarization | aggregated (5 mM sodium phosphate)   |
| Hardison et al. (1975)      | C.T. chromatin                    | MMB                       | H1 oligomerization   |
| Smerdon and Isenberg (1976) | purified H1                       | fluorescence anisotropy   | no H1 interaction  |
|                             | purified H1                       | sedimentation analysis    | no H1 interaction  |

Table 1.2 (Continued)

|                            |                                     |         |   |
|----------------------------|-------------------------------------|---------|---|
| Nikolaev et al. (1983b)    | C.T. chromatin                      | MMB     | H1 oligomerization with head-to-head, head-to-tail, and tail-to-tail contact <sup>1</sup> |
| Nikolaev et al. (1981)     | C.T. nuclei                         | MMB     | H1 oligomerization with head-to-head, head-to-tail, and tail-to-tail contact <sup>1</sup> |
| Clark and Thomas (1988)    | H5 (.012 mg/ml) on DNA (800 b.p.)   | DSP     | H5 oligomerization up to n=9, independent of salt and protein concentration               |
|                            | H5/H1 (.012 mg/ml) free in solution | DSP     | no crosslinking   |
| Thomas and Kornberg (1975) | rat liver chromatin                 | DS, M3M | H1 oligomerization  |
| Draves et al. (1992)       | GH5 (.012 mg/ml) free in solution   | DSP     | no crosslinking   |
|                            | GH5 (.012 mg/ml) on linear DNA      | DSP     | oligomerization up to hexamers  |
| Dashkevich et al. (1983)   | mouse liver nuclei                  | DTP     | H1 <sup>o</sup> contacts with other histone proteins                                      |
| Glotov et al. (1978)       | C. T. nuclei                        | MMB     | H1 contacts with H3 and H4  |

The list of crosslinking reagents (crosslinkers) includes: DSP, dithiobis (succinimidyl propionate); DS, dimethyl suberimidate (dihydrochloride); DTBP, dimethyl 3,3'-dithiobis-(propionimidate); DTSSP, 3,3'-dithiobis (sulfosuccinimidyl propionate); DST, disuccinimidyl tartarate; ; MMB, methyl-4-mercapto- butyrimidate; EDAC, 1-ethyl-3(3-dimethylaminopropyl) carbodiimide; CMTD, N,N'-bis(2-carboxyimidomethyl) tartaramide; DTP, dimethyl-3,3'-dithiobispropionimidate dihydrochloride; DMSI, dimethylsuberimidate dihydrochloride; M3M, methyl 3-mercaptopropionimidate. GH5, the trypsin-resistant globular domain of H5; GH1, the trypsin-resistant globular domain of H1; N-GH1, the combined N-terminal and globular domains.

<sup>1</sup> Contacts refer to the relative orientation of neighboring linker histone molecules with head-to-head indicating crosslinked contact between two N-GH1 domains, and tail-to-tail indicating crosslinked contact between two C-terminal domains. Frequently, analysis is performed using a two-dimensional SDS-PAGE gel technique described in (Thomas, 1989).

and Thomas, 1988b). While H5 (and the globular domains) is cooperative, independent of the salt concentration<sup>1</sup>, H1 displays negligible cooperativity in low salt (Table 1.1).

However, it should be noted that from fluorescence anisotropy measurements presented in (Watanabe, 1986) H1 binding remains cooperative, albeit only weakly so, at low salt concentrations. None-the-less, a number of reports identify a salt range in which H1 binding becomes more cooperative: 20-40 mM NaCl for linear DNA and 40-100 mM NaCl for supercoiled DNA (Table 1.1).

Linker histone cooperativity in binding is reflected by the coexistence of naked DNA and saturated DNA-protein complexes in the same reaction solution (De Bernardin et al., 1986). This "all or nothing binding" has been observed with sucrose gradient (Renz and Day, 1976), and metrizamide gradient analysis (Singer and Singer, 1978) in which nucleoprotein complexes are observed to migrate discretely rather than continuously, and suggest DNA saturation. The same effect has been observed with gel electrophoresis (Yaneva et al., 1991; see Chapter 3). Gel electrophoresis of linear DNA in the presence of linker histones does not exhibit the "retardation" usually associated with complex formation. Rather, the bands remain unchanged in mobility, but gradually decrease in intensity as material is transferred into large aggregates. Interestingly, crosslinking studies suggests that cooperativity results in increased contact between linker histones, possibly reflecting saturated binding (Clark and Thomas, 1986; Thomas et al., 1992; De Bernardin et al., 1986).

---

<sup>1</sup> The terms salt and NaCl are interchanged throughout the thesis, and reflect the almost-exclusive use of NaCl in linker histone-DNA binding studies.

Despite the amount of effort devoted to studies of linker histone interactions with DNA, the basis of linker histone cooperativity remains a matter of some debate. In general, two separate possibilities appear to underlie the phenomenon and include either: (a) the "tramline" model (Clark and Thomas, 1988; Thomas et al., 1992; Goytisolo et al., 1996), or (b) cooperativity based on protein-protein contacts as described by (Kowalczykowski et al., 1986; McGhee and von Hippel, 1974). The "tramline" model essentially proposes that cooperativity is a function of DNA substrate availability. The cooperative process begins when a single linker histone acquires two DNA strands via two separate DNA binding sites on GH5. Once the tramline nucleus forms, the proximity of two parallel DNA strands makes a preferred binding substrate for binding, and hence a basis for cooperativity. The model is supported by numerous EM micrographs apparently showing tramlines or DNA-linker histone complex containing multiple DNAs, and site-directed mutagenesis studies support the presence of two DNA binding sites on GH5 that may facilitate multiple DNA binding. The second model to explain linker histone cooperativity is based on a more classical view. That is, contact between adjacently-bound proteins leads to increased binding affinity (McGhee and von Hippel, 1974). The free energy associated with this contact effectively increases the overall binding free energy, and leads to a higher binding coefficient. The importance of linker histone self-association in this second model suggests that protein interactions should be readily observable under a variety of conditions. To this end, linker histones have been self-crosslinked on DNA, in chromatin, and free in solution (Table 1.2). Additionally, EM micrographs consistently show that linker histones (and the globular) domain bind DNA in

closely associated groups, rather than randomly, on the DNA (Clark and Thomas, 1988). Despite all this work, results have been inconclusive; a number of studies contradict linker histone self-association including the report that H1 does not associate in solution based on fluorescence anisotropy results (Smerdon and Isenberg, 1976), and reports that GH5 does not associate (Draves et al., 1992; Thomas et al., 1992).

#### **1.4 DNA-linker histone complexes from a macromolecular perspective**

As previously described, linker histones are able to bind multiple DNAs. Not only does the globular domain appear to have at least two DNA-binding domains, but the long terminal tail domains contain many putative DNA binding elements, comprised of a large number of basic residues. Together this suggests that a single linker histone may interact with separate DNA fragments, and collectively form a vast nucleoprotein network. Such a network, because of its potentially large size might be expected to have low solubility, and this appears to be the case, since linker histones have been repeatedly reported to precipitate DNA (Osipova et al., 1985; Clark and Thomas, 1988; Welch and Cole, 1979; Liao and Cole, 1981; Segers et al., 1991). Additionally, the term aggregation point has been used to describe the onset of aggregation. The aggregation point is characterized by: (a) appearance of material in the sample well in gel electrophoresis (Yaneva et al., 1991, De Bernardin et al., 1986), (b) large fiber-like structures (visible by EM) consisting of a thick cable of protein with many DNA molecules protruding, accompanied by free DNA (De Bernardin et al., 1986; Draves et al., 1992), (c) increased turbidity as molecules become insoluble (Glotov et al., 1978c; Matthews and Bradbury,

1978), and (d) nucleoprotein complexes pelleting in a sucrose gradients (Clark and Thomas, 1988) and metrizamide gradients (Liao and Cole, 1981; Singer and Singer, 1978). The appearance of such an infinite network structure in a polymerizing system is an inevitable consequence of the presence of multifunctional constituents (Flory, 1953). The interaction of DNA and linker histones is multifunctional, since the proteins and DNAs both contain multiple sites for binding.

The basis for linker histone-induced aggregation of DNA may be a combination of both DNA-protein, and protein-protein interactions, though protein-DNA binding appears to be the single most important element. In particular, the lengthy C-terminal tail may be particularly pivotal as it is in a solvent accessible location within the linker histone nucleoprotein complex, potentially positioned to "grab" other nucleoprotein complexes (Glotov et al., 1978c). Different linker histone subtypes have varying ability to aggregate DNA (Welch and Cole, 1979; Liao and Cole, 1981). This is likely a consequence the number of basic residues and the DNA aggregation rate for linker histones as demonstrated from a study with  $H1_T$  from calf thymus, and  $H1_S$  from sea urchin sperm.  $H1_S$ , the more basic subtype, aggregates DNA better than  $H1_T$ , and indicates that higher DNA binding affinity enhances aggregation (Osipova et al., 1985). Interestingly, the aggregate-inducing effects of the C-terminal domain can be reproduced with general polyamines (Olins et al., 1967; Garcia-Ramirez and Subirana, 1994), and repeats of the SPKK sequence found in the C-terminal tail (Bailly et al., 1993), all of which bind to, and preferentially aggregate AT-rich DNA.

Evidence for protein-protein contacts in facilitating aggregation comes mainly from E.M. and crosslinking studies (Table 1.2). For the former, a number of DNA-linker histone structures have been identified that indicate close linker histone contact, and suggest protein-protein contacts in DNA aggregation. These structures include rods and filaments, and DNA circles or hairpins from overlapping segments of the same DNA fragment (Clark and Thomas, 1988). In addition, the dimension of linker histone-saturated-DNA filaments suggest that the protein is sandwiched (presumably in close contact) between DNA strands. To be specific, separation of DNA duplexes in the putative "tramline" complex is reported to be 3 nm in width, which is roughly the size of the globular domain (Thomas et al., 1992). Crosslinking studies indicate that linker histones make extensive contacts in chromatin, on DNA, and, possibly free in solution (Table 1.2), although the latter has been a matter of controversy.

Both similarities and differences exist between the way linker histones bind to supercoiled DNA, and to linear DNA. Gel electrophoresis studies of the titration of linear DNA with linker histones do not reveal the "gel shifts" usually associated with DNA-protein association. Instead, bands decrease in intensity, and then vanish entirely above a critical histone loading. It will be shown in Chapter 3 that this is a natural consequence of high cooperativity. On the other hand, gel electrophoresis, as well as gradient studies indicate that linker histones bind supercoiled DNA in a more uniform manner, exhibiting a mobility shift as linker histones are added. However, H1 bound to supercoiled DNA at higher salt concentrations appears to mimic linear DNA binding. At higher salts, soluble H1-supercoiled DNA complexes are observed to increase in electrophoretic mobility as aggregates begin to appear in the well up to around 100 mM

NaCl (Yaneva and Zlatanova, 1991; reviewed in Zlatanova and Yaneva, 1991). In effect by 100 mM NaCl, the aggregate acts "like a magnet" in attracting nearly all of the linker histones leaving some supercoiled DNAs with fewer proteins (De Bernardin et al., 1986). These observations are corroborated by metrizamide gradient sedimentation which show that by 100 mM NaCl most H1 becomes associated with the aggregate complex for supercoiled DNA (Singer and Singer, 1978). It is also reported that linear DNA aggregates more readily than supercoiled DNA in response to increased salt and protein concentration (Liao and Cole, 1981). For linear DNA, light scattering studies with H1 and long, linear DNA indicates that maximum precipitation occurs at around 300 mM NaCl, and is negligible below 50 mM NaCl and above 500 mM NaCl-the approximate ionic strength required for H1 dissociation from DNA (Glotov et al., 1978b; Matthews and Bradbury, 1978). Interestingly, linker histones appear to uniformly bind linear DNA above 20 mM NaCl to produce a "fast migrating complex", and this property is used as an indicator of cooperativity in sucrose gradient analysis (Table 1.1) (Renz and Day, 1976; Thomas et al., 1992; Clark and Thomas, 1986; Clark and Thomas, 1988).

These observations suggest that charge neutralization of the DNA is, at least in part, responsible for the difference in aggregation for linear and supercoiled DNA. This is based on: (a) the universality of salt in inducing aggregation for both linear, and supercoiled DNA, and (b) an apparent limit in the H1-DNA ratio that supercoiled DNA can absorb and still remain soluble. For example, the 4,500 b.p. SV40 plasmid is soluble when 12 molecules of H1 are bound, but becomes insoluble when 40-85 molecules are bound, as demonstrated by the sedimentation of two complexes in metrizamide gradients

(Singer and Singer, 1978). Both salt and linker histone binding to DNA act to "reduce" the effective surface charge density of the linker histone nucleoprotein complex. Salt produces a cloud of counterions around the nucleoprotein complex thus masking the charge, and also acts to increase the solution permittivity. Similarly, bound linker histones effectively neutralize DNA phosphate groups by adding basic residues with each linker histone reportedly neutralizing about 6 phosphate groups (Watanabe, 1986; Segers, 1991). Conceivably, reduction of the net surface density allows closer contact, oligomerization, and, ultimately, precipitation of DNA that for supercoiled nucleoprotein complexes is impeded by fewer bound molecules per DNA as compared to linear DNA (Singer and Singer, 1978). Instead, linker histones appear to bind relatively uniformly amongst all supercoiled DNA molecules (Singer and Singer, 1978, Laio and Cole, 1981; Yaneva, 1991). Interestingly, polyamines, and cationic peptides also condense and aggregate DNA, indicating that the process is not linker histone specific (Olins et al., 1967). Other reasons for a salt- and protein- dependent aggregation may exist and could include salt-dependent alterations in protein structure that increases cooperativity (Clark and Thomas, 1988).

But what is the basis for the observed differences of linker histone binding to and aggregation of linear and supercoiled DNA? First, superhelicity may influence linker protein assembly on the DNA. Perhaps crossovers (that appear to act as high affinity binding substrate) facilitate uniform linker histone binding (Krylov et al., 1993; Singer and Singer, 1976). Additionally supercoiled DNA may be unable to fully saturate like linear fragments due to limited binding sites or effects related to bending or untwisting

(Ivanchenko et al., 1996). Particularly revealing are EM of H1 bound to plasmid DNA in which linker histones are shown to bind in clusters that are separate by regions of what appear to be stress-related "bubbled DNA" (De Bernardin et al., 1986). These micrographs not only tend to support the presence of structural-related impediments to linker histone binding onto supercoiled DNA, but also show that the DNA clearly forms internal "tramlines" by H1 bridging distal parts of the plasmid. The latter observation is informative in that the multiple DNA-binding domains of H1 may be satisfied "internally" by the plasmid DNA. For linear DNA, unbound DNA-binding domains would be available to interact with other DNAs, and promote oligomerization, or as revealed by E.M. form hairpins or other structures on the same DNA fragment. Certainly, it seems odd that while supercoiled DNA acts as a preferred substrate for linker histone binding, linear DNA binds linker histones leading more readily to aggregation (Liao and Cole, 1981). For rather thorough reviews on the subject refer to Zlatanova and Yaneva (1991) and Zlatanova and van Holde (1995).

While the mechanisms involved in linker histone-DNA binding and aggregation are not completely understood, at least three fundamental factors appear to be involved in the aggregation process. First, linker histones deposit in a cooperative, close-neighbor fashion that for H1 is salt dependent. Second, a dynamic movement of linker histones and DNA from soluble complexes into massive, insoluble structures accompanies a salt increase. Third, the association of large aggregates appears to be largely the consequence of charge neutralization of the linker histone-DNA nucleoprotein complex. It has also been speculated that salt-dependent alteration in linker histone structure may facilitate the aggregation process (Welch and Cole, 1979; Liao and Cole, 1981).

### 1.5 Interaction of linker histones with chromatin

As described previously, H5 and H1 have been reported to stabilize or compact chromatin fibers. For example at low salt, linker histones induce "three dimensionality" in chromatin fibers composed only of octamers. Chromatin fibers are considered to exist between two morphological endpoints including an extended, flattened form observed in chromatin fibers without linker histones at low salt, and a poorly-characterized compacted isoform observed at high ionic strength. To complicate matters, salt and linker histones both compact chromatin, though it is unlikely that the compacted structures are the same. SFM studies indicate that the native chromatin fiber is quite heterogeneous, but neutron scattering results appear to support a fiber with more homogeneity. The fiber predicted by neutron scattering has linker histones located internally-similar to the original 30 nm fiber (Graziano et al., 1994). Over the years numerous attempts to identify the location of linker histones within chromatin have been conducted, commonly relying on the access of either antibodies or proteases to chromatin-bound linker histones. The results, for the most part, are difficult to interpret, and, in sum total, are contradictory. For an extensive overview on the location of linker histones in the chromatin fiber refer to (Zlatanova and van Holde, 1995).

The mechanism by which linker histones condense chromatin is another relevant topic that remains unelucidated. To begin, protein-protein interactions appear to drive the compaction process as suggested by reports of self-association of both histone octamers (Dubochet and Noll, 1978) and linker histones (Table 1.2). Evidence also supports that

extensive contacts between proteins exists in chromatin as indicated by extensive linker histone self-crosslinking (Table 1.2), and the finding that protein-protein contacts in chromatin stabilize DNA from thermal melting (Riehm and Harrington, 1989). In what may be a related issue, isolated nucleosomes or core particles undergo oligomerization and aggregation in the presence of salt and linker histones. Nucleosomes (Ali and Singh, 1987; Segers et al., 1991) and small oligonucleosomes (Jin and Cole, 1986) have been reported to aggregate in the presence of linker histones, with the C-terminus apparently producing most of the effect. Another group found that "aggregated" chromatosomes produced large crosslinked H1 homopolymers (Thomas and Khabaza, 1980). Based on EM, H1 reconstituted nucleosome oligomers actually resemble chromatin fibers (Grau et al., 1982; Finch and Klug, 1976), indicating that chromatin fiber morphology may be facilitated by linker histone-promoted bridging between separate nucleosomes. Whether such parallels exist in chromatin is unknown. None-the-less, these results suggest that linker DNA is not necessary for the formation of some kinds of chromatin fibers, and support the prospect of protein-protein contacts in chromatin stability.

For chromatin compaction to occur, nucleosomes are required to make close contact. Since linker DNA length is well below the persistence length of DNA, the linker should act like a rod in preventing nucleosome interactions. The result, as indicated by EM, is that chromatin in low salt devoid of linker histones appears as isolated octamers spatially separated on a "string" of extended, rigid DNA. Linker histones are believed to somehow alter or circumvent linker DNA rigidity. To this end, two models have in recent years become popularized. The first model contends that linker histones bend linker

DNA, and ultimately facilitating nucleosome contact (Figure 1.3). Particularly supportive of this model are EM studies in which dinucleosomes (bound to the same DNA fragment) appear to condense with increasing salt concentration (Yao et al., 1991; Garcia-Ramirez, 1992). Yao et al. (1991) further corroborate this by showing that the diffusion coefficient increases with NaCl concentration, indicating a more compact structure. The second model proposes that DNA does not bend during compaction, but rather chromatin condenses much like an accordion with the linker DNA remaining relatively rigid during the process. Linker histones bring the entering and exiting DNA (Figure 1.3) together much like the parallel running "tramlines" observed in naked DNA binding studies (Hamiche et al., 1996; Furrer et al., 1995). Furthermore, the C-terminal tail domain appears to play an important role in stabilizing the "tramline" of the entering and exiting DNA strands. This may explain analytical sedimentation results reported by (Allan et al., 1986) in which the linker histone C-terminal domain was required for the fiber compaction. Evidence for this model is building and includes sedimentation analysis, diffusion coefficients, cryo-EM, and measurements made from SFM. images. For a more in-depth overview of the mechanism of chromatin compaction refer to van Holde and Zlatanova (1996).

Model H1-DNA studies are performed with the aim of better understanding H1 interactions in chromatin. However, the use of model studies in obtaining physiologically-relevant data is questionable due to the constraints placed on linker histones within chromatin. In short, chromatin presents challenges that warrant a certain amount of skepticism in applying DNA modeling results. Obviously, the octamer histone, and the resulting nucleosome substrate presents an environment that cannot be duplicated

Figure 1.3. Simplified schematic of two models for chromatin compaction. One model contends that linker DNA bends in the chromatosome, while the other model does not require bent linker DNA. In low salt in the absence of linker histones, chromatin is extended with individual nucleosomes appearing like "beads on a string". With the addition of linker histones, chromatin is observed to compact leading to the closer contact between nucleosomes (Thoma and Koller, 1977, reviewed in van Holde and Zlatanova, 1996). To accomplish this task, linker histones may either bend linker DNA, or linker histones may bring the entering and exiting DNAs together, and, in effect, allow every other nucleosome to interact.

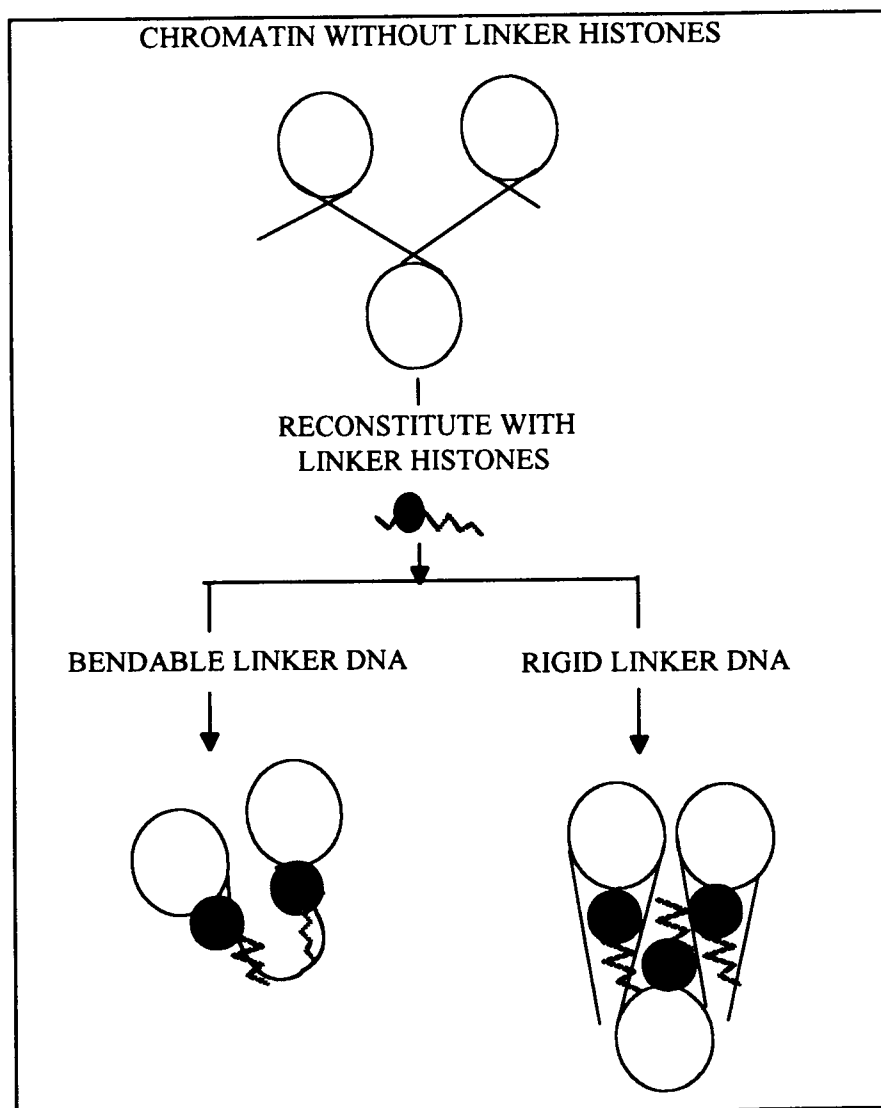


Figure 1.3

with naked DNA. For example, while it is established that linker histones cooperatively saturate DNA, it is unclear whether such structures exist in chromatin. With this said, what information can be applied from simple in vitro DNA binding studies? Certainly a better understanding of linker histone cooperativity, self-association, and DNA-binding properties can be gained using simplified models, but again without conducting parallel chromatin assays, application of this information remains highly speculative. Nonetheless, as in all biochemical studies, it is necessary to begin with the simplified system in order to build the background upon which more biologically relevant studies can be constructed.

## **1.6 Organization of thesis**

From the introduction, it should be obvious that the topic of H5 linker histone binding and assembly onto DNA is both expansive in scope, and complicated in nature. From this vast field of linker histone biochemistry, the research topic was originally focused on the self-association of DNA-bound H5 (and GH5) as measured by dithiobis (succinimidyl propionate) crosslinking. During the course of the initial research, other related experimental "avenues" opened and were explored. In short, this thesis forms a mosaic of projects that address both H5 and GH5 self-interaction, and H5 and GH5 interaction with DNA. It was discovered that a full understanding of linker histone binding to DNA will require a composite of these elements.

In summary, the following general questions were asked during the course of research, and provided a basis for the experiments described in this thesis:

1. Do linker histones self-associate in solution? Contradictory results have been reported.
2. Do linker histones organize into specific crosslinked assemblies, either in solution or on DNA?
3. Does H5 bind DNA via the recognition helix as the prototypical helix-turn-helix model predicts?
4. How does DNA topology (superhelicity) affect linker histone assembly onto DNA?
5. Does H5 affect chromatin morphology?

The experimental results are subdivided into three chapters, and represent closely related themes that are anticipated to comprise research papers to be submitted for publication in research journals, and include: Chapter 2: Self Association and Complexing of H5-related Proteins in Solution and onto DNA: Potential Implications for Chromatin Stability, focuses principally on evidence for linker histone self-association free-in-solution and bound to DNA. Particular emphasis is place on determining whether self-interaction is specific, and the effect of DNA, salt and protein concentration on linker histone self-association. Chapter 3: Biochemical Studies of H5 Linker Histone: Evidence for a Novel DNA-Binding Strategy by a Winged-Helix Motif Protein, primarily addresses the way in which linker histones bind to DNA. Included is evidence for specific motifs involved in DNA binding, results that directly counter the popular "major groove binding model" for GH5, some quantitation of linker histone-induced aggregation of DNA, and the analysis of H5-induced compaction of small reconstituted chromatin fibers. Finally, Chapter 4:

Analysis of Linker Histone-DNA Complexes by SDS-PAGE, both summarizes novel techniques applying glutaraldehyde crosslinking discussed (in part) in previous chapter, and introduces a nonradioactive method for approximating protein-DNA ratios of nucleoprotein complexes separated with PAGE. All the techniques described in this chapter employ SDS-PAGE, and the results are hoped to be submitted to biotechniques-oriented journal.

## CHAPTER 2

### **Self-Association and Complexing of H5-Related Proteins Free in Solution and Bound to DNA: Evidence for Specific Contacts**

#### **2.0 Summary**

The ability for GH5 and H5 to self-associate either free in solution, or when bound to DNA was investigated. Salt-induced turbidity, analytical equilibrium ultracentrifugation and chemical crosslinking with dithiobis (succinimidyl propionate) (DSP) were used to measure the ability for the linker histones to self-interact. While all the proteins were observed to scatter light appreciably at high salt concentrations and crosslink over a wide range of salt concentrations, only H5 appeared to self-associate appreciably in solution as measured by equilibrium analytical ultracentrifugation. GH5 self-crosslinked differently when bound to supercoiled DNA, than when bound to linear DNA or crosslinked free in solution. The latter showed a relative high abundance of uncrosslinked monomers, and crosslinking in solution was slower than for GH5 bound to linear DNA, under similar condition. In the same set of experiments, GH5 crosslinked, detectably on supercoiled DNA only up to a trimeric complex. The rate of GH5-crosslinking on supercoiled DNA was a relatively slow, indicating a difference in assembly as compared to that on linear DNA. Finally, using a novel strategy, referred to as quantitative proteolysis, that may be applicable to other protein self-association studies, crosslinked-GH5 complexes were cleaved with chymotrypsin in order to elucidate

their organization. GH5 assembled onto a 22 b.p. oligonucleotide DNA in a manner that involved specific protein-protein contacts that appeared to involve the C-terminal part of the protein. Results support the premise that linker histones assemble specifically both in solution and on DNA.

## 2.1 Introduction

The main protein constituent of chromatin is a class of basic, structural proteins known as histones. Histones are further subdivided into *linker histones* and the *octamer complex* which consists of two subunits each of histones H2A, H2B, H3 and H4 (van Holde, 1989). Linker histones bind to the octamer and associated DNA in roughly a 1:1 stoichiometry (Bates and Thomas, 1981), and stabilize the nucleoprotein assembly (otherwise known as a nucleosome), as assayed by resistance of the core DNA to nuclease digestion (Noll and Kornberg, 1977). The exact location of linker histone binding on the nucleosome is unclear, and may actually involve multiple sites (Allan et al., 1980; Pruss et al., 1996). Additionally, it is well established that chromatin exists between two extreme conformations: extended and compacted fibers. Extended fibers were originally reported as being relatively planar structures 10 nm in width as observed by EM (Olins and Olins, 1974; Woodcock, 1973; Finch and Klug, 1976), and in similar studies, compacted fibers were reported to be relatively homogenous structures with a diameter of around 30 nm and solenoidal in appearance (reviewed in Widom, 1989). However, recent scanning force microscopy indicates that chromatin is considerably more heterogeneous in structure with more three-dimensional organization even at a lower salt concentration than indicated

earlier from EM (Leuba et al., 1994a; reviewed in van Holde, K. E. and Zlatanova, J., 1995).

Chromatin experiences condensation with the addition of linker histones (Thoma and Koller, 1977) or by an increase in ionic strength (Thoma et al., 1979; Hansen et al., 1989). The basis for fiber compaction remains a matter of some debate, though protein-protein interactions may contribute significantly. Histone octamers (Dubochet and Noll, 1978), linker histones (Maman et al., 1994), and nucleosomes have all been reported to self-associate in solution (Finch and Klug, 1976). Particularly intriguing is the finding that nucleosomes or small chromatin oligonucleosomes self-associate only after the addition of linker histones (Segers et al., 1991; Ali and Singh, 1987; Grau et al., 1982) which suggests that linker histones may act like a tether in joining separate nucleosomes. Early models of chromatin, in fact, predicted such chromatin infrastructure based on the extensive crosslinking between linker proteins that could be accomplished when these were present in chromatin (Table 1.2).

Considering that chromatin proteins self interact, it seems plausible that linker DNA rigidity may impede contact between neighboring nucleosomes. How then does the chromatin compaction process circumvent linker DNA rigidity? One proposal relies on increased contact between neighboring nucleosomes through DNA bending (Yao et al., 1991). Presumably, the highly basic C-terminal linker histone tail interacts with the linker DNA, as the trypsin-resistant globular domain by itself has been reported not to be sufficient for native-like fiber compaction (Allan et al., 1986) though EM micrographs reveal that some GH5-facilitated compaction does occur (Thoma et al, 1983). Alternatively, it is proposed that chromatin compaction occurs much like the collapse of

an accordion with the linker DNA remaining relatively rigid throughout the process. In this model, the linker histone, binding at the dyad axis, "sandwiches" the entering and exiting DNAs together, and, in effect, brings every-other nucleosome together (Furrer et al., 1995) (see [Figure 1.2](#) for a depiction of these models). For a thorough review on the topic of linker histone induced chromatin compaction refer to van Holde and Zlatanova (1996).

Because protein-protein contacts appear to be important for chromatin stability, a number of experiments were conducted in order to better characterize linker histone self-interaction. Self-association was assayed by chemical crosslinking with dithiobis (succinimidyl propionate) (DSP), salt-induced turbidity and analytical ultracentrifugation. Additionally, a novel assay called *quantitative proteolysis* was developed to elucidate crosslinked-GH5 organization; it utilizes chemical crosslinking followed by chymotrypsin proteolysis. In summary, it was found that: (a) both avian erythrocyte-specific linker histone H5, and the trypsin-resistant globular domain of H5 (GH5), crosslinked into aggregate complexes free in solution, (b) DNA topology influenced the self-interaction of DNA-bound GH5, and (c) GH5 assembled onto DNA in a specific manner that appears to involve protein-protein contacts near the C-terminus of the globular domain.

## 2.2 Methods and materials

### 2.2.1 Protein purification

#### *2.2.1.1 Expression of recombinant human GH1.3, human GH1° and avian GH5*

The trypsin-resistant globular domains of human subtypes H1° (reviewed in Zlatanova and Doenecke, 1994) and H1.3, referred to respectively as GH1° and GH1.3, were both cloned into pET-15b (Novagen) (Moffat and Studier, 1986), an *E. coli* expression vector. To begin, residues 26 to 96 of human H1° were PCR amplified from a genomic DNA fragment containing the human H1° gene that had been cloned into pBluescript II SK (+) (Doenecke and Tonjes, 1986). The forward primer, ACC ACC CCA TGG GGT ATT CAG ACC TGA TCG TG, included Met followed by Gly and residue 26-31 of native H1° protein. The GH1° reverse primer had the sequence CTT GGG CCA TGG TCA CTT GGC TAG CCG GA. Similarly, residues 37 to 110 of human H1.3 were PCR amplified from a genomic fragment containing the human H1.3 gene cloned into pUC19 (Albig et al., 1991). The forward primer had the sequence AAA GCA TCC ATG GGA CCC CCA GTA TCT GA, and the reverse primer had the sequence CCC GGA CCA TGG TCA CTT GTT GAG TTT GAA GGA. Included in all primers was the recognition sequence for Nco I restriction enzyme which was used for cloning purposes. The gene fragments containing GH1° or GH1.3 were PCR-amplified and cloned into pET-15b as follows: the plasmids containing the gene for H1° and H1.3 were linearized, treated with phenol and ethanol precipitated. PCR reactions were

performed as 100  $\mu$ l reactions and included: 50 ng of template DNA, 0.7  $\mu$ g of both forward and reverse primers, 2.5 unit of Taq polymerase (Pharmacia), and 0.125 mM of each dNTP. The reaction solution consisted of 100 mM Tris-HCl (pH 9.0), 15 mM  $MgCl_2$ , 500 mM KCl. A layer of mineral oil was placed over the PCR reaction solution, and contents were placed in a thermocycler. The first cycle included a denaturation step at 94  $^{\circ}C$  for 5 minutes, a primer annealing step at 65  $^{\circ}C$  for 1 minute, and an extension step at 72  $^{\circ}C$  for 1.5 minutes. Subsequent steps included as shorter 1 minute denaturation step with the final step also including a 10 minutes extension step. Significant amounts of PCR produced insert were detected by 30 cycles. Nco I along with NEB4 buffer (New England Biolabs) was added directly to the PCR reaction and incubated at 37  $^{\circ}C$  overnight. The DNA was purified by phenol extracted and ethanol precipitated. The Nco I-cut insert containing the globular domain was ligating into pET-15b (cut with NcoI and reacted with calf intestinal phosphatase). The ligation reaction included: 15% PEG 8000, 800 unit /  $\mu$ l of T4 DNA ligase (New England Biolabs) using reaction buffer provided, and was conducted at 15  $^{\circ}C$  for 24 hours. The ligated-DNA reaction mixture was transformed into DH5 $\alpha$  cells made competent following a common  $CaCl_2$  procedure. Subsequently, the cells were grown in LB broth at 37  $^{\circ}C$  and plated on LB-agarose plates containing 100  $\mu$ g/ml of ampicillin. Plasmids from ampicillin-resistant colonies were isolated by the alkaline lysis method (Maniatis et al., 1982), and plasmids containing the insert were then transformed into BL21 *E. coli* cells (Novagen). Cells were induced to express either GH1 $^{\circ}$  or GH1.3 with the addition of 0.6 mM IPTG at 0.35-0.6 O.D. (600 nm). Cells were induced for several hours while shaking at 37  $^{\circ}C$ . Clones expressing large quantities of peptide migrating at the expected location of the globular domain were isolated and stored

in 20% glycerol. One of these clones was randomly selected for large scale expression and purification.

GH5, expressed from GH5pLK (generously provided by V. Ramakrishnan) (Gerchman et al., 1994), and GH1<sup>o</sup> were expressed and isolated using virtually identical protocols based on the procedure originally described by Cerf et al. (1993). BL21 E. coli cells were grown in LB in 50 ml starter cultures overnight. The LB contained either 50 µg/ml kanamycin (for GH5 in pET-3a) or 50 µg/ml ampicillin (for GH1<sup>o</sup> and GH1.3 in pET-15b). 25 mls of the starter culture was then added to 1 liter of LB with the proper antibiotic and induced to express protein as described above. The culture was then pelleted in J6B rotor at 3.5 krpm for 15 minutes. The pellet was resuspended in 13 mls of E. coli. wash buffer containing: 25 mM Tris-HCl (pH 7.8), 0.5 M NaCl, 0.2 mM EDTA, 0.35 mM PMSF and placed on ice with all subsequent steps being conducted either on ice or at 4 °C. The samples were sonicated for about 10 minutes with 3 separate pulses lasting about 3 minutes each. Cellular debris was then spun down for 30 minutes in an SS-34 rotor. The supernatant was removed with the pellet being resuspended (by vortexing) in 8 mls of wash buffer. The resuspended pellet was centrifuged again as above with the supernatant being removed and added to the previous supernatant. Partially purified protein was precipitated with ammonium sulfate at 0.38 mg/ml. After brief vortexing, the solution was placed on ice for 30 minutes then centrifuged for 30 minutes at 12,000 rpm in an SS34 rotor. The sample was then dialyzed into 100 mM NaCl, 10 mM Tris-HCl (pH 7.8), 0.2 mM EDTA in a Spectrapore 3 (molecular weight cut off (MWCO) of 3500) overnight. After dialysis, the sample was then loaded (with gravity feed) onto a

CM Sephadex C25 (Sigma) column (5 cm x 2.7 cm) that had been preincubated with 300 mM NaCl, 10 mM Tris-HCl (pH 7.8), 0.2 mM EDTA. The protein was eluted off the column at 20 mls/hr with a peristaltic pump, and a gradient starting with 50 mls of 300 mM NaCl, 10 mM Tris-HCl (pH 7.6), 1 mM EDTA, 0.1 mM PMSF and ending with 50 mls of 1 M NaCl, 10 mM Tris-HCl (pH 7.6), 1 mM EDTA, 0.1 mM PMSF. Material eluted from the column was detected both by gel electrophoresis and absorbance at 190 nm. Aliquots were combined and the protein was extensively dialyzed into water using Spectrapore 3 dialysis tubing. The sample was frozen and lyophilized down to several mls then further dialyzed. Samples were stored frozen in water.

#### *2.2.1.2 Native avian erythrocyte-specific linker histone H5 isolation*

Native H5 was isolated from chicken blood as described in Chapter 3, based on an original procedure described in Garcia-Ramirez, et al. (1990). Briefly, chicken nuclei were isolated by disrupting chicken erythrocyte cells in 10 mM Tris-HCl (pH 7.8), 0.4 mM EDTA, 120 mM KCl, 30 mM NaCl, 0.2% nonident P-40, 0.3 mM PMSF. Nuclei were hypotonically lysed in 0.2 mM EDTA, 0.1 mM PMSF and linker histones were salt extracted by bringing the resulting chromatin "jelly" to 0.65 M NaCl. CM Sephadex C25 cation exchange chromatography was used to separate purified linker histone H5 from linker histone H1 and other contaminants by washing extracted linker proteins from the CM Sephadex C25 column with 800 mM NaCl, 10 mM Tris-HCl (pH 7.8), 0.2 mM EDTA. H5 was subsequently eluted off the column in 1.6 M NaCl, 10 mM Tris-HCl (pH 7.8), 0.2 mM EDTA, 0.1 mM PMSF, dialyzed extensively into water, and stored frozen.

### 2.2.2 Extinction coefficients determination

The extinction coefficients were determined for GH5, GH1°, and H5, based on the absorbance of three tyrosine residues per protein. Following a procedure outlined by Gill and von Hippel (1989), the protein was denatured in 6 M guanidine HCl by diluting a small volume of "protein stock solution" in either 7.5 M guanidine HCl or 8 M guanidine HCl. The absorbance of this sample ( $A_{theor}$ ) was measured "simultaneously" from 190-320 nm with the final absorbance adjusted to a background absorbance of 6 M guanidine HCl. This was done to maximally expose the protein residues to solution, and as closely as possible mimic conditions used originally to estimate the molar extinction coefficient for tyrosines with glycyl-L-tyrosylglycine (Edelhoch, 1967). The absorbance was also recorded for the native protein (taken from the same "stock solution") suspended in water ( $A_{native}$ ). Based on Beer's law, the the extinction coefficient for the native protein in water ( $\epsilon_{native}$ ) is:

$$(2.1) \quad \epsilon_{native}(\lambda_2) = \epsilon_{theor}(\lambda_1) \times \frac{A_{native}(\lambda_2)}{A_{theor}(\lambda_1)},$$

where  $\lambda_1$  is the wavelength where the theoretical extinction coefficient ( $\epsilon_{theor}$ ) for the protein is known, and  $\lambda_2$  is the wavelength at which  $\epsilon_{native}$  is to be calculated.  $\epsilon_{theor}$  was determine from the following: (a) each protein (GH1°, GH5 and H5) contains three tyrosines, and (b) each tyrosine has estimated extinction coefficients of 1200 M<sup>-1</sup>cm<sup>-1</sup> at 280 nm, 1400 M<sup>-1</sup>cm<sup>-1</sup> at 278 nm, and 1450 M<sup>-1</sup>cm<sup>-1</sup> at 276 nm (Edelhoch, 1967).

Protein concentrations were subsequently estimated by averaging the calculated protein concentrations over a number of widely spaced wavelengths. The protein

concentration was only measured if the absorbance at 420 nm was less than 0.02 O.D., in order to minimize light scattering and artificially high O.D. values. If values exceeded 0.02 O.D. (420 nm) for the stock sample, the sample was centrifuged for 30 minutes at 13,000 rpm at 4 °C in a table-top centrifuge to remove light-scattering precipitate. If values exceeded 0.02 O.D. (420 nm) for sample treated with guanidine HCl, the data were discarded. Absorbances were measured using a Hewlett Packard 8452A Diode Array Spectrophotometer in a quartz glass cuvette with a pathlength of 1 cm.

### 2.2.3 Circular dichroism studies

Protein samples, stored frozen in water, were thawed, and centrifuged for 30 minutes in a table-top centrifuge to pellet precipitate. Using a Cary 15 spectrophotometer purged with nitrogen gas, protein samples were initially diluted in water to give an absorbance at 184 nm of <1 O.D. in a quartz glass cuvette with a 1 mm path length. The cuvette was immediately transferred to a JASCO 720 Spectropolarimeter, also purged with nitrogen gas, and scanned from 184 nm - 260 nm at 1nm intervals at 20 nm/min. In observing the effect of sodium phosphate (pH 7.2), samples were removed from the cuvette, and 100 mM sodium phosphate (pH 7.2) buffer stock was added dropwise with the solution vigorously pipeted up-and-down after each drop. Values were initially measured as ellipticity in millidegrees ( $\theta$ ), and were converted to  $\Delta\epsilon$  by the relationship:

$$(2.1) \quad \Delta\epsilon = \frac{\Delta\epsilon_{STD}}{\theta_{STD}} \cdot \frac{\theta}{lC}$$

Here,  $\Delta\epsilon_{STD}$  is the known  $\Delta\epsilon$  of (+)-10-camphorsulfonic acid at 290.5 nm,  $l$  is the pathlength of the of the cuvette (in cm),  $\theta_{STD}$  is the ellipticity of (+)-10-camphorsulfonic acid at 290.5 nm,  $\theta$  is the ellipticity of the sample, and  $C$  is the molar concentration of protein amide bonds. Thus, the units of  $\Delta\epsilon$  are  $\text{cm}^{-1} (\text{mol/L})^{-1}$ . Sodium phosphate buffer was prepared as a 200 mM sodium phosphate stock solution by titrating 200 mM sodium phosphate dibasic ( $\text{Na}_2\text{HPO}_4$ ) with a smaller volume of 200 mM sodium phosphate monobasic ( $\text{NaH}_2\text{PO}_4$ ) until a pH of 7.2 was reached.

#### 2.2.4 DNA preparation

A 22 b.p. oligonucleotide duplex was formed by annealing the sequence GTA GTA ACG GAA GCC AGG TAT T to its complement strand. Separately, a 42 b.p. oligonucleotide duplex with the sequence CCG GAA TTC GCA TCA TTG CCT TCG GTC CAT AAA GGA ATT CGG was annealed to its complementary strand following a procedure outlined in Chapter 3. The former sequence represents a putative linker histone H1 binding site based on a DNA footprinting result (Sevall, 1988). DNA concentrations were approximated by UV absorbance spectroscopy with  $\epsilon (260 \text{ nm}) = 20 \mu\text{g}^{-1} \text{ ml}^1 \text{ cm}^{-1}$ .

Plasmid pPol208-12 was isolated from DH5 $\alpha$  *E. coli* cells using the alkaline lysis procedure (Maniatis et al., 1982). DNA was further purified from a CsCl gradient, and cut with Hha I (New England Biolabs) following methods outlined by the manufacturer. pPol08-12 contains Twelve tandem copies of a 5S rDNA nucleosome positioning sequence (208 b.p.) from *Lytechinus variegatus*, that is cloned into the multiple cloning site of pUC19 (Georgel et al., 1993) based on the original construct from

Simpson et al. (1985). The final product consisted of the insert, over 2600 b.p. in length, as well as up to 16 smaller fragments, less than 400 b.p. in length, from Hha I cut pUC19 ( Table 4.1).

#### 2.2.5 Salt-induced turbidity analysis of GH5, GH1°, and H5

An aliquot of concentrated protein stock was diluted with water and the absorbance of the sample was measured at 420 nm. If the absorbance was above 0.02 ODs, the sample was centrifuged for 30 minutes at 13,000 rpm at 4 °C in a table-top microcentrifuge in order to remove aggregates. Starting protein sample concentrations were as follows: (a) GH5, 0.27 mg/ml; (b) GH1°, 0.27 mg/ml; (c) H5, 0.85 mg/ml; and (d) bovine serum albumin (Sigma), 2 mg/ml. Samples were then brought to 1 mM sodium phosphate (pH 7.2) by adding 100 mM sodium phosphate (pH 7.2), dropwise, followed by vigorously pipeting the solution up-and-down. UV absorbance at 420 nm, or turbidity, was then measured to detect aggregation. The sample was subsequently centrifuged at 13,000 rpm at room temperature for several minutes to pellet salt-induced aggregates. The supernatant was then carefully decanted and its absorbance was measured at 420 nm as before. After measuring the absorbance of the supernatant, the supernatant was used to resolublize the pelleted protein. The effect of NaCl on linker histone aggregation was analyzed by increasing the salt concentration in 50 mM NaCl increments by adding 5 M NaCl, dropwise to samples, then by incubating the samples on ice for 15 minutes. After each increase in NaCl concentration, the absorbance was measured as described above.

Aggregate dissociation was measured by resuspending aggregate collected from concentrated stock solution in a small volume of water to obtain a starting solution or suspension. The absorbance at 420 nm was recorded at different dilutions by resuspending the pellet in increasingly large volumes of ice cold water and allowing the sample to equilibrate for 15 minutes on ice.

#### 2.2.6 Chemical crosslinking of GH5 and H5 free in solution

First, NaCl was added dropwise from a 5 M NaCl stock as 50 mM steps to GH5 at 0.036 mM in 1 mM sodium phosphate (pH 7.2), 0.2 mM EDTA with vigorous pipeting (mixing) after the addition of each drop. Samples were then incubated on ice for 10 -15 minutes after each 50 mM NaCl increment with these step repeated until a final predetermined NaCl concentration was reached. The final solution also contained 0.2 mM EDTA (pH 7.8) and 1 mM sodium phosphate (pH 7.2). Dithiobis (succinimidyl propionate) was prepared by making a stock solution of 5 mg/ml in formamide following previously described work (Maman et al., 1994; Thomas et al., 1992; Draves et al., 1992). Lyophilized DSP was suspended in formamide to a 20 x stock then added to the reaction solution for a final concentration of 0.1 mg/ml. The crosslinking reaction was conducted at room temperature with continuous shaking. Crosslinking was stopped by adding 2 x SDS loading buffer (0.125 M Tris-HCl (pH 6.8), 4% SDS, 20% glycerol, and 0.04% bromophenol blue), and freezing the samples in liquid nitrogen. Samples were thawed immediately before analysis with SDS-PAGE. Crosslinking with H5 at 0.018 mM was performed as described for GH5.

### 2.2.7 Equilibrium analytical ultracentrifugation

Protein samples (originally stored frozen in water) were maintained in 1 mM sodium phosphate (pH 7.2), 0.2 mM EDTA, and incrementally increased in 50 mM NaCl steps by adding, dropwise, 5 M NaCl then storing the sample on ice for 15 minutes before proceeding to the next step. 160  $\mu$ l samples were loaded into a Beckman XLA, and run at 4 °C. Equilibrium was generally reached after 16 hours, and absorbance was read at 234 nm. Typical sample concentrations were about 0.5 mg/ml for H5, and 0.3 mg/ml for GH5.

### 2.2.8 Chemical crosslinking of GH5 assembled onto linear DNA

Unless otherwise stated in the text, DNA at 0.05 mg/ml was incubated with GH5 in 10 mM NaCl, 10 mM Tris-HCl (pH 7.8), 0.2 mM EDTA for 1 hour at room temperature. Samples were then treated to 0.1 mg/ml DSP for 30 minutes with the reaction stopped with 0.1 M glycine. The reaction solution was brought to 28% v/v with ice cold TCA, precipitated on ice for 30 minutes, and centrifuged at 13,000 rpm for 1 hour at 4 °C. After removing the supernatant, ice cold 10 mM HCl-acetone was used to wash the pellet. The mixture was centrifuged for 30 minutes at 13,000 rpm using a table top centrifuge at 4 °C. All samples were resuspended in a common final volume of 10 mM Tris-HCl (pH 7.8), 0.2 mM EDTA. For experiments investigating the concentration-dependent effects of GH5 on crosslinked polymer distribution, reaction volumes were

made inversely proportional to the GH5/DNA ratio, and ranged from less than 100  $\mu$ l for 140% GH5:DNA (w/w) to over 1 ml for samples at 10% GH5:DNA (w/w).

### 2.2.9 Quantitative proteolysis of GH5

GH5 at 0.04 mg/ml was incubated with the 22 b.p. oligonucleotide at 100% w/w for 35 minutes at 4 °C in buffered solution containing: 10 mM sodium phosphate (pH 7.2), 8 mM NaCl, 0.2 mM EDTA. The sample was then crosslinked in 0.01 mg/ml DSP (or 0.001 mg/ml for GH5 bound to the 42 b.p. fragment) from a 20 x stock solution for 2 hours at room temperature with constant shaking. The reaction was "stopped" with 50 mM glycine by shaking for five minutes. Chymotrypsin frozen in 10 mM Tris-HCl (pH 7.8) was added to 0.3  $\mu$ g/ml from a 20 x stock solution and incubated at room temperature for different time points. Proteolysis was stopped with 1 mM PMSF, followed by the addition of 2 x SDS loading buffer and freezing the resulting solution in liquid nitrogen. Products were analyzed by SDS-PAGE (18% polyacrylamide, 30:8 acrylamide:bisacrylamide). Similarly, GH5 at 0.04 mg/ml, free in solution, was crosslinked and proteolyzed with chymotrypsin, but with the following exceptions: DSP at 0.001 mg/ml was added to GH5 without preincubation.

### 2.2.10 Analysis with SDS-PAGE

SDS/polyacrylamide gels were constructed based on (Laemmli, 1970; Chapter 4). Gels were silver stained by a diamine silver staining protocol (Sasse and Gallagher, 1991;

Chapter 4) that included: fixing the gels in 45% methanol / 9 % acetic acid for several hours, washing the gel for about a day with repeated changes of water, then staining and developing the gel. Gels were silver stained as described in Chapter 4). For coomassie staining: the gel was stained for 30 minutes in 45% methanol (v/v), 9% acetic acid, and 0.25% (w/v) coomassie G-250 then destained in 7.5% acetic acid and 5% methanol with a kimwipe to absorb coomassie from gel. Gels were quantitated by analyzing the scans of photographs with NIH Image (version 1.57) (O'Neill et al., 1989).

## **2.3 Results**

### **2.3.1 Protein purification and characterization**

The globular domains of avian erythrocyte-specific linker histone H5, human subtype H1<sup>o</sup> (reviewed in Zlatanova and Doenecke, 1994), and human subtype H1.3 were expressed and purified as described in Methods and Materials. While the GH5 and GH1<sup>o</sup> expression vectors, GH5plk and pET-15b-GH1<sup>o</sup>t, respectively, were found to express a protein at around 8500 daltons, pET-15b-GH1.3 expressed a protein closer to 25,000 daltons (data not shown). In the latter case, the ribosome appeared to have read through the three stop codons placed at the end of the O.R.F., reaching the end of the transcript at the point of the T7 RNA polymerase termination sequence (Moffat and Studier, 1986). Because of this, recombinant GH1.3 was not used in further experiments. GH1<sup>o</sup> and GH5 both were purified using an ammonium sulfate precipitation step and ion exchange chromatography (Methods and Materials). In the ion exchange chromatography

step, GH1° and GH5 eluted at nearly identical salt concentrations from the CM Sephadex C25 column (Figure 2.1A). This was expected since the net number of positive residues<sup>1</sup> for GH1° is 10 and GH5 is 11, and the molecular weights are approximately 7795 daltons and 8125 daltons respectively. H5 is reported to elute from the same column at around 0.95 M NaCl, owed primarily to its greater net number of positive residues of 41 and molecular weight of 20880 daltons. No contaminating protein products were detected in either the GH1° or GH5 purified protein preparations (Figure 2.1B).

Recombinant GH1°, GH5 and native H5 were further characterized by determining each protein's extinction coefficient based on the respective amino acid sequences (see Appendix A1) following the procedure by Gill and von Hippel (1989); see also Methods and Materials. GH5, GH1°, and H5 had nearly identical molar extinction coefficients at around 275 nm which was expected since each protein has three tyrosines, though the  $\epsilon$  for H5 increased significantly by 220 nm (compared to GH5 and GH1°) due to an increased amide bond absorbance (Table 2.1). Overall, the extinction coefficients reported here corresponded well, more or less, with other authors (Table 2.2), and in effect, unify previously-reported values that were made at different wavelengths. Of particular significance are the results of Thomas et al. (1992), whose reported extinction coefficient for GH5 of 4.5 mg/ml (at 230 nm) was determined from amino acid analysis. Considering our estimated value of 4.2 mg/ml, the use of UV absorbance spectroscopy appears to provide accurate protein concentration (providing that the turbidity is low). Besides the values reported in Table 2.2, additional extinction coefficients can be calculated for wavelengths between 250-300 nm using Figure 2.2 and equation (2.2).

---

<sup>1</sup> Net number of positive residues = number of basic residues (at pH 7.8) - number of acidic residues (at pH 7.8).

Figure 2.1. Purification of recombinant GH1° and GH5. BL21 *E. coli* cells transformed with expression plasmids containing the genes for GH1° and GH5 were induced as 1 liter cultures with IPTG. Cells were sonicated in buffer containing 500 mM NaCl. Following precipitation of protein contaminants in 0.38 mg/ml ammonium sulfate, the crude preparation was loaded onto CM Sephadex C25 column. Using a peristaltic pump, a salt gradient from 300 mM NaCl to 1 M NaCl (including 10 mM Tris-HCl (pH 7.8), 1 mM EDTA, 0.1 mM PMSF) was used to separate GH1° and GH5 from protein contaminants. (a) The elution of GH5 (*solid squares*) and GH1° (*open squares*) measured by the absorbance at 230 nm as a function of NaCl concentration. (b) about 1 µg of each protein was run on an 18% Laemmli gel that was stained with coomassie. The proteins appeared to migrate close to the position previous reported for native GH5.

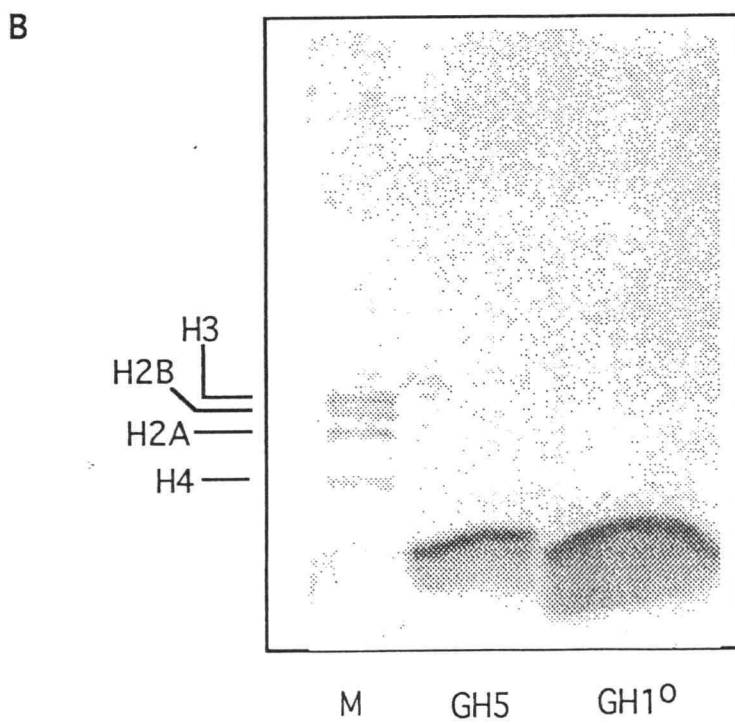
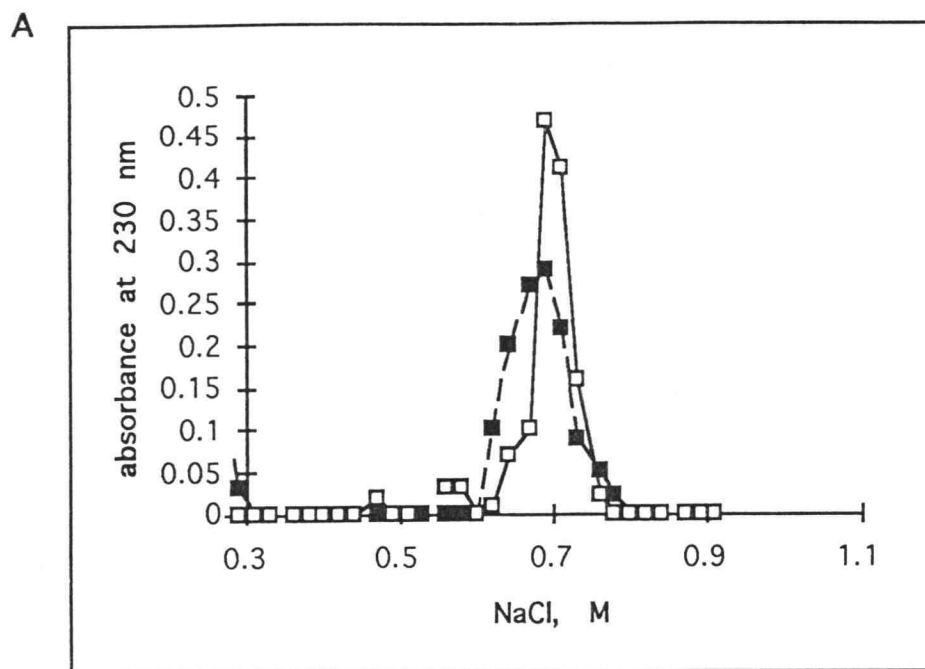


Figure 2.1

Table 2.1. List of calculated extinction for H5 and related proteins.

| $\lambda$ (nm) | H5 <sup>†</sup>                                  |  | GH5 <sup>‡</sup>                                 |  | GH1 <sup>§</sup>                                 |  |
|----------------|--|--|--|--|--|--|
|                | $\epsilon$<br>(M <sup>1</sup> cm <sup>-1</sup> ) | $\epsilon$<br>(ml <sup>1</sup> mg <sup>-1</sup> cm <sup>-1</sup> ) | $\epsilon$<br>(M <sup>1</sup> cm <sup>-1</sup> ) | $\epsilon$<br>(ml <sup>1</sup> mg <sup>-1</sup> cm <sup>-1</sup> ) | $\epsilon$<br>(M <sup>1</sup> cm <sup>-1</sup> ) | $\epsilon$<br>(ml <sup>1</sup> mg <sup>-1</sup> cm <sup>-1</sup> ) |
| 280            | 3,920  | 0.189<br>(0.00891)   | 4,140  | 0.520<br>(0.0258)  | 4,010  | 0.514<br>(0.0283)  |
| 278            | 4,070  | 0.196<br>(0.00969)   | 4,230  | .531<br>(0.0268)   | 4,210  | 0.540<br>(0.0296)  |
| 276            | 4,130  | 0.199<br>(0.0109)  | 4,130  | .518<br>(0.0263)   | 4,220  | 0.541<br>(0.0298)  |
| 236            | 18,400   | 0.888<br>(0.0553)  | 14,100   | 1.78<br>(0.11)   | 13,800   | 1.77<br>(0.0971)   |
| 234            | 26,100   | 1.27<br>(0.0506)   | 21,400   | 2.69<br>(0.259)  | 18,600   | 2.39<br>(0.131)  |
| 230            | 48,100   | 2.31<br>(0.134)  | 34,000   | 4.27<br>(0.409)  | 30,600   | 3.93<br>(0.216)  |
| 226            | 82,000   | 3.95<br>(0.176)  | 47,100   | 5.92<br>(0.567)  | 41,900   | 5.38<br>(0.296)  |
| 220            | 136,000  | 6.26<br>(0.666)  | 66,100   | 8.58<br>(0.820)  | 58,200   | 7.46<br>(0.410)  |
| 214            |  |  | 95,100   | 11.9<br>(1.15)   | 81,800   | 10.5<br>(0.575)  |

The extinction coefficients were determined using the molar extinction coefficient of Tyr at 280 nm, 278 nm, and 276 nm as described in Methods and Materials. The reported values are an average of these three calculation.

Standard deviations in brackets.

<sup>†</sup> Values based on seven samples, and a molecular weight of 20880.

<sup>‡</sup> Values based on six samples, and a molecular weight of 8125.

<sup>§</sup> Values based on nine samples, and a molecular weight of 7795.

Table 2.2. Previously reported extinction coefficients for GH5 and H5.

| Protein | $\lambda$ (nm) | Extinction Coefficient                    | Author                       |
|---------|----------------|---|------------------------------|
| H5      | 275            | 4,020 M <sup>-1</sup> cm <sup>-1</sup>    | Garcia-Ramirez et al. (1990) |
| H5      | 280            | 2.00 ml mg <sup>-1</sup> cm <sup>-1</sup> | Johns, E. W. (1971)          |
| H5      | 230            | 1.85 ml mg <sup>-1</sup> cm <sup>-1</sup> | Camerini-Otero et al. (1976) |
| GH5     | 230            | 4.5 ml mg <sup>-1</sup> cm <sup>-1</sup>  | Thomas et al. (1992)         |
| GH5     | 275.5          | 4,500 M <sup>-1</sup> cm <sup>-1</sup>    | Maman et al. (1994)          |

The secondary structure of each linker histone proteins was analyzed using circular dichroism (CD). The proteins differed in their relative proportion of secondary elements, and in their response to sodium phosphate (pH 7.2). While GH1<sup>o</sup> (Figure 2.3A) and GH5 (Figure 2.3B) were relatively unaffected by the presence of sodium phosphate (pH 7.2), H5 underwent considerable restructuring which presumably involved folding of the tail domains (Figure 2.3C). The presence of 1 mM sodium phosphate (pH 7.2) appeared sufficient for H5 folding as the CD profile changed relatively little more at 10 mM sodium phosphate (pH 7.2). The results support previous reports of linker histone tail folding in the presence of PO<sub>4</sub><sup>-3</sup> (Hill et al., 1989; Clark et al., 1988). It has been reported that terminal tail folding also occurs when H5 binds to DNA (Hill et al., 1989; Clark et al., 1988; Bohm and Creemers, 1993). Based on the general form of the CD spectra, the folding behavior in PO<sub>4</sub><sup>-3</sup>, and the estimated amount of  $\alpha$ -helices based on Clark and Thomas (1988) (data not shown), the purified proteins appear to have been properly folded.

Figure 2.2. Absorbance spectra for purified proteins, and the effect of 6 M guanidine HCl on the UV absorbance profile. (a) GH5, (b) GH1°, and (c) H5. Legend symbols: stock protein (*solid circles*) diluted in water; stock protein in 6 M urea (*open circles*)

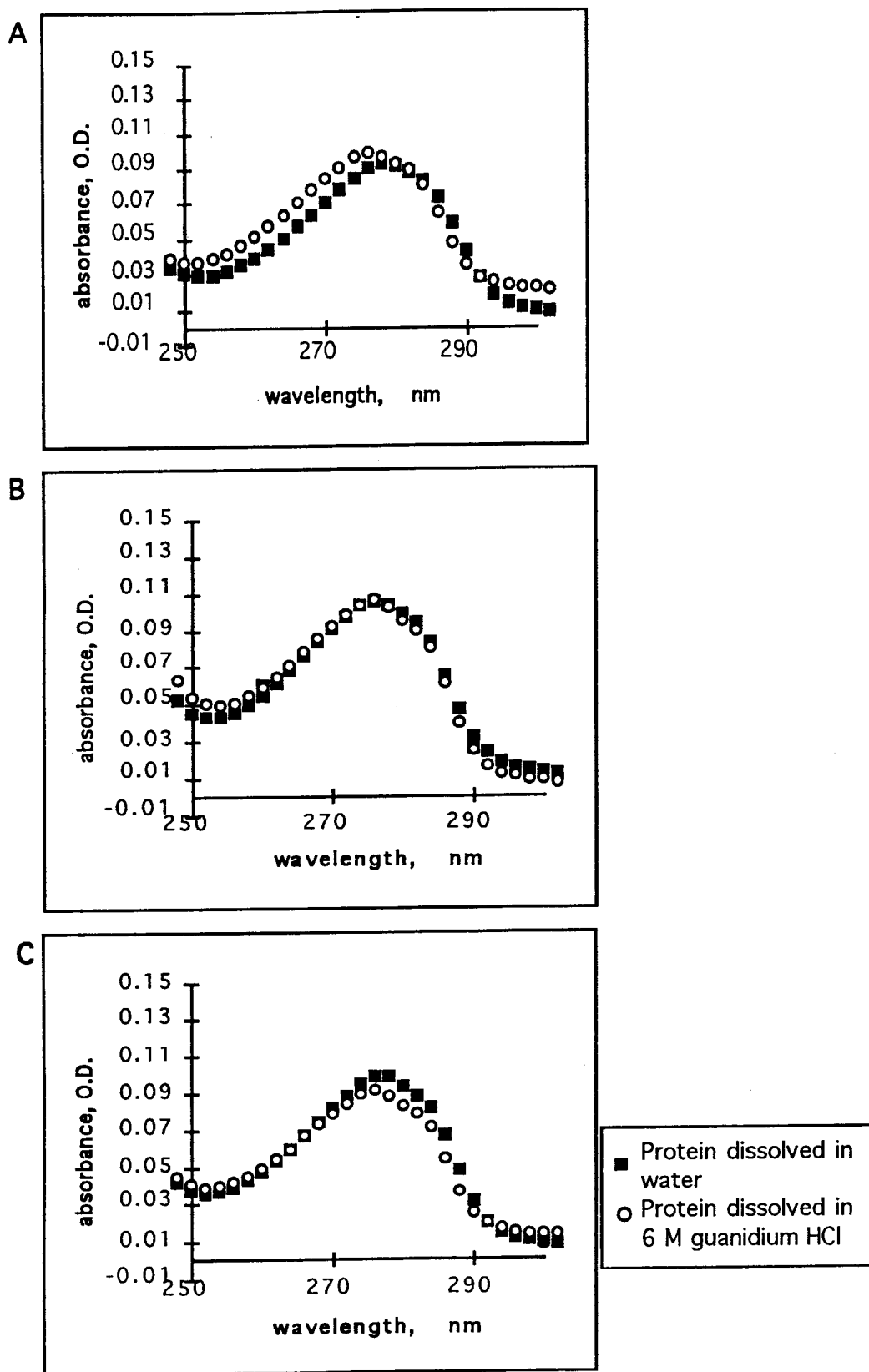


Figure 2.2

Figure 2.3. Circular dichroism of linker histone proteins, and the effect of  $\text{PO}_4^{3-}$ . The CD spectra of (a) recombinant GH1°, (b) native H5 and (c) recombinant GH5 were measured using a Jasco 720 Spectropolarimeter. Samples were measured in water (---), in 1 mM sodium phosphate (pH 7.2) (----), and in 10 mM sodium phosphate (—).  $\Delta\epsilon$  ( $\text{cm}^{-1}$   $(\text{mg/ml})^{-1}$ ) expressed as a function of wavelength (nm).

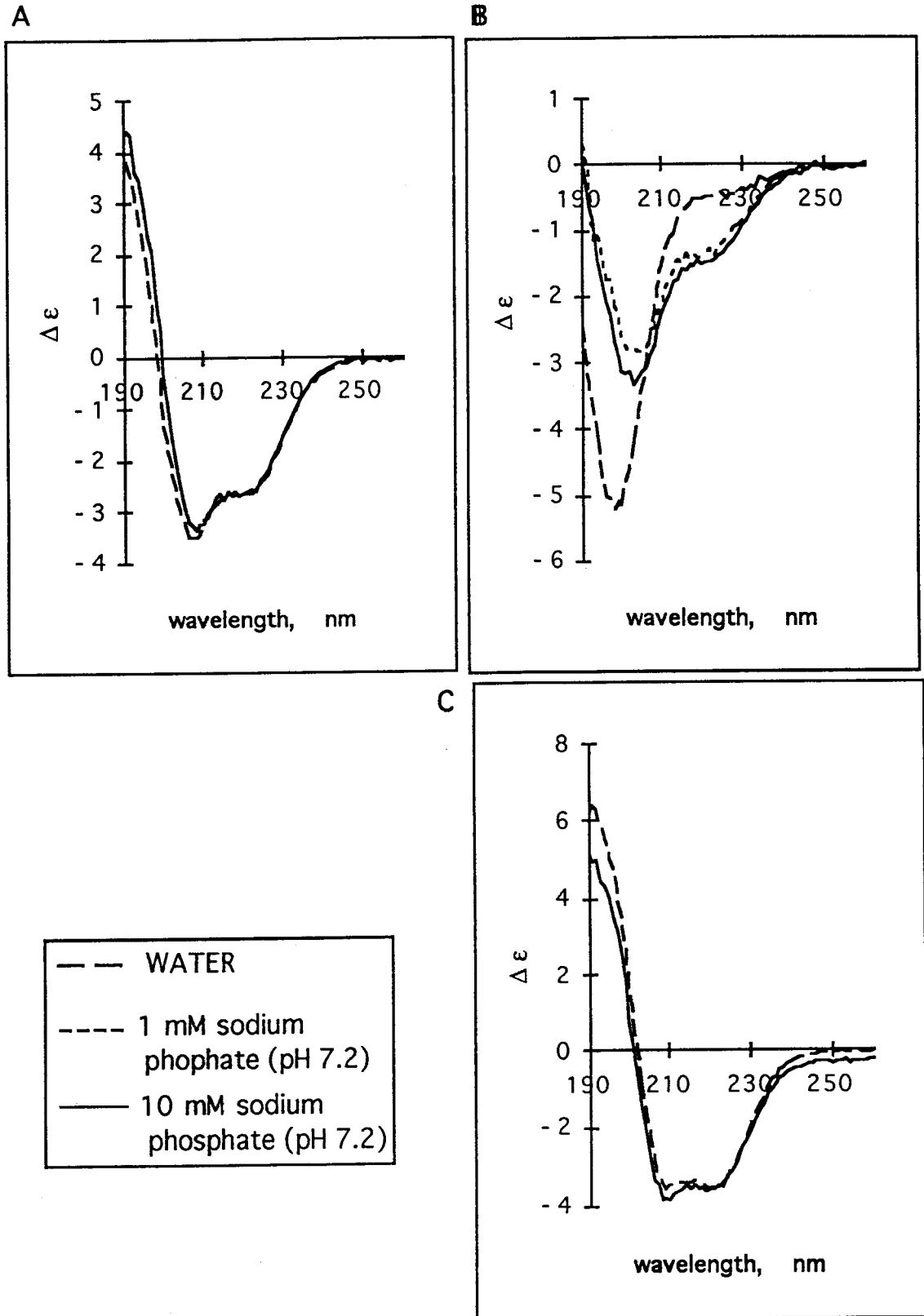


Figure 2.3

## 2.3.2 Self-Association of H5, GH1° and GH5 free in solution

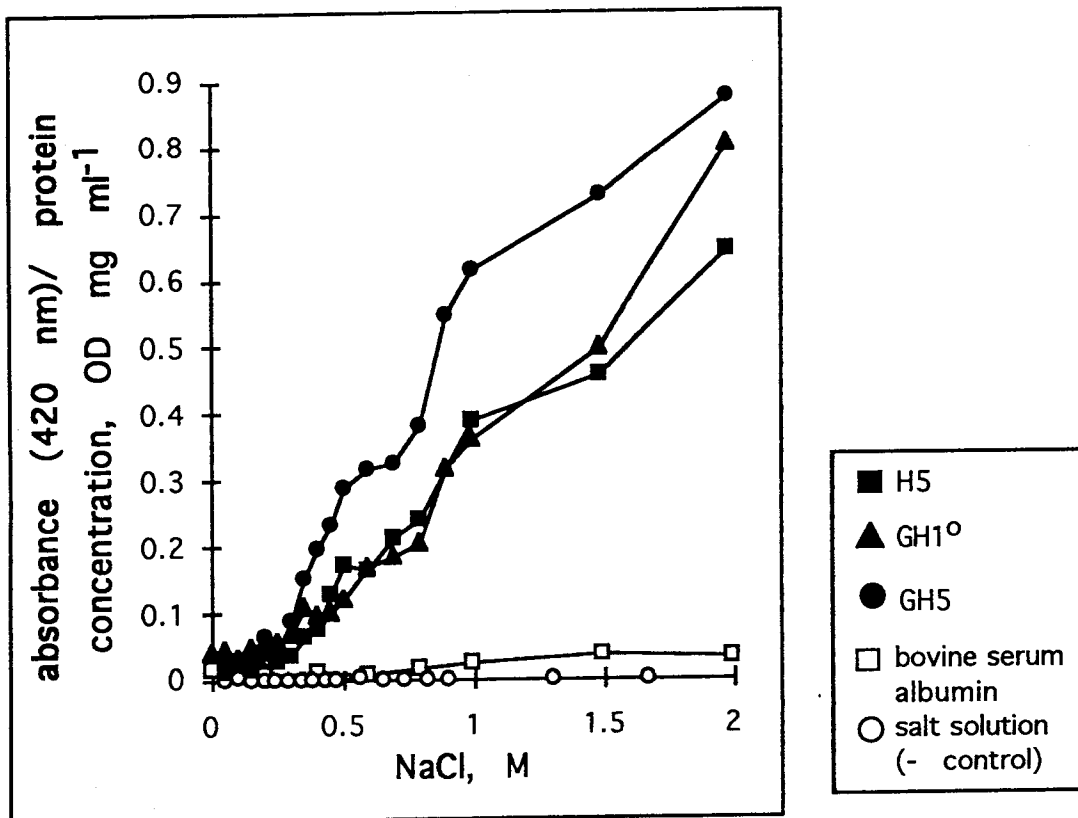
### *2.3.2.1 Salt-induced turbidity of H5, GH1° and GH5 free in solution*

Salt-induced turbidity has previously been used to determine whether DNA-H1 linker histone complexes interact in solution (Matthews and Bradbury, 1978; Glotov et al., 1978c). In those studies it was reported that DNA-protein aggregation is a salt-dependent process with maximum turbidity occurring at around 0.25 M NaCl. As a comparison, we examined the effect of NaCl on the turbidity of linker histones free in solution with the premise that similarities in the response to increased salt concentration may be a potential measure of the importance of protein-protein contacts in linker histone-DNA aggregation.

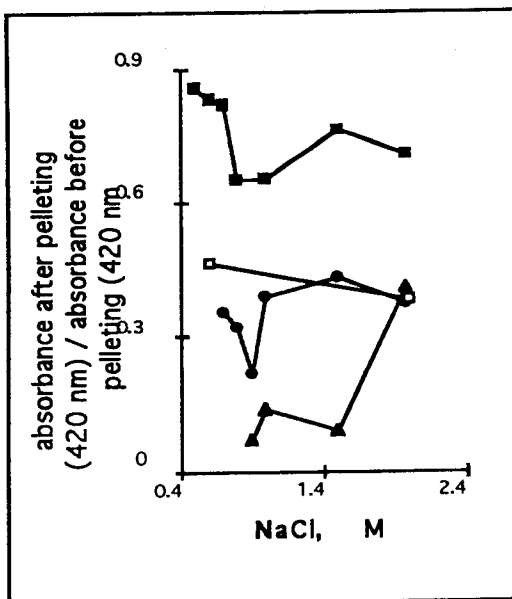
Results indicate that above about 0.25 M NaCl GH1°, GH5, and H5 all experienced a salt-dependent increase in turbidity, with all H5-related proteins displaying nearly equivalent responses (Figure 2.4A), and all linker proteins producing considerably more salt-induced turbidity than bovine serum albumin in this salt range. At lower salt concentrations, the low turbidity was not significantly greater than that of BSA. Interestingly, each linker protein exhibited similar inflection points at about 0.45 M and 0.85 M NaCl at which point the turbidity increased abruptly. The pelleting behavior of the proteins was also investigated by comparing the absorbance at 420 nm before and after pelleting (Figure 2.4B). The H5 aggregate was far more resistant to pelleting than was either the GH5 or GH1° aggregate--which both pelleted similar to bovine serum albumin. Finally, aggregate reversibility was measured by resuspending the pelleted aggregate in

Figure 2.4. Salt-dependent turbidity analysis of linker histone proteins. Proteins were treated to increasing ionic strength by adding NaCl in 50 mM increments while in 1 mM sodium phosphate (pH 7.2), 0.2 mM EDTA. (A) Turbidity was measured by the absorbance at 420 nm ( $A(420\text{ nm})$ ), and all values are adjusted to reflect dilution by the addition of NaCl stock, and normalized by the protein concentration. (B) The ability for the aggregate to sediment was also investigated. After adding salt, the sample was stored for a few minutes on ice, and the  $A(420\text{ nm})$  was measured. This is referred to as the "absorbance before pelleting (420 nm)". Then the sample was pelleted at 13,000 rpm for 15 minutes at room temperature in a table top centrifuge for several minutes. This is referred to as the "absorbance after pelleting (420 nm)". (C) Aggregate isolated from concentrated protein stocks was assessed for reversibility by diluting the aggregate in increasing volumes of ice cold water. Samples included: H5 (*solid squares*), GH5 (*solid circles*), GH1° (*solid triangles*), serum albumin (*open squares*) or buffered solution (negative control) (*open circles*).

A



B



C

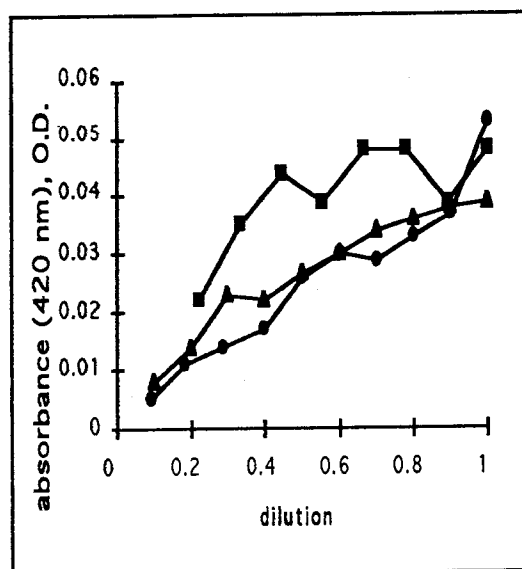


Figure 2.4

increasing volumes of water. Since the plot of the normalized absorbance as a function of dilution was not concave but roughly linear, as would be expected from simple dilution, the aggregation process appears to have been irreversible for all three proteins (Figure 2.4C).

In summary, the salt dependent increase in turbidity indicates that the linker histone proteins themselves, without the presence of DNA, were capable of interacting to form large aggregates at high salt concentrations. The common inflection points, and roughly equivalent response to NaCl for H5, GH5 and GH1<sup>o</sup>, as well as the common step-wise increases in turbidity suggests that the proteins were interacting (and aggregating) similarly. What this actually represents from a protein interaction model is unclear. The aggregation process did not appear to be enhanced by the presence of the linker histone tails; rather self-interaction of the globular domain appears to have been responsible for the salt concentration-dependent effect as judged by the common response by all three proteins. The tail domains did however increase the ability for the H5 aggregate to resist sedimentation (as compared to the globular domains), though it is uncertain whether the tail domains increased nucleoprotein complex solubility or remodeled the aggregate complex structure. The former is implied by the ubiquitous "inflection points".

Based on the irreversibility of the aggregation process by dilution, it follows that the contacts involved in aggregation are not the same as the weak protein-protein interactions reported in Maman et al. (1994). Certainly, the aggregates would have undergone dissociation with dilution, if the two were the same. The difference between

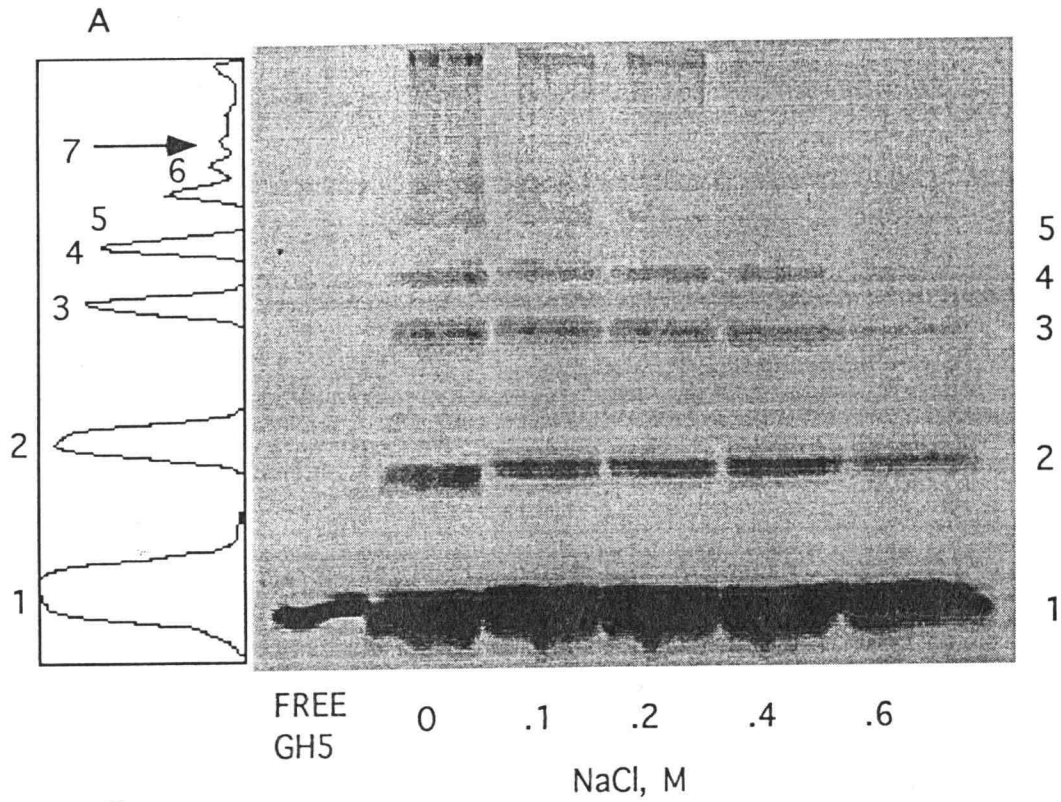
the bell-shaped turbidity curve for H1-DNA (in which turbidity reaches a maximum at 0.3 M NaCl) (Matthews and Bradbury, 1978; Glotov et al., 1978c) and the turbidity profile for linker histones free in solution (Figure 2.4B) suggests that the aggregation process is quite different in the two cases; other mechanisms must be involved in DNA-linker histone aggregation. It should also be emphasized that the turbidity measurements give no indication of fraction of the protein involved in these aggregates; it could be very small, and produce measurable turbidity.

#### *2.3.2.2 Crosslinking of GH5 and H5 free in solution*

Chemical crosslinking has previously been used to determine whether linker histone proteins make contact free in solution (Table 1.2). Extensive crosslinking in solution is taken to be indicative of specific interactions, since random collisions are expected to produce a minimal amount of crosslinking (Maman et al., 1994). DSP was used as the crosslinking molecule; and has a 1.2 nm crosslinking length, and reacts primarily with  $\epsilon$ -amines of lysine residues. In recent years three separate authors have used DSP in attempts to determine whether GH5 self-associates in solution (Draves et al., 1992; Thomas et al., 1992; Maman et al., 1994). However, the data in the literature are contradictory; only Maman et al. (1994) successfully crosslinked GH5, reporting a  $K_a$  of  $4.8 \times 10^3 \text{ M}^{-1}$ .

GH5 at 0.036 mM (0.29 mg/ml) was incrementally increased in 50 mM NaCl steps to salt concentrations between 0 and 600 mM NaCl, then crosslinked with 0.1 mg/ml DSP. Polymers of various sizes were observed by SDS-PAGE after 30 minutes of

**Figure 2.5.** Crosslinking GH5 free in solution with DSP. (A) GH5 at 0.036 mM was crosslinked for 30 minutes at room temperature in 0.1 mg/ml DSP at various NaCl concentration buffered by 10 mM sodium phosphate (pH 7.2). Samples were separated on an 18% Laemli gel (30: .8) acrylamide: bisacrylamide), and silver stained. A representative scan of the crosslinked complexes is presented to the side of the gel. *Arrow* denotes location of GH5 septamer. (B) The effect of salt on crosslinking efficiency was measured by the fraction of GH5 monomer left uncomplexed at various salt concentrations as scanned from a representative gel at 30 minutes under conditions described in (A). (C) GH5 at 0.04 mg/ml was crosslinked free in solution in 10 mM NaCl, 10 mM sodium phosphate (pH 7.2), 0.2 mM EDTA. (D) A graph of the log of the relative molar amount of each polymer is plotted as a function of polymer size. Conditions are as described above with (A). Crosslinking was performed in 10 mM NaCl, 0.2 mM EDTA, 10 mM sodium phosphate (pH 7.2). For all parts, the DSP crosslinking reaction was "stopped" by freezing the reaction in 2 x SDS loading buffer. The relative molar amount for each polymer at the indicated time was calculated by dividing the mass of a respective polymer by the mass of the monomer product (at the indicated time) as determined from a silver-stained gel. This value was then equated to a molar value by dividing the relative mass by the number proteins found in the polymer complex (for a dimer this value is two, and for a trimer this value is three).



**B**

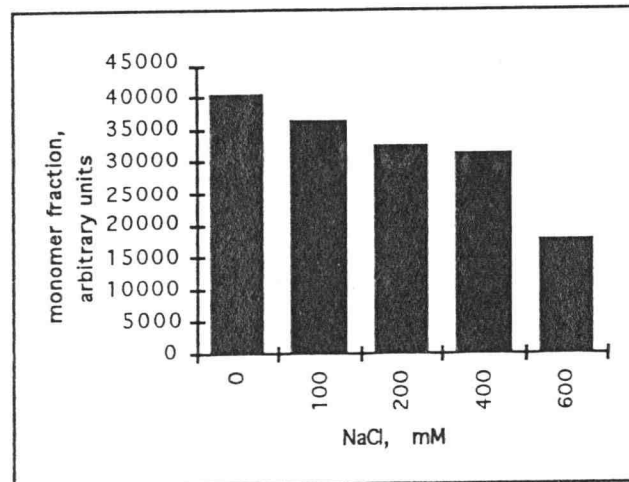
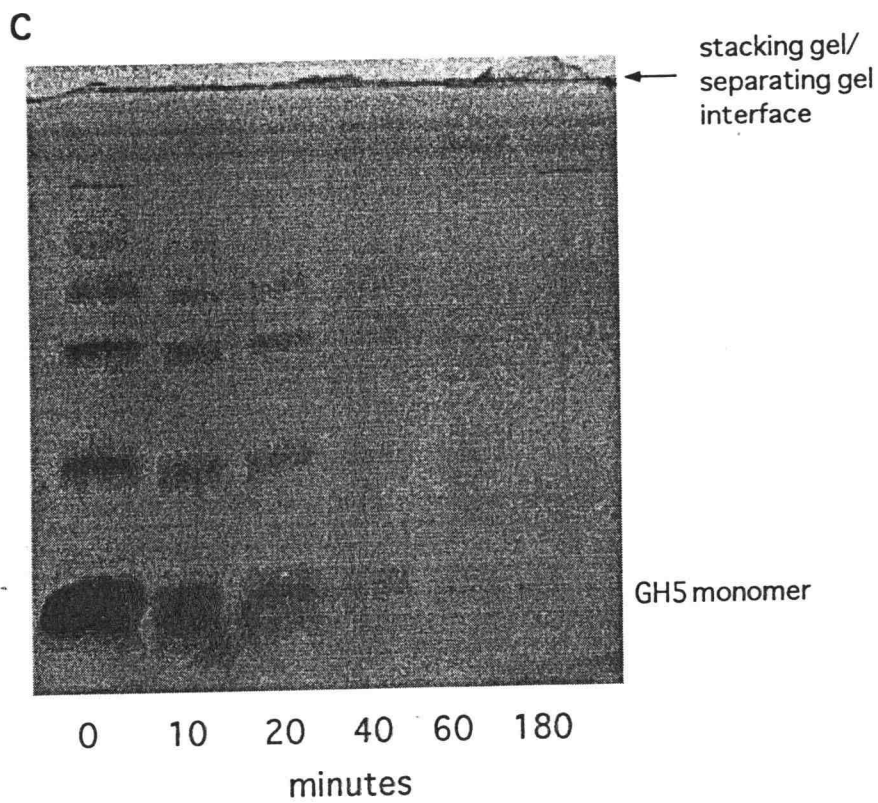
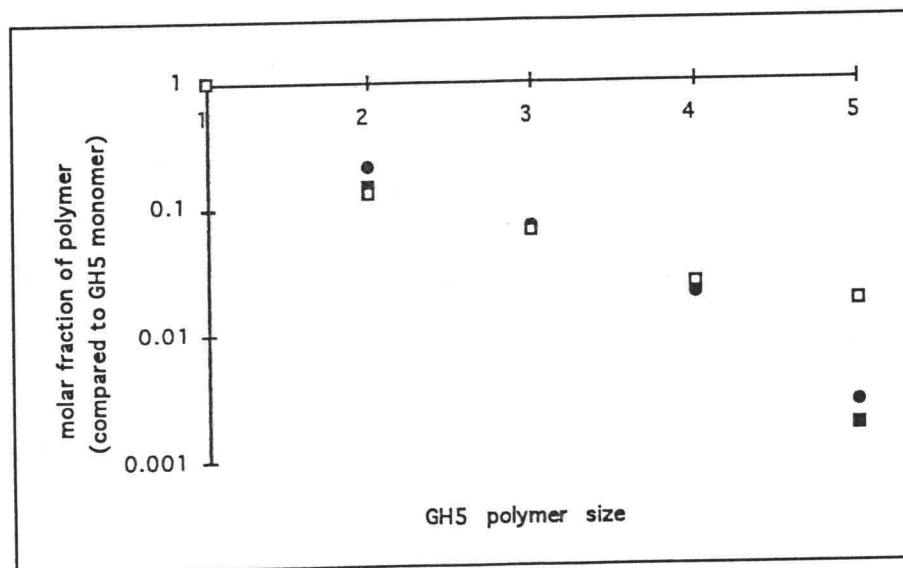


Figure 2.5



**D**



- GH5 DSP crosslinked free in solution, 10 minutes
- GH5 DSP crosslinked free in solution, 20 minutes
- GH5 DSP crosslinked free in solution, 40 minutes

Figure 2.5 (continued)

crosslinking. (Figure 2.5A). Crosslinking was a dynamic process with nearly all GH5 becoming crosslinked into large aggregate complexes within a couple of hours (Figure 2.5C). Also noteworthy was an observed increase in the electrophoretic mobility of monomeric GH5 due to neutralization of lysine residues by DSP; this increase in electrophoretic mobility was greatest for GH5 crosslinked in the absence of NaCl as was noted originally by Maman et al. (1994).

The crosslinking rate as measured by monomer disappearance increased as a function of the NaCl concentration, with samples in 600 mM NaCl crosslinking about twice as fast as those in 0 mM NaCl (Figure 2.5B). Crosslinking at a higher salt concentration resulted in a reduction in both the amount of monomeric GH5 as well as other small-sized polymer products presumably as a consequence of the formation of very large aggregates. A plot of the logarithm of the relative molar proportion for each polymer (relative to amount of GH5 monomer product) as a function of polymer size revealed a linear relationship (Figure 2.5C). According to Flory (1953) such a relationship is a consequence of "divalency" in which monomers form linear filaments via a single, repeating interaction interface. This is in contrast to more complicated contacts that lead to "branching". For linear polymerization,

$$(2.3) \quad \frac{N_x}{N_1} = p^{(x-1)},$$

$$(2.4) \quad \ln\left(\frac{N_x}{N_1}\right) = (x-1)\ln p,$$

where  $N_x$  is the molar amount of polymer of size  $x$ ,  $N_1$  is the molar amount of monomer, and  $p$  is the probability that any randomly chosen reactive surface has reacted. By applying the relationship,

$$(2.5) \quad N_x = N_1 \frac{m_x}{xm_1}$$

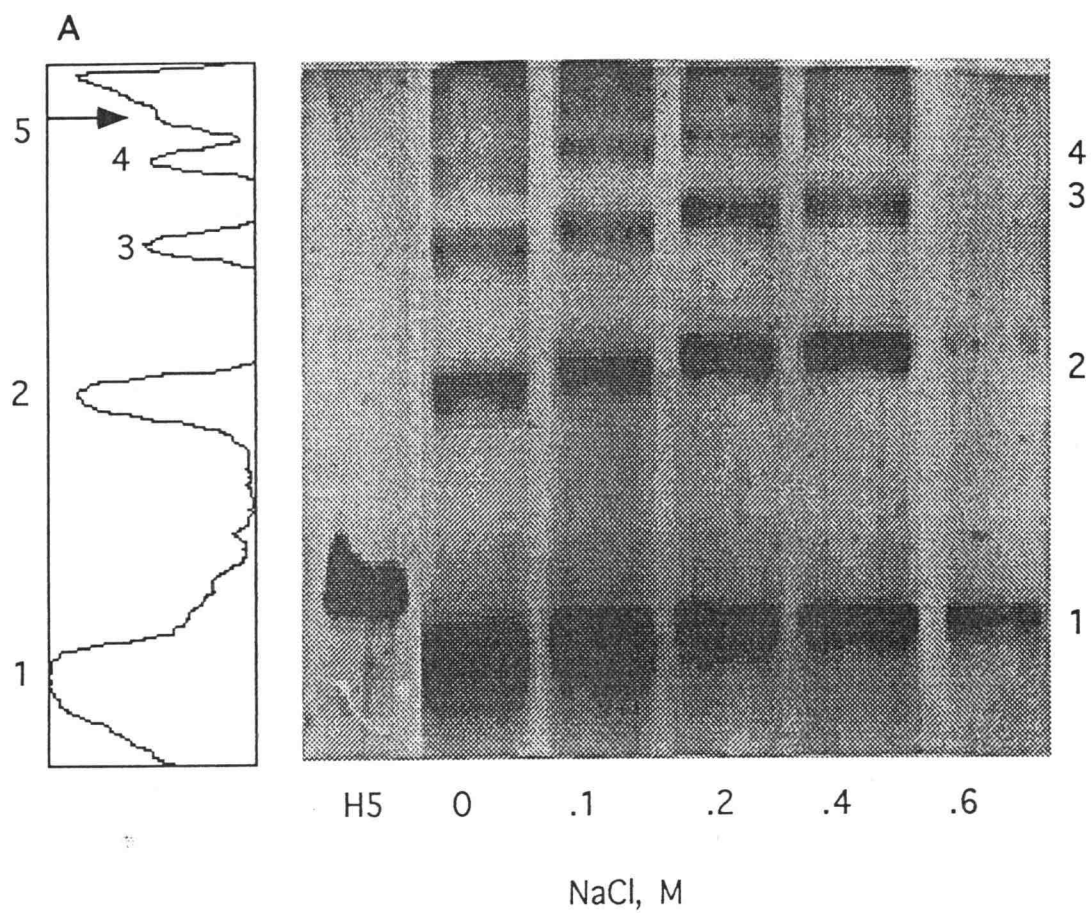
the relative molar concentration of polymers (as observed from silver-stained SDS-polyacrylamide gels) can be used as an estimate of polymer mass. Here,  $m_x$  is the mass of a polymer of size  $x$ , and  $m_1$  is the mass of the monomer component. Solving for  $p$ , GH5 crosslinked in 8 mM NaCl, 10 mM sodium phosphate (pH 7.2) showed some variation with time of crosslinking; values ranged from an estimate of 0.25 to 0.34 (Figure 2.5B). The lower value was typical of early time points, while the higher value was general detected after about 30 minutes of crosslinking. At longer times, some deviation from what appears to be linearity (Figure 2.5B) is seen. This is expected when crosslinking produces branched aggregates.

In an effort to elucidate the role of the basic tail domains in promoting linker histone self association, H5 free in solution was crosslinked with DSP; for a comparison with GH5 results. H5 was previously reported to crosslink in 1% formaldehyde into polymers up to trimers (Russo et al., 1983), but was observed not to crosslink under "less invasive" conditions used for GH5 crosslinking with DSP (Clark and Thomas, 1988). In this study, H5 at 0.38 mg/ml was crosslinked in 0.1 mg/ml DSP as described for GH5. Like GH5, H5 was crosslinked into polymers extending from monomers to complexes too

large to enter the 12% polyacrylamide gel (Figure 2.6A). Upon crosslinking, monomeric H5 experienced a larger increase in electrophoretic mobility than GH5; this was likely due to the neutralization of the many more lysine amines carried by H5 than GH5. With the addition of 1 mM sodium phosphate (pH 7.2), the electrophoretic mobility increased even more, suggesting that lysines in the tail made close enough contact to crosslink, reducing the effective size of the protein. Alternatively, this effect may be related to C-terminal tail structuring as described in the CD experiments. Crosslinking efficiency was dependent on ionic strength with the largest increase in crosslinking rate occurring with addition of 1mM sodium phosphate (Figure 2.6B). Like GH5, all H5 molecules eventually became crosslinked with DSP, producing protein complexes too large to enter the 5% polyacrylamide stacking gel with no detectable monomer-sized particles remaining. Initially, 50 mM glycine was used to stop the crosslinking reaction, but appeared to only slow the crosslinking reaction as storage on ice overnight lead to the production of massive aggregates (data not shown). Because of this, samples were commonly frozen with liquid nitrogen in 2x SDS loading buffer, which appeared quite effectively stop the reaction.

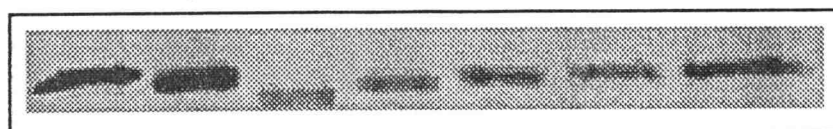
The electrophoretic mobility and the relative molar proportion of polymers (normalized to the moles of monomer) was used to further characterize the H5 crosslinked complexes. Plotting the log of the molecular weight of the crosslinked polymers as a function of electrophoretic mobility, revealed that GH5 and H5 both complex as a ladder of peptides with each step reflecting the addition of a single protein molecule (Figure 2.6C). The slope of this line is greater for GH5 than for H5, probably reflecting different polyacrylamide concentration used in the experiment, 18% and 12%,

Figure 2.6. Crosslinking H5 free in solution with DSP. (A) H5 at 0.018 mM was crosslinked for 30 minutes at room temperature in 0.1 mg/ml DSP at various NaCl concentrations buffered by 1 mM sodium phosphate (pH 7.2). Samples were separated on an 12% Laemmli gel (30: .8 acrylamide: bisacrylamide), and silver stained. A representative scan of the crosslinked complexes is presented to the side of the gel. *Arrow* denotes the location of the GH5 pentamer. (B) The effect of salt on crosslinking efficiency was measured by the amount of uncomplexed monomer. A note to prevent possible confusion: the samples labeled water and 0 were different in that the water sample had no buffer while the 0 sample was buffered by 1 mM sodium phosphate. (C) The relative electrophoretic mobility (as referenced to the mobility of the monomer fragment) is plotted versus the effective molecular weight of the crosslinked complex. (D) A plot of the log of the relative molar amount of each polymer is plotted as a function of polymer size for samples in (A) as described in Figure 2.5C.



**B**

|                  |   |   |   |   |   |   |   |
|------------------|---|---|---|---|---|---|---|
| sodium phosphate | - | - | + | + | + | + | + |
| DSP              | - | + | + | + | + | + | + |

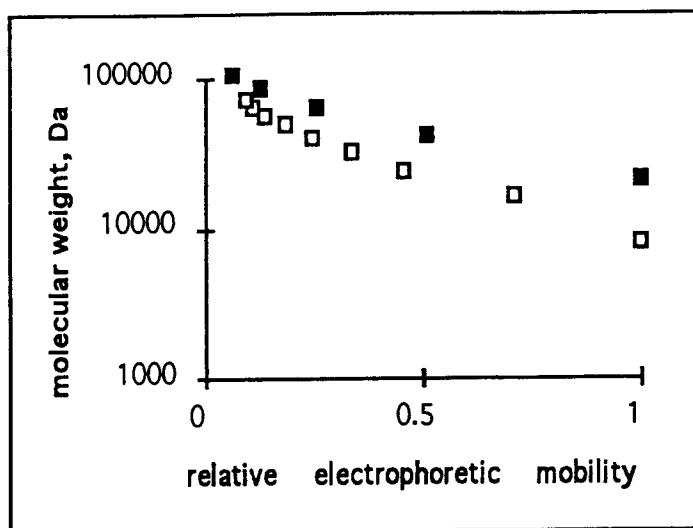


H5 water 0 .1 .2 .4 .6

NaCl, M

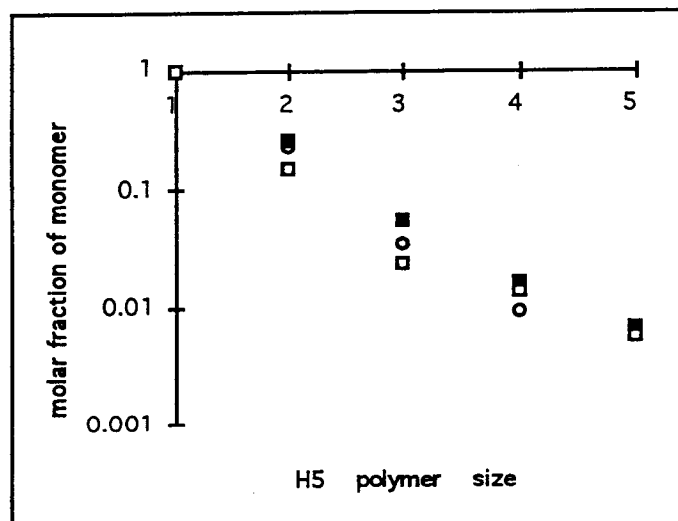
Figure 2.6

C



■ H5 DSP-crosslinked in solution  
 □ GH5 DSP-crosslinked in solution

D



■ H5 DSP crosslinked free in solution,  
 200 mM NaCl, 1 mM sodium phosphate (pH 7.2)  
 □ H5 DSP crosslinked free in solution,  
 100 mM NaCl, 1 mM sodium phosphate (pH 7.2)  
 ○ H5 DSP crosslinked free in solution,  
 water

Figure 2.6 (continued)

respectively. The deviations from linearity seen at very high molecular weights are to be also expected in such graphs. The general linearity of the plotted data is an expected result based on the electrophoretic mobility of homogeneous polymers by Ferguson analysis, and essentially reproduce results reported by Maman et al (1994). A plot of the log of the relative molar fraction for each polymer as a function of polymer size appeared to be nonlinear (Figure 2.6D). The non-linearity could be explained if H5 assembled with a valency greater than two (see Flory, 1953); larger, branched aggregates have more opportunities to add units, and thus larger aggregate formation is more abundant than for comparable linear polymerization. Quite possibly, the long, flexible C-terminal tail domains provide additional interaction sites, and facilitate enhanced self-interaction of separate crosslinked H5 polymers.

### *2.3.3.3 Self-Association of GH5 and H5 as studied by equilibrium analytical ultracentrifugation*

GH5 at 0.3 mg/ml, and H5 at 0.5 mg/ml in 1mM sodium phosphate (pH 7.2), 0.2 mM EDTA were incrementally increased from water to a target salt concentration as described for samples in the turbidity and crosslinking studies. Samples were then analyzed with an XLA analytical ultracentrifuge according to the following equation:

$$(2.6) \quad \frac{d \ln C}{d(r^2)} = \frac{M(1-\nu\rho)}{2RT} \omega^2$$

Here,  $C$  is the concentration of the protein,  $M$  is the molecular weight of the protein,  $R$  is the gas constant ( $8.314 \text{ joules deg}^{-1} \text{ mole}^{-1}$ ),  $T$  is the temperature (Kelvin),  $\rho$  is the solution density,  $\omega$  is the rotor speed,  $\nu$  is the specific volume of the sample and  $r$  is the distance from the center of the rotor to any point in the cell. In this case  $\nu$  for H5 was set to  $0.766 \text{ ml/g}$  and is based on measurements for H1 (Smerdon and Isenberg, 1976), and the value for GH5 was estimated to be  $0.74 \text{ ml/g}$ , based on its amino acid composition. The significant difference in the two values is a consequence of the unusual amino acid composition of the "tails" of intact H5. The solution density  $\rho$  was estimated based solely on the contribution of NaCl, neglecting a minor contribution from buffer..

Distinct differences in the ability to self-associate as judged by this criterion were observed for GH5 and H5. GH5 showed no apparent ability to self-associate at low salt since the plot of  $r^2$  vs  $\ln C$  is linear, and the molecular weight calculated from equation (2.6) was close to the expected value (Table 2.3; Figure 2.7). Even at increased salt concentration up to  $400 \text{ mM NaCl}$  (Figure 2.7C), which have been shown to promote aggregation and crosslinking, GH5 still gave straight line  $\ln C$  vs  $r^2$  graphs, suggesting homogeneity. However, the apparent molecular weight of GH5 actually decreases as the salt concentration increases; this is most likely a non-ideality effect, common in concentrated salt solutions. It is possible that this effect could mask a weak tendency for GH5 to self-associate. In contrast, H5 appeared to assemble free in solution in a salt concentration-dependent manner. In  $1 \text{ mM sodium phosphate (pH 7.2)}$ ,  $0.2 \text{ mM EDTA}$ , H5 existed primarily as a monomer with of molecular weight of  $20,000 \text{ daltons}$  (approximately the expected size of H5) (Figure 2.8A). However, with the addition of

Table 2.3. Results of equilibrium analytical sedimentation

| protein | NaCl<br>(mM) | slope<br>(cm <sup>-2</sup> ) | $\rho$<br>(g ml <sup>-1</sup> ) | 1- $\nu\rho$ | MW approx<br>(dalton) |
|---------|--------------|------------------------------|---------------------------------|--------------|-----------------------|
| H5      | 0            | 0.29                         | 1.000                           | 0.234        | 20,200                |
|         | 200          | na                           | 1.0082                          | 0.228        | na                    |
|         | 400          | na                           | 1.0165                          | 0.227        | na                    |
| GH5     | 0            | 0.32                         | 1.000                           | 0.260        | 8,270                 |
|         | 100          | 0.29                         | 1.0041                          | 0.257        | 7,580                 |
|         | 200          | 0.28                         | 1.0082                          | 0.254        | 7,408                 |
|         | 250          | 0.26                         | 1.0104                          | 0.252        | 6,800                 |
|         | 300          | 0.25                         | 1.0124                          | 0.250        | 6,720                 |
|         | 400          | 0.24                         | 1.0165                          | 0.248        | 6,503                 |

na: complex non-linearity in  $\ln C$  vs  $r^2$  graph prevented the calculation of the molecular weights, for these samples.

**Figure 2.7.** Equilibrium analytical ultracentrifugation of GH5 free in solution. GH5 at 0.3 mg/ml in 1 mM sodium phosphate (pH 7.2), 0.2 mM EDTA was centrifuged for 16 hours at 25,000 rpm. Data are plotted as natural log  $C$  vs  $r^2$ .  $C$  is the absorbance at 234 nm. Lines were fit to the data based on linear regression (Microsoft Excel). Samples were examined with (A) 0 NaCl, (B) 200 mM NaCl, and (C) 400 mM NaCl.

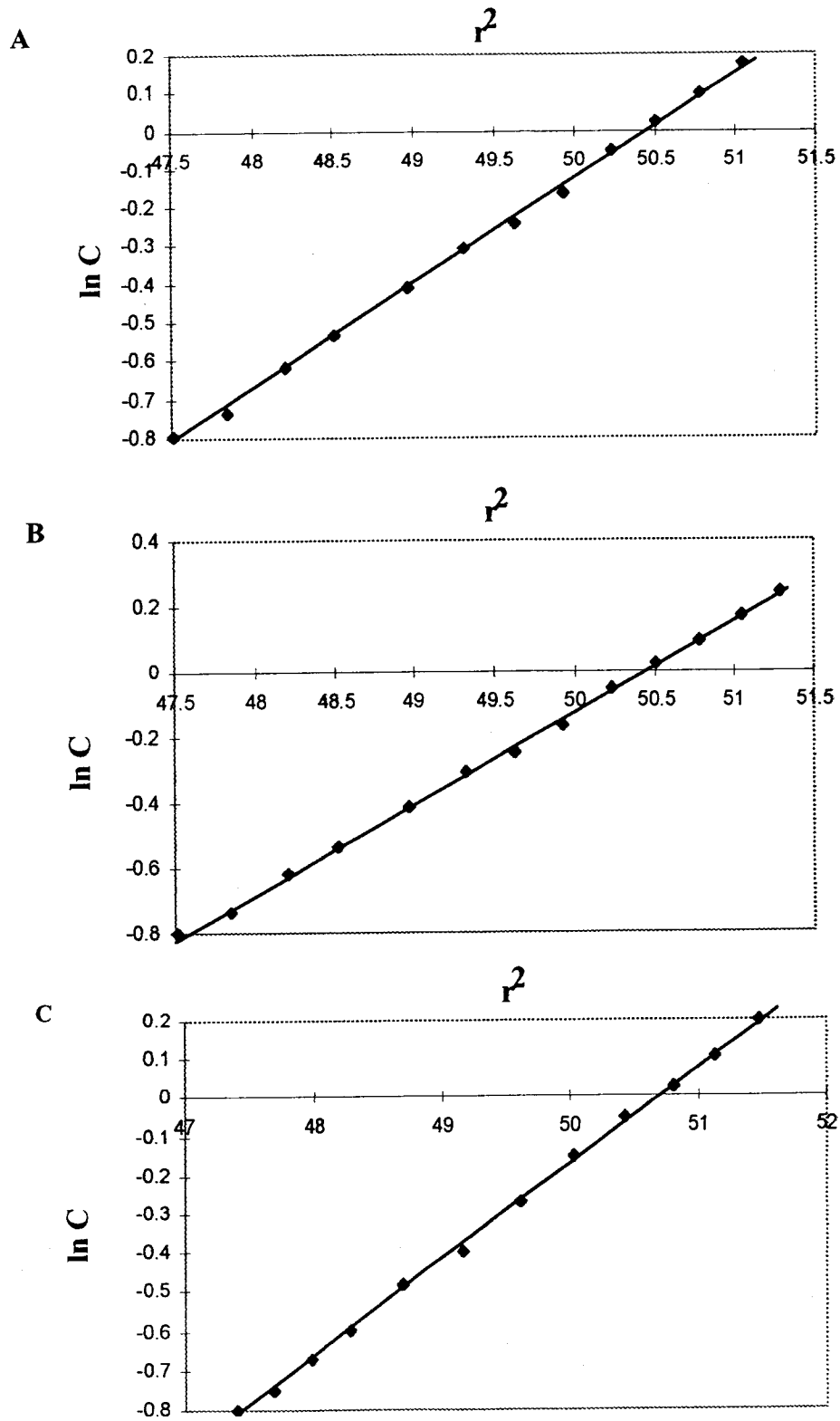
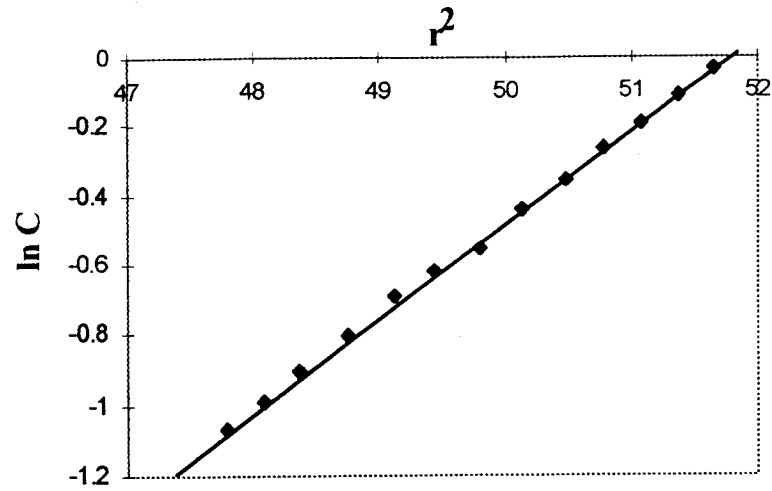


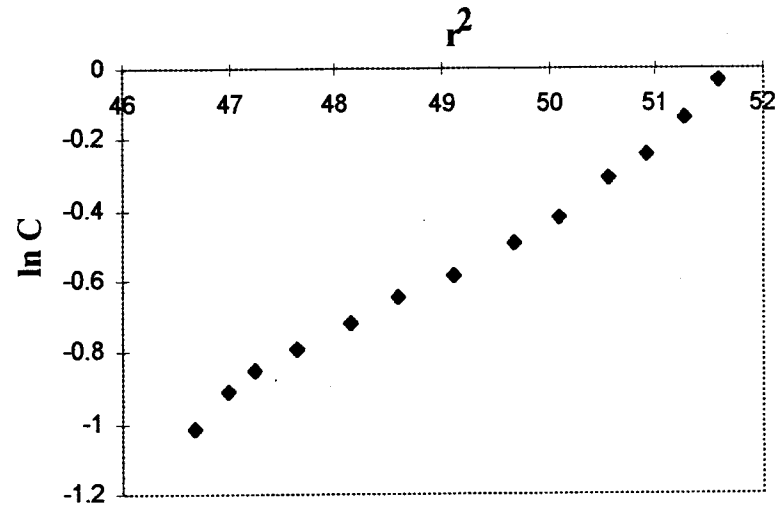
Figure 2.7

Figure 2.8. Equilibrium analytical ultracentrifugation of H5 free in solution. H5 at 0.5 mg/ml in 1 mM sodium phosphate, .2 mM EDTA was centrifuged for 16 hours at 16,000 rpm. Data are plotted as natural log  $C$  vs  $r^2$ .  $C$  is the absorbance at 234 nm. Lines were fit to the data based on linear regression (Microsoft Excel). Samples were examined with (A) 0 NaCl, (B) 200 mM NaCl, and (C) 400 mM NaCl.

A



B



C

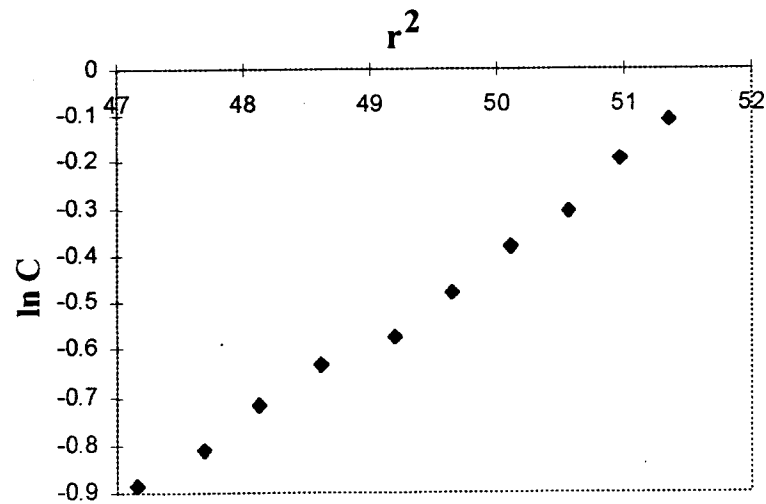


Figure 2.8

200 mM NaCl ([Figure 2.8B](#)), and 400 mM NaCl ([Figure 2.8C](#)) nonlinearity in the sedimentation profile suggests a heterogeneous population of H5 complexes, and thus, self-association. The non-ideality effects observed with GH5 are certain to be operative here as well. Such a combination of heterogeneity, and non-ideality makes quantitative analysis almost impossible, so no attempt has been made to determine the exact polymer distribution. It should also be noted that the turbidity studies do not necessarily contradict the sedimentation equilibrium results. A small fraction of very large aggregates would simply sediment to the bottom of the cell, and not be observed in the gradient.

#### 2.3.4 Association of GH5 molecules on DNA

##### *2.3.4.1 Interaction of GH5 molecules bound to linear DNA: effect of GH5-DNA ratio and NaCl concentration*

Previously, Clark and Thomas (1988) reported that the distribution of H5 polymers formed by crosslinking while bound to an 800 b.p. DNA is largely independent of protein and NaCl concentration. In contrast, H1 crosslinking increased with protein concentration (only at low salt concentration), and with NaCl concentration (Clark and Thomas, 1986). Together these results illustrate important differences in the binding properties of H1, and H5. H1 displays low cooperativity in low salt, and increased cooperativity in high salt ([Table 1.1](#)), while the cooperativity of H5 is independent of salt. Cooperativity should result in H5 molecules cooperatively associating in contiguous patches on DNA even in low salt (5 mM NaCl), whereas under these same conditions H1

is thought to be spatially distributed over the fragment. Thus, for H1 bound to DNA in low salt conditions, crosslinking becomes sensitive to the protein-DNA ratio. Similar studies on the effect of salt concentration and protein concentration have not been performed with GH5, though both Draves et al. (1992) and Thomas et al. (1992) find that GH5 extensively crosslinks when bound to DNA in long linear DNA in low salt solutions.

In this work, GH5 was bound to a mixture of linear DNA fragments obtained by Hha I-cutting pPol208-12. The fragment sizes ranged from 2600 b.p. to small fragments of less than 400 b.p. GH5:DNA ratios 10-140% (w/w) were used in order to elucidate the effects of protein concentration and NaCl on protein-protein contacts. Crosslinking appeared to be independent of the GH5-DNA ratio, as a change from 10-140% produced a nearly-identical distribution of crosslinked polymer sizes at all GH5-DNA ratios analyzed (Figure 2.9A). This is in contrast to the effect of NaCl on the polymer distribution. Samples at 140% GH5:DNA (w/w) showed a considerable increase in the number of crosslinkable protein-protein contacts with increasing salt concentration (Figure 2.9B). The difference was considerably more dramatic for polymers larger than a dimer, with GH5 bound to DNA in 100 mM NaCl crosslinking more extensively than in 10 mM NaCl.

It has been previously reported that GH5 cooperatively binds to DNA independently of protein concentration, with the exception of concentrations less than 10% GH5: DNA (w/w) (Thomas et al., 1992; Draves et al., 1992). Additionally, GH5 has been reported to bind to DNA independently of NaCl concentration, as an increase in ionic strength from 15 mM NaCl to 40 mM NaCl at 70% GH5:DNA (w/w) produced little

Figure 2.9. Effect of GH5:DNA ratio and ionic strength on the polymer distribution of GH5 crosslinked onto DNA. (A) Comparison of the distribution of GH5 polymers as a function of GH5:DNA (w/w) ratios. GH5 was incubated with Hha I cut pPol208-12 in 10 mM NaCl, 10 mM Tris-HCl (pH 7.8), 0.2 mM EDTA, crosslinked with 0.1 mg/ml DSP for 30 minutes and precipitated with 28% TCA (as described in the text). The distribution reflects the mass of each polymer normalized by the mass of uncrosslinked monomer. (B) Comparison of the distribution of GH5 polymers as a function of either 10 mM NaCl or 100 mM NaCl at 140% GH5:DNA (w/w). The mass of each polymer is normalized as in (A) with the mass estimated from silver stained SDS/polyacrylamide gels.

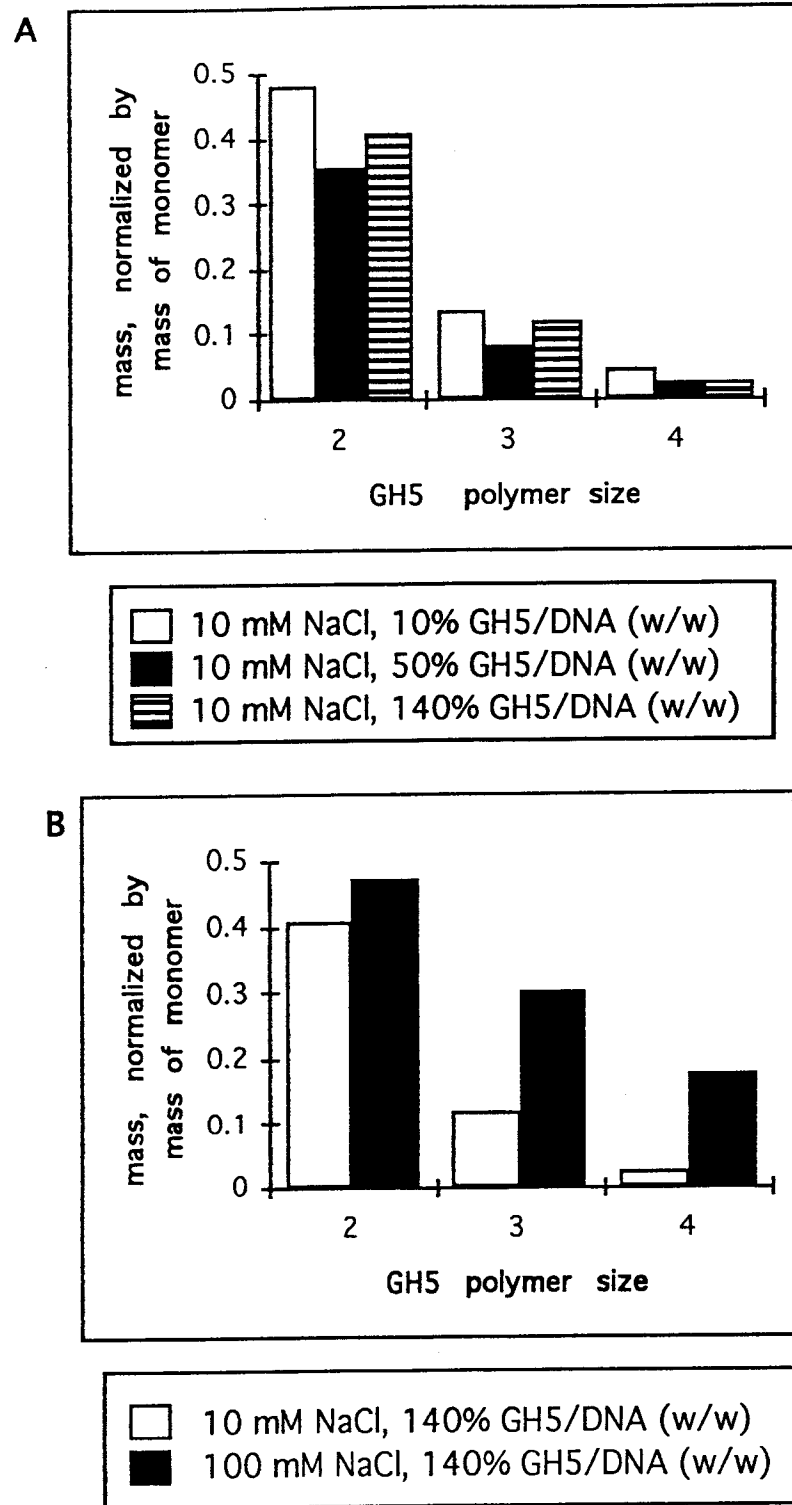


Figure 2.9

discernible difference in GH5-DNA electrophoretic mobility, sedimentation in a sucrose gradient or in the general appearance of the nucleoprotein complex as observed from EM pictures (Draves et al., 1992). The salt-concentration dependency of GH5 crosslinking (Figure 2.9B) came as a surprise, considering that Clark and Thomas (1988) interpret increased crosslinking between DNA-bound linker histones to be directly related to cooperativity. According to Clark and Thomas (1988) and Clark and Thomas (1986), GH5 and H5 display a similar salt concentration-independence in DNA assembly (Draves et al., 1992; Thomas et al., 1992), and therefore would be expected to produce the same crosslinking results; namely independence from salt-dependent effects. In explaining the apparent inconsistency between crosslinking results presented here and previous reports, it must be emphasized that GH5-DNA oligomerization and aggregation results in an increase in the number of GH5 contacts between molecules on separate DNAs (see below). So, increased crosslinking may reflect either increased GH5-DNA nucleoprotein complex interactions, or increased cooperativity as reported for H5 by (Clark and Thomas, 1988).

#### 2.3.4.2 *Effect of type of DNA substrate on GH5 crosslinking*

It is well established that linker histones interact with linear DNA and supercoiled DNA differently. First, linker histones bind supercoiled DNA in preference to linear DNA (Vogel and Singer, 1974) with binding affinity increasing with superhelicity. Second, linker histones distribute relatively evenly amongst the population of supercoiled DNA (Singer and Singer, 1978; De Bernardin et al., 1991), but for linear DNA, linker histones cooperatively bind some DNA fragments while leaving others DNA fragments completely

unbound (Draves et al., 1992). Third, linker histones more readily associate and aggregate linear DNA than supercoiled DNA (Liao and Cole, 1981). DSP-facilitated crosslinking was used to better understand how DNA topology affects the frequency of GH5 self-interactions, and mechanism of assembly. This is especially relevant since the importance of DNA topology on linker histone binding continues to be a current topic of interest (Zlatanova and van Holde, 1996)

To investigate these questions, GH5 was crosslinked for various periods of time in the presence and absence of a 42 b.p. oligonucleotide, and as a comparison a parallel study was conducted with supercoiled pUC19 plasmid DNA (2600 b.p. in size). For DNA-dependent crosslinking, GH5 and DNA both at 0.04 mg/ml were incubated on ice for 30 minutes in buffered solution containing 10 mM NaCl, 10 mM sodium phosphate (pH 7.2), 0.2 mM EDTA, and reacted with DSP at 0.1 mg/ml. For solution crosslinking, GH5 at 0.04 mg/ml in 10 mM NaCl, 10 mM sodium phosphate buffer (pH 7.2), 0.2 mM EDTA was reacted with DSP at a final concentration of 0.1 mg/ml. At various time points, DSP reactions were stopped with the addition of 2 x SDS loading buffer, and by freezing the contents of the reaction mixture in liquid nitrogen.

Based on the disappearance of GH5 monomers into larger crosslinked complexes, the presence of DNA clearly influenced the crosslinking rate. GH5 that was bound to the 42 b.p. oligonucleotide, crosslinked faster than GH5 free in solution (Figure 2.10A). The increased crosslinking rate for GH5 bound to DNA (42 b.p. oligonucleotide), as compared to GH5 free in solution, was not simply due to the interaction of proteins bound to a single DNA molecule. The basis for this argument is the following, the 42 b.p. DNA can

Figure 2.10. Influence of the type of DNA substrate (or lack of substrate) on GH5 self-interaction. (A) A time course of GH5 crosslinking was measured by plotting the normalized mass of uncrosslinked monomers (to the initial monomer mass). As discussed in more detail in the text, GH5 at 0.04 mg/ml was incubated with either pUC19 plasmid DNA (*solid squares*), a 42 b.p. oligonucleotide (*solid circles*) or free in solution (*solid triangles*) in buffer containing: 10 mM NaCl, 10 mM sodium phosphate (pH 7.2), 0.2 mM EDTA. Samples were brought to 0.1 mg/ml DSP for various lengths of time. The reactions were stopped by freezing the reaction in 2 x SDS loading buffer. Values represent uncrosslinked monomer masses normalized by the amount of monomer detected at the initial time point. (B) Analyzing the distribution of crosslinked polymers for GH5 bound to the 42 b.p. oligonucleotide as described in (A). A comparison of the distribution of GH5 (as described in Figure 2.5D) is included as a comparison. A graph of the log of the relative molar amount of each polymer is plotted as a function of polymer size.

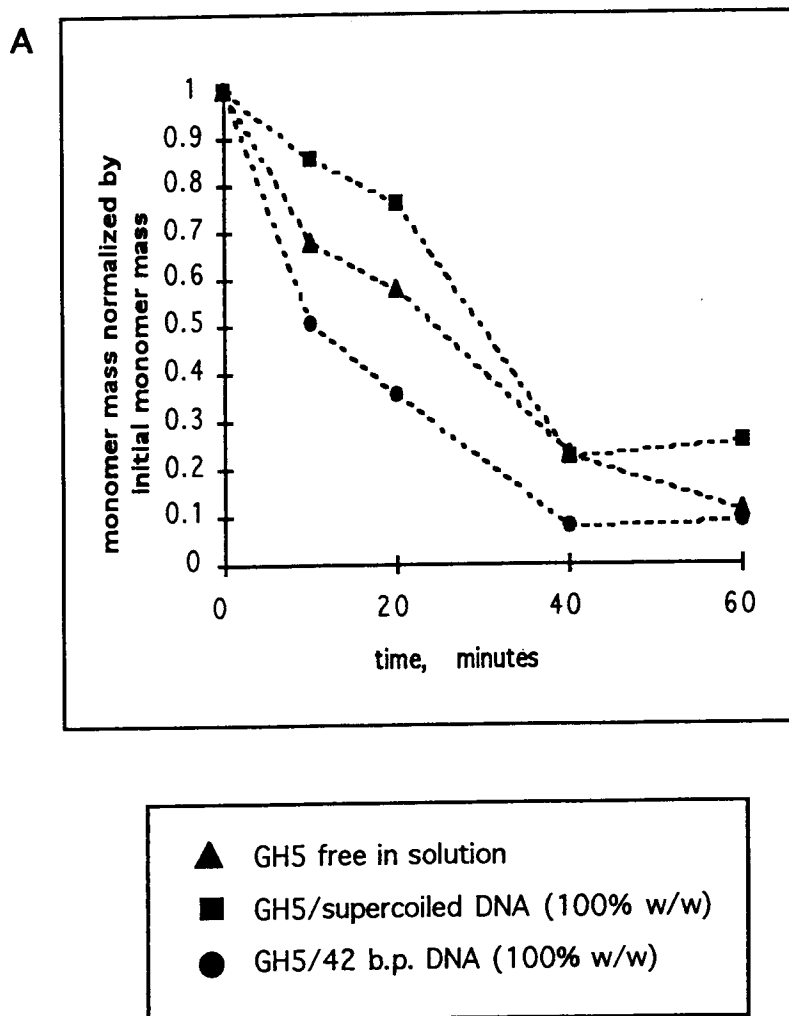
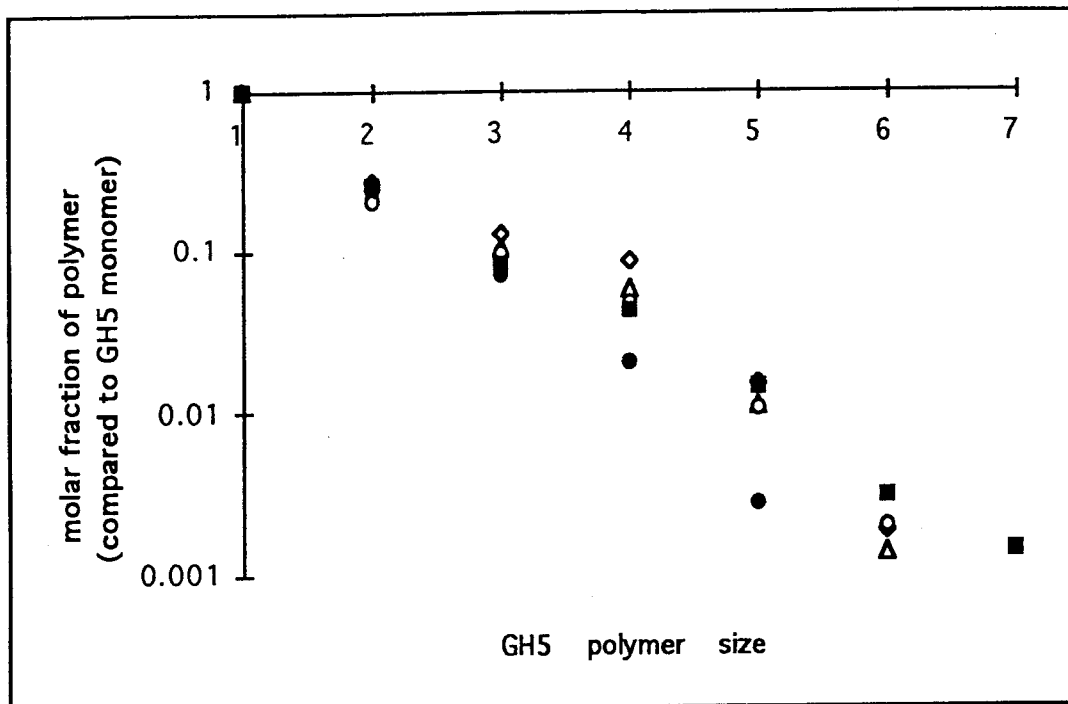


Figure 2.10

B



- GH5 DSP crosslinked free in solution, 10 minutes
- GH5 DSP crosslinked free in solution, 30 minutes
- △ GH5 DSP crosslinked onto a 42 b.p. oligonucleotide, 1 minute
- GH5 DSP crosslinked onto a 42 b.p. oligonucleotide, 10 minutes
- ◇ GH5 DSP crosslinked onto a 42 b.p. oligonucleotide, 20 minutes

Figure 2.10 (continued)

accommodate the binding of no more than three GH5 molecules (see Chapter 3), yet GH5 was able to crosslink into complexes too large to enter the gel, and complexes as large as heptamers that were resolved in the 18% SDS/polyacrylamide gel. Instead, it is likely that individual nucleoprotein complexes oligomerized, forming an extensive network of crosslinked GH5 molecules, an explanation that is supported by the reported susceptibility of GH5-DNA complexes to form aggregates (Chapter 3).

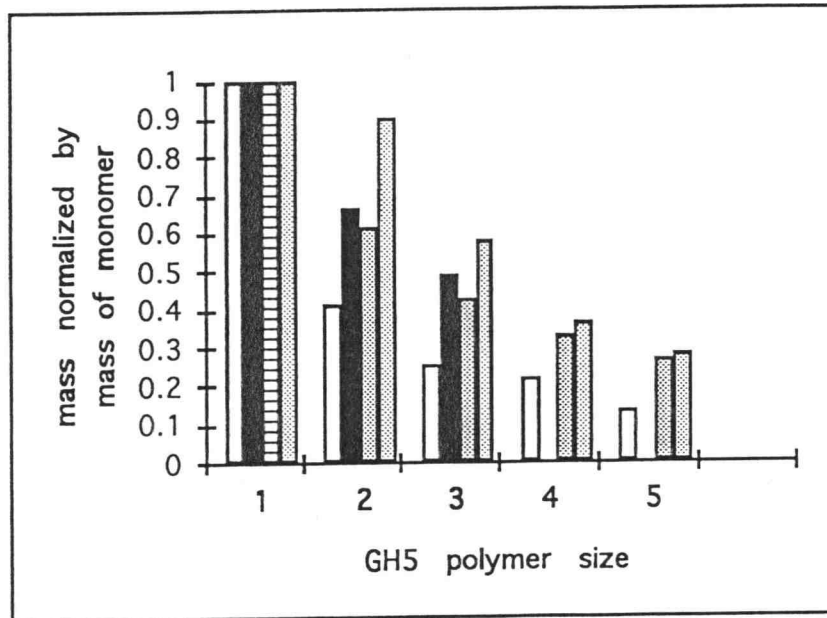
The effect of the 42 b.p. oligonucleotide on GH5 crosslinking was further analyzed by plotting the relative molar proportion of each polymer (relative to the amount of GH5 monomer product) as a function of polymer size (Figure 2.10B). Results indicate that samples examined at 1, 10, and 20 minutes produced similar relative amounts of each size of crosslinked polymer; the distribution compared well to that obtained with free GH5 after 30 minutes. Qualitatively, this finding appears to be in accord with the result of kinetic study in which the 42 b.p. oligonucleotide enhanced GH5 crosslinking (Figure 2.10A).

While it is clear that the 42 b.p. oligonucleotide enhanced the ability for GH5 to self-interact, the reason for this result is unclear. Possibly, binding to DNA effectively neutralized GH5, allowing closer contact between GH5 molecules from separate nucleoprotein complexes. Alternatively, GH5, via its two binding domains, may have been able to bridge two or more DNA molecules, ultimately bringing GH5 molecules from separate nucleoprotein complexes into contact. The former implies that GH5-DNA aggregates are stabilized by protein-protein contacts, while the latter implicates protein-DNA contacts; it is likely that both are important for network formation.

Interestingly, GH5 crosslinked into aggregate complexes more slowly when bound to supercoiled pUC19 plasmid than for even GH5 in free solution (Figure 2.10A). This may be consistent with the finding that H5 is relatively poor at aggregating supercoiled DNA as compared to linear DNA (Chapter 3).

In examining the influence of DNA topology on GH5 assembly, and crosslinking, GH5 was crosslinked, separately, onto a 42 b.p. oligonucleotide, onto Hha I cut pPol208-12 DNA, and onto a supercoiled pUC19 plasmid. Time points were chosen for comparison where roughly the same amount crosslinking had occurred (as judged by the disappearance of GH5 monomers). GH5 bound to DNA (both the 42 b.p. oligonucleotide and Hha I cut pPol 208-12 DNA) clearly formed a larger proportion of high molecular weight GH5 homopolymers than did GH5 crosslinked free in solution (Figure 2.11). GH5 also crosslinked differently on supercoiled DNA than for other samples. GH5 DSP-crosslinked on supercoiled DNA showed a strong propensity to form only small GH5 oligomers (trimers and smaller), or to become involved in complexes too large to enter the running gel (Figure 2.11) and data not shown). In contrast, GH5 bound to linear DNA and free in solution appeared to crosslink to form a continuous, logarithmic distribution as previously described (Figure 2.5C). As in the above-described rate study, results suggest that DNA-binding promoted GH5 self-association, since GH5 bound even to short linear DNA produced more larger-sized crosslinked polymers than did GH5 crosslinked free in solution. Furthermore, the length of linear DNA (42 b.p. vs 2600 b.p.) did not appear to markedly influence the size distribution.

**Figure 2.11.** Effect of DNA substrate on the distribution of DSP crosslinked polymers. The distribution of DSP-crosslinked polymers was measured for a number of samples including: (a) GH5 free in solution, (b) GH5 bound to supercoiled pUC19 DNA, (c) GH5 bound to a 42 oligonucleotide, and (d) GH5 bound to Hha I cut pPol208-12. Refer to the legend for a summary of conditions used for crosslinking. GH5 that was DSP crosslinked onto Hha I cut pPol208-12 DNA was prepared differently from the other samples that were simply dissociated in 2 X SDS loading buffer. Briefly, GH5 was incubated with HhaI cut pPol208-12 (producing fragments from 30 b.p. to 2600 b.p.) for 1 hour at room temperature and crosslinked with DSP at 0.1 mg/ml added from a stock of 5 mg/ml. Samples were then precipitated with TCA as described in Methods and Materials. Since the crosslinking rates varied depending on the sample conditions, time points were chosen to give roughly comparable levels of disappearance of the GH5 monomer .



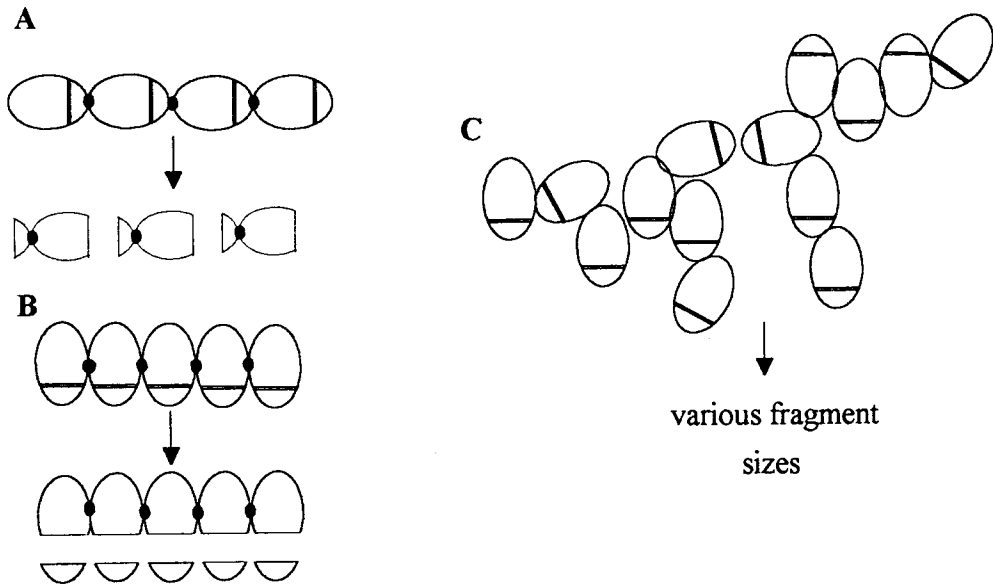
- GH5: 10 mM NaCl, 10 mM sodium phosphate buffer (pH 7.2), 20' time point
- GH5/supercoiled DNA (100% w/w): 1 mM sodium phosphate buffer (pH 7.2), 40' time point
- ▨ GH5/42 b.p. DNA (100% w/w): 10 mM sodium phosphate buffer (pH 7.2), 20' time point
- ▩ GH5/Hha I cut pPol208-12 (140% w/w): 10 mM NaCl, 1 mM sodium phosphate buffer (pH 7.2), 30' time point

Figure 2.11

### 2.3.5 Characterizing crosslinked GH5 organization by quantitative proteolysis

In order to elucidate the organization of crosslinked GH5 complexes and to obtain evidence for specific contacts in crosslinking, a technique involving crosslinking and proteolysis was developed, and is referred to as *quantitative proteolysis*. In this method, GH5 was first crosslinked with DSP then proteolyzed with chymotrypsin which cleaves preferentially at a single site, Phe 93. Information on filament structure was then determined based on the size distribution of the proteolyzed peptide products-hence the name quantitative proteolysis. Figure 2.12 presents a number of hypothetical case studies which better illustrate this technique. As originally envisioned, quantitative proteolysis relies on a protease that cleaves once per protein within an "indefinite filament". The technique can be easily used for characterizing indefinite filaments in which proteins self-interact via two surfaces (Figure 2.12A). Conceivably, smaller peptides would be released if cleavage is not along the main chain of the crosslinked protein polymer (Figure 2.12B). However, more complicated filaments resulting from random collisions or branching limits the utility of quantitative proteolysis (Figure 2.12C). Furthermore, it is plausible that a multiple-site proteases could be used, and as described below for GH5 crosslinked to a 22 b.p. oligonucleotide, finite-sized complexes can also be characterized with quantitative proteolysis.

Quantitative proteolysis was used to elucidate the crosslinked organization of GH5 assembled free in solution and on oligonucleotides. For the later analysis, GH5 at 0.04 mg/ml was mixed with a 22 b.p. oligonucleotide at 0.04 mg/ml in 10 mM sodium phosphate (pH 7.2) for 35 minutes on ice before being crosslinked with DSP for 2 hours



**Figure 2.12.** Examples of indefinite protein filaments and the expected results of quantitative proteolysis. (A) Two separate surface contacts per protein produces a "simple" filament. A protease cuts once (per protein) along the "chain" of the filament resulting in the release of monomer-sized peptides. (B) In the event that the filament is "simple", but the site of proteolysis is peripherally located away from the main protein covalent linkage, only peptides representing the distance between the site of proteolysis to the free terminal end of the protein will be observed. (C) Quantitative proteolysis of random or complex filaments will produce a collection of various-size polymers.

at 4 °C. After "quenching" the crosslinking reaction in 50 mM glycine, the GH5-DNA sample was proteolyzed with chymotrypsin. It was found that samples at 0.01 mg/ml DSP produced the best results, since GH5-DNA crosslinked at higher concentration seemed to be unaffected by chymotrypsin proteolysis (data not shown). Interestingly, the lower concentration of GH5 crosslinked primarily as a dimer with the dimer rapidly becoming reduced to mostly a monomer complex after 15 minutes of room temperature digestion with chymotrypsin at 0.3 µg/ml (Figure 2.13A). Upon further digestion, up to 2 hours, only monomer products were detected (data not shown). The mass of each GH5 crosslinked polymer before chymotrypsin digestion was divided into the mass of the corresponding GH5 polymer after 15 minutes of digestion. This value is referred to as the relative change in mass, and values greater than one indicate an increase in the amount of a particular polymer size with the larger the number, the greater the increase. For GH5 crosslinking onto the 22 b.p. oligonucleotide, the relative change in mass for the GH5 monomer complex was 4.8, and reflects cleavage of most of the dimer-sized GH5 complex into a monomer-sized peptide (Figure 2.13A, 2.13B).

It is striking that such a significant fraction of dimer-sized GH5 complexes were reduced to monomer-sized peptides, and suggests that the two GH5 molecules that crosslinked together on the 22 b.p. oligonucleotide interacted largely via a single interaction surface (Figure 2.14A). This is in contrast to nonspecific interaction that would have resulted in largely dimer-sized peptide (Figure 2.14B). Perhaps indirectly, these results argue that GH5 assembles onto DNA in an organized fashion, though the type of complex or filament remains to be elucidated. Results also suggests that the

**Figure 2.13.** Determining DSP-crosslinked GH5 complex organization by quantitative proteolysis. (A) GH5 at 0.04 mg/ml was bound to a 22 b.p. oligonucleotide at 100% (w/w), treated to 0.01 mg/ml DSP for two hours, brought to 50 mM glycine, and cleaved with 0.3  $\mu$ g/ml chymotrypsin for the indicated amount of time. (B) The relative change in mass for crosslinked GH5 monomers, dimer, and trimers as a result of the quantitative proteolysis of GH5 bound to a 22 b.p. oligonucleotide. The mass of each crosslinked GH5 polymer after 15 minutes of chymotrypsin digestion was divided by the respective polymer mass before proteolysis, and plotted as a function of GH5 polymer size. (C) The relative change in mass for crosslinked GH5 monomers, dimer, and trimers as a result of the quantitative proteolysis of GH5 free in solution. GH5 at 0.04 mg/ml was treated to 0.001 mg/ml DSP for two hours, brought to 50 mM glycine, and cleaved with 0.3  $\mu$ g/ml chymotrypsin for the indicated amount of time.

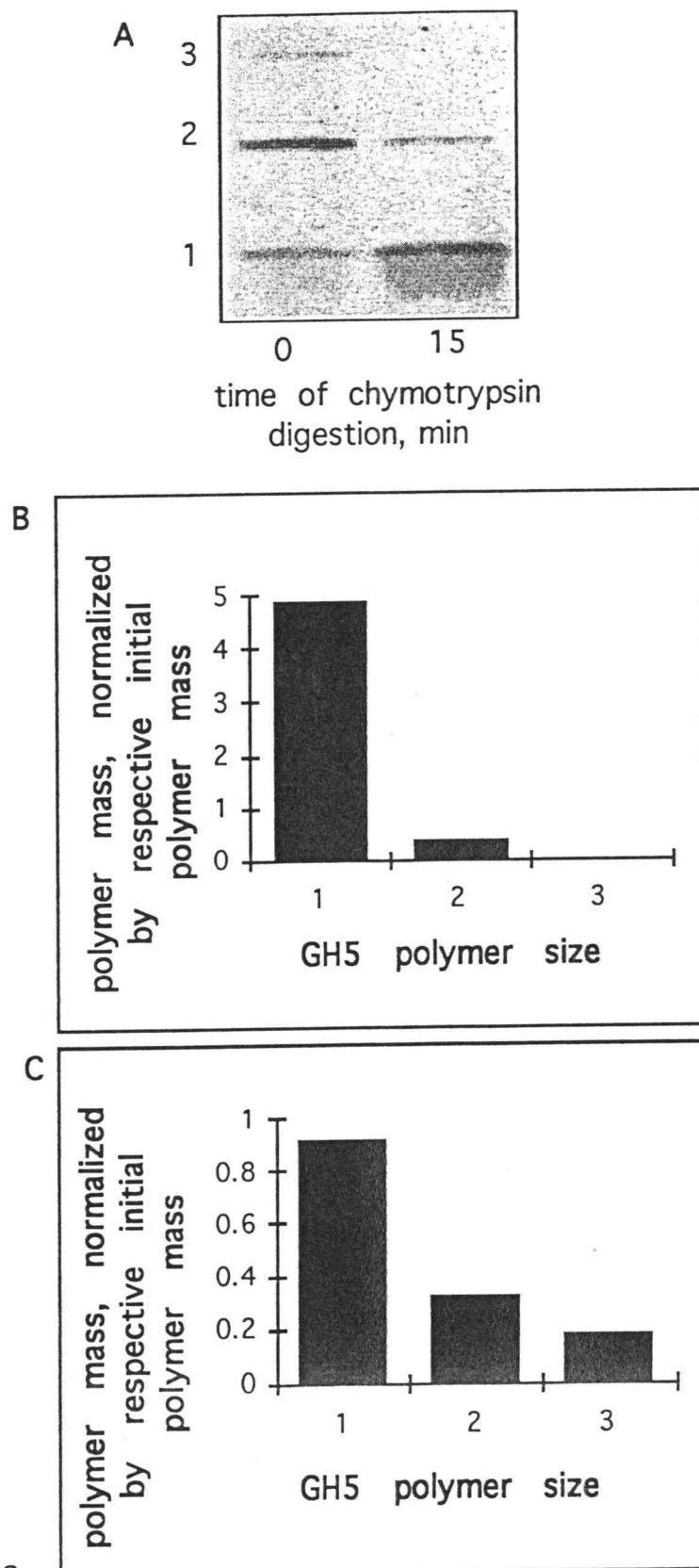
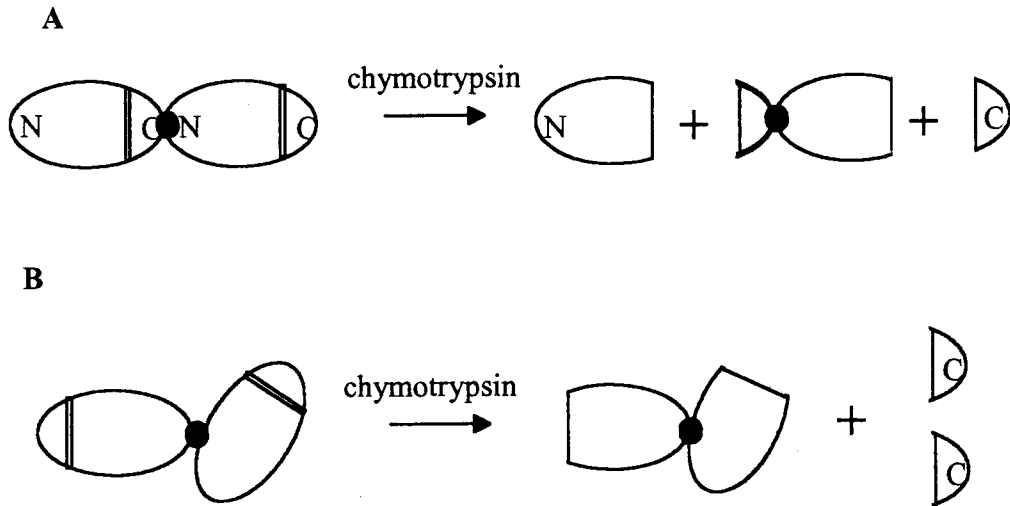


Figure 2.13

C-terminus was near the site of the protein-protein contact. A single lysine, Lys 97, lies C-terminal from the primary chymotrypsin digestion site, Phe 93, and is an excellent candidate to be the primary crosslinking site. Crosslinking via any other residue would have only resulted in the release of a small 4 amino acid peptide and conservation of dimer-sized fragments, as cleavage would not have been along the main chain of the protein filament (Figure 2.14B) The importance of the C-terminal end for GH5 self-association was also reflected by the inability for GH5 to re-crosslink after its removal with chymotrypsin (data not shown). In summary, these observations support specific self-interactions of GH5 bound to the 22 b.p. oligonucleotide.

Quantitative proteolysis was also applied to GH5 assembled free in solution. GH5 at 0.04 mg/ml in 10 mM sodium phosphate (pH 7.2) was titrated with DSP to identify optimal crosslinking conditions as described for the study with the 22 b.p. oligonucleotide. Crosslinking at 4 °C for 2 hours in 0.001 mg/ml DSP produced a GH5 ladder (data not shown)--that was cleaved with 0.3 µg/ml of chymotrypsin for 15 minutes. Unlike the finite filament case for GH5 crosslinked to the 22 b.p. oligonucleotide, crosslinked free GH5 represented an indefinite model as polymers were observed to extend from monomer-sized peptides to complexes too large to enter the stacking gel (Figure 2.5). The results of quantitative proteolysis were clearly different for GH5 free in solution (Figure 2.13C) as compared to GH5 bound to the 22 b.p. oligonucleotide (Figure 2.13B). First, proteolysis of the GH5 crosslinked filament produced peptides with a considerable size heterogeneity (data not shown). This was reflected by the relatively large quantity of different-sized polymers larger than monomers that appeared after proteolysis. In



**Figure 2.14.** Models for potential contacts of adjacent GH5 molecules bound to a 22 b.p. DNA. (A) Uniform contacts in which the C-terminal region of one molecule contacts a more N-terminal portion of another molecule. Chymotrypsin cleavage results in the production of two peptides roughly the size of a monomer, along with small peptides 4 amino acids in size. (B) Random contacts in which one molecule interacts with another via arbitrary parts of the protein. Chymotrypsin cleavage results in the production of a dimer size molecule as well as small peptides 4 amino acids in size. Symbols: (*dots*) represent DSP crosslinking points that covalently attach two separate molecules, and (*double lines*) represent chymotrypsin cleavage sites.

contrast, proteolysis of GH5 bound/crosslinked to the 22 b.p. DNA resulted in virtually all monomer-sized products. Second, the relative change in mass was consistently less than 1 for all polymer sizes (Figure 2.13C), and indicates that crosslinking continued despite DSP quenching in 50 mM glycine before proteolysis. Curiously, a parallel study of the quantitative proteolysis of GH5 DSP-crosslinked on a 42 b.p. oligonucleotide produced results similar to that for GH5 free in solution (data not shown), and suggests that GH5 may assemble differently on 22 b.p. and 42 b.p. oligonucleotides.

Results of quantitative proteolysis, while supporting the potential for GH5 to specifically interact on DNA, provided no clear evidence that GH5 forms specifically-interacting crosslinked complexes free in solution. First, proteolysis of GH5 crosslinked free in solution resulted in greater heterogeneity in the size of released polymers than for GH5 bound to the 22 b.p. oligonucleotide, which casts doubt as to simple, uniform assembly. Second, GH5 free in solution continued to crosslink after chymotrypsin digestion (data not shown) quite unlike the results observed for GH5 crosslinked to the 22 b.p. oligonucleotide. Besides indicating that 50 mM glycine may have been ineffective in quenching the crosslinking reaction, continued crosslinking of free GH5 even after chymotrypsin proteolysis may also indicate any number of possibilities including: (a) crosslinked GH5 complexes were organized in such a way as to prevent access to Phe 93, chymotrypsin's primary cleavage substrate, and (b) GH5 once cleaved with chymotrypsin was able to reassemble again, suggesting multiple surfaces available for interaction and placing no unique importance to the C-terminal part of GH5 in self-association. So, based on quantitative proteolysis it is uncertain whether free GH5

associated randomly or, specifically. However, the accord between the polymer size distribution found in solution with that expected for a random, bifunctional condensation argues that chain branching is minimized. Perhaps the most reasonable conclusion is that when GH5 associates in solution, most the interactions are specific, but some non-specific interactions also occur, some eventually leading to branching and network formation..

In developing quantitative proteolysis as a practical method for determining crosslinked filament organization, two major problems were encountered that presented major technical challenges. First, 50 mM glycine did not appear to stop DSP crosslinking, and may have compounded problems in interpreting the results of proteolysis. This was particular evident when working with GH5 crosslinked free in solution, and bound to the 42 b.p. oligonucleotide. While 50 mM glycine has been utilized in the past to terminate DSP crosslinking, perhaps lysine or Tris may make a better "quencher". As mentioned here, freezing samples in SDS loading buffer also proved effective. Second, some difficulty was encountered in optimizing crosslinking concentrations. Over-crosslinking appeared to prevented cleavage of the complex into smaller polymers while under-crosslinking produced too little polymers for analysis. However, this obstacle seemed to be satisfactorily overcome by conducting chymotrypsin proteolysis on samples treated over a wide range of DSP concentrations.

## 2.4 Discussion

### 2.4.1 Association and assembly of linker histones

Three separate methods were used to analyze linker histone protein self-association: (a) salt-induced turbidity, (b) chemical crosslinking, and (c) equilibrium analytical ultracentrifugation. These techniques are complimentary, for they measure different aspect of the self-association process. Turbidity is very sensitive to the formation of very large aggregates, as appear in high salt concentrations, and can detect small amounts of such aggregate. Chemical crosslinking is useful in the detection of weak or transient contacts whether they occur in solution or on a DNA substrate, since it is essentially a non-equilibrium process. Finally, equilibrium sedimentation examines relatively stable interactions that are capable of being maintained free in solution.

For GH5 and H5, chemical crosslinking free in solution with DSP resulted in the formation of a broad spectrum of polymers, including some aggregate complexes too large to enter the SDS/polyacrylamide stacking gel. At first glance, these results appear to contradict those of Smerdon and Isenberg (1976) who report that H1 does not self associate based on fluroescence anisotropy, and analytical centrifugation. Equilibrium centrifugation studies of H5 described in this thesis show clear evidence for self-association at higher salt concentrations. Smerdon and Isenberg (1976) do not show their sedimentation data, but it is perhaps significant that their reported average molecular weights increase somewhat with increasing salt as would be expected from self-association.

With GH5, self-association in solution was demonstrated by crosslinking, but was not evident from the sedimentation equilibrium studies. This could be a consequence of non-ideality (or decrease in the specific volume) at high salt concentrations compensated by protein self-association. Such a phenomenon was clearly observed for H5.

Alternatively, it may be that while the globular domains are able to dynamically interact, the dissociation constant is too high to allow detection by equilibrium solution studies.

Maman et al. (1994) contend that their calculated value of  $K_s$  for GH5 self-association may be large enough to account for physiologically important interactions. However, it should be noted that this reported  $K_s$  was derived from a chemical crosslinking study, and may be without meaning because of the non-equilibrium nature of such experiments.

Overall, it is clear that observations made in this thesis support reports that GH5 does interact in solution, although weakly.

Parallel analysis of H5 self-association shows that the protein clearly interacts in dilute solution, and with a larger association coefficient than for GH5. Like GH5, H5 crosslinked into large aggregates in a salt-dependent manner. In particular, H5 showed a dramatic increase in crosslinking efficiency with the addition of 1 mM sodium phosphate, suggesting that structuring of the terminal tail domains (as indicated by circular dichroism), or salt-dependent shielding of basic residues might be responsible. Unlike GH5, the crosslinking data for H5 appears to be supported by equilibrium analytical ultracentrifugation data. Interestingly, all linker histone proteins were found to undergo a salt-dependent increase in turbidity that showed increased sensitivity at certain salt concentrations. However these experiments appear to be following another aspect of the

association process--the irreversible formation of very large aggregates, so a correlation, if any, with the other studies is unknown..

Maman et al. (1994) makes a case that GH5 crosslinks specifically since: (a) the use of crosslinking reagents with different crosslinking lengths led to different crosslinking results, and (b) successfully crosslinking proteins in solution is, in itself, indicative of specific interactions. None-the-less, nonspecific crosslinking due to random collisions cannot be ruled out. So, in an attempt to provide more concrete evidence that GH5 self-associates in a specific manner, a technique referred to as quantitative proteolysis was developed to analyze complex organization. After cleaving the crosslinked complex with a protease that cuts once per protein, products of cleavage were detected with SDS-PAGE. Ideally, the distribution of released peptides provides information as to complex organization. While quantitative proteolysis of crosslinked GH5, free in solution, produced mainly monomer-sized polymers--which are indicative of a simple filament, the presence of larger-sized GH5 polymers makes definitive identification of the type of crosslinked structure impossible. The possibility that GH5 crosslinked into organized filaments was further investigated by logarithmically plotting the relative abundance of each polymer size as a function the number of GH5 molecules bound in each complex. The resulting linear relationship is characteristic of a simple, nonbranching filament, though the limited size of the crosslinked complexes included in the analysis leaves some uncertainty in the interpretation. Considering the present level of uncertainty, the use of a high resolution imaging technique might be valuable in providing more definitive proof that GH5 crosslinks specifically as simple, unbranched filaments.

#### 2.4.2 Linker histone binding and complexing to DNA molecules

DSP crosslinking results indicate that GH5 molecular self-associates more readily when bound to linear DNA than when bound to supercoiled DNA. Additionally, GH5-linear DNA oligomerization and aggregation appears to have played a major part in the relatively high crosslinking rate. In support of this conclusion: contact between separate nucleoprotein complexes was particularly evident for GH5 crosslinked on the 42 b.p. oligonucleotide. Protein oligomers included sizes that extend to the well, and were far too large to have complexed on an individual DNA fragment. In effect, extensive crosslinking could only be indicative of contacts made between separate GH5-DNA complexes. Furthermore, studies examining SDS-dependent solubility of H5-DNA complexes, presented in Chapter 3, as well as a previous published metrizamide gradient work both clearly identify linear DNA as being particularly vulnerable to linker histone-induced aggregation (Singer and Singer, 1978; Liao and Cole, 1981), as compared to supercoiled DNA.

Supercoiled DNA is distinctly different from linear DNA as a binding substrate for linker histones. Particularly intriguing was the finding that GH5 crosslinked as clusters, up to three proteins in size, onto supercoiled DNA. The most apparent explanation: GH5 binds at DNA crossover in a spatially separated manner in small groups up to trimers. Crossovers appear to act as a high affinity sites for linker histones (Vogel and Singer, 1974; Krylov et al., 1993) with the globular domain apparently recognizing these DNA structures (Singer and Singer, 1976). Interestingly, four-way junction DNA, which may

mimic crossovers, loads three-to- four GH5 molecules (Varga-Weisz et al., 1994; Goytisolo et al., 1996), a result that is analogous to and consistent with this GH5 crosslinking study. Crossovers in superhelical DNA may resemble four-way junctions and provide linker histones with a "super affinity substrate". Alternatively, GH5 may not bind at crossover points, but instead be separated on the DNA by stress-induced structures. For example, EM shows H1 linker histone cooperatively coating isolated portions of a plasmid DNA (De Bernardin et al., 1986). Separation between H1 clusters appears to be due to stress-related, "bubble shaped" structures that formed in the plasmid due to H1 binding. However, it should be noted that these experiments used the intact protein, rather than the globular domain. Ultimately, a high-resolution imaging technique may be require to determine whether in fact GH5 binds in small clusters at crossover points.

In a related study, the effects of the protein-to-DNA ratio and salt concentration on GH5 assembly onto linear DNA were examined. Crosslinking results demonstrate that protein concentration (from 10% to 140% GH5:DNA w/w) had relatively little effect on the overall distribution of GH5 crosslinked polymers. This finding may be consistent with previously reported EM (and sucrose gradient work) in which the general appearance GH5-DNA complexes change little with increasing protein concentration above 10% GH5:DNA (w/w) (Draves et al., 1992). GH5-DNA crosslinking produced results similar to those for H5 (Clark and Thomas, 1988). The relative distribution of crosslinked H5 complexes were reported to be independent of the H5-DNA ratio, which according to Clark and Thomas (1988) is indicative of cooperative binding. However, these authors also report that the H5 crosslinked polymer distribution was independent of the NaCl

concentration; we instead found that GH5 crosslinking was highly sensitive to the NaCl concentration. What is the reason for the salt-dependence of GH5 crosslinking to DNA? Either an increase in salt concentration lead to closer contact between GH5 molecules on a single DNA fragment or facilitated the oligomerization of separate nucleoprotein complexes. In determining which of these possibilities accounted for the salt-dependent increase in GH5 crosslinking, the following reports may be relevant: (a) GH5 displays salt-independent cooperativity in binding (Thomas et al., 1992; Draves et al., 1992), and (b) GH5-DNA aggregation increases with ionic strength (Chapter 3). Together, these results suggest that salt did not effect protein binding density as described for linker histone H1 (Clark and Thomas, 1986). Instead, the salt-dependent increase in GH5 self-crosslinking in GH5-DNA complexes may been the result of salt promotion of nucleoprotein oligomerization and aggregation.

Finally, quantitative proteolysis was used to elucidate whether GH5 crosslinked onto DNA in a specific manner. GH5 crosslinked and cleaved on a 22 b.p. oligonucleotide produced results expected for specific contacts. The interaction also appears to have involved the C-terminal tail of GH5, and supports the importance of specific protein-protein contacts in GH5 binding and assembly onto DNA. The identification of specific contacts between GH5 bound to DNA, suggests that the same surfaces responsible for GH5 self-interactions on DNA may facilitate the self-association of GH5 free in solution. However, as described above, attempts to identify such contacts free in solution were unsuccessful.

### 2.4.3 Implications of studies on linker histone self-association

This study adds independent verification that GH5 crosslinks with DSP in dilute solution, a question that has been given contradictory answers over the last few years. Furthermore, results presented here suggest that GH5 may associate specifically, thus supporting the proposal of Maman et al. (1994). But what is the significance of specific self-association? For one, specific interactions in solution suggests that protein-protein contacts are the basis for cooperative binding to DNA, and may necessitate revision of the "tramline model" (Thomas et al., 1992). In the tramline model, cooperativity is based solely on the availability of two DNA strands (to satisfy the two binding sites on the protein), and does not consider protein-protein interactions. While not totally dismissing the tramline model, results included in this study suggest that protein-protein interactions must be an integral part of GH5 assembly onto DNA, and presumably may offer at least a partial explanation for linker histone's cooperative behavior. The importance of protein-protein contacts are also suggested by the disruption of aggregates in low urea concentrations (Chapter 3) and prominent GH5 self-crosslinking onto DNA (as compared to GH5-DNA crosslinking) (Chapter 4).

Linker histone self-association may also have relevance to chromatin fiber compaction. It has been recognized for some time that linker histones H5 and H1 can be extensively chemically crosslinked within the chromatin fiber *in situ* (Table 1.2) though crosslinking of the globular domain *in situ* is limited sizes up to trimers (Nikolaev et al., 1984). Steric problems associated with nucleosome binding may be partially responsible for the difference; whereas the globular domain is securely isolated on the nucleosome, the

long linker histone tails are free to interact beyond the nucleosome. In a possibly related topic, nucleosomes reconstituted with linker histones are able to assemble (Ali and Singh, 1987; Segers et al., 1991), and form structures that resemble chromatin (Grau et al., 1982; Klug and Finch, 1976). This suggests that linker histone tails are capable of bridging separate nucleosomes with this "bridging" mechanism being potentially important in chromatin compaction and stability. Based on both the DSP-crosslinking studies and equilibrium analytical ultracentrifugation analysis, it appears that part of H5-dependent aggregation of nucleosomes may include protein-protein interactions involving the terminal tail domains though (as described above) it is unclear whether tail folding enhances protein-protein contacts. In summary, the finding that H5 self interacts with a relatively high affinity is particularly important because it helps explain *in situ* crosslinking results, and offers a possible explanation for linker histone induced chromatin stability.

## CHAPTER 3

### Linker Histone H5 (and the Globular Domain of H5) Binding to DNA and Chromatin

#### 3.0 Summary

A number of diverse biochemical-related studies were conducted with the ultimate goal of characterizing the binding of avian erythrocyte linker histone H5, and its globular domain (GH5), to naked DNA and small chromatin fibers. First, it was found that H5 bound to DNA was more sensitive to chymotrypsin digestion, than was H5 free in solution. This was unexpected based on predictions by a popular model in which the third helix of the globular domain of H5 is "buried" in the major groove, and suggests that this model may not accurately reflect the actual H5-DNA complex. H5 differed from GH5 in that DNA-binding was highly resistant to the effects of NaCl, urea, and SDS. This suggests that H5 bound to DNA principally through the highly-basic, terminal tail domains, and that binding elements in the tail domains did not require solution-stable secondary structure. On the other hand, results of the urea studies indicate that the aggregation by GH5 was strongly dependent on protein-protein contacts. In a group of experiments intended to parallel the DNA-binding study, H5 was bound to DNA reconstituted *in vitro* with octamers. Results based on protection of an EcoR I recognition site suggest that H5 either bound asymmetrically upstream of the nucleosome--near the dyad axis (where DNA enters and exits the nucleosome) or symmetrically on the dyad axis. Furthermore, H5 compacted reconstituted chromatin into

a solenoidal-like fiber as determined from velocity analytical ultracentrifugation, but only upon the addition of 30 mM NaCl.

### 3.1 Introduction

Linker histones are an essential protein component of higher eukaryotic chromatin. Structurally, each linker histone is comprised of three separate parts: (a) the N-terminal tail domain, (b) the trypsin-resistant globular domain, and (c) the C-terminal tail domain (Aviles et al., 1978). X-ray diffraction data and NMR analysis both indicate that the globular domain folds into a winged-helix motif with a highly-conserved, flexible loop or wing, known as the  $\beta$ -hairpin, at the C-terminus of the peptide (Ramakrishnan et al., 1993). It has been proposed that the globular domain has at least two separate binding sites based: (a) on the appearance of at least two closely associated DNA fragments emerging from linker histone-DNA complexes in electron micrographs (Clark and Thomas, 1988; Thomas et al., 1992; Draves et al., 1992) and (b) the identification of basic residue "patches" on three separate parts of the globular domain (Cerf et al., 1994). Goytisolo et al. (1996) further strengthen the two DNA binding-site model by showing that elimination of arginine and lysines in either of the putative binding sites weakens DNA binding.

The molecular structures of a number of winged-helix motif proteins have been solved for proteins both in solution and bound to DNA and include (in part): jun, transcription factor ETS DNA-binding domain (Werner et al., 1995), MU transposase internal activation element (Clubb et al., 1994), HNF-3 $\gamma$  hepatocyte specific transcription

regulator (Clark et al., 1993), and yeast heat shock factor transcriptional regulator (Harrison et al., 1994). The family is characterized by a globular domain that consists of a three  $\alpha$ -helix bundle with extended loops that connect separate individual  $\alpha$ -helices (Brennan, 1993). To date, all winged-helix proteins that have been so studied have been shown to bind DNA in a way similar to many helix-turn-helix proteins, like CAP (Schultz et al., 1991). That is, the interaction is primarily made through a recognition helix with additional contacts via loops along the "contact interface" between the DNA and protein (Overdier et al., 1994). The way in which linker histones bind to DNA remains speculative, but evidence based on homology with other winged-helix-motif family members argues that the higher affinity site includes insertion of a recognition  $\alpha$ -helix into the major groove, as with HNF-3 $\gamma$ , a close structural homologue (Clark et al., 1993). However, since the structure of a linker histone bound to DNA has not been solved at molecular resolution, characterization of DNA binding has instead relied on limited biochemical-based reports. These studies include the finding that Lys 85 is protected from reductive methylation upon DNA binding (Thomas and Wilson, 1986), and that binding is largely mediated by several basic residues (Goytisolo et al., 1996). While these results have been used to support the idea of globular domain binding to DNA via interaction of the recognition helix with the DNA major groove, the conclusions are far from definitive. Furthermore, it should be noted that those winged-helix proteins whose mode of binding are known, each bind to a specific consensus sequence, whereas linker histone show little sequence specificity. Rather they bind preferentially to structures like four way junctions (Varga-Weisz et al., 1993; Varga-Weisz et al., 1994), DNA

crossovers (Vogel and Singer, 1974), and to entering-and-exiting DNAs near the dyad axis of nucleosomes (Allan et al., 1980).

Less is known about the role of the terminal tail domains though it has been established that the C-terminal tail binds DNA with a higher affinity than does the N-terminal tail combined with the globular domain (Glotov et al., 1978b), and the entire protein (with both terminal tail domains) binds considerable more tightly than does the globular domain (Segers et al., 1991). The C-terminal tail has also been reported to interact with DNA via motifs containing  $\alpha$ -helicies (Clark et al., 1988). It is unclear whether binding principally involves interaction of basic residues with the DNA phosphate backbone or whether binding is more base specific with contacts involving van der Waals interactions or hydrogen bonding in the DNA grooves. In this regard, the putative SPKK DNA-binding motif found repeatedly throughout the terminal tail domains preferentially interacts with narrow minor grooves of B-DNA (Hill et al., 1991; Churchill and Suzuki, 1989; Bailly et al., 1993), and likely plays a major part in linker histone binding to DNA. The C-terminal tail also appears to serve a role in promoting chromatin stability as it is necessary for fiber condensation (Allan et al., 1980). The N-terminal tail is considerably shorter than the C-terminal tail and has been reported to help anchor the globular domain onto the nucleosome (Allan et al., 1986), possible through interactions with the octamer core (Boulikas et al., 1980).

Linker histones appear to play an important role in facilitating chromatin stability. Upon binding nucleosomes either at the dyad axis, where DNA enters and exits from the octamer (Allan et al., 1980), or possibly at a position just off the dyad axis (Pruss et al.,

1996; Hayes and Wolffe, 1993), the linker histone is able to convert chromatin that exists in an extended form into a compacted form (reviewed in van Holde and Zlatanova, 1996). The compacted form is characterized by closely associated octamers, and has been reported to form a solenoid 30 nm in diameter with a pitch of six octamers per turn (Finch and Klug, 1976, reviewed in Widom, 1989). However, the uniform 30 nm solenoid may be an exception to the rule as recent scanning force microscopy (SFM) results suggests that the chromatin filament is far more heterogeneous ( Leuba et al., 1994; reviewed in van Holde and Zlatanova, 1995). The basis for linker histone-induced compaction is uncertain. Linker histones may bend or reduce the rigidity of the linker DNA to facilitate octamer-octamer contact (Yao et al., 1991). Alternatively, linker histone binding to the nucleosome may change the angle that the entering and exiting DNA make at the dyad axis-collapsing chromatin like an accordion in the process ( Furrer et al., 1995).

Chromatin stability may also involve protein-protein interactions between octamer proteins and linker histones (Riehm and Harrington, 1989). This hypothesis is supported by reports that linker histones induce aggregation of mononucleosomes (Segers et al., 1991; Ali and Singh, 1987; Grau et al., 1982), linker histones can be extensively crosslinked in chromatin (Table 1.2), as well as by solution studies, reported in Chapter 2, showing that H5 tail domains enhance self-association.

In the studies described herein, interaction of linker histone H5 (an avian erythrocyte-specific subtype) with DNA and chromatin was investigated in order to better understand the way H5 binds to chromatin. First, results of a protease protection assay suggests that H5 may not interact with the DNA major groove via insertion of the

recognition  $\alpha$ -helix as do other winged-helix motif proteins, and thus directly contests the popular major-groove-binding model. In another set of experiments, the ability for H5 and GH5 to aggregate DNA was characterized in considerable detail as a means of mimicing potential interactions found in chromatin (Matthews and Bradbury, 1978). Evidence for potential cooperative protein-protein contacts within the aggregate complex are presented. Interestingly, H5 was relatively resistant to the effects of increased salt and urea concentrations on maintaining aggregate stability, which suggests that unlike GH5, the terminal tail domains required no solution stable secondary structure for binding. This supports previous circular dichroism studies (Hill et al., 1989; Clark et al., 1988), as well as the generally recognized importance of flexibility in high affinity protein binding to DNA (Kwon et al., 1997). Finally, H5 was bound to artificially reconstituted chromatin fibers, and the effects thereof analyzed by a number of methods including restriction nuclease digestion, analytical ultracentrifugation and agarose gel electrophoresis. H5 appeared to bind at the point on the nucleosome where the DNA enters and exits, as binding conferred protection to an endonuclease restriction site. H5 binding also results in restructuring of the fiber into a condensed form.

## 3.2 Methods and materials

### 3.2.1 Protein Purification

#### *3.2.1.1 Purification of recombinant GH5*

Recombinant GH5 was expressed and isolated as described in Chapter 2. Briefly, BL21 *E. coli* cells transformed with GH5pLK, a pET-3a expression vector (Novagen) inserted with the coding sequence for GH5 (Gerchman et al., 1994), were grown to 0.35-0.6 OD(600 nm) and induced with 0.6 mM IPTG for several hours. Cells were sonicated, and proteins were extracted in buffer containing 25 mM Tris-HCl (pH 7.8), 500 mM NaCl, 0.2 mM EDTA, 0.35 mM PMSF. After precipitating protein contaminants in 0.38 mg/ml ammonium sulfate, the decanted supernatant was dialyzed into 300 mM NaCl, 0.2 mM EDTA, 10 mM Tris-HCl (pH 7.2) and purified on a CM Sephadex C25 (Sigma) column with a gradient from 0.3 - 1 M NaCl. After extensive dialysis into water, purified GH5 was stored frozen in water. GH5 concentrations were determined from extinction coefficients as described in Chapter 2.

#### *3.2.1.2 Isolation of H5 from chicken erythrocytes*

Native H5 was purified in a protocol based on Garcia-Martinez et al. (1991). 15 mls of chicken blood (Lampire) were disrupted (by pipeting vigorously) in ice cold homogenization buffer (10 mM Tris-HCl (pH 7.8), 0.4 mM EDTA, 120 mM KCl, 30 mM

NaCl, 0.2% nonidet P-40, 0.3 mM PMSF) with 10 volumes of homogenization buffer for every volume of chick blood. Cells were then pelleted at 9 krpm for 10 minutes in a GSA rotor at 4 °C. The pellet was resuspended in ice cold homogenization buffer (without nonidet P-40) by initially adding a small volume of buffer, disrupting the cells as stated above (with mild homogenization with a tissuemize if necessary), then diluting the suspension in a larger volume of ice cold homogenization buffer (without nonidet P-40). The suspension was then spun down in a GSA rotor at 7 krpm for 10 minutes. This step was repeated until the pellet appeared white, indicating purified nuclei. Nuclei were stored in homogenization buffer on ice at this point, if necessary.

Chromatin was extracted by hypotonically lysing the pelleted nuclei in roughly 50 volumes of 0.2 mM EDTA and 0.1 mM PMSF per nuclei volume. The nuclear pellet was stirred briskly for 1 hour, then homogenized with a tissuemizer to break up the aggregated chromatin "blob". The suspension was sedimented in an SS-34 rotor at 13,000 rpm for 30 minutes, the supernatant decanted, and the chromatin "jelly" resuspended in roughly 50 "pellet volumes" of 625 mM NaCl, 0.2 mM EDTA, 0.1 mM PMSF and stirred briskly overnight. Chromatin was subsequently pelleted, and the supernatant (containing linker histones) was decanted and stored separately on ice. The chromatin gel was resuspended, a second time, in 625 mM NaCl, 0.2 mM EDTA, vortexed briefly, and pelleted; the supernatants (containing linker binding proteins) from the two extraction were combined. The supernatant was diluted to 500 mM NaCl and applied at 20 mls/hour to a CM Sephadex C25 (Sigma) column (2.7 cm x 5.0 cm) equilibrated with 500 mM NaCl, 10 mM Tris-HCl (pH 7.8), 0.2 mM EDTA, 0.1 mM PMSF by washing the column with 3 flow-through volumes of buffer (as determined by bromophenol blue dye). Linker

high mobility group proteins were then eluted off the column with four bed volumes of 500 mM NaCl, 10 mM Tris-HCl (pH 7.8), 0.2 mM EDTA, 0.1 mM PMSF; H1 was eluted off with four bed volumes of 800 mM NaCl, 10 mM Tris-HCl (pH 7.8), 0.2 mM EDTA, 0.1 mM PMSF; and H5 was eluted off in two volumes of 1.6 M NaCl, 10 mM Tris-HCl (pH 7.8) 0.2 mM EDTA, 0.1 mM PMSF discrete salt steps. H5 was extensively dialyzed in water, and stored frozen in water. H5 concentrations were determined from an extinction coefficients as described in Chapter 2.

### *3.2.1.3 Octamer Preparation isolation from chicken erythrocytes*

Octamers were isolated by a procedure loosely based on the original procedure from Yager et al. (1989). Briefly, chicken erythrocyte nuclei (isolated as described in the isolation of H5) were diluted to 70 OD(260 nm) (as measured in 0.1 M NaOH) in homogenization buffer, and digested with micrococcal nuclease (Worthington) at a final concentration of 150 units/ml at 37 °C for 20 minutes. The micrococcal nuclease was stored frozen in 15% glycerol at 45,000 units/ml. After pelleting, the nuclei were hypotonically lysed in 0.25 mM EDTA, 0.1 mM PMSF with nuclei diluted to 50 O.D.s (as measured in 0.1 M NaOH). Linker histones were removed by bringing the solution to 350 mM NaCl, and stirring for 3 hours on ice with 30 mg/ml of CM Sephadex C25. The CM Sephadex C25 was pelleted with an HB4 rotor at 6.5 krpm for 30 minutes. Soluble chromatin was diluted to 50 OD(260 nm), and further digested with micrococcal nuclease until sub-core particles were detected on a 6% polyacrylamide gel buffered in TAE. Sample were then concentrated to 1000 OD(260 nm) with a XM50 filter (Amicon), and a

1 ml sample was loaded onto a hydroxyapatite column in 0.1 M potassium-phosphate (pH 6.7), 2.2 M NaCl as described by Simon and Felsenfeld (1979). Eluted samples were pool and identified by SDS-PAGE (Laemmli, 1970). The concentration of finally purified octamers was determined from  $\epsilon = 4.3 \text{ mg}^{-1} \text{ cm}^{-1} \text{ ml}$  at 230 nm (Stein, 1979).

### 3.2.2 DNA purification

#### *3.2.2.1 Oligonucleotide preparation*

A 22 b.p. single-stranded oligonucleotide with the sequence GTA GTA ACG GAA GCC AGG TAT T, and it's complementary were generated using a 380A DNA synthesizer (Applied Biosystems, Inc.). The 22 b.p. sequence represents a putative linker histone H1 binding site based on DNA footprinting (Sevall, 1988). Annealed DNA concentrations were roughly approximated by  $\epsilon (260 \text{ nm}) = 20 \text{ } \mu\text{g}^{-1} \text{ ml}^1 \text{ cm}^{-1}$ . Salts associated with DNA synthesis were removed by first dissolving the oligonucleotides in water, then passing the solution through a 0.9 x 2.0 cm G-50 Sephadex NICK column (Pharmacia). The single-stranded oligonucleotide were combined in roughly equimolar proportions in 10 mM NaCl, .2 mM EDTA, (based on  $\epsilon(260 \text{ nm}) = 30.3 \text{ } \mu\text{g}^{-1} \text{ ml}^1 \text{ cm}^{-1}$ ). Samples were raised to 90 °C in a heating block and cooled slowly back to room temperature at the rate of the cooling heating block. Separately, a 42 b.p. oligonucleotide duplex with the sequence CCG GAA TTC GCA TCA TTG CCT TCG GTC CAT AAA GGA ATT CGG was constructed as described for the 22 b.p. oligonucleotide.

It is recognized that the above-described extinction coefficients, in general, are only approximate, and applicable to long DNA's of average GC/AT ratio. However, in the case of the 42 b.p. oligonucleotide, each base is represented in nearly equal proportions, thus making the approximation a valid one. For purposes of annealing, approximating the 22 b.p. anneal oligonucleotide with an average value for the extinction coefficient resulted in a slight overabundance of one strand that theoretically should have resulted in about 10% of the DNA remaining unannealed<sup>1</sup>. However, based on PAGE, no single-stranded oligonucleotides were detected, and using the average extinction coefficient resulted in approximately equal concentrations of DNA for the duplex 22 b.p. and 42 b.p. oligonucleotides (based on gels stained with ethidium bromide stain and UV illuminated) (see Results).

### 3.2.2.2 Long DNA isolation

Two separate protocols were used to produce long DNA for the experiments. For the chymotrypsin studies, pUC19 was prepared using PEG 8000 (Maniatis et al., 1982). Plasmids were isolated from *E. coli* using the alkaline lysis procedure and resuspended in 5 M LiCl which preferential precipitates DNA over RNA. The solution was kept on ice for several hours, brought to 50% isopropanol, then centrifuged for 30 minutes in an SS40 rotor at 10,000 rpm. The samples were treated with RNAase then brought to 0.8 M NaCl / 13% w/v PEG 8000, centrifuged with the pellet resuspended in 10 mM Tris-HCl (pH

---

<sup>1</sup> Estimate based on an  $\epsilon(260)$  of 25,000  $M^{-1} cm^{-1}$  and 22,000  $M^{-1} cm^{-1}$  for the 22 b.p. oligonucleotide and its complimentary strand based the molar extinction coefficients of each base (Wallace and Miyada, 1987).

=7.8). DNA was further purified with phenol:chloroform:isoamyl alcohol (25:24:1) extraction and ethanol precipitated following common procedures (Maniatis et al, 1982).

Studies of reconstituted chromatin utilized pPol208-12, which includes twelve tandem copies of a 5S rDNA nucleosome positioning sequence (208 b.p.) from *Lytechinus variegatus* cloned into pUC19 (Georgel et al., 1993). Briefly, DH5 $\alpha$  *E. Coli* transformed with pPol208-12 were grown to 0.6 O.D.s in LB broth with chloramphenicol added to 0.017 mg/ml and shaken overnight at 37 °C. Cells were then processed by the alkaline lysis procedure (Maniatis et al, 1982). DNA was further purified by resuspending ethanol-precipitated pPol208-12 in 25 mls of T.E. (10 mM Tris-HCl (pH 7.8), 0.2 mM EDTA), with 2 mls of ethidium bromide (10 mg/ml), and 27 g of CsCl for a final solution with a density of 1.55 g/ml. The solution was transferred to quick-seal tubes (Beckman) and centrifuged for 18 hours in a Ti65.2 rotor at 45,000 at room temperature. The band corresponding to supercoiled DNA was extracted from the quick-seal tube, and ethidium bromide was removed with n-butanol. The DNA sample were then diluted with 3 volumes of water, and precipitated in 70% ethanol. pPol208-12 was cleaved with either Hha I or Hinp I according to manufactures recommended procedure (New England Biolabs), and the 2600 b.p. insert was separated by pUC19-related fragments (< 400 b.p.) using a 115 ml Ultragel A2 column as described in (Hansen et al., 1989). DNA concentrations were determined by  $\epsilon(260 \text{ nm}) = 20 \mu\text{g}^{-1}\text{cm}^{-1}\text{ml}$ .

### 3.2.3 Salt extraction studies of the GH5-DNA aggregate

GH5 at 0.05 mg/ml was incubated with DNA at 0.05 mg/ml in 0.2 mM EDTA, 10 mM sodium phosphate (pH 7.2). Samples were then stored on ice overnight to induce aggregation. NaCl was added from a 10x NaCl stock dropwise (with rapid pipeting after each drop) to final salt concentration between 0 - 500 mM NaCl. Samples were set on ice for 1 hour, shaken at 4 °C for 30 minutes, then set on ice for 3 more hours. Release of DNA from the complex was detected by removing an aliquot and analyzing it with native PAGE run in TBE buffer. SDS solubility of GH5 in the aggregate complex was determined by mixing a sample briefly in 2 x SDS loading buffer (0.125 M Tris-HCl (pH 6.8), 4% SDS, 20% glycerol, 0.04% bromophenol blue) then analyzing the sample with SDS-PAGE (Laemmli, 1970).

### 3.2.4 Effect of urea on aggregate formation

First, nucleoprotein aggregates were formed by incubating GH5 or H5 with DNA overnight on ice. GH5 at 170% (w/w) was incubated with the 22 b.p. DNA at 0.033 mg/ml in 10 mM NaCl, 0.2 mM EDTA, 5 mM sodium phosphate (pH 7.2), and from 0 M- 6 M urea for 30 minutes at 4 °C (with shaking). Similarly, H5:DNA at 120% (w/w) was incubated with Hha I cut pPol208-12 at 0.033 mg/ml. Samples were mixed with SDS loading buffer as described above for the salt-dependent dissociation experiments.

### 3.2.5 Chymotrypsin digestion of H5 bound to DNA

H5 at 0.032 mg/ml was incubated in the presence and absence of pUC19 (purified by the PEG 8000 protocol) in 10 mM NaCl, 0.2 mM EDTA, 10 mM sodium phosphate buffer (pH 7.2) with H5 bound to DNA at 80% H5:DNA (w/w). Samples were shaken at room temperature or 37 °C for 45 minutes, chymotrypsin (frozen in 10 mM Tris-HCl (pH 7.8)) was added from a 6 µg/ml stock to a final concentration of 0.2 µg/ml. Chymotrypsin digestion was conducted at either room temperature or at 37°C with proteolysis stopped by bringing the reaction to 1 mM PMSF, and adding SDS loading buffer. Samples were immediately frozen in liquid nitrogen and stored at -20 °C until analysis with SDS-PAGE.

### 3.2.6 Computer modeling study of GH5 bound to DNA

Modeling was performed with INSIGHT II (Biosyms Inc., San Diego) with molecular coordinates obtained from the PDB data base via the Brookhaven National Laboratories internet web site (<http://www.bnl.gov/bnl.html>).

### 3.2.7 Reconstitution of octamers and H5 onto the 208-12 DNA

Proteins and DNA were combined at a high NaCl concentration, and dialyzed into T.E. buffer in a technique referred to as salt dialysis (Hansen et al., 1989). Briefly, DNA between 0.04-0.075 mg/ml was mixed with octamers in 2 M NaCl, 10 mM Tris-HCl (pH 7.8), 0.2 mM EDTA, and 0.1% nonidet P-40 (Sigma), and placed in Spectrapore 3 (M.W.C.O. 3500) dialysis tubing that was soaked overnight in the same buffer

(Meersseman et al., 1991). Samples were then dialyzed (at 4 °C with stirring) into 1 M NaCl, T.E. for several hours, then to 0.75 M NaCl, T.E for several hours. After the 0.75 M, T.E. step, the dialysis bag contents were removed from the dialysis bag, the sample volume was measured, then returned with H5 and polyglutamic acid (Sigma) (with an average molecular weight of 10 kDa) in 0.75 M NaCl. PGA was added to a final concentration of 2 mg/ml as reported by Stein and Mitchell (1988). The dialysis bag was then placed in 0.63 M NaCl, T.E. for several hours. The sample was reduced by 100 mM NaCl increments down to T.E. with each step lasting about an hour and a half; the sample was dialyzed twice in T.E. for several hours each. Reconstituted chromatin was generally run on either 1% or 0.3 % agarose gels (TAE) and detected by ethidium bromide staining / UV illuminance. Reconstituted chromatin was stored on ice.

### 3.2.8 Velocity analytical ultracentrifugation

A Beckman XLA was used to analyze reconstituted 208-12 DNA. Typically, 400  $\mu$ l samples (along with buffer control) were analyzed at 260 nm at 20 minute time points over a couple hours. Rotor speeds were set between 20,000-25,000 rpm with the high speeds applied to octamer reconstitutes, and the slower speeds generally applied to reconstitutes which included H5. Sedimentation experiments were conducted at 21 °C. Data was plotted as the natural log of the distance of the boundary half-way point as a function of time (seconds). The sedimentation coefficient was determined from,  $s \times \omega^2 = \Delta \ln r / \Delta t$ , where  $s$  is the sedimentation coefficient,  $\omega$  is the rotor speed (rads/second),  $t$  is time (seconds), and  $r$  is the midpoint of the boundary at time  $t$ . All data were recorded at 21°C, and were corrected to  $s_{20,w}$  values by standard methods (van Holde, 1985).

### 3.2.9 Restriction digestion of reconstituted chromatin

Chromatin reconstituted with H5 and histone octamers were digested at room temperature basically following Hansen and Lohr (1993). DNA reconstituted with histone octamers and H5 was digested for up to 10 hours at room with EcoR I at 0.7 units/ $\mu$ l in 3.5 mM MgCl<sub>2</sub>, 30 mM Tris-HCl (pH 7.8), 50 mM NaCl, 0.01% Triton X-100. Reaction were brought to 5 mM EDTA to stop DNA digestion. The amount of chromatin (in terms of DNA) for the reactions was typically about 0.05 mg/ml. After digestion, samples were analyzed by PAGE (see below).

### 3.2.10 Dialysis of H5 from the reconstituted chromatin

Chromatin reconstituted with H5 in 10 mM NaCl, T.E. (at a final DNA concentration of 0.05 mg/ml) was placed in Spectrapore 6 dialysis bag which has a molecular weight cut-off of 50,000 daltons. Bovine serum album was added to a final concentration of 0.05 mg/ml. Samples were dialyzed into a large volume of the same buffer with samples removed directly from the bag at the appropriate time points. Each aliquot was immediately treated with 7.5 units/ml of micrococcal for a couple hours at room temperature in 1 mM CaCl<sub>2</sub>, 50 mM NaCl, in order to digest chromatin for efficient removal of H5 in 2 x SDS loading buffer. Samples were then analyzed by silver stained SDS/polyacrylamide gels, and referenced to albumin which has a MW of 66,000, and was retained within the dialysis bag.

### 3.2.11 Polyacrylamide gel electrophoresis (PAGE)

#### *3.2.11.1 SDS-PAGE*

SDS/polyacrylamide gels were constructed based on Laemmli (1970)(see also Chapter 4). Gels were silver stained by a diamine silver staining protocol (Sasse and Gallagher, 1991; see also Chapter 4) that included: fixing the gels in 45% methanol / 9 % acetic acid for several hours, washing the gel for about a day with repeated changes of water, then staining and developing the gel. Gels were then silver stained as described in Chapter 4. For coomassie staining: the gel was stained for 30 minutes in 45% methanol (v/v), 9% acetic acid, and 0.25% (w/v) coomassie G-250 then destained in 7.5% acetic acid and 5% methanol with a kimwipe to absorb coomassie from gel. Gels were quantitated by analyzing the scans of photographs with NIH Image (version 1.57) (O'Neill et al., 1989).

#### *3.2.11.2 Native PAGE*

For linker histone/oligonucleotide binding studies, samples (usually 0.5  $\mu$ g of material with respect to DNA) were analyzed on gels consisting of 15% polyacrylamide:bisacrylamide (30:8), and were run on slab gels (about 0.75 mm), typically, at 3.8 volts/cm at room temperature in TBE / Tris-base:borate:EDTA (5x: 109 g Tris-base, 55.6 g boric acid, 9.31 g EDTA / 1 liter). Nucleosome-related analysis was

performed with 6% polyacrylamide:bisacrylamide (29:1) at 13.5 volts/cm at room temperature in TAE / Tris-base:acetic acid:EDTA (50x: 242 g Tris-base, 57.1 mls glacial acetic acid, 14.6 g EDTA / 1 liter). DNA and nucleoprotein complexes were detected by the UV illuminance of gels stained in 0.5 µg/ml ethidium bromide. Samples were mixed with loading buffer (10x: 1 % bromophenol blue, 1 % xylene cyanol, 50 % glycerol) immediately before application to gel. Gel quantitation was performed as described above for SDS-PAGE.

### **3.3 Results of model H5 (and GH5) DNA binding studies**

#### **3.3.1 Interaction of H5 and GH5 with small DNA oligonucleotides**

H5 and GH5 were bound to 22 b.p. and 42 b.p. oligonucleotides. The 22 b.p. oligonucleotide contained a putative H1-binding sequence from the rat serum albumin gene (Sevall, 1988). In the first experiment, the two oligonucleotides were competed against one another, and results unambiguously show that both GH5 and H5 were preferentially bound to the 42 b.p. oligonucleotide (Figure 3.1A). This figure also demonstrates a common feature of linker histone binding to linear DNA. Gel shifts were never observed; the DNA was divided, because of aggregation and cooperativity, into two fractions--a fraction of very large aggregates, which could not enter the gel, and uncomplexed free DNA molecules. As more histones were added, the fraction of the latter decreased until it eventually vanished. Because of the complexity of this reaction,

**Figure 3.1.** Competitive binding between a 22 b.p. and 42 b.p. oligonucleotides by GH5 and H5. (A) Separately, GH5 and H5 were incubated with equal concentrations of the two oligonucleotides both at 0.04 mg/ml in buffered solution containing 10 mM NaCl, 10 mM sodium phosphate, 0.2 mM EDTA. GH5 was titrated at GH5:DNA(w/w) ratios of 50%, lane a; 100%, lane b; 200%, lane c; and 300%, lane d. H5 was titrated at H5:DNA (w/w) ratios of 25%, lane e; 50%, lane f; 100%, lane g; and 150%, lane h. (B) Plotting the mass amount of free DNA for both the 22 b.p. (*solid squares*), and 42 b.p. (*solid circles*) oligonucleotides in the H5 binding study (lanes e-h). (C) Plotting the mass amount of free DNA for both the 22 b.p. (*open squares*), and 42 b.p. (*open circles*) oligonucleotides in the GH5 binding study (lanes a-d). The *dashed line* indicates the approximate average of the first four values for the 22 b.p. oligonucleotide, and serve as an initial reference point. The concentration of the 42 b.p. oligonucleotide was approximated by  $\epsilon_{260} = 50 \mu\text{g ml}^{-1} \text{cm}^{-1}$ . The concentration of the 22 b.p. oligonucleotide was made roughly equivalent by comparing it to the 42 b.p. oligonucleotide via ethidium bromide-stained polyacrylamide gels.

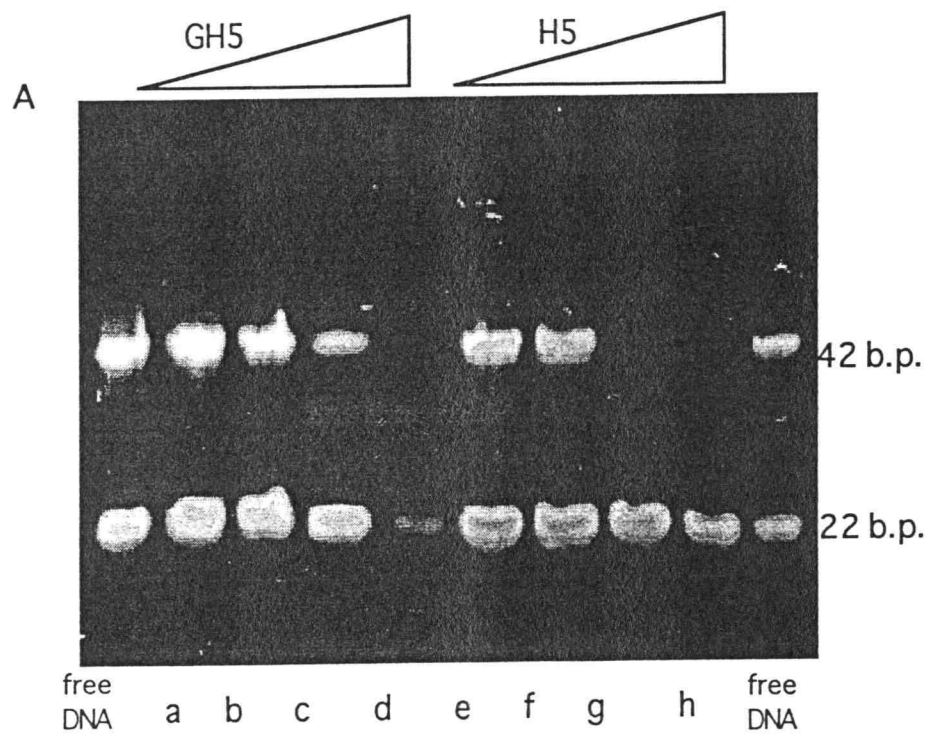
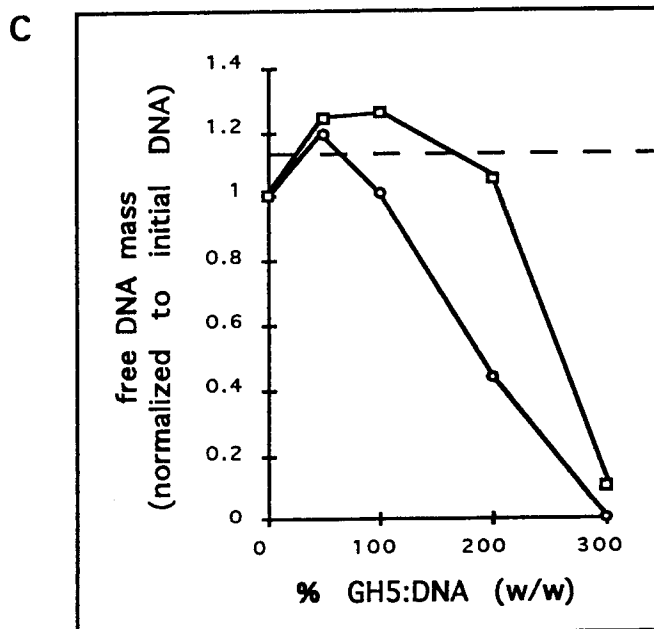
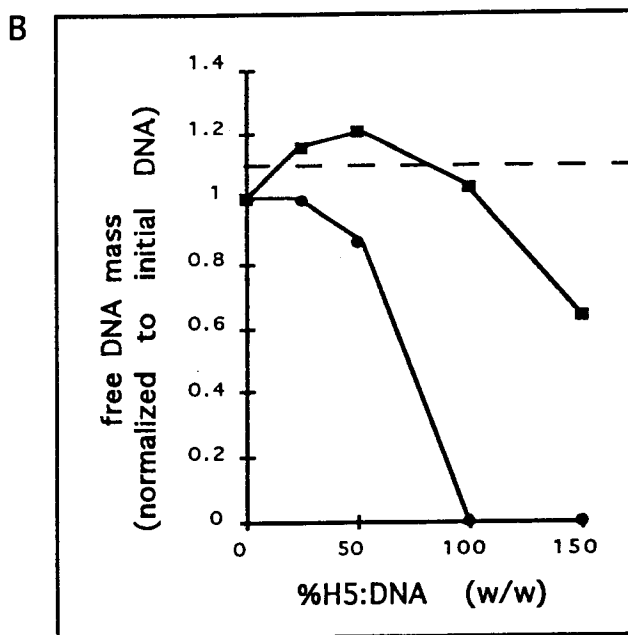


Figure 3.1



- H5-42 b.p. DNA oligonucleotide
- H5-22 b.p. DNA oligonucleotide
- GH5-42 b.p. DNA oligonucleotide
- GH5-22 b.p. DNA oligonucleotide

Figure 3.1 (continued)

which involves both cooperative binding and aggregation, it was not possible to describe linker histone/ DNA binding by any simple binding model.

The results, shown in Figure 3.1, while highlighting the nonspecific nature of linker histone binding to DNA, also demonstrated that the putative H1 binding sequence showed no strong preference for GH5 and H5 binding. Furthermore, the way GH5 and H5 preferentially bound the 42 b.p. oligonucleotide illustrates an interesting difference between the proteins in DNA binding. By comparing the free DNA plots for H5 (Figure 3.1B), and for GH5 (Figure 3.1C), H5 was observed to display a much stronger preference for to the 42 b.p. oligonucleotide with nearly all of it being bound before H5 began to bind the 22 b.p. DNA (Figure 3.1B, 100% w/w point; Figure 3.1A, lane g). This may indicate that the 22 b.p. DNA was too small a substrate for effective H5 binding, and would support a binding site size of 47 b.p. reported by Clark and Thomas (1988).

More complete binding titrations, using the 22 b.p. oligonucleotide with either GH5 or H5 in 10 mM sodium phosphate (pH 7.2) are shown in Figure 3.2A and Figure 3.2B. The plots represent the amount of unbound DNA as a function of input protein concentration. Because we cannot describe the complex binding process by a simple model, the data has been fitted by empirical polynomial equations, which may have no mechanistic meaning. It is possible to derive "cooperative" binding models which fit such data, but it would be very difficult to take into account the accompanying aggregation process. The general form of the equation that was found to describe protein "binding" to the oligonucleotides,  $y^5 = a - b x^3$ , is the same for GH5 and H5, though it is unclear whether this has any mechanistic significance. The apparently enhanced apparent binding

Figure 3.2. Binding curves of GH5 or H5 titrated onto a 22 b.p. oligonucleotide. (A) GH5 incubated for 1-2 hours with the 22 b.p. oligonucleotide at approximately 0.04 mg/ml on ice in buffer containing 10 mM sodium phosphate (pH 7.2), 0.2 mM EDTA. The curve describing a best-fit of the data is:  $y^5 = 1.04 - 1.80x^3$  ( $R^2 = 0.775$ ). (B) H5 was bound to the 22 b.p. oligonucleotide at approximately 0.03 mg/ml and 0.04 mg/ml as described for GH5. The curve describing the best-fit of the data is:  $y^5 = 1.01 - 5.24x^3$  ( $R^2 = 0.879$ ). Refer to legend for symbol explanation. Plots based on 15% native polyacrylamide gels stained with ethidium bromide with curves generated by Table Curves 4 (Jandel Scientific).

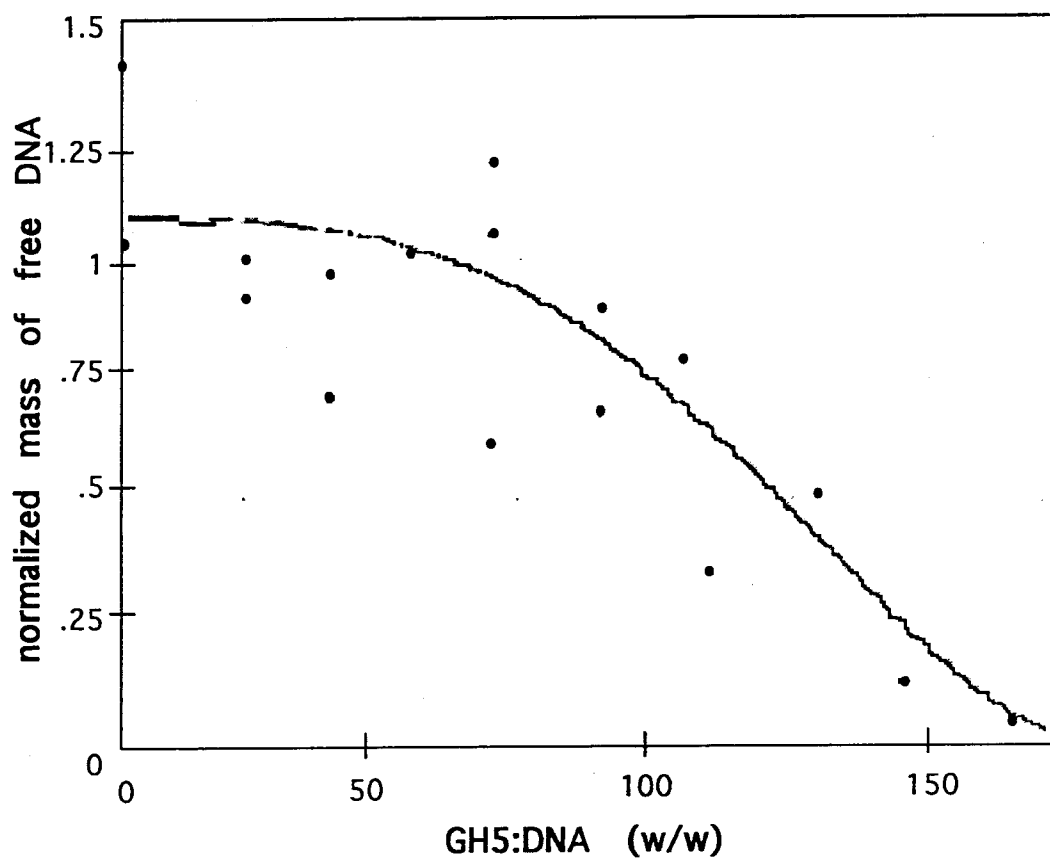


Figure 3.2

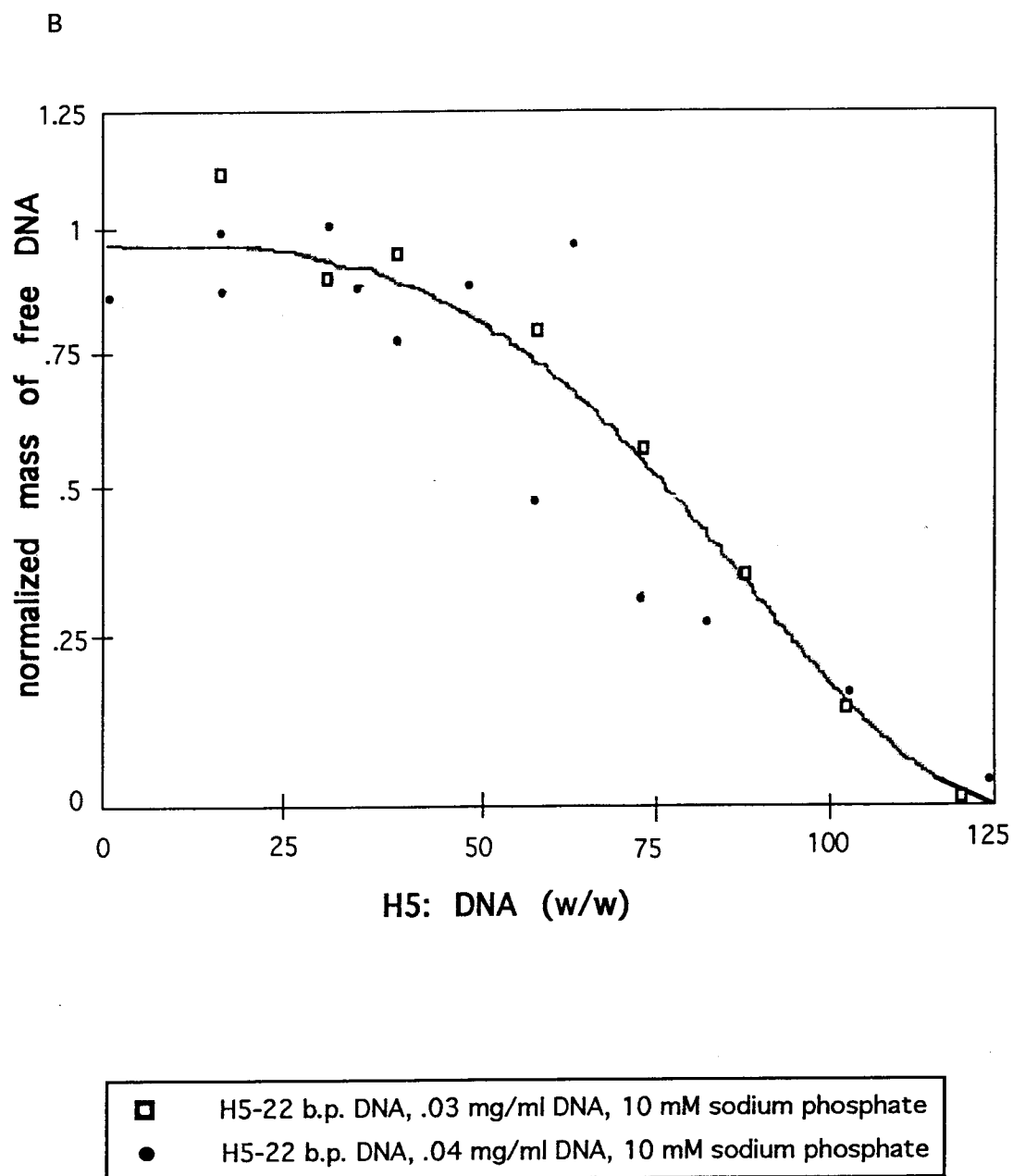


Figure 3.2 (continued)

by H5 (compared to GH5) may be the result of a higher binding affinity for DNA (relative to GH5) (Segers et al., 1991). However, considering that the DNA concentrations used in the study were well above the reported  $K_d$  of  $3 \times 10^{-9}$  M at 10 mM NaCl (Watanabe, 1985), meaningful quantitation of binding affinities is impossible. Another important observation: H5 appeared to interact identically with the oligonucleotides at a DNA concentration of 0.03 mg/ml and 0.04 mg/ml (Figure 3.2B). This suggests that H5 did not bind as a preformed complex, but rather bound as individual isolated proteins (Lohman, 1992). Of course, interpretation of any binding data would have to take into consideration the effects of aggregation, which appears to involve non-uniform binding affinities for DNA by the aggregate complex (Draves et al., 1992).

### 3.3.2 Determining the binding-site size of GH5

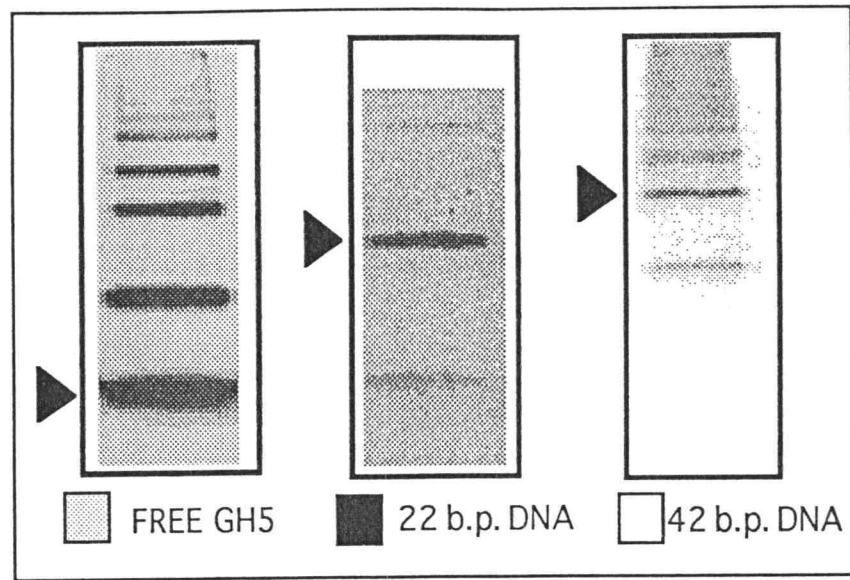
An effective, straight-forward technique was developed to determine the number of GH5 molecules preferentially crosslinked when bound to a DNA oligonucleotide, which likely represents the maximum number of GH5 molecules that can be easily accommodated on that oligonucleotide. The technique entails crosslinking GH5 with DSP on oligonucleotides of various sizes. In this study, GH5 at 0.04 mg/ml was bound to either a 22 b.p. oligonucleotide or a 42 b.p. oligonucleotide at 100% GH5:DNA (w/w) in 8 mM NaCl, 10 mM sodium phosphate buffer, 0.2 mM EDTA for 35 minutes, then reacted with DSP for 2 hours at room temperature, then quenched in 0.05 M glycine. Loading buffer 2 X SDS was then added to the reaction mixture with subsequent separation on an 18% Laemmli gel. Under these conditions, 0.001 mg/ml DSP was optimal for GH5

crosslinking onto the 42 b.p. oligonucleotide, and 0.01 mg/ml was optimal for GH5 crosslinking onto the 22 b.p. oligonucleotide. In the above-described reaction conditions, greater DSP concentrations lead to over-crosslinking in which no clear preferred number of crosslinked molecules was observed (data not shown). As a comparison, GH5 free in solution at 0.036 mM was crosslinked in 0.1 mg/ml DSP for 30 minutes in 400 mM NaCl, 5 mM sodium phosphate, 0.2 mM EDTA. The reaction was also quenched by bringing the reaction to 0.05 M glycine.

A comparative histogram plotting the abundance for various protein oligomers clearly shows that the distribution was influenced markedly by the oligonucleotide size (Figure 3.3A,3.3B). While GH5 crosslinked free in solution displayed a molar logarithmic distribution (see Chapter 2), the histograms for GH5 DSP-crosslinked on the 22 b.p. and 42 b.p. oligonucleotides showed a preference for crosslinking at 2 and 3 GH5 molecules, respectively. However, there was also extensive interaction between separate GH5-DNA complexes (particularly for the 42 b.p.-histone complexes) as reflected by protein oligomer sizes extending to the well of the gel (Figure 3.3A). The complexes larger than trimers must result from crosslinking between GH5 molecules on different complexes. In summary, a core group of closely-associated, DNA-bound proteins were crosslinked together onto the oligonucleotide at low DSP concentrations. The clear dependence of the number of crosslinked molecules on the size of the oligonucleotide suggests that protein-protein contacts were due to protein assembly on individual DNA fragments. Therefore, these results argue that contacts between GH5 molecules bound to the same DNA molecule was preferred over interactions between GH5 molecules bound to separate

**Figure 3.3.** Estimating the number of GH5 molecules bound to 22 b.p. and 42 b.p. oligonucleotides. Histogram of GH5 (mass amount) for individual protein oligomer sizes normalized to the total mass amount (up to a pentamer-sized complex). (white bar, GH5 DSP crosslinked bound to a 42 b.p. oligonucleotide; black bar, GH5 DSP crosslinked free in solution; and gray bar, GH5 DSP crosslinked to a 22 b.p. oligonucleotide). Insert: representative lanes of 18% Laemmli gel from crosslinking experiment. From left to right, GH5 at 0.036 mM crosslinked free in solution at 0.1 mg/ml DSP; GH5 crosslinked to a 22 b.p. oligonucleotide at approximately 100% (w/w) in 0.01 mg/ml DSP; and GH5 crosslinked to a 42 b.p. oligonucleotide at 100% (w/w) in 0.01 mg/ml DSP. Arrows point to the single most populous GH5 oligomer (mass amount), in each case.

A



B

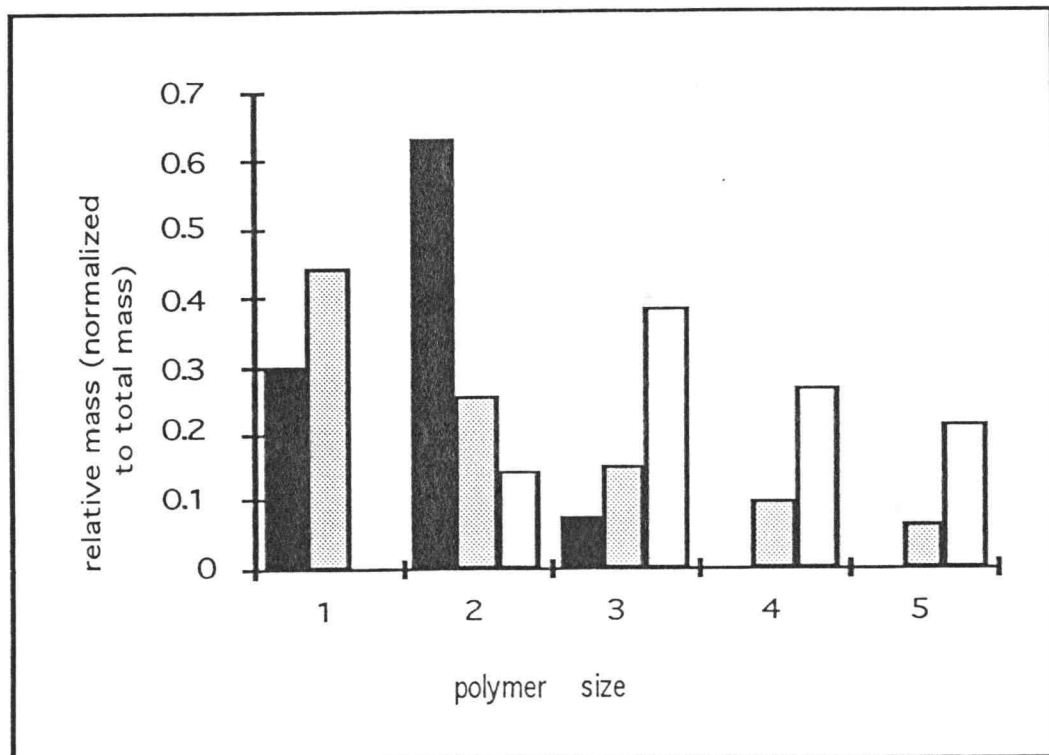


Figure 3.3

DNA complexes, though these contacts were observed, and gave rise to nucleoprotein complex oligomerization.

By dividing the number of base pairs of the oligonucleotide by the mode of the number of crosslinked GH5 molecules the binding site size can be estimated, though it is probably an overestimate since the ends of the DNA (that are normally unbound) are included in the calculation. A binding site size of 11 b.p./GH5 was calculated in this way for the 22 b.p. DNA, and 14 b.p./GH5 for the 42 b.p. DNA. These values are experimentally indistinguishable, and are also consistent with the value of 10 b.p./GH5 previously estimated by Thomas et al. (1992) in a less direct fashion.

### 3.3.3 Binding H5 and GH5 to "long" linear and supercoiled DNA

It is well established that linker histones interact with linear and supercoiled DNA differently. First, supercoiled DNA has a higher binding affinity for linker histones than does the corresponding linear or relaxed forms (Vogel and Singer, 1974)), and binding affinity increases with increasing linking number (Krylov et al., 1993). Second, linker histones bind and organize linear and supercoiled DNA differently. In the former case, binding saturates some fragments while leaving other DNAs completely unbound as described here (Figure 3.1A) and by other authors (Singer and Singer, 1978; Liao and Cole, 1981). For supercoiled DNA, linker histones bind plasmid DNA more uniformly with all available DNA molecules receiving approximately equivalent amount of protein (Yaneva and Zlatanova, 1991). Additionally, crosslinking studies presented in Chapter 2, suggest that GH5 binds supercoiled DNA in relatively isolated clusters-possibly indicating

binding at crossovers, while linear DNA appears to become cooperatively saturated.

Despite these differences, linker histones appear to exhibit some cooperativity with both types of DNAs, since proteins are observed to closely associate in clusters on both DNA conformations (De Bernardin et al., 1986).

GH5 and H5 binding to supercoiled and linear DNA was further elucidated by conducting binding studies with native gel electrophoresis. For linear DNA binding, GH5 and H5, separately, were incubated with Hha I cut pPol208-12, which produces a large 2600 b.p. pUC19-based fragment and a number of smaller fragments around 200 b.p. The reaction solution included 1 mM sodium phosphate (pH 7.2), 0.2 mM EDTA, and either 10 mM or 100 mM NaCl with DNA at 0.024 mg/ml. Complexes were then crosslinked with 0.1% glutaraldehyde at 4 °C overnight, and separated on a native 1% agarose gel run in TAE. As reported previously, linear fragments underwent the signature of all-or-none binding (Figure 3.4A, 3.4B) with H5 complexing with considerably more DNA than GH5. An increase in NaCl led to an apparent reduction in the amount of free DNA for both GH5 and H5. But as suggested by a plot of free DNA (normalized to a standard) from Figure 3.4A, NaCl only effected apparent binding at low GH5:DNA ratios (Figure 3.4D); at higher GH5:DNA (w/w) ratios no effect of salt on the amount of free DNA was observed. This is best illustrated by comparing samples 10% GH5:DNA (w/w) and 80% GH5:DNA (w/w) at the two salt concentrations (Figure 3.4D). For the former, about 10% of the DNA was complexed to GH5 in samples incubated in 10 mM NaCl, compared to 35% for samples incubated in 100 mM NaCl. For the latter, the amount of DNA complexed to GH5 was about 40% at both salt concentrations. Finally, in corroboration with the

**Figure 3.4.** The effect of NaCl concentration and DNA topology on GH5 and H5 binding to long DNA. (A) Either GH5 or H5 was incubated with Hha I cut pPol208-12 in buffered solution containing either 10 mM or 100 mM NaCl. Hha I cut pPol208-12 produces a large 2600 b.p. fragment consisting of 12 tandem copies of the *Lytechinus variegatus* 5S DNA (pictured in illustration), along with fragments smaller than 400 b.p. that are not shown. The reaction was incubated on ice for 1 hour with DNA at 0.024 mg/ml as described in the accompanying text. Samples were loaded onto a 1% agarose gel, and stained in ethidium bromide (0.5 µg/ml). Lanes a-d, GH5 bound to Hha I cut pPol208-12 in buffered solution containing 10 mM NaCl; lanes e-h, GH5 bound to Hha I cut pPol208-12 in buffer solution containing 100 mM NaCl. From left to right, (GH5:DNA (w/w)): lanes a and e, 10%; lanes b and f, 50%; lanes c and g, 80%; and lanes d and h, 140%. (B) Similarly, H5 was bound to Hha I cut pPol208-12 DNA; lanes i-l, H5 bound in buffered solution containing 10 mM NaCl, and lanes m-p, H5 bound in buffered solution containing 100 mM NaCl. (H5:DNA (w/w)): lanes a and e, 10%; lanes b and f, 50%; lanes c and g, 80%; and lanes d and h, 140%. (C) Either GH5 or H5 was incubated with plasmid pUC19 at 0.04 mg/ml on ice for 2 hours as described in the text. Lanes a-d, GH5 bound to pUC19, and lanes e-g, H5 bound to pUC19. From left to right, (GH5:DNA (w/w)): lane a, 50%; lane b, 100%; lane c, 150%; and lane d, 200%; (H5:DNA (w/w)): lane e, 50%; lane f, 100%; and lane g, 150%. (D) Plot of free DNA normalized to the initial DNA from (A) for GH5 bound to Hha I cut pPol208-12 in buffered solution containing either 10 mM NaCl (*filled circles*), and 100 mM NaCl (*filled squares*).

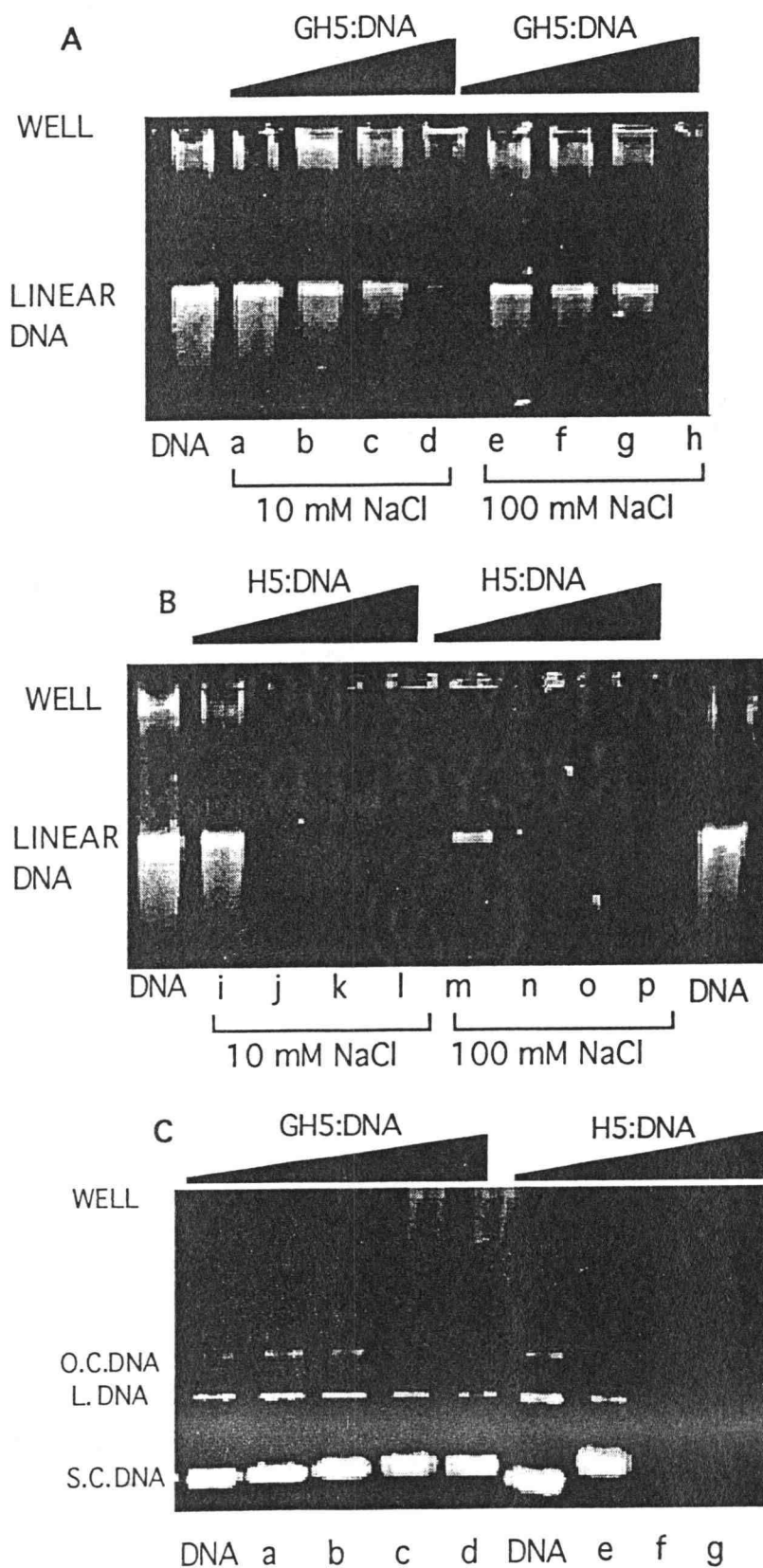


Figure 3.4

D

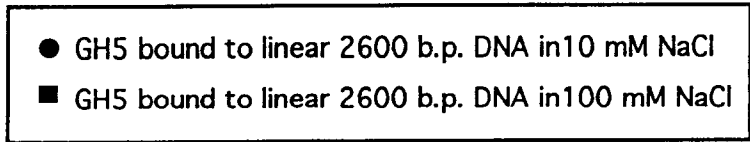
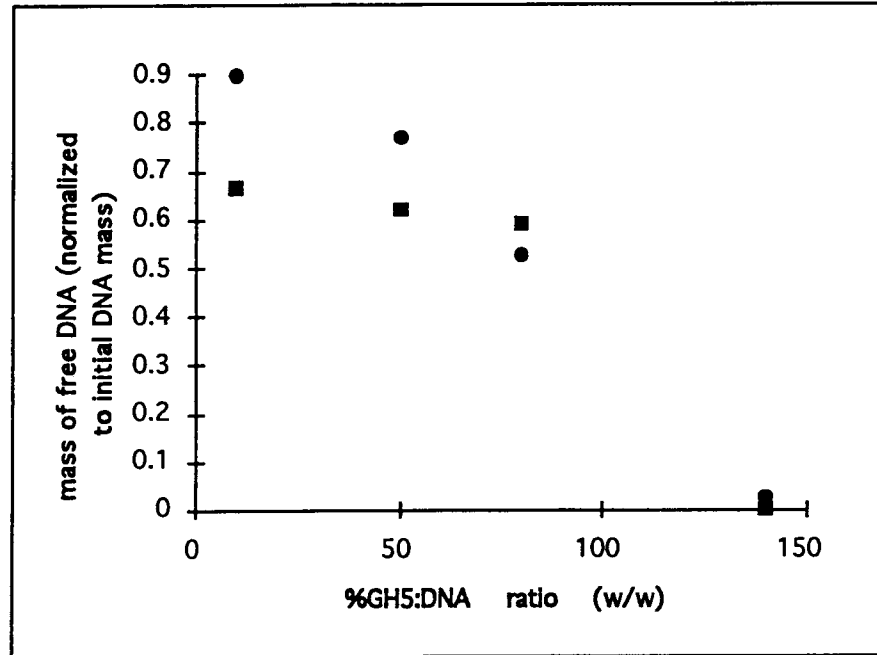


Figure 3.4 (continued)

above-described finding that GH5 bound the 22 b.p. oligonucleotide with a lower affinity than did H5, more Hha I cut pPol208-12 was associated in aggregate with H5 than was GH5, under similar binding conditions.

Curiously, the finding that higher NaCl concentrations increased apparent DNA binding affinity is contrary to results expected from counterion binding theory. Counterion binding theory predicts that protein binding to DNA is an entropy driven process facilitated by the release of sodium ions from DNA phosphate groups, and related by:  $d \log K_{\text{obs}} = -Z \psi d \log MX$ , where  $K_{\text{obs}}$  is the affinity constant,  $Z$  is the number of phosphates neutralized by the DNA binding site of the protein,  $\psi$  is a constant reflecting the fraction of phosphates neutralized by NaCl, and  $MX$  is the NaCl concentration (Lohman, 1986). From this relationship,  $K_{\text{obs}}$  should decrease with increasing NaCl quite unlike the results observed for H5 and GH5. In order to explain this counterintuitive result, the higher NaCl concentration may instead be affecting protein cooperativity (Watanabe, 1986; Clark and Thomas, 1986). Cooperativity,  $\omega$ , a unitless parameter, contributes to overall binding free energy,  $\Delta G^{\circ}_{\text{total binding}}$  by  $\Delta G^{\circ}_{\text{coop}} = -RT \ln \omega$ . Thus positive cooperativity (where  $\omega > 1$ ), increases binding affinity, as reflected by  $\Delta G^{\circ}_{\text{total binding}} = \Delta G^{\circ}_{\text{monomer}} + \Delta G^{\circ}_{\text{coop}}$ , where  $\Delta G^{\circ}_{\text{monomer}}$  is the binding free energy for a singly-bound protein. As an alternative explanation, salt may enhance the ability for nucleoprotein complexes to acquire additional DNA, and thereby aggregate. Previous reports support the latter explanation since: (a) neither GH5 (Thomas et al., 1992; Draves et al., 1992) nor H5 (Clark and Thomas, 1988) have been reported to experience a salt-dependent increase in cooperativity, unlike H1 (Table 1.1), (b) E.M. (and other

techniques) indicates that aggregation increases with salt concentrations (Singer and Singer et al., 1978; Laio and Cole, 1981; Clark and Thomas, 1988; De Bernardin et al., 1986), and (c) aggregation is dependent on the number of basic residues in the C-terminal tail, thus supporting the differences in binding between GH5 and H5 (Osipova et al., 1985). While increased cooperativity cannot be completely dismissed in explaining the salt-dependent increase in apparent GH5 and H5 binding to DNA, ubiquitous reports of linker histone-DNA aggregation (Osipova et al., 1985; Clark and Thomas, 1988; Welch and Cole, 1979; Liao and Cole, 1981; Sergers et al., 1991; Singer and Singer, 1978) makes salt-dependent aggregation all the more likely in explaining these results.

In a comparative study, GH5 and H5, separately, were titrated onto supercoiled pUC19 DNA at 0.04 mg/ml in 10 mM sodium phosphate (pH 7.2) and 0.2 mM EDTA (Figure 3.4C). Unlike linear DNA, supercoiled plasmid DNA experienced a retardation rather than saturation and/or aggregation supporting the previous observation by Laio and Cole (1981). Additionally, supercoiled DNA apparently can absorb a larger amount of GH5 and remain solution-soluble than linear DNA. This was evident by the absence of free linear DNA at 140% GH5:DNA (w/w) for linear DNA (Figure 3.4A, lane d and lane h), but little apparent diminishment of free DNA observed for supercoiled DNA even at 200% GH5:DNA (w/w) (Figure 3.4C, lane d). At sufficiently high protein concentration, however, H5 (in contrast to GH5) could also produce aggregation of supercoiled DNA as was evident by the disappearance of soluble H5-pUC19 complexes at 100% H5:DNA (w/w) (Figure 3.4C, lane f and g). As with linear DNA, H5 appeared to have a considerably higher affinity for DNA than did GH5. This difference in effect of GH5 and

H5 on supercoiled DNA is intriguing, and may reflect the ability of H5 tails to reach several distant DNA strands, whereas GH5 can contact only nearby strands.

### 3.3.4 Dissociation of GH5- and H5-induced nucleoprotein aggregates

#### *3.3.4.1 Solubilization of linker histone-DNA complexes (and aggregates) in 2% sodium dodecyl sulfate (SDS)*

Sodium dodecyl sulfate (SDS) is a strong denaturant of protein structure, and insolubility in SDS has been used as a measure of protein aggregation, and plaque formation (Castano et al., 1986). The technique was applied here to the analysis of linker histone-DNA binding on the premise that proteins should be extractable from solution-soluble nucleoprotein complexes by SDS. On the other hand, proteins protected within the aggregated nucleoprotein complex are expected to be less extractable, possibly due to exclusion of SDS molecules. Two general studies were performed to better quantitate the effect of SDS: (a) a comparative treatment of GH5- and H5-DNA complexes with SDS, and (b) a time course of H5-DNA complex solubility in SDS as a function of DNA topology. In the first study, GH5 and H5, separately, were titrated onto Hha I cut pPol208-12 at 0.041 mg/ml in 0.2 mM EDTA, 10 mM sodium phosphate (pH 7.2). The binding reaction was incubated on ice for 1-2 hours, then the contents were treated to 2 x SDS (2% SDS) loading buffer by rapidly pipeting the solution up-and-down. Samples were then separated by SDS-PAGE (0.1% SDS) and silver stained as described in Methods and Materials.

GH5 and H5 complexed to DNA reacted quite differently to the effects of SDS. SDS seemed to have relatively little effect on the H5-DNA complex (Figure 3.5A), while GH5 appeared to be readily dissociated from DNA under nearly identical conditions (Figure 3.5B). This is based on the appearance of free GH5, and absence of H5 entering 18% Laemmli gels in the respective experiments. DNA was also observed to enter the SDS/polyacrylamide gel along with free GH5 (Figure 3.5B). In contrast, free DNA entering SDS/polyacrylamide gels diminished proportional to the H5:DNA input ratio (Figure 3.5A), indicating that the H5 bound the DNA despite the presence of SDS. The H5-DNA binding complex appeared to be in the form of massive aggregates since only free DNA was observed, suggesting the binding complex was too large to enter the stacking gel. Additionally, H5 bound larger DNA fragments preferentially to smaller DNA fragments as previously reported (reviewed in Zlatanova and van Holde, 1996) which suggests nonspecific binding. Overall, under the conditions used, H5 appeared to organize itself into nucleoprotein aggregates, while GH5-DNA complexes were readily dissociated in SDS which suggests a lack of aggregation. It should be noted that GH5-DNA complexes also became insoluble in 2% SDS with longer incubation time (see below).

In a second series of separate experiments that addressed the effects of SDS on linker histone binding, the solubility of H5 in SDS was determined for H5 bound to linear DNA, H5 bound to supercoiled DNA, as well as control without DNA (Figure 3.6). The linear DNA was Hind III cut pBR322, a 4265 b.p. plasmid, and the supercoiled DNA was pML2 $\alpha$ G, pBR322 which contains a portion of the mouse  $\alpha$ -globin gene (Yaneva and Zlatanova, 1992). H5 was bound to the respective DNA at room temperature with samples removed over a time course extending up to about 2 hours. Contents were mixed

**Figure 3.5.** Solubility of GH5 and H5 complexed to Hha I cut pPol208-12 in 2% SDS. (A) Solubility of H5 bound to Hind III linearized pBR322 in 2% SDS as observed from a silver-stained 18% polyacrylamide Laemmli gel (with a final concentration of .1% SDS). From left to right (H5:DNA (w/w), lane a, 0%; lane b, 15%; lane c, 35%; lane d, 50%; lane e, 65%; lane f, 85%; lane g, 105%; lane h, 125%; and lane i, 145%. (B) Solubility of GH5 bound pMAL in 2% SDS as in (A). From left to right (GH5:DNA (w/w), lane a, 25%; lane b, 40%; lane c, 55%; lane d, 70%; lane e, 90%; lane f, 110%; lane g, 130%; and lane h, 165%.

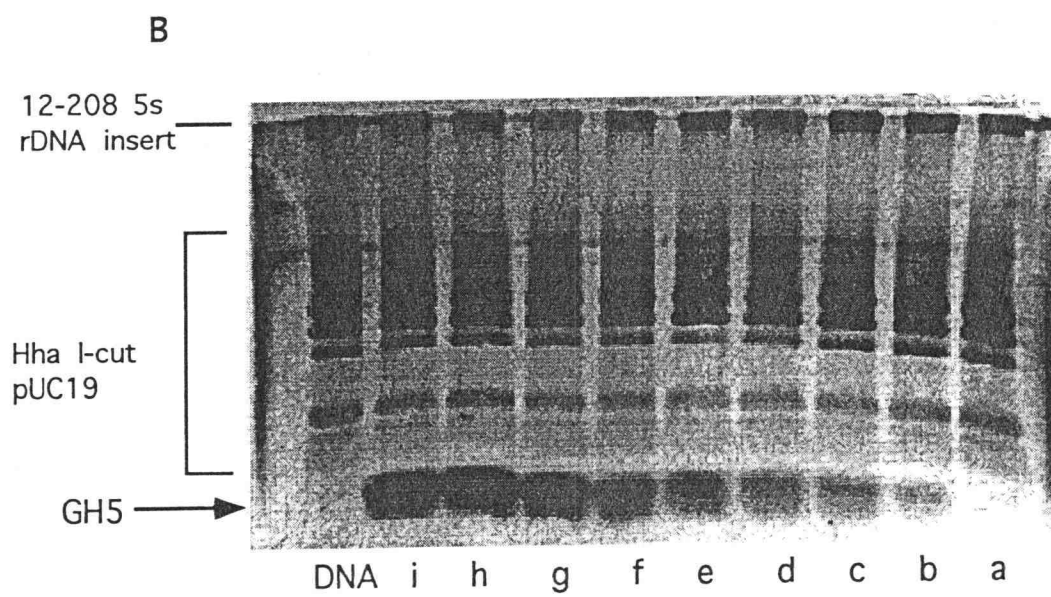
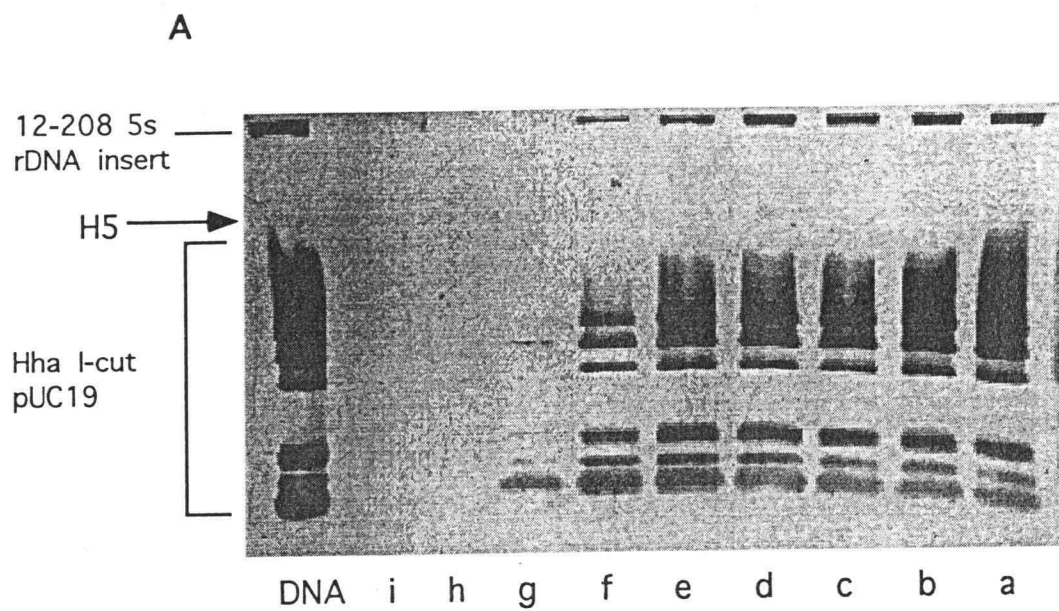


Figure 3.5

Figure 3.6. The solubility of H5 in 2% SDS as a function of DNA topology as detected by SDS-PAGE. Samples included: H5 bound to Hha I cut pPol208-12 (*open square*), H5 bound to pUC19 (*solid squares*), and free H5 (*solid circles*). Values were normalized to the input quantity of H5. Conditions were as follows: H5 at 0.03 mg/ml was incubated with the respective DNA at 0.04 mg/ml in 10 mM sodium phosphate (pH 7.2), 0.2 mM EDTA, 20 mM NaCl. Binding reactions were conducted at room temperature for time indicated, and stopped by adding 2 X SDS loading buffer.

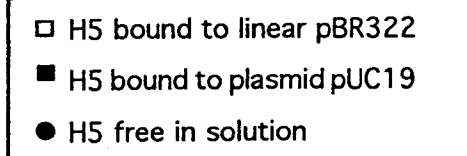
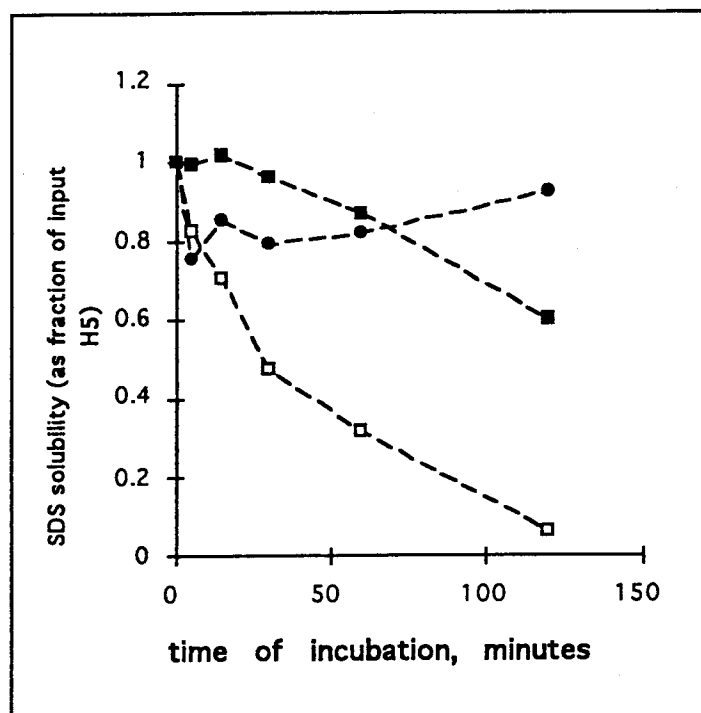


Figure 3.6

with 2 x SDS loading buffer, frozen in liquid nitrogen, and thawed immediately before analysis by SDS-PAGE. Linear DNA experienced rapid insolubilization in 2% SDS as compared to supercoiled DNA. Since supercoiled DNA actually has a higher affinity for H5 than does linear DNA (Vogel and Singer, 1974), H5 insolubility in SDS was not simply a result of DNA binding. Rather insolubility in SDS appears to reflect aggregation, with this interpretation supported by other studies including: results presented here in which H5 bound linear DNA to form aggregates that were too large to enter a 1% agarose gel while binding supercoiled DNA as a soluble complex (Figure 3.4), and (b) sedimentation studies indicating that linear DNA pellets as large aggregates upon binding H1 (Laio and Cole, 1981; Osipova et al., 1985). These difference may reflect the possibility that linker histone binding to supercoiled DNA is largely intramolecular, whereas linker histone binding to linear DNA is intermolecular, at least at lower histone/DNA ratios.

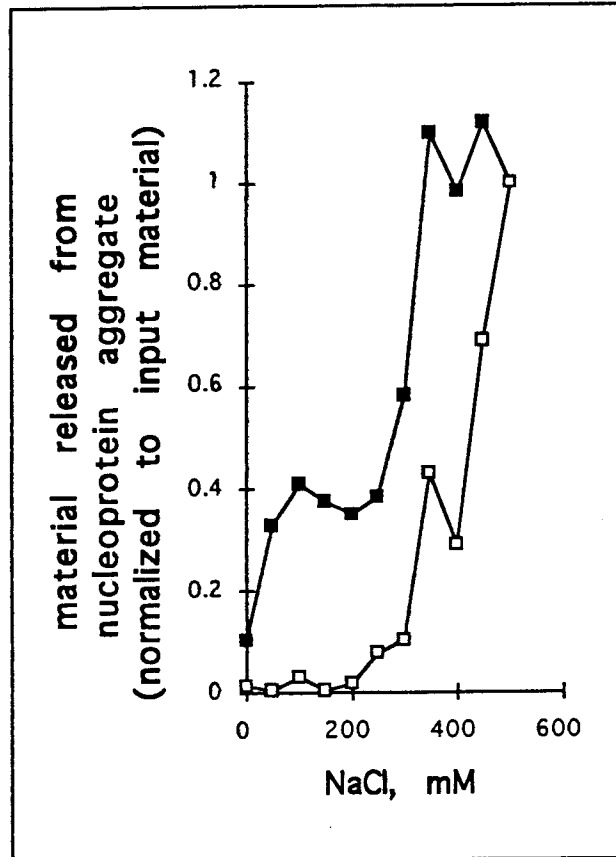
#### *3.3.4.2 Salt induced disruption of the GH5-DNA aggregate*

Salt-dependent dissociation of linker histones from DNA and chromatin has been used previously to elucidate general binding characteristics. In a rather novel approach, NaCl was used to probe preformed GH5-DNA aggregates as a means of better understanding stabilizing elements, and perhaps discriminate between protein-protein and DNA-protein contacts. GH5 at 0.05 mg/ml was bound to the 22 b.p. oligonucleotide at 100% GH5:DNA (w/w) in 10 mM sodium phosphate (pH 7.2), 0.2 mM EDTA. The incubation reaction were then allowed to stand overnight on ice, leading to production of

aggregates that were largely insoluble in SDS (as assayed by SDS-PAGE). The aggregates were then analyzed via the salt-dependent release of DNA, and by the solubility of GH5 in SDS (Figure 3.7). This was accomplished by removing a sample from the GH5-DNA binding reaction, then applying one portion to a native polyacrylamide gel (run in TBE), and another portion to an SDS/polyacrylamide gel. The former was performed to track the release of free DNA, while the latter was used to gauge the SDS-solubility of GH5, as a function of salt concentration. SDS insolubility was used as an assay to measure the amount of GH5 not accessible to dissociation, and thus served as an indicator of general GH5-DNA aggregation as described above for H5-DNA complexes.

Results suggest that the salt-induced solubilization of the GH5-DNA aggregate occurred in a multistep process. In the first the step, extending to 200 mM NaCl, roughly 35% of GH5 became SDS-extractable, but this was not accompanied by any significant salt-dependent dissociation of DNA. This may indicate that while GH5-DNA complexes were still aggregated, the aggregate was slightly deconsolidated--resulting in some SDS-dependent release of solution-exposed GH5 which could not occur without some disruption of the DNA-protein network. The second step, from 250 mM - 350 mM NaCl, resulted in the remaining aggregated GH5 becoming accessible to SDS solubilization. Over this range of salt concentrations, about 30% of the DNA also became extractable, suggesting major GH5-DNA reorganization--from an aggregate complex to a largely solution-accessible complex. Between 350 mM - 500 mM (with all GH5 soluble in SDS), the remaining >70% of the 22 b.p. oligonucleotide then became salt-dissociated.

Figure 3.7. Salt-dependent release of GH5 and the 22 b.p. oligonucleotide from the nucleoprotein aggregate. Aggregates were created by incubating the GH5 at 300% GH5:DNA (w/w) and a 22 b.p. oligonucleotide on ice overnight in 10 mM sodium phosphate (pH 7.2). NaCl was used to dissociate GH5 and the 22 b.p. oligonucleotide from the nucleoprotein aggregate. The amount of released DNA (mass amount normalized to the initial mass of DNA) was determined by scanning a picture of an ethidium bromide (0.5  $\mu\text{g/ml}$ ) stained 18% polyacrylamide gel (*open squares*) run in TBE. Similarly, the mass amount of SDS-soluble GH5 was determined from silver-stained 18% Laemmli gels (*solid squares*).



■ GH5 soluble in 2% SDS  
□ 22 b.p. oligonucleotide released from GH5-DNA complex

Figure 3.7

In interpreting the results, other relevant studies include Sergers et al. (1991) who reports that the globular domain appears to dissociate from DNA at around 200 mM NaCl; Thoma et al. (1983) finds that GH5 partially dissociates from chromatin at 200 mM. Additionally, Glotov et al. (1978b), using fluorescence polarization to measure salt-dependent binding, describes a two-step dissociation of the combined globular-domain-and-N-terminal domain of H1 with the first step occurring at 250 mM NaCl, and the second step occurred at 400 mM NaCl with complete dissociation at 700 mM NaCl (though the effect of the N-terminus must also be considered). Salt-dependent binding and crosslinking studies presented in Chapter 4 indicate that GH5 stops binding DNA between 180 mM and 270 mM NaCl. From these results, it appears that GH5 which has been bound to DNA within highly-condensed aggregates requires a higher salt-concentration for dissociation than would be expected from previous binding studies, though the salt-concentration required for SDS-solubilization of GH5 within aggregates was close to that previous reported to prevent GH5 binding to DNA.

An exact interpretation of the salt-dependent dissociation of the GH5-DNA aggregate would be highly speculative, but it does appear that at least two DNA binding elements may have been involved in stabilizing the aggregate. The first element was affected from around 250 - 350 mM NaCl, which appears to correspond to the "consensus" salt concentration believed to disrupt GH5 binding to DNA. Certainly, over this range of salt concentrations GH5 became largely accessible to SDS extraction (consistent with previous reports), but retention of DNA in the aggregate continued to higher salt concentrations. The second element was affected from 350 - 500 mM NaCl

with subsequent cooperative dissociation of GH5 from the 22 b.p. oligonucleotide in which only free DNA was observed to enter the native polyacrylamide gel ; that is, no discrete GH5-DNA complexes were observed (data not shown). While the data may support the popularized two-binding site model for GH5 (Ramakrishnan et al., 1993; Goytisolo et al., 1996), the effect of protein-protein contacts in stabilizing the GH5-DNA aggregate may make this correlation an oversimplification.

#### 3.3.4.2 Urea extraction studies of the GH5-DNA aggregate

Urea was used to dissociate GH5 and H5 from DNA, as a counterpart to the salt-dependent GH5/H5 studies. While NaCl should affect aggregate solubility primarily by dissociating DNA-protein contacts, urea was employed an agent that primarily affects protein-protein contacts, and at high concentrations is a powerful protein denaturant. Thus, urea was used to examine the importance of protein structure in aggregate stabilization. GH5 at 120% GH5:DNA (w/w) was aggregated with the 22 b.p. oligonucleotide at 0.033 mg/ml as described for the salt dissociation studies. Samples were then diluted in a water-urea mixture that brought the final urea concentration from between 0 M and 6 M. The solution was then shaken for 30 minutes with part of the sample treated briefly to 2 x SDS loading buffer then analyzed with SDS-PAGE, and a portion of the reaction mixture analyzed with native PAGE. The former was used to examine protein extractability by SDS and the latter was used to assess the amount of free DNA released by urea.

Results of the urea-dependent dissociation of GH5-DNA somewhat resembles the salt-dependent results. First, a rapid increase in GH5 solubility in 2% SDS was detected from 0 M - 2 M urea, followed by the release of DNA from the aggregate complex. By 2 M urea, around 80% of the GH5 in the aggregate complex had become extractable in 2% SDS. At the same time, most of the DNA still remained complexed (as observed by native PAGE). Above 2 M urea, it appears that DNA became increasingly susceptible to dissociation, and by 6 M urea the GH5- DNA was completely dissociated. As described for the salt-dependent aggregate dissociation study, urea-dependent DNA dissociation occurred cooperatively with the release of only free DNA; no GH5-bound 22 b.p. oligonucleotides were observed to enter the 15% polyacrylamide gel (data not shown). As proposed for the salt-dependent dissociation study, two binding elements may be involved in aggregate stabilization. For urea-induced aggregate dissociation, one possible element appears to have been disrupted from 0 to 2 M urea, allowing 2% SDS solubilization of most of the GH5, but under these circumstances most large aggregates remained intact, sequestering most of the DNA. Another element appeared to be affected from 2 M to 6 M urea, resulting in complete aggregate dissociation, and the release of DNA. The urea dissociation results are of special interest, because the range of urea concentrations in which most GH5 became accessible (0-2 M) is the range usually associated with a breakdown of intermolecular protein interactions, rather than denaturation (Creighton, 1993).

The urea-dependent solubilization of H5-DNA aggregates was co-plotted with GH5-DNA data (Figure 3.8). H5 at 170% H5:DNA (w/w) was aggregated with Hha

I-cut pPol208-12 DNA in 10 mM sodium phosphate (pH 7.2), 0.2 mM EDTA on ice overnight. Clearly, H5 aggregation (and binding) was highly resistant to the effects of urea, though by 6 M urea H5 appears to have also become soluble in 2% SDS. The additional resistance of H5 to urea must have been the result of the tail domains, suggesting that protein structures responsible for DNA binding via tail-domains were relatively resistant to urea denaturation. It is conceivable that urea was relatively ineffective because H5 binding structure is more reliant on DNA-induced stability, and less on internal protein stabilization. Such DNA-dependent protein folding and stabilization is common amongst DNA-binding proteins (Petersen et al., 1995; Newman et al., 1995; Kwon et al., 1997; Spolar and Record, 1994), and this also appears to be the case for linker histones (Aviles et al., 1979; Hill et al., 1989; Clark et al., 1988; Bohm and Creemers, 1993). Alternatively, resistance of H5-DNA aggregates to dissociation with both SDS and urea may be the result of highly condensed or stable H5-DNA structures (as compared to GH5-DNA aggregates) that exclude the denaturants. Earlier result comparing the SDS extractability of H5 bound to supercoiled DNA and linear DNA is particularly supportive of this interpretation. H5 bound to supercoiled DNA, which was believed to be solution soluble, was readily extractable in SDS, but H5 bound to linear DNA, which was believed to be solution insoluble, was resistant to SDS extraction (Figure 3.6). Regardless of the mechanistic explanation, it is clear that tail-DNA contacts act in place of histone-histone contacts (as observed for GH5) in importance for stabilizing H5-DNA complexes.

**Figure 3.8.** Urea-dependent disruption of linker histone-DNA complexes. The stability of aggregates involving GH5 bound to a 22 b.p. oligonucleotide, and separately, H5 bound to Hha I cut pPol208-12 were examined at various urea concentrations. GH5 at 175% GH5:DNA (w/w) or H5 at 120% H5:DNA (w/w) were incubated overnight with the 22 b.p. oligonucleotide or Hha I cut pPol208-12, respectively, in various concentrations of urea. Samples included: GH5 that became extractable in 2 % SDS (*solid squares*), H5 that became extractable in 2 % SDS (*solid circles*), and the 22 b.p. oligonucleotide released from the GH5-DNA aggregate (*open squares*).

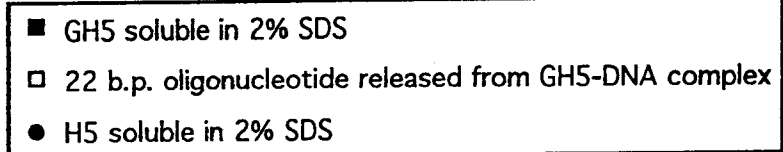
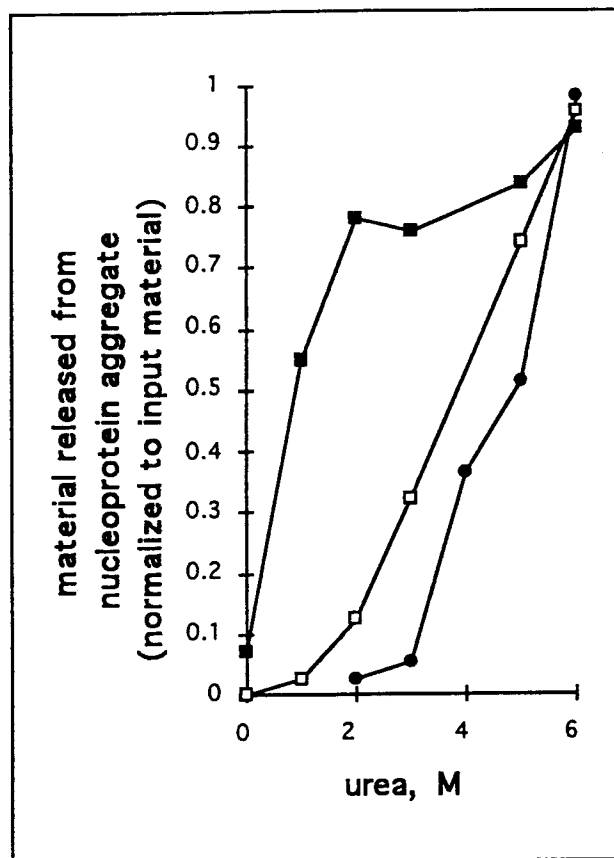


Figure 3.8

### 3.3.6 Chymotrypsin digestion of H5 bound to DNA

#### *3.3.6.1 Exposure of Phe 93 to chymotrypsin proteolysis as a result of H5-DNA binding*

Many helix-turn-helix and winged-helix motif proteins have been shown to bind to DNA via the recognition helix, thus leading to the speculation that GH5 (and presumably all linker histones) bind DNA the same way (Ramakrishan et al., 1993). The crystal structure of HNF-3 $\gamma$  bound to DNA (Clark et al., 1993) is considered to be representative of GH5 bound to DNA because: (a) HNF-3 $\gamma$  is the closest structural homologue to GH5 (Zlatanova and van Holde, 1997), (b) crystallized HNF-3 $\gamma$  contains prominent loops or wings that appear to be similar to the wings of GH5 (Brennan, 1993), and (c) a number of important residues are homologously positioned for both proteins. One such pair of residues, Phe 93 of GH5 and Trp 193 of HNF-3 $\gamma$  closely co-position when the two protein structures are superimposed (data not shown), and because both these residues have largely hydrophobic, aromatic groups, it can be argued that the residues serve similar purposes. Trp 193 of HNF-3 $\gamma$  makes close Van der Waals interactions with a ribose moiety in DNA, suggesting the aromatic ring doesn't actually intercalate into the DNA (Clark et al., 1993).

Phe 93 has properties that make it ideal as part of a protease protection assay to elucidate details of the GH5-DNA binding complex. First, Phe 93 is the primary site of proteolysis by chymotrypsin. Second, Trp 193 of HNF-3 $\gamma$  crystallized bound to DNA makes close contact with a ribose moiety, and would thus be expected to be protected upon HNF-3 $\gamma$  binding to DNA. It follows that by identifying the accessibility of Phe 93

(either protected or exposed upon H5 binding to DNA) with chymotrypsin, a reasonable argument can be made as to whether GH5 binds like HNF-3 $\gamma$ . Figure 1.2 illustrates a hypothetical GH5-DNA complex modeled after a typical helix-turn-helix motif protein with a recognition helix inserted in the major groove (Ramakrishnan, 1993). From Figure 1.2 it is also apparent that Phe 93 is located in the cluster of residues referred to as the primary binding site, and should be expected to be protected against cleavage if such a model is correct. Considering this, chymotrypsin was used as part of a protease protection assay to determine whether the globular domain of H5 binds to DNA via the putative primary DNA-binding site.

In the study, plasmid pUC19 at 0.04 mg/ml was incubated with H5 at 0.032 mg/ml in 10 mM NaCl, .2 mM EDTA, 10 mM sodium phosphate (pH 7.2) for 45 minutes.

Chymotrypsin was added to a final concentration of 0.2  $\mu$ g/ml with the reaction conducted at room temperature (Figure 3.9B). As a comparison, H5 was cleaved with chymotrypsin in identical conditions but without DNA (Figure 3.9A). In comparing the digestion of H5 to smaller peptides, it is clear that H5 is digested faster when bound to plasmid pUC19 than when free in solution. At 50 minutes no remaining H5 was detected for the sample digested when bound to DNA, while for H5 free in solution over 20% still remained, it too had also been completely digested. The digestion of H5 followed an expected exponential behavior; the chymotrypsin digestion rate for H5 bound to supercoiled pUC19 DNA was several-fold greater than that for H5 free in solution (Figure 3.9C). The difference in digestion rates were even more striking when the reactions were performed at 37 °C for H5 free in solution (Figure 3.10A) and for H5 bound to pUC19 (Figure 3.10B). Together, these results strongly suggest that for H5 bound to DNA, Phe

Figure 3.9. Plot of H5-related peptides as a result of chymotrypsin digestion of free protein at room temperature. (A) H5 at 0.032 mg/ml was digested by 0.2  $\mu$ g/ml chymotrypsin. At the indicated time points, samples were treated to 1 mM PMSF, and frozen after the addition of 2x SDS loading buffer. *Insert:* representative silver stained 18% Laemmli gel (30:8) of digestion timecourse. The peptides are referred to as *H5*, the full-length protein (*solid squares*); *C*, the C-terminal tail domain of H5 (*solid triangles*); and *NG*, the combined N-terminal tail and trypsin resistant globular domains (*solid circle*). (B) H5 at 0.032 mg/ml was bound to plasmid pUC19 at 0.04 mg/ml and processed as in (A). *Insert:* as described for (A). (C) The data from (A) and (B) re-plotted as a semilog graph. Legend: digests of H5 bound to supercoiled pUC19 (*squares*) and H5 digested free in solution (*diamonds*). Lines represent results of linear regression (Microsoft Excel 4.0). The mass of each peptides was determined by scanning the silver stained gel, and processing the data using NIH Image. Final values were normalized to the starting amount of H5 (shown at the extreme right in the inserted panel). Note that each peptide has been reported to silver stain at a different relative intensity compare to the entire linker histone. Thus, silver staining intensity cannot be used in comparing relative quantities between peptides.

A

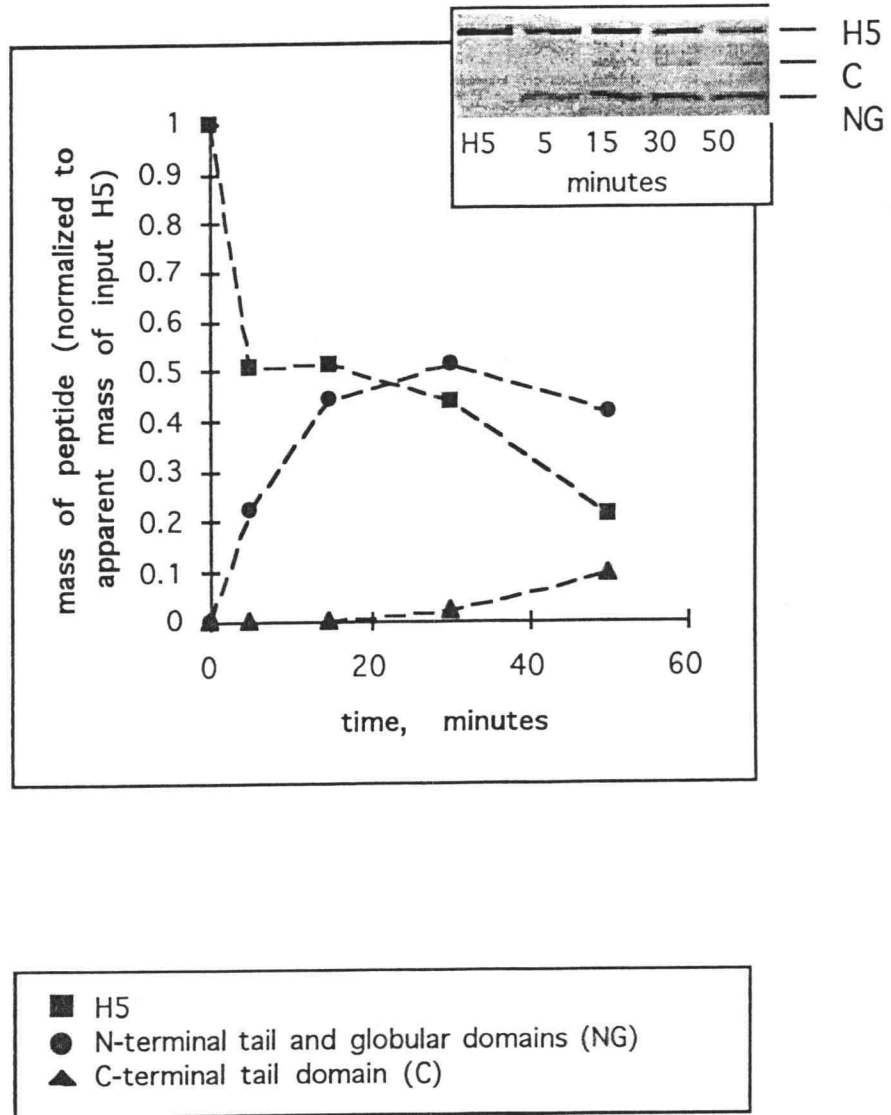


Figure 3.9

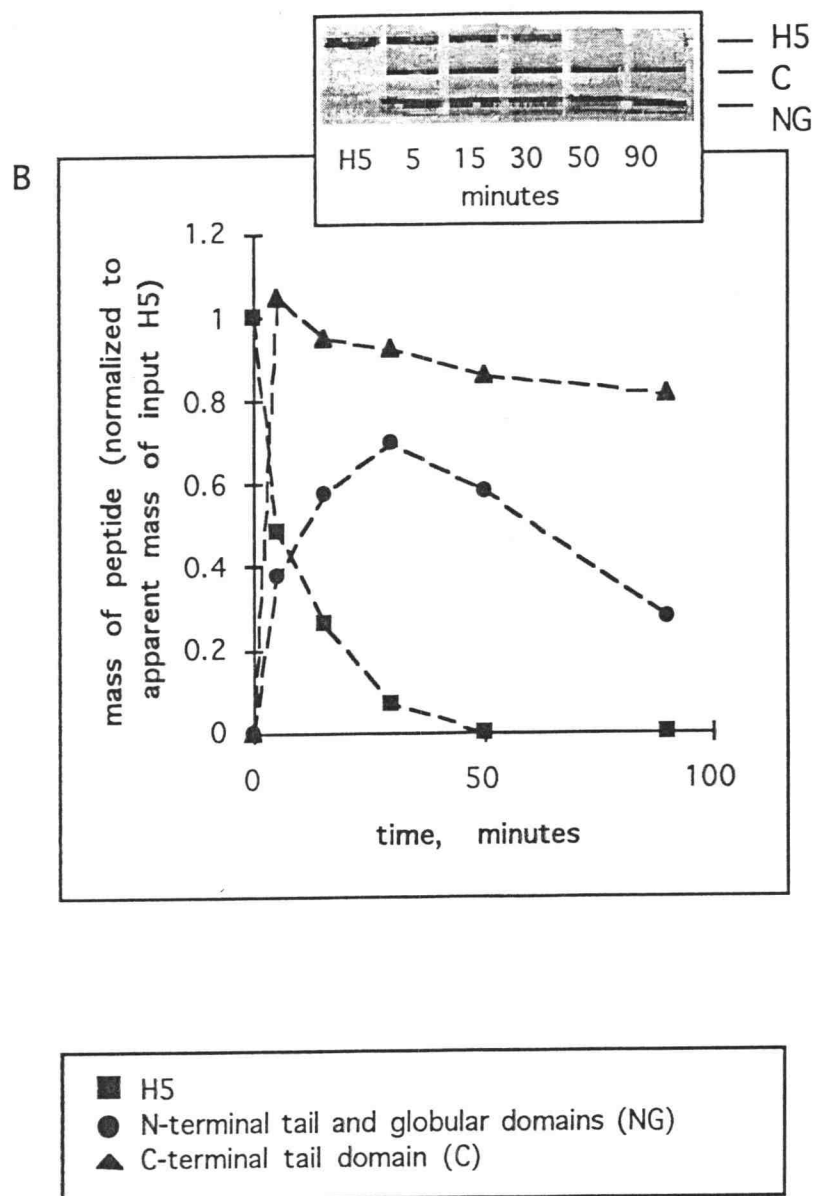


Figure 3.9 (continued)

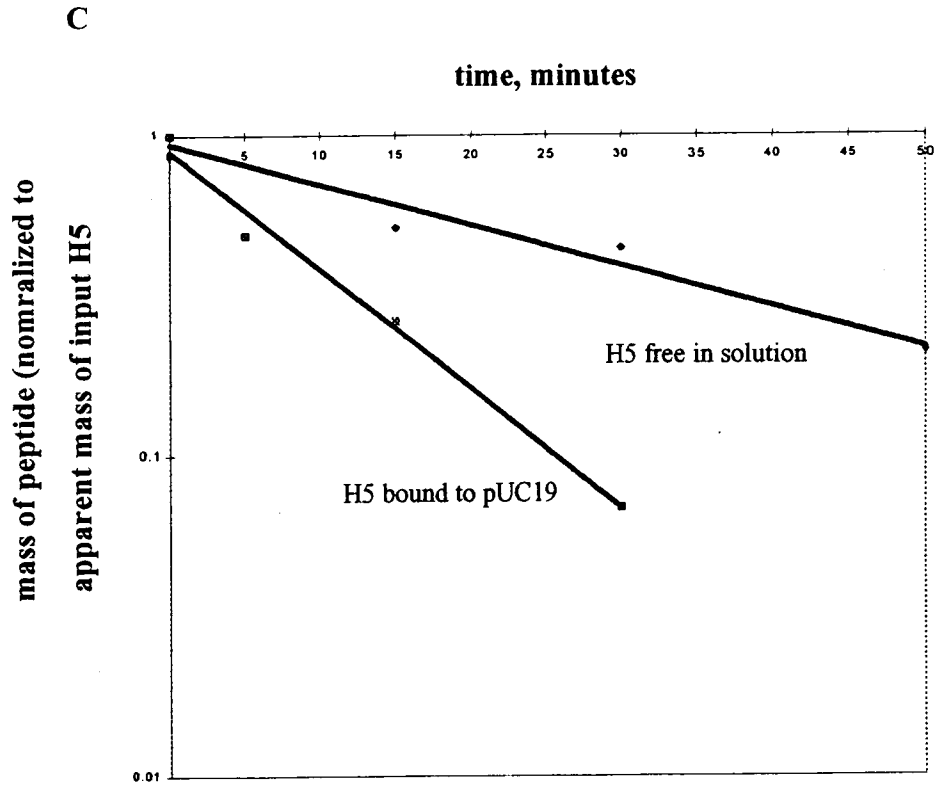


Figure 3.9 (continued)

**Figure 3.10.** Plot of H5-related peptides as a result of chymotrypsin digestion of DNA-bound protein at 37°C. (A) H5 at 0.032 mg/ml was digested by 0.2 µg/ml chymotrypsin. At the indicated time points, samples were treated to 1 mM PMSF, and frozen after the addition of 2x SDS loading buffer. *Insert:* representative silver stained 18% Laemmli gel (30:8) of digestion timecourse. The peptides are referred to as *H5*, the full-length protein (*solid squares*); *C*, the C-terminal tail domain of H5 (*solid triangles*); and *NG*, the combined N-terminal tail and trypsin resistant globular domains (*solid circle*). (B) H5 at 0.032 mg/ml was bound to plasmid pUC19 at 0.04 mg/ml and processed as in (A). *Insert:* as described for (A). Gels were quantitated as described in [Figure 3.9](#).

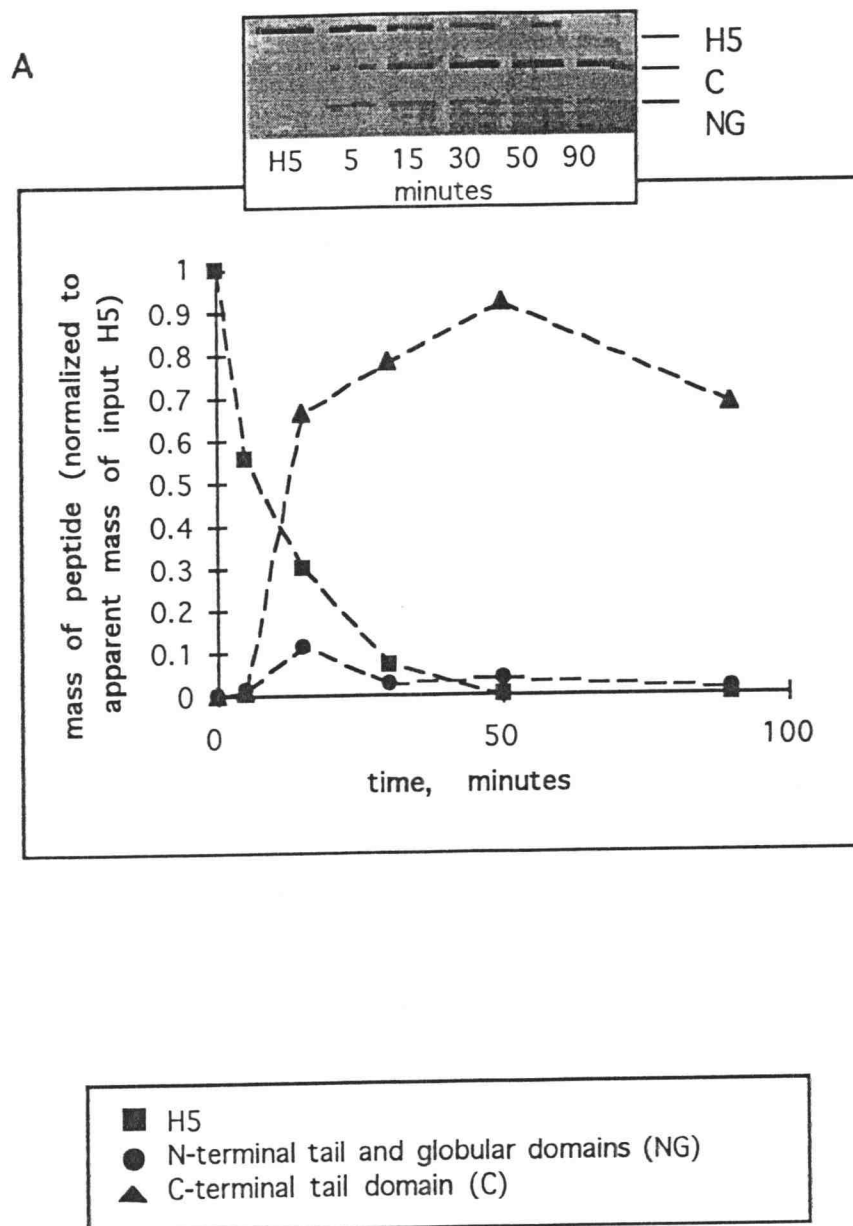


Figure 3.10

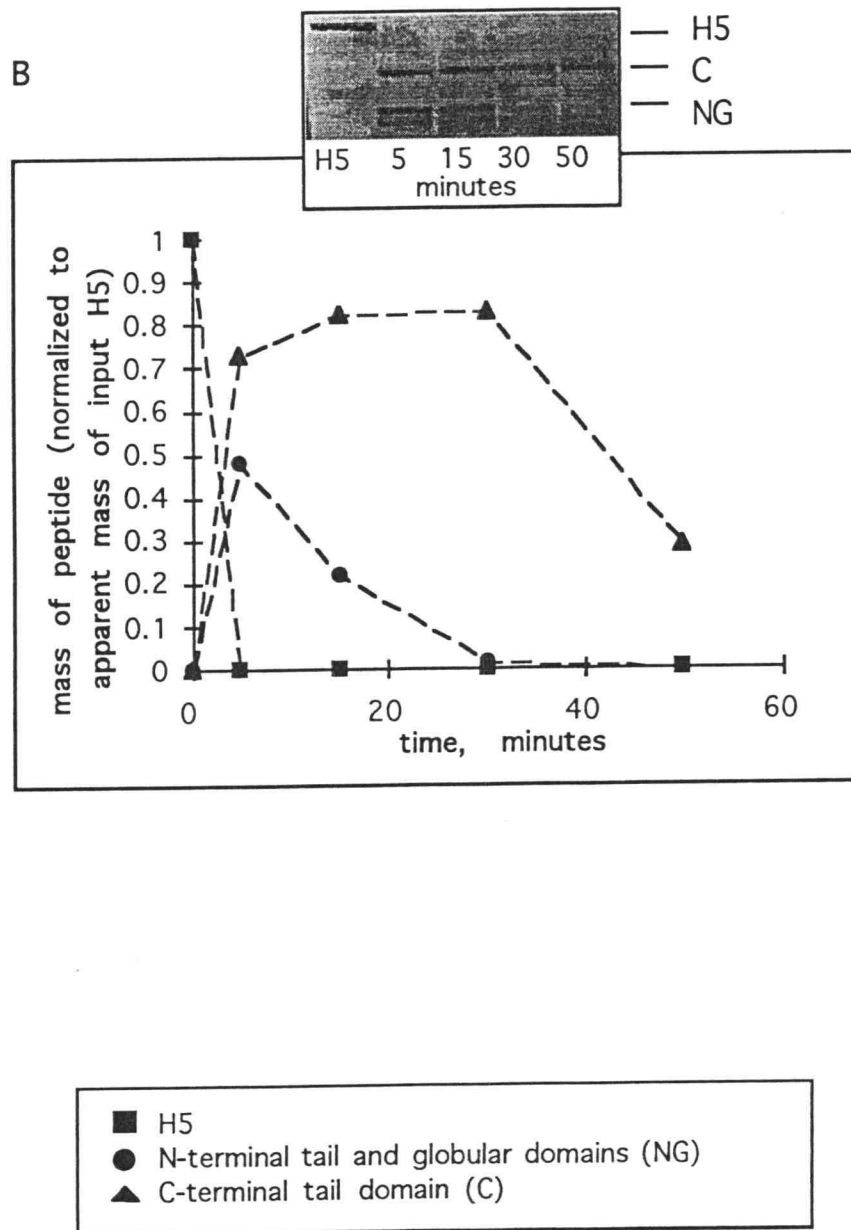


Figure 3.10 (continued)

93 was considerably more accessible to chymotrypsin cleavage than for solution-soluble H5.

Chymotrypsin cleavage (at Phe 93) resulted in the production of two principle peptides: (a) the C-terminal tail domain (C), and the combined N-terminal tail domain and the trypsin-resistant globular domain (NG). The C-terminal tail domain migrates noticeably slower than the N-terminal domains even though the molecular weights are nearly identical, presumably as a result of the large number of basic residues present in the C-terminal tail. While chymotrypsin preferentially recognizes Phe 93 as a primary cleavage site, other low-affinity, secondary sites also exist throughout the protein--eventually leading to general protein degradation (De Bernardin et al., 1986). Interestingly, further degradation of the globular domain appeared to be roughly independent of the presence of DNA, with a peak in the globular domain concentration occurring at 30 minutes in both experiments. In contrast, the C-terminal tail domain was clearly protected from digestion when H5 was bound to DNA at room temperature, as the peptide was present at considerably higher levels in comparison to those observed for unbound H5. Curiously, the C-terminal tail domains was protected at 37 °C for both for H5 bound to pUC19 and for H5 free in solution under the experimental conditions. Protection of the C-terminal tail upon DNA binding has also been reported for H1 linker histone (De Bernardin, et al., 1986), and the peptides most protected from proteolysis in the C-terminal domain upon DNA binding have been found to consist largely of  $\alpha$ -helical secondary structure (Hill et al., 1989).

### 3.3.7 Computer modeling the GH5-DNA complex

As an additional, theoretically-based, method for analyzing linker histone binding and assembly, the published crystal lattice of GH5 was used in a DNA-docking experiment. This "experiment" was based on a similar approach used for crystallized recA protein. The recA crystal lattice was found to consist of filaments of recA molecules arranged in roughly a six-fold screw axis (Story et al., 1992), similar to complexes observed with EM--both bound to DNA and free in solution (Heuser and Griffith, 1989). Additionally, the recA crystallized filaments allowed for the docking of DNA, corroborating the solution studies that indicate recA complexes are primarily driven by protein-protein contacts (reviewed in Takahashi and Norden, 1994). In summary, the finding that the recA crystal lattice forms helical filaments with P6<sub>1</sub> symmetry, corroborate both EM, and results of the biochemical characterization of recA.

Admittedly, the use of the crystal lattice in obtaining information on GH5 assembly onto DNA is not as compelling as for recA. First, GH5 has an estimated K<sub>d</sub> of protein self-association of 2 x 10<sup>-4</sup> M (Maman et al., 1994) which is about two order of magnitude higher than the apparent K<sub>d</sub> for GH5 binding to small oligonucleotides (Figure 3.1A). In fact, GH5 has thus far been shown only to self-associate into solution-soluble complex via chemical crosslinking whereas equilibrium analytical centrifugation results under similar conditions showed no clear evidence for self-association. Equally, no evidence for GH5 assembly in solution is available from high-resolution imaging techniques. Second, unlike recA, the importance of protein-protein contacts in GH5 self-assembly (on DNA and in solution) remains unresolved. For example, while it has

been known for some time that linker histones bind to DNA cooperatively, it is still unknown whether cooperativity stems from protein-protein contacts or a DNA-structure related phenomenon (reviewed in Yaneva and Zlatanova, 1991). While evidence for protein-protein contacts in GH5 assembly is less compelling than for recA, results presented in Chapter 2 suggest that GH5 may assemble through specific interactions. This includes: (a) the finding that GH5 appears to assemble uniformly onto a 22 b.p. oligonucleotide, apparently making self-contact primarily via the C-terminus, (b) GH5 crosslinking free in solution implicating specific self-assembly (Maman et al., 1994), (c) and crosslinked polymer distribution indicative of simple filament formation. Considering that GH5 may associate specifically both in solution and onto DNA, it was felt appropriate to analyze the GH5 crystal lattice for uniform filaments that, like recA filaments, would dock B-DNA.

In the course of analyzing the GH5 crystal lattice for features that would dock B-DNA, it was observed that the crystal lattice is comprised of interconnecting GH5 filaments with the filament axis running along the z-axis of the lattice unit cell (see [Figure 3.11](#)). The filaments consist of alternating GH5 monomers in two conformations--A monomers, containing an extended  $\beta$ -hairpin, and, B monomers, containing a  $\beta$ -hairpin that curls back toward the third  $\alpha$ -helix (Ramakrishnan et al., 1993). The filament has two-fold symmetry, and if the difference between A and B monomers is neglected, the filament has a pseudo four-fold screw axis. The filament contains a, roughly, 1.5 nm central hole that runs parallel to the filament axis. DNA failed to dock into this hole primarily due to a steric-related problem involving the B monomer. In the same docking

Figure 3.11. GH5 filament based on crystalized GH5 lattice. The complete GH5 crystal lattice (Ramakrishnan et al., 1993). is comprised of filaments in turn comprised of two "sub-filaments" that are related by a two-fold axis of symmetry. Also identified are the monomer type (A or B), and the location of the b-hairpin and the third helix. (Shown is a representative "sub-filament" strand.)

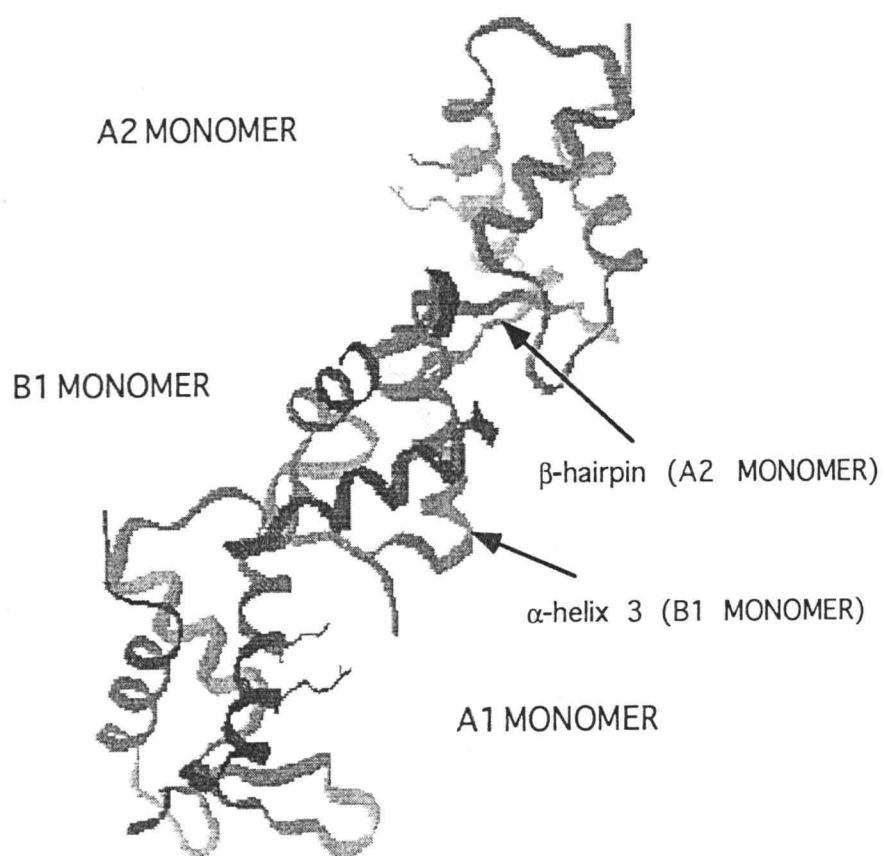


Figure 3.11

experiment, the A monomer appeared to interact with the DNA primarily via an extended  $\beta$ -hairpin that contacts either the minor or major groove depending on the individual A monomer. From this model, the GH5 monomer that docked into the major groove had a poor fit with limited contact of Lys 85, Lys 69, and Arg 73 with DNA phosphate groups. In contrast, the GH5 monomer that docked into the minor groove did so in a way that qualitatively positioned Lys 85, Lys 69, and Arg 73 in close contact with the DNA phosphate backbone; the third  $\alpha$ -helix (which contains Lys 69 and Arg 73) actually straddles the phosphate backbone (Figure 3.12A). Because of this, the model is referred to as the "minor groove binding model" (MnGBM).

The "major groove binding model" (MjGBM) originally proposed by Ramakrishnan et al. (1993) (Figure 3.12B) and the "minor groove binding model" (MnGBM) (Figure 3.12A) are similar, in that the same surface of GH5 interacts with DNA in both cases--making distinction (using biochemical tools) between the two models extremely difficult. However, some experimental evidence does support the MnGBM. Distamycin, a minor groove binding molecule is reported to disrupt linker histone-DNA complexes (Kas et al., 1989), though it is unclear whether this effect is due to distamycin-dependent disruption of binding by the globular domain or terminal tails domains. The importance of narrow minor groove binding is also reflected by the affinity of linker histones for A-T rich DNA (Izaurralde et al., 1989; unpublished data<sup>2</sup>), but again the full protein was used in these studies. This is considered a problem especially since it is known that the SPKK motif found in the terminal tail domains prefers minor groove

---

<sup>2</sup> H1 was found to preferentially bind AT-rich DNA as determined by SELEX method of consensus sequence identification (Tuerk and Gold, 1990).

**Figure 3.12.** Computer generated picture of putative minor groove binding GH5-DNA model and the prototypical major groove binding model (A) An approximation to the interaction of the GH5 A monomer bound to DNA based on interactions observed by docking DNA into the GH5 crystal lattice, otherwise described as the "minor groove binding model". Protein contact is made primarily by  $\beta$ -hairpin interaction with the minor groove, while  $\alpha$ -helix 3 (H3) appears to nonspecifically interact with the DNA strand. (B) An A monomer was bound to DNA based on homology with HNF-3 $\gamma$  from the HNF-3 $\gamma$ /DNA crystal structure (Clark et al., 1993), in which nucleoprotein contact includes insertion of the third helix into the major groove. *Black circles* represent points where Lys 69, Arg 73, and Lys 85 appear to contact the phosphate backbone. Abbreviation: H3,  $\alpha$ -helix 3; H2,  $\alpha$ -helix 2; H1,  $\alpha$ -helix 1; and W1, the  $\beta$ -hairpin.  $\beta$ -strands are represented by light-colored ribbons, and  $\alpha$ -helices are represented by cylinders. Modeling work was done with Insight II (Biosyms, San Diego, CA).

A

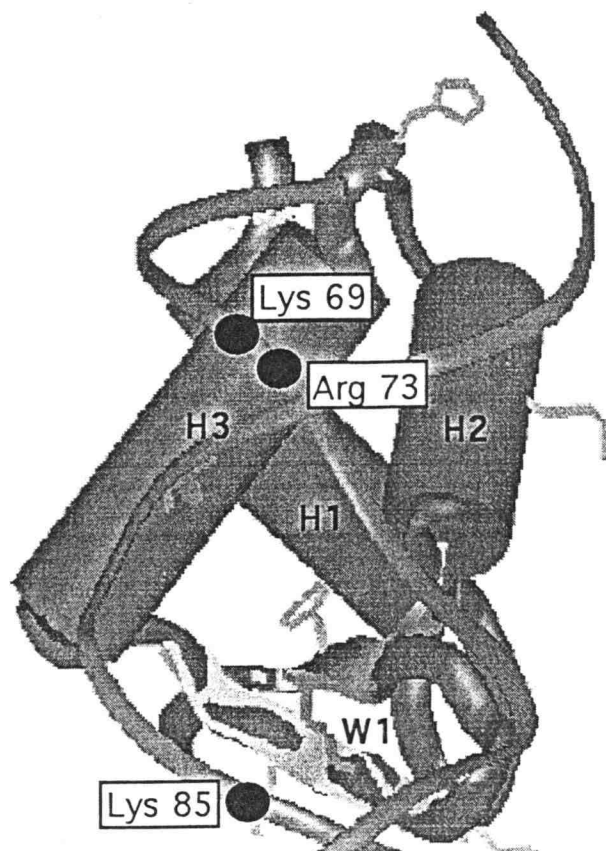


Figure 3.12

B

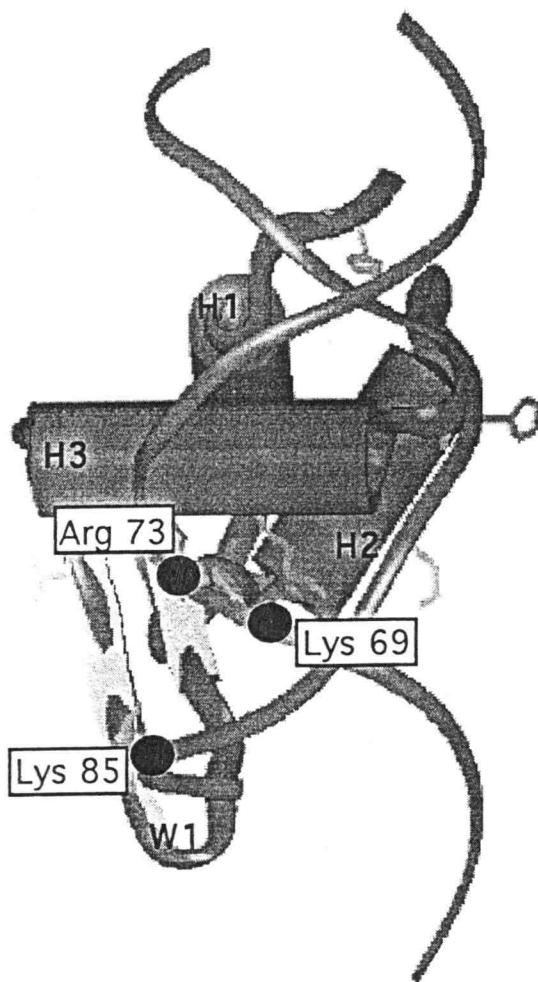


Figure 3.12 (continued)

binding (Churchill and Suzuki, 1989). Similar experiments to assay for minor groove binding will need to be conducted with the globular domain, in order to provide more definite evidence for either the MjGBM or MnGBM.

Closer inspection of the crystalized "GH5 filaments" suggests a possible model for GH5 self-associated in solution. One may envision the crystalized filament as a composite of two "sub-filaments" each related by a four-fold screw axis, and comprised of alternating A and B GH5 monomers (Figure 3.11). Such a fiber would be compatible with the divalent GH5 molecule described in Chapter 2, which self-interacts primarily through two contact surfaces. From the crystal filament contact appears to involve the B-hairpin, as one surface, and either the third helix or loop between the second or third  $\alpha$  helix, as the second surface. Interestingly, the importance of the C-terminal end of GH5 (including the  $\beta$ -hairpin) has been implicated in self-interaction of GH5 bound to a 22 b.p. oligonucleotide.

### 3.4 Results of small chromatin fiber reconstitution with H5

H5 was bound to small "artificially" reconstituted chromatin fibers as a counterpart to the model DNA studies. This comparison was considered necessary because of obvious differences between chromatin and naked DNA models. For the chromatin study, the 208-12 DNA (Simpson et al., 1985) as discussed above was chosen, and is available as a high-expression clone with the DNA inserted into the multiple cloning site of pUC19 (resulting in pPol208-12) (Georgel et al., 1993). The 208-12 DNA insert contains twelve tandem repeats of a 208 b.p. portion of the 5S RNA gene from *Lytechinus variegatus*

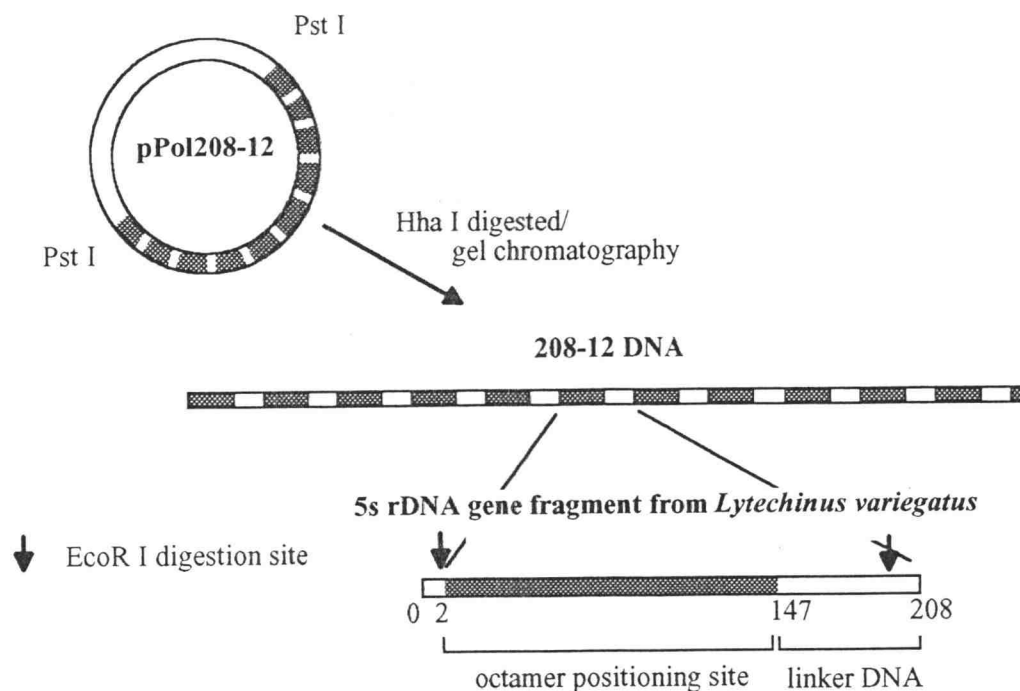


**Figure 3.13.** Schematic representation of the 208-12 DNA used in the small fiber chromatin reconstitution studies. The plasmid pPol208-12, which contains the 208-12 DNA inserted into the multiple cloning site of pUC19 (Georgel et al., 1993), was cleaved with Hha I—resulting in a number of DNA fragments less than 400 b.p., and the 208-12 DNA which is over 2600 b.p. The 208-12 DNA was subsequently separated by gel chromatography with ultragel A2 resin. Each 208-12 DNA is comprised of twelve tandem copies of a 208 b.p. fragment from the 5s rDNA gene from *Lytechinus variegatus*. The 208 b.p. fragment contains an octamer positioning site leading to protection from nucleotides 2 to 147 from micrococcal nuclease digestion upon octamer deposition (Dong et al., 1990). In addition, the fragment also contains two EcoR I nuclease digestion sites at nucleotide 2 and nucleotide 197.

(Figure 3.13). The 208 b.p. fragment has been well-characterized as containing an octamer positioning sequence, and the 208-12 DNA has been extensively utilized in previous reconstituted-chromatin studies, making the DNA ideal for analyzing the effects of H5 binding to chromatin fibers. The major octamer position protects base pairs 2 to 147 on the 208 b.p. fragment from micrococcal nuclease digestion, with the rest of the DNA repeat comprised of octamer-unbound, unprotected linker DNA (Figure 3.14) (Dong et al., 1990).

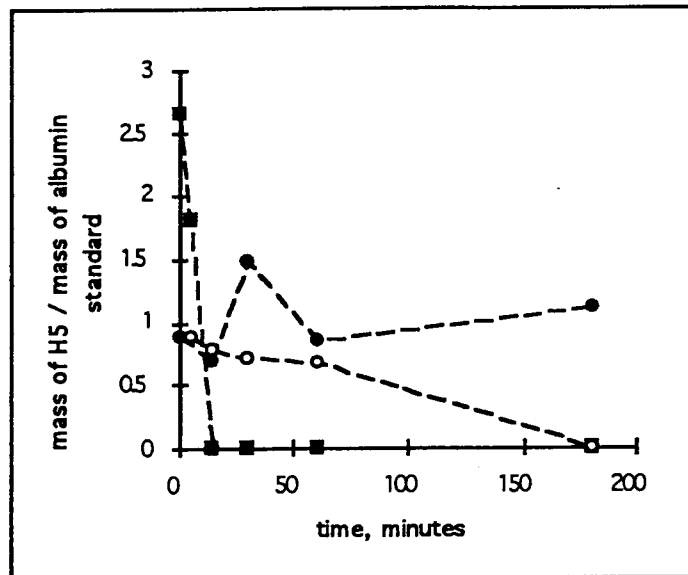
The techniques for isolation of the 208-12 repeat, its reconstitution with histone cores, and the addition of GH5 or H5 are described in Methods and Materials. In this section, four separate assays were used to characterize H5 binding to chromatin and included: (a) dialysis-dependent release and quantitation of H5 bound to the reconstituted fiber, (b) endonuclease digestion as a measure of DNA exposure in the reconstituted fiber, (c) agarose gel electrophoresis, and (d) analytical ultracentrifugation. The principle objective of these experiments was to identify H5 binding on reconstituted chromatin fibers, to elucidate whether H5 binding led to protection of linker DNA, and to examine the impact of H5 binding on fiber morphology. The development of a model chromatin system containing linker histones as well as octamers is an important prerequisite for further analysis of chromatin fiber structure.

#### 3.4.1 Dialysis of reconstituted fibers

A simple dialysis technique was designed to verify that H5 bound to reconstituted 208-12 DNA. The strategy is as follows: H5 was bound to reconstituted 208-12 DNA at

Figure 3.14. Use of large-pore dialysis membrane to detect binding and dissociation of H5 from reconstituted 208-12 DNA. Solution soluble H5 (*solid squares*), and chromatin associated H5 bound at 2 H5:octamer (mole/mole) (*open circles*), and 4 H5:octamer (mole/mole) (*solid circles*). Reconstituted fibers were placed in Spectrapore 6 (MWCO 50 kDa) dialysis bags and dialyzed into a large volume of 10 mM NaCl, T.E. (pH 7.8) at 4 °C. At indicated time points samples were removed, digested with micrococcal nuclease with the products of digestion analyzed on silver-stain SDS/polyacrylamide gels (12% polyacrylamide).

A



■ Free H5

○ H5 reconstituted 208-12 5s rDNA (n=15) at 24 H5 molecules/DNA

● H5 reconstituted 208-12 5s rDNA (n=15) at 48 H5 molecules/DNA

Figure 3.14

a final concentration of 0.03 mg/ml, as described in Methods and materials, and the samples were dialyzed along with 5 µg/ml of bovine serum albumin in Spectrapore 6 (MWCO = 50,000 Da) dialysis tubing into a large volume of low salt solution (T.E., 10 mM NaCl). H5 is a 20,900 dalton protein, so it readily passed through the dialysis membrane while the chromatin fiber, with a molecular weight of over 1.3 million dalton, and albumin with a 66 kilodalton molecular weight were retained inside the dialysis bag. The amount of H5 remaining inside the dialysis bag was measured by removed a sample from the dialysis bag, digesting the sample with micrococcal nuclease (0.007 units/µl, 1 mM CaCl<sub>2</sub>) at room temperature for a few hours, then measuring the amount of H5 relative to the retained amount of serum albumin by a coomassie-stained SDS polyacrylamide gel.

Results show that H5 was preferentially retained in the dialysis bag for 208-12 DNA reconstituted samples (Figure 3.14). While free H5 was dialyzed away from the bag within 15 minutes, H5 was detected in the 2 H5:octamer (mole/mole) reconstitute after 1 hour. For 208-12 DNA reconstituted with 4 H5:octamer (mole/mole), no discernible H5 dissociation from the chromatin fiber was detected, though precipitate was observed in the dialysis bag, suggesting the effect was due to aggregation. Only a small reduction in the amount of H5 retained in the dialysis bag for the reconstituted 208-12 at 2 H5:octamer (mole/mole) was observed within the first several minutes. This suggests that nearly all the input H5 was bound to the chromatin fiber, though a small amount (<10%) appeared to be unbound. However, H5 did exhibit some slow dissociation from the fiber, since it was dialyzed out by 3 hours for the 208-12 DNA reconstituted with 2 H5:octamer (mole/mole). Proteins that pass out through the dialysis bag are essentially prevented from

rebinding. It follows that these results probably represent a very slow histone dissociation or exchange reaction, which is also supported by evidence for linker histone turnover in chromatin (van Holde, 1989). Though not fully exploited in this work, dialysis appears to be well suited for chromatin-related protein competition studies, since small unbound proteins can rapidly be removed from the reaction solution. Indeed, the use of such membranes could provide a very useful alternative to the more conventional (and imprecise) techniques like filter binding for any studies of binding of small proteins to DNA.

#### 3.4.2 Endonuclease digestion of the reconstituted fibers

Restriction enzyme EcoR I was used as a tool to measure the exposure of linker DNA in the reconstituted fiber. The 208 b.p. fragment contains a number of restriction sites including two EcoR I restriction sites: one of which lies in a partially protected position at the edge of the nucleosome core (base pair 2), and another that lies in the unprotected linker DNA (base pair 197). Reconstituted 208-12 DNA chromatin fibers were digested with EcoR I to determine whether H5 binding to the fibers restricted access to the restriction site located at base pair 197. To accomplish this, H5 and octamers were reconstituted onto the 208-12 DNA following the protocol outlined in Methods and Materials. Reconstituted fibers were then digested with EcoR I at 0.7 units/ $\mu$ l in reaction buffer containing 30 mM Tris-HCl (pH 7.8), 3.5 mM MgCl<sub>2</sub>, 50 mM NaCl, 0.01 % Triton X-100 at room temperature. Results clearly indicate that the addition of H5 to chromatin limited access to linker DNA. While stripped chromatin fibers (without H5) appeared to

be completely digested by 3 hours (as measured by the relative amounts of released mononucleosomes), 1 H5:octamer (mole/mole) was found to reduce the digestion rate significantly ([Figure 3.15](#)). In contrast 3 H5:octamer (mole/mole) produced no discernible digestion which could indicate either strong protection or simple aggregation.

A reduction in EcoR I access to cleavage sites upon the addition of H5 apparently reflects steric-related protection of linker DNA. The basis for this protection is uncertain since a number of possible factors may be responsible. First, H5 may actually bind to the linker DNA in the region of the EcoR I site at 197, preventing cleavage. It is well established that a linker histone bound to a nucleosome (chromatosome) increases the amount of DNA protected from micrococcal nuclease digestion from 146 b.p. to 166 b.p. (Noll and Kornber, 1977), and thus, H5 could be covering the EcoR I site at 197 ([Figure 3.13](#)) as a result of binding of the globular domain to the nucleosome. While open to some interpretation, this is consistent with H5 binding at the dyad axis of the nucleosome to confer protection as predicted by a popular model ([Figure 1.1](#); Allan et al., 1980), and supports similar observations by Meersseman et al. (1991) using Ava I which cleaves at 203. Alternatively, the long H5 C-terminal domain may bind to the linker DNA, and as a result, prevent EcoR I cleavage, though analogous accessibility of micrococcal nuclease to chromatin DNA makes such terminal-tail protection unlikely. Second, H5 may reposition the octamer to cover the EcoR I site. It has been reported that H5 repositions the octamer laterally on the *Lytechinus vareigatus* 5s rRNA gene about 20 b.p. "upstream" upon binding (Meersseman et al., 1991), but asymmetric binding of H5 may also be responsible for this effect (Hayes and Wolffe, 1993; Pruss et al., 1996). It is of interest to note that if binding is asymmetric, it exhibits preference to the upstream

Figure 3.15. EcoR I endonuclease digestion of reconstituted 208-12 DNA chromatin fibers. Digestion occurred under the following molar H5/octamer stoichiometry H5: 0 (*solid squares*), 1 (*solid circles*), and 3 (*open squares*). The amount of digestion was measure by the release of mononucleosomes into a 6% native polyacrylamide gel run in TAE as measured by the amount of ethidium bromide UV illumination. Reaction conditions included 30 mM Tris (pH 7.6), 3.5 mM MgCl<sub>2</sub>, 50 mM NaCl, 0.01 % Triton X-100 with 0.7 ug/ml of EcoR I used to digest 0.05 mg/ml chromatin DNA at room temperature.

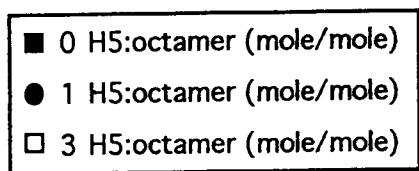
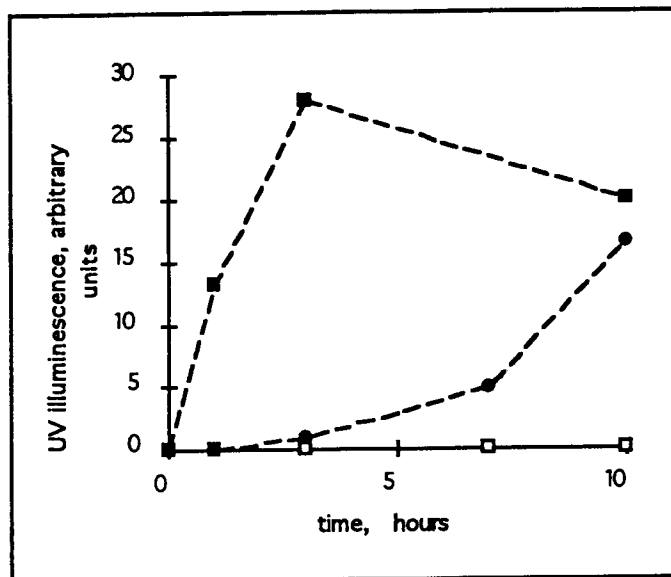


Figure 3.15

position; preferential downstream binding (in the vicinity of residues 147-167) would not give protection (see [Figure 3.13](#)). Third, H5 may induce structural changes in the fiber that prevent access to linker DNA. Compaction or stabilization of a more condensed form of chromatin is known to limit access to linker DNA (Leuba et al., 1994). However, at the  $MgCl_2$  and NaCl concentrations used for the restriction digestion, the stripped chromatin should also be maximally compacted for the fiber digested in either the presence and absence of H5 (Schwarz and Hansen, 1994). Finally, H5-induced aggregation of the reconstituted chromatin fibers may have limited access to EcoR I. In addressing this concern, fibers reconstituted at 1 H5 / octamer entered a 1% agarose gel run in TAE, indicating solution solubility. However, it is conceivable that  $MgCl_2$  may have induced aggregation of the H5 bound-reconstitutes in the reaction conditions. It should also be noted that octamer-reconstituted 208-12 DNA has been reported to remain soluble under the reaction conditions used in this study (Hansen and Lohr, 1993). Certainly, the accessibility of fibers reconstituted at 1 H5 / octamer (compared to 3 H5 / octamer), suggests solubility, as does the noticable lack of precipitate.

#### 3.4.3 Agarose gel electrophoresis of the reconstituted fibers

Gel electrophoresis has been previously used to analyze small reconstituted chromatin fibers (reviewed in (Hansen et al. (1997))). As with other macromolecules like DNA, chromatin migrates under the influence of an electric field due to a net negative surface charge density, but is impeded by the collisions with the gel matrix. In general, electrophoresis of a macromolecules through gel matrix is described by the equation,

$$\frac{\mu}{\mu_o} = \left(1 - \frac{R}{P_e}\right)^2,$$

where  $\mu$  is the relative electrophoretic mobility (usually relative to a viral capsid standard),  $\mu_o$  is the mobility in free solution,  $P_e$  is the effective pore radius, and  $R$  is the effective radius of the molecule (Griess et al., 1989). Polymers, including chromatin, also experience a phenomenon known as reptation in which the complex can travel, in a worm-like fashion, through a gel matrix with a pore size considerably smaller than its radius of gyration. Reptation is defined at the point where  $R$  decreases with decreasing  $P_e$  (Fletcher et al., 1994a). These parameters have been calculated for chromatin fibers (i.e. fiber effective radius, fiber surface charge density) from Ferguson-type plots by a technique known as quantitative gel electrophoresis in which chromatin samples are analyzed with agarose gel electrophoresis at different percent agarose (Fletcher et al., 1994a; Fletcher et al., 1994b).

In this study, the effect of H5 binding to small chromatin fibers was measured by changes in the relative mobility in a simplified form of quantitative proteolysis. Instead of measuring the electrophoretic mobility of samples for many agarose concentration, samples were analyzed with either 0.3% or 1% agarose gel electrophoresis. As observed for 208-12 DNA reconstituted at various octamer saturations (Appendix A3), the 0.3% agarose gel emphasizes  $\mu_o$  or surface-charge-density-related difference between reconstitutes. In contrast, the 1% agarose gel was used to compare not only surface-charge-densities but also incorporated shape-related differences. H5 was incubated with a slightly over-saturated ( $n=13-14$ ) reconstituted 208-12 DNA. This value of  $n$  is based on estimates from the sedimentation coefficient (see Appendix A2), and may

indicate that more octamers were bound than available positioning sites. The mobilities (relative to free DNA) of reconstitutes containing 0, 1, and 3 moles of H5/ moles of nucleosomes, were 0.85, 0.91, and 0.87, respectively in a 0.3% agarose gel, and 1.0, 1.07 and 1.06, respectively, in a 1% agarose gel (Figure 3.16). So, it appears that the addition of linker histones increased the electrophoretic mobility at both concentrations. H5 also appeared to "stabilize" the reconstitutes, as observed by gel electrophoresis, as the band corresponding to the nucleoprotein complex was sharpened with the addition of H5 (data not shown).

Raising the ratio to 3 H5:octamer (mole/mole) appeared to reduce the surface charge density ( $\mu_o$ ) but without significantly altering shape. This is best demonstrated by a significant reduction in the electrophoretic mobility of reconstitutes with 3 H5:octamer in the 0.3% agarose gel as compared to samples at 1 H5:octamer; samples applied to a 1% agarose gel experienced a similar, albeit considerably smaller, difference (Figure 3.16). The 1% agarose gel which is sensitive to shape-related factors appeared to show no major changes in fiber structure going from 1 to 3 H5:octamer, though the 0.3% agarose gel (which is sensitive to the  $\mu$  of the fiber) did measure an increase in H5 binding. Certainly, these results strongly suggest that H5 remodeled reconstituted 208-12 into a more compact shape, but that "over saturation" of H5 onto the chromatin fiber did not appear to significantly increase compaction, though binding did clearly take place. Admittedly, these conclusions are speculative, especially consider that chromatin fiber compaction can be "masked" by a reduction in surface charge density from linker histone binding. To

Figure 3.16. Histogram of electrophoretic mobilities for samples of chromatin fibers reconstituted in the presence of H5. 5-10  $\mu$ l of reconstituted samples at 0.05 mg/ml DNA were applied to each lane. Histogram the electrophoretic mobility (relative to free 208-12 DNA) of H5 bound to reconstituted 208-12 DNA (n = 15) chromatin fibers at 0, 1, and 3 H5-octamer molar ratios. The histogram includes the relative mobility of samples analyzed on 1% agarose gel (*white bar*), and 0.3 % agarose gel (*solid bar*).

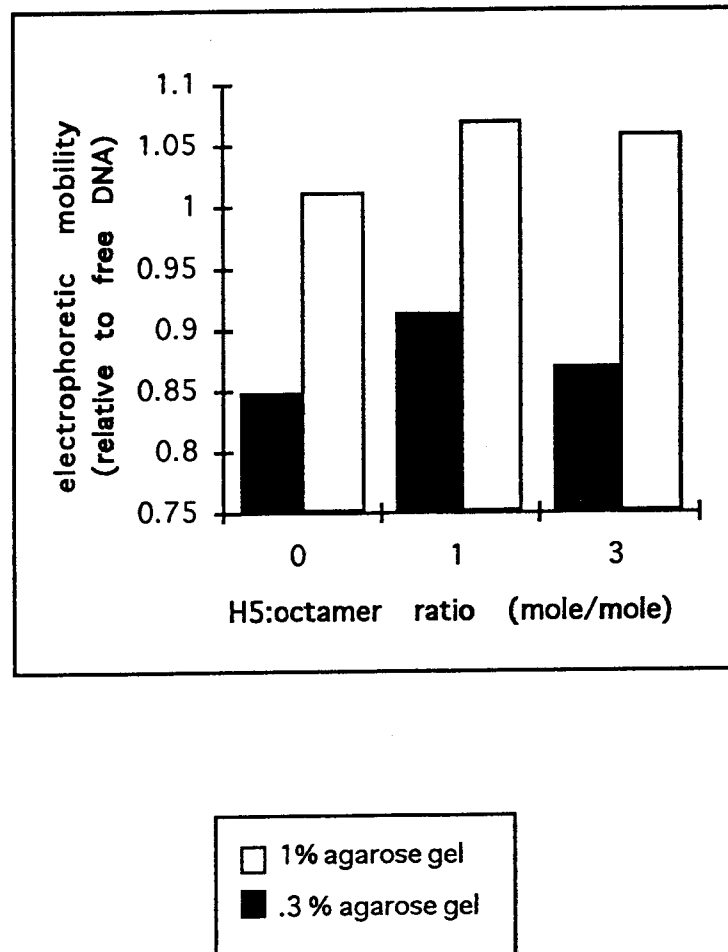


Figure 3.16

circumvent this problem, sedimentation analysis was used to characterize H5-induced compaction of DNA based on hydrodynamic properties.

#### 3.4.4 Analytical velocity ultracentrifugation of the reconstituted fibers

Analytical ultracentrifugation has been an indispensable tool for characterizing reconstituted chromatin fibers. Comparative sedimentation coefficients have previously been used to establish that NaCl (Hansen et al., 1989) and MgCl<sub>2</sub> (Schwarz and Hansen, 1994) condense 208-12 DNA reconstituted with histone octamers. In addition, sedimentation coefficients (in low salt) have also been previously used to estimate the number of octamers bound to the 208-12 DNA (Lohr and Hansen, 1993; Appendix A3). Here, analytical ultracentrifugation was used to examine H5-induced fiber compaction as both a function of NaCl concentration and H5-octamer ratio. Chromatin fibers were reconstituted according to the protocol described above and analyzed with a Beckman XLA analytical ultracentrifuge. The 208-12 DNA was reconstituted with about 13-14 octamers<sup>3</sup> (as estimated by the sedimentation of the fiber in 10 mM Tris-HCl (pH 7.8), 0.2 mM EDTA), which is considered over-saturated since only 12 sites are theoretically available for octamer deposition.

In the first study, the effect of the H5 / octamer ratio on fiber compaction was investigated. The reconstituted 208-12 DNA ( $n \cong 13$ ) was bound with H5 at 1 and 3 H5:octamer (mole/mole). At 10 mM NaCl, 10 mM Tris-HCl (pH 7.8), 0.2 mM EDTA the sedimentation coefficients were 32.5 S, and 36.0 S, respectively (Table 3.1). This

---

<sup>3</sup> The number of octamers was estimated from the  $s_{20,w}$  as outline in Fig. 3 of Hansen and Lohr (1993) (see also Appendix 2). The number of octamers bound in over-saturated fibers ( $n > 12$ ) was estimated by (Hansen and Lohr, 1993, Fig. 8) (see also Figure A2.1).

relatively small change in  $s_{20,w}$  suggests that saturation or even oversaturation with linker histone H5 does not lead to significantly greater compaction in low salt, and supports conclusions based upon agarose gel electrophoresis (see above). In fact, the increase in  $s_{20,w}$  with the addition of 1 or 3 H5/octamer (mole/mole) is close to that expected simply from the increased mass of the chromatin complex.

Table 3.1. The effect of H5 binding and NaCl on the sedimentation coefficient of octamer-supersaturated reconstituted 208-12 DNA chromatin fibers.

|                             | H5 / nucleosome<br>(mole/mole) | NaCl, mM | Sedimentation<br>Coefficient |
|-----------------------------|--------------------------------|----------|------------------------------|
| Preparation 1 <sup>i</sup>  | 0                              | 0        | 31.4                         |
|                             | 1                              | 10       | 32.5                         |
|                             | 3                              | 10       | 36.0                         |
| Preparation 2 <sup>ii</sup> | 0                              | 0        | 34.8                         |
|                             | 2                              | 0        | 38.9                         |
|                             | 2                              | 30       | 50                           |
|                             | 2                              | 60       | aggregation                  |

The estimated concentration 208-12 DNA of the samples was 0.046 mg/ml<sup>i</sup>, and 0.04 mg/ml<sup>ii</sup>. Samples included 2 mg/ml polyglutamic acid (PGA). PGA was found not to effect the compaction of octamer histone-reconstituted 208-12 DNA based on the observation that the sedimentation coefficient of reconstituted 208-12 did not change with PGA concentration up to 2 mg/ml PGA (data not shown). However, Meersseman et al. (1991) do report that PGA may effect the ability for linker histones to produce a chromatosome stop. The H5-octamer ratio was based on input quantities. Values of  $s_{20,w}$  adjusted from values obtained for samples run at 21°C as described in Methods and Materials.

In the second study, the effect of NaCl on fiber compaction at a constant H5 / octamer ratio was examined. The sedimentation coefficient was determined for the

reconstituted 208-12 DNA ( $n \cong 14$ ) bound with 2 H5:octamer (mole/mole) in T.E. and in 30 mM NaCl, T.E. In T.E., H5-bound fibers had a greater sedimentation coefficient than did fibers without H5 (38.9 S and 34.8 S, respectively (Table 3.1)). Again, however, this increase would be largely accounted for by the increase in mass of the chromatin. On the other hand, increasing the NaCl concentration appeared to drastically further compact H5-bound chromatin as the sedimentation coefficient increased to 50.0 S in 30 mM NaCl (Table 3.1). As in the first experiment, these results demonstrate that H5 binding leads to little if any compaction of the reconstituted 208-12 chromatin in low salt. On the other hand, the dramatic increase to 50.0 S for H5 reconstitutes at 30 mM NaCl indicates substantial compaction. Indeed, it is close to the value estimated for "fully compacted", reconstituted 208-DNA (Hansen et al., 1989), comprising approximately two turns of a 6 nucleosome-per-turn solenoid.

### 3.5 Discussion

The experiments in this study, collectively, take a broad approach in examining H5 binding to DNA. Ultimately this was considered necessary due to the multifaceted nature of the binding process. Linker histones: (a) bind DNA, (b) display cooperativity, and (c) organize DNA into extensive aggregate complexes. Additionally, within the cell, H5 binds DNA in association with assembled histone octamers. This study sought to better quantitate H5 interactions with DNA by considering all of these elements. Furthermore, by conducting parallel studies on both H5, and its trypsin resistant globular domain, the

role of linker histone tails in DNA binding, and nucleoprotein aggregation was also elucidated.

### 3.5.1 GH5/H5 binding to DNA

A number of important observations were made in characterizing H5 binding to DNA. A comparison of chymotrypsin digestion rates of H5 in solution and H5 bound to DNA demonstrated that upon H5 binding to DNA, Phe 93 is placed in a position or conformation more exposed to the enzyme than when the protein is free in solution. The finding that Phe 93 became more exposed upon H5 binding to DNA may be particularly important especially since biochemical data addressing the way H5 actually interacts with DNA is limited. Arguably in the most definitive study on how GH5 binds to DNA, Goytisolo et al. (1996) demonstrated that neutralization of a cluster of basic residues around the third  $\alpha$ -helix (Arg 73, Lys 69, and Lys 85) leads to weaker DNA binding. However, the same is also true when a cluster of basic residues (Lys 40, Arg 42, Lys 52, Arg 94) on the opposite side of the protein from are neutralized. The results of Goytisolo et al. (1996) do not resolve the question as to which part of GH5 binds to DNA more tightly ; data indicates that neutralization of residues on either of the sites has an almost equivalent effect on GH5-DNA interactions. While the exact reasons for increased chymotrypsin digestion of Phe 93 upon H5 DNA-binding reported here is unclear, results indicate that the mechanism of DNA binding is likely unlike structurally similar major groove helix-turn-helix, and winged-helix proteins.

To further study details of the GH5-DNA complex a computer modeling experiment was conducted in which DNA was docked into the GH5 crystal lattice as deduced by Ramakrishnan et al. (1993). Results suggest that Arg 73, Lys 69, and Lys 85 may be able to make contact with the DNA backbone either by binding in the minor groove or major groove. Minor groove binding by intact linker histones is well established based on distamycin competition studies (Kas et al., 1989), though it is unclear whether the globular domain itself actually interacts with the minor groove--especially since the SPKK motif in the C-terminal tail preferentially binds A-T rich sequences in the minor groove with a relatively-high binding affinity (Churchill and Suzuki, 1989). However, neither proposed GH5-DNA model satisfactorily predicts the observed enhanced exposure of Phe 93 to chymotrypsin digestion upon GH5 binding to DNA. These differences may be reconciled by any of the following: (a) GH5 binds to DNA via sites other than the third  $\alpha$ -helix (as described above), (b) DNA binding involves major groove binding by the third  $\alpha$ -helix but the binding complex rearranges as to exposes Phe 93 to solution (unlike the homologous residue of HNF-3 $\gamma$  (Clark et al., 1993)), or (c) H5 tails, which bind considerably tighter than the globular domain, sterically prevent GH5 from binding via the third  $\alpha$ -helix (and associated residues), thus leading to preferential Phe 93 digestion. The last possible explanation exemplifies a potentially serious problem in using GH5 to determine how the globular domain interacts with DNA in the context with the entire protein: such GH5 studies assume that the tail domains do not influence the binding of the globular domain. For example, the second wing of GH5 (W2) is located in the C-terminal tail, and likely influences binding--based on the homologous interaction of W2 with DNA

from HNF-3 $\gamma$ /DNA crystal data (Clark et al., 1993). Other studies tend to support primary site binding, since Phe 93 has been reported to be protected from chymotrypsin digestion upon H5 binding to nucleosomes (Leuba et al., 1993), and salt-compacted chromatin (Losa et al., 1984). However, binding to nucleosomes may involve special placement, or reformation of the linker histone, or a linker histone adjacent to a bulky nucleosome may not allow appropriate approach of a proteolytic enzyme. Furthermore, salt compaction may simply prevent access of chymotrypsin to much of the fiber. Because of such caveats, it is important for studies to be conducted with naked DNA.

By comparing binding of GH5 and H5, the importance of the terminal tail domains in DNA binding was demonstrated. It is well established that H5 displays higher affinity binding to both DNA and chromatin than does GH5 (Segers et al., 1991; Thoma et al., 1983). This was corroborated here by the finding that H5 bound a 22 b.p. oligonucleotide with a higher affinity than GH5. The tails domains also appear to require considerable more DNA for binding than GH5. The binding site size of GH5 was estimated at between 11-14 b.p. based on the preferential of GH5 molecules bound and crosslinked to DNA for each oligonucleotide. On the other hand, the binding site size for H5 appeared to be greater than 22 b.p., since the 22 b.p. oligonucleotide competed extremely poorly against a 42 b.p. oligonucleotide for H5. This conclusion supports an estimate of 41 b.p. / H5 by Clark and Thomas (1988).

In this chapter, GH5/H5-DNA aggregates served as an experimental system to elucidate DNA binding, and protein-protein interactions that might contribute to chromatin stability (which also experiences salt induced aggregation). It has been recognized for some time that linker histones readily aggregate DNA (Glotov et al.,

1978c). Matthews and Bradbury (1978) and Glotov et al. (1978c) proposed that linker histone aggregation was a result of the bridging of separate nucleoprotein complexes via the terminal tail domains. However, based on solubility in 2% SDS, both GH5 and H5 aggregated DNA after an overnight incubation with DNA on ice in low salt buffer. Therefore, linker histone tails were not necessary for DNA aggregation, but appeared to only to increase the aggregation rate. Additionally, aggregates containing H5 were much more resistant to disruption by urea than those involving GH5, indicating fundamentally different modes of aggregation.

Linker histones were found to aggregate linear DNA more efficiently than supercoiled DNA, suggesting that linker histones assemble onto the DNA conformers differently. Since aggregation increased with NaCl concentration, this may indicate that the phenomenon is related to a reduction in the effective charge of the H5-DNA complex. Osipova et al. (1985) reports that aggregation increases with the number of basic residues found in the terminal tail domains; so that salt and linker histone binding may serve the same purpose. H5 may saturate onto linear DNA more easily than onto supercoiled DNA, leading to greater charge neutralization, and aggregation. In support of this interpretation, Singer and Singer (1978) found that soluble plasmid DNA bound significantly fewer H1 molecules than aggregated plasmid DNA; hence nucleoprotein complexes with a higher net negative charge were more soluble than those with a lower net negative charge.

The GH5-DNA aggregate provided a model to better understand the interactions that constitute GH5-DNA complexes. Through salt, and separately, urea dissociation studies, GH5 was found to stabilize the aggregate by at least two binding "elements".

The first "element" was disrupted from 250 mM - 350 mM NaCl, and 0 M - 2 M urea, and appeared to convert the GH5-DNA complex from a solution-insoluble to a solution-soluble complex, though little DNA was released as a result of this structural reorganization. The second "element" was disrupted from 350 mM - 500 mM NaCl, and 2 M - 6 M urea, and resulted in the complete dissociation of the "solublized" GH5-DNA complex. Because GH5 assembly onto DNA is poorly characterized, it is unclear whether "elements" refer to protein-protein contacts or protein-DNA interactions, though the higher affinity element was clearly cooperative in nature, since only free DNA (and not partially GH5-saturated oligonucleotides) were dissociated from the aggregate.

Increased aggregate solubility in relatively low concentrations of urea indicates that hydrogen bonding is important in aggregate stabilization. For GH5, aggregates appear to be strongly reliant on hydrogen bond interactions since even 2 M urea was sufficient to solublize the GH5-DNA aggregate complex. In contrast, H5-DNA aggregates required nearly 6 M urea to produce significant solubilization, which likely was the result of protein structure destabilization. Arguably, hydrogen bonding involved protein-protein interactions, and not DNA-protein contacts, as the destabilization observed for GH5-DNA complexes at low urea concentration was not observed H5-DNA complexes. Instead, GH5 induced aggregation appears to be a phenomenon based largely on protein-protein hydrogen bonding, while H5 emphasizes DNA-protein contacts in forming aggregates.

The finding that DNA dissociated from the aggregate complex in a cooperative fashion may be a significant observation, since the basis for linker histone cooperativity remains unelucidated. Cooperativity may follow two separate models

including: (a) the "tramline" model in which closely associated, parallel-running DNA act as high affinity DNA substrates (Thomas et al., 1992), and (b) cooperativity that is based on strong protein-protein interaction following more classical perspectives (McGhee and von Hippel, 1974). Unfortunately, the salt-dissociation results, though significant since the cooperative nature of linker histone binding was reaffirmed (Watanabe, 1986), still do not elucidate the basis for cooperativity. Kinetic analysis may ultimately be required to determine the basis of cooperativity since the "thermodynamic endpoints" appear to be identical for both models.

### 3.5.2 H5 binding to chromatin

Model linker histone-DNA models have been effectively utilized to better understand how linker histones interact with naked DNA. But these studies are limited since the effects of the nucleosome are not considered. To provide a more physiologically-relevant analysis of H5 binding to DNA (in the context of the octamers), a DNA comprised of twelve tandem repeats of the 5S rRNA gene of *Lytechinus variegatus* (208-12 DNA) (Simpson et al., 1985; Georgel et al., 1993) was reconstituted with octamers and H5. The 208-12 DNA construct was specifically chosen for this study because: (a) the number of octamers bound is readily determined by calibration curves based on the sedimentation coefficient (Hansen and Lohr, 1993; see Appendix A2), (b) the precise effects of NaCl and MgCl<sub>2</sub> on the compaction of 208-12 DNA has been elucidated (Hansen et al., 1989; Schwarz and Hansen, 1994), and (c) the effects of H5 on the reconstituted 208-12 remained to be elucidated--the reconstitution studies reported

here are the first to include linker histones. Linker histone binding to reconstituted 208-12 DNA was characterized by agarose gel electrophoresis, velocity analytical ultracentrifugation, and endonuclease digestion studies.

Results presented here clearly support H5-induced compaction of the reconstituted fibers as others have also demonstrated (reviewed in van Holde, 1989). Gel electrophoresis indicated that in 40 mM Tris-acetic acid (TAE electrophoresis running buffer), H5 readily "compacted" the reconstituted 208-12 DNA, as indicated by an increase in electrophoretic mobility for both 0.3% and 1% agarose gel electrophoresis (relative to saturated reconstitutes without H5). Interestingly, the fibers appeared to be relatively unaffected by the input concentration of H5 as indicated by both velocity analytical ultracentrifugation and gel electrophoresis. In order to "properly" fold chromatin, the presence of both H5 and NaCl were required to produce maximally compacted fibers supporting the studies of Losa et al. (1984) utilizing native chromatin. The maximum observed sedimentation coefficient ( $s_{20,w}$ ) of 50.0 S is close to the value of 51.5 S predicted by hydrodynamic modeling (Bloomfield et al., 1967) for reconstituted 208-12 DNA making two turns of a 30 nm diameter solenoid (with six nucleosomes per turn) (Hansen et al., 1989). Thus, H5 may have packaged the reconstituted 208-12 DNA (lacking linker histones) into a compacted solenoidal-like structure by 30 mM NaCl.

It was also of interest to compare H5-induced fiber compaction to salt-dependent effects which have been well documented (Finch and Klug, 1976; Losa et al., 1984; Leuba et al., 1994). From sedimentation studies, reconstituted 208-12 DNA (lacking linker histones) has been reported to reach a maximal state of compaction of 40 S at 200 mM

NaCl (Hansen et al., 1989), and 55 S in 2 M MgCl<sub>2</sub> (Schwartz and Hansen, 1994). This indicates that the effects of NaCl and MgCl<sub>2</sub> on fiber compaction result in different compacted isoforms. By comparing physiologically-relevant compaction achieved by adding H5, and NaCl, to reconstituted 208-12 DNA, it appears that neither MgCl<sub>2</sub> nor NaCl can by themselves properly compact chromatin. MgCl<sub>2</sub> appears to "over-compact" the fiber, and NaCl clearly forms "under-compacted" fibers; results supported from electron micrographs (Losa et al., 1984). In explaining the necessity for H5 to properly compacting chromatin, it is not possible to distinguish whether H5 is required to bend linker DNA or bring the entering and exiting DNAs together on the nucleosomes (reviewed in van Holde and Zlatanova, 1996). However, based on similarities in  $s_{20,w}$ , MgCl<sub>2</sub> and H5 may induce fiber compaction via the same general mechanism.

Reconstituted 208-12 DNA was also digested with the EcoR I, a restriction endonuclease that cleaves at a site near the dyad axis of the nucleosome. Results indicate that H5 binding conferred protection to the site, as the digestion rate for chromatin fibers reconstituted with H5 was significantly less than that for fibers not reconstituted with H5. These results are consistent with (Meersseman et al., 1991) who report that H5 reconstituted onto 18 tandem repeats of the 5S rRNA gene of *Lytechinus variegatus* results in chromosome protection that is expected to include 197 (the EcoR I cleavage site). Such specific exclusion argues for an asymmetric site with preferred orientation upstream from the histone octamer position.

## CHAPTER 4

### Analysis of Linker Histone-DNA Complexes Using SDS-PAGE

#### 4.0 Summary

Glutaraldehyde is a protein-DNA crosslinking reagent that has been extensively used in fixing histones to DNA in chromatin-related studies. In this chapter, glutaraldehyde crosslinking is used to investigate the equilibrium between soluble DNA molecules and those involved in larger DNA-histone networks. In a second study, a comparison is made between linker histone H5, and its globular domain in salt concentration-dependent binding and crosslinking to DNA. The effect of the globular domain on overall H5-DNA interactions was observed, and results suggest that DNA-binding domains of linker histones crosslink to DNA in a relatively independent fashion. Finally, a clear demarcation at 0.06% glutaraldehyde for "complete" and "partial" crosslinking of GH5 to short oligonucleotides was observed. Between "saturated" and "under-saturated" crosslinking was observed. When applied to an SDS/polyacrylamide gel, "partially-crosslinked" samples were separated into a number of intermediate complexes. By combining diamine and non-diamine silver staining, the relative amount of DNA and GH5 in each intermediate complex was estimated, non-isotopically, in a technique referred to as differential staining SDS-PAGE.

## 4.1 Introduction

Linker histones belong to a class of eukaryotic chromatin structural proteins. Each linker histone is composed of a tripartite structure consisting of a basic N-terminal tail domain, a compact, trypsin-resistant globular domain, and a very basic C-terminal tail domain (Aviles et al., 1978). Linker histones bind nucleosomes and stabilize the DNA-octamer complex, though the location of the binding site is still a matter of some debate (reviewed in Zlatanova and van Holde, 1996). Functionally, linker histones compact or condense chromatin from an extended fiber to a somewhat heterogeneous solenoidal-shaped fiber around 30 nm in diameter (Thoma et al., 1979; Leuba et al., 1994). The exact mechanism by which linker histones compact chromatin is unknown though histone-histone interactions play an important role (Riehm and Harrington, 1989), and the C-terminal linker histone tail appears to be necessary (Allan et al., 1986). The C-terminal tail is distinct from the other domains in that: (a) it is considerably more basic, (b) it binds DNA more tightly than the combined globular domain and N-terminal peptide (Thoma et al., 1983; Glotov et al., 1978b), and (c) it facilitates enhanced linker histone self-association (Chapter 2).

Linker histones bind cooperatively to DNA and are generally believed to interact with linear DNA nonspecifically, though oligonucleotides that contain poly-A tracks (unpublished data), and AT-rich DNA (Izaurrealde et al., 1989) as well as other particular sequences have been shown to display some preference in binding (reviewed in Zlatanova and Yaneva, 1991). Linker histone H1, a ubiquitous class of linker histone binds DNA cooperatively in a salt-dependent manner (Renz and Day, 1978; Clark and Thomas, 1986;

Singer and Singer, 1978; Liao and Cole, 1981). In low salt, H1 binds with low cooperativity, but at ionic strengths above 20-40 mM NaCl, H1 displays enhanced cooperativity. On the hand, the avian erythrocyte-specific linker histone H5 (Clark and Thomas, 1988), and the globular domain of H5 (GH5) (Thomas et al., 1992) cooperatively bind to DNA in a salt-independent manner. In a related phenomenon, linker histones have been reported to associate as multiple DNA-protein complexes that result in aggregation, as observed from electron micrographs (De Bernardin et al., 1986), gel electrophoresis (Yaneva et al., 1991; Chapter 3), and sedimentation analysis (Osipova et al., 1985; Liao and Cole, 1981). Aggregation increases with salt concentration likely due to diminished charge repulsion between DNA-protein complexes or possibly due to salt effect protein-protein interactions. Additionally, linker histones bound to supercoiled DNA experience less aggregation than linear DNA (Chapter 3). It has been proposed that aggregation involves "crosslinks" between separate DNA-protein complexes in which the C-terminal tail acts as a bridge. In this way, the aggregates may reflect a network of DNA-protein complexes linked by the lengthy C-terminal tails (Glotov et al., 1978c; Matthews and Bradbury, 1978). However, the globular domain is also capable of aggregating DNA, thus indicating that the tails are not absolutely necessary but only increase the potential for aggregation (Chapter 3).

In this study, the effect of glutaraldehyde crosslinking was used as a tool to better understand histone-DNA interactions. Glutaraldehyde is a bis-aldehyde homobifunctional protein-DNA crosslinker that has been extensively utilized in the study of histone proteins and chromatin (De Bernardin et al., 1986; Olins and Wright, 1973, Thoma and Koller,

1977; Leuba et al., 1994; ). It has been speculated that glutaraldehyde covalently links amine groups via a Schiff base pathway (Figure 4.1) (Hermanson, 1996).

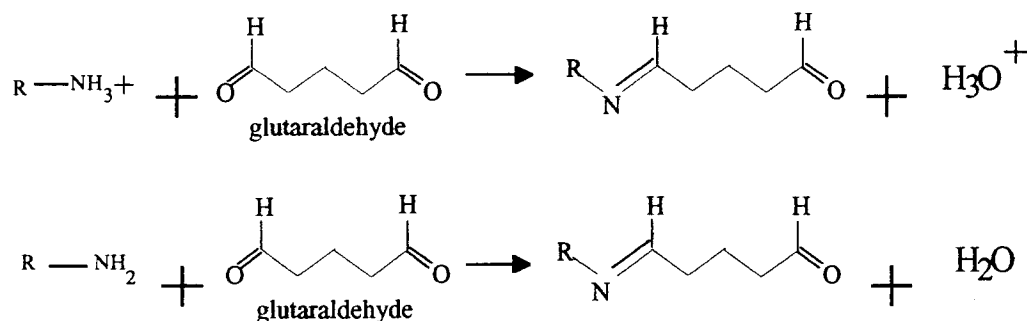


**Figure 4.1.** Modification of amine groups upon reaction with glutaraldehyde (Hermanson, 1996).

In the following work, it is reported that for samples briefly crosslinked, glutaraldehyde actually may have interfered with DNA-histone interactions; possibly from electrostatic neutralization of charged amines or steric interference with DNA-protein contacts. However, glutaraldehyde crosslinking for long time periods clearly resulted in linker histone-DNA "fixation" indicating that linker histones bind DNA despite the covalent attachment of glutaraldehyde molecules. In two related technical reports, methods that apply glutaraldehyde and SDS-PAGE are presented. First, a non-isotopic strategy for estimating the relative amounts of protein and nucleic acids in mixtures and complexes was developed. It is reliant on two silver staining protocols, and appears to be well suited for examining nucleoprotein complexes, especially those that are prone to aggregation, by maintaining solubility in SDS. Second, the salt-dependent dissociation of crosslinked linker histone-DNA complexes was used to compare the binding/crosslinking

of GH5 and H5. Results suggest that the technique can be used to identify separate DNA-binding motifs on a protein, based on the relative affinities for DNA.

## **4.2 Methods and materials**

### 4.2.1 Protein purification procedure

Recombinant GH5 was expressed and isolated based on a previous report by Cerf et al. (1993) as described in Chapter 2. Briefly, BL21 *E. coli* cells transformed with GH5pLK, a pET-3a expression vector (Novagen) inserted with the coding sequence for GH5 (Gerchman et al., 1994), were grown to 0.35-0.6 OD(600 nm) and induced with 0.6 mM IPTG for several hours. Cells were sonicated, and proteins were extracted in buffer containing 25 mM Tris-HCl (pH 7.8), 500 mM NaCl, 0.2 mM EDTA, 0.35 mM PMSF. After precipitating protein contaminants in 0.38 mg/ml ammonium sulfate, the decanted supernatant was dialyzed into 300 mM NaCl, 0.2 mM EDTA, 10 mM Tris-HCl (pH 7.8) and purified on a CM Sephadex C25 (Sigma) column with a gradient from 0.3 - 1 M NaCl. After extensive dialysis into water, purified GH5 was stored frozen in water. GH5 concentrations were determined from extinction coefficients as described in Chapter 2.

Native H5 was isolated from frozen chicken blood (Lampire) with some alterations to the procedure described in Garcia-Martinez et al. (1990). As described in Chapter 3, chicken nuclei were isolated by disrupting erythrocytes in frozen blood (Lampire). Nuclei were hypotonically lysed in 0.2 mM EDTA, 0.1 mM PMSF and linker histones were salt extracted by bringing the resulting chromatin "jelly" to 0.65 M NaCl. CM Sephadex C25 cation exchange chromatography was used to purify linker histone H5 in a stepwise

elution process in which linker histone H1 and other contaminants were eluted from the column in 800 mM NaCl, 10 mM Tris-HCl (pH 7.8), 0.2 mM EDTA. H5 was subsequently eluted off the column in 1.6 M NaCl, 10 mM Tris-HCl (pH 7.8), 0.2 mM EDTA, 0.1 mM PMSF, dialyzed extensively into water and stored frozen.

#### 4.2.2 Preparation of DNA

A 22 b.p. oligonucleotide duplex was formed by annealing the sequence GTA GTA ACG GAA GCC AGG TAT T to its complement strand. Separately, a 42 b.p. oligonucleotide duplex with the sequence CCG GAA TTC GCA TCA TTG CCT TCG GTC CAT AAA GGA ATT CGG was annealed to its complementary strand. The former sequence represents a putative linker histone H1 binding site that is based on a DNA footprinting sequences from the mouse serum albumin gene (Sevall, 1988).

Oligonucleotides were generated using a 380A DNA synthesizer (Applied Biosystems, Inc.). Salts associated with DNA synthesis were removed by first dissolving the oligonucleotides in water, then passing the solution through a 0.9 x 2.0 cm G-50 Sephadex NICK column (Pharmacia). The single-stranded oligonucleotide were combined in roughly equimolar proportions in 10 mM NaCl, 0.2 mM EDTA. Samples were raised to 90 °C in a heating block, and cooled slowly back to room temperature at a rate determined by the cooling of the heating block. DNA concentrations were roughly approximated by UV absorbance spectroscopy with  $\epsilon$  (260 nm) = 20  $\mu\text{g}^{-1}$  ml  $\text{cm}^{-1}$ .

Plasmid pPol208-12 was isolated from DH5 $\alpha$  *E. coli* cells using the alkaline lysis procedure (Maniatis et al., 1982). DNA was further purified from a CsCl gradient, and cut with Hha I (New England Biolabs) following methods outlined by the manufacturer.

pPol08-12 contains twelve tandem copies of a 5S rDNA nucleosome positioning sequence (208 b.p.) from *Lytechinus variegatus* that is inserted into the multiple cloning site of pUC19 (Georgel et al., 1993) and is based on the original construct from (Simpson et al., 1985). The final product consisted of the insert, over 2600 b.p. in length, as well as up to 16 smaller fragments, each less than 400 b.p. in length, from Hha I cut pUC19 ( Table 4.1).

#### 4.2.3 Gel staining procedures

A diamine stain protocol, as reported in Sasse and Gallagher (1991), was found to work well in staining both DNA and proteins. Samples were separated by SDS-PAGE (Laemmli, 1970), and the 18% polyacrylamide gel was immediately soaked in 10% glutaraldehyde for 30 minutes. Uncrosslinked glutaraldehyde was removed from the gel by washing it in water (frequently changed) inside a covered container. Washing was continued until the wash water was clear instead of a greenish color caused by glutaraldehyde. The gel was placed in a diamine staining solution for thirty minutes. The diamine staining solution was prepared by adding 0.4 g of  $\text{AgNO}_3$  to 2 mls of distilled water, then by combined this with a solution composed of 190  $\mu\text{l}$  of NaOH and 0.7 mls of  $\text{NH}_4\text{OH}$  that had been brought to 48 mls in distilled water. If the thoroughly-mixed solution was turbid,  $\text{NH}_4\text{OH}$  was added, dropwise, until the solution cleared. The gel was then washed (twice) in distilled water for one minute, and placed in developing solution: 0.5 g sodium citrate and 0.5 mls formaldehyde brought to 100 mls with distilled water. Upon coloration, the gel was removed from the developing solution and soaked in a large

volume of distilled water with frequent change of water. Farmer reagent (Kodak) was used if gels became "over stained". The destaining reaction was stopped by soaking the gel in a large volume of water with repeated changes of water.

A non-diamine stain protocol (personal communicated by Dr. Julia Yaneva) was found to preferentially silver stained nucleic acids. The SDS / polyacrylamide gel were first fixed in 10% glutaraldehyde as described above. The gel was then "pre-soaked" in 5% nitric acid for 15 minutes, and washed in distilled water for 10 minutes. Gel staining consisted of shaking the gel in 0.4 %  $\text{AgNO}_3$  for 30 minutes, and washing the gel (twice) in distilled water for 1 minute. The developing solution consisted of either 0.5 mls of formaldehyde and 0.5 g of sodium citrate dissolved in 100 mls of distilled water, or alternatively, 5.67 g of sodium carbonate and 0.5 mls of formaldehyde dissolved in 200 mls of distilled water. Gels were destained with Farmer's Reagent (Kodak), if necessary, as described above.

SDS / polyacrylamide gels were stained with coomassie for 30 minutes in 45% methanol (v/v), 9% acetic acid, and 0.25% (w/v) coomassie G-250 then destained in 7.5% acetic acid and 5% methanol with a kimwipe to absorb coomassie from gel.

#### 4.2.4 PAGE-related analysis

SDS / polyacrylamide gels were constructed based on (Laemmli, 1970). The stacking gel composed of 6.35 % polyacrylamide:bisacrylamide (30:0.8), 0.135 M Tris-HCl (pH 6.8), 0.1% SDS; the separating gels consisted of 18% polyacrylamide:bisacrylamide (30:0.8), 0.375 M Tris-HCl (pH 8.7), 0.1% SDS. Gels

were run in buffered solution (5x: 15.1 g Tris-base, 94 g glycine, 5 g SDS / 1 liter) typically at 13.5 volts/cm. Before loading, samples were mixed with 2x SDS loading buffer (0.125 M Tris (pH 6.8), 4% SDS, 20% glycerol, and 0.04% bromophenol blue) briefly at room temperature. Native PAGE was conducted in TBE with 15% polyacrylamide:bisacrylamide (30:0.8) gels at 12.5 volts/cm. Before loading, samples were mixed with 10x loading buffer (1 % bromophenol blue, 1 % xylene cyanol, and 50% glycerol). Gels were processed by staining in ethidium bromide (0.5 µg/ml), and fluoresced with UV luminescence. Gels were quantitated from photographs processed with NIH Image (version 1.57) (O'Neill, et al., 1989).

#### 4.2.5 Crosslinking GH5 to DNA with glutaraldehyde

Unless otherwise stated, GH5 was bound to DNA in 10 mM sodium phosphate (pH 7.2), 0.2 mM EDTA, and incubated for 30 minutes at room temperature. Glutaraldehyde was added dropwise (and repeatedly pipetted after each drop) from a 10 x stock solution, samples were shaken for 5-15 minutes and incubated for about 3 hours at room temperature, then rapidly frozen in SDS loading buffer by placing the eppendorf tubes in liquid nitrogen.

For studies involving salt-dependent crosslinking, GH5 at 0.12 mg/ml was bound to Hha I cut pPol208-12 at 0.04 mg/ml for 30 minutes at room temperature in 0.2 mM EDTA, 10 mM sodium phosphate (pH 7.2) with the salt concentration adjusted to between 0 and 800 mM NaCl. Glutaraldehyde was added from a 10 x stock to 0.06% as

described above, and allowed to crosslink for several hours at room temperature. Samples were subsequently frozen (in liquid in liquid nitrogen) in SDS loading buffer. H5 at 0.07 mg/ml was added to Hha I cut pPol208-12 in a fashion identical to that for GH5.

#### 4.2.6 Differential staining SDS-PAGE methodology

GH5 at 0.045 mg/ml and DNA at 0.045 mg/ml were mixed in buffered solution containing 0.2 mM EDTA, 10 mM Tris-HCl (pH 7.8) and incubated at room temperature for 45 minutes. Glutaraldehyde (Sigma) initially at 25% w/v was diluted in reaction buffer to a 10 x concentration (with respect to the final concentration used in the experiment). The 10 x glutaraldehyde stock was added, dropwise, to the GH5-DNA reaction solution followed by rapidly pipeting the mixture up-and-down. Samples were incubated at room temperature for about two hours, followed by rapidly freezing the reaction contents (in an eppendorf tube) in liquid nitrogen. Identical 15  $\mu$ l samples were loaded on two separate 18% SDS / polyacrylamide gels. One gel was silver stained with the diamine silver-staining protocol, and the other gel was silver stained with the non-diamine silver-staining protocol.

### **4.3 Results**

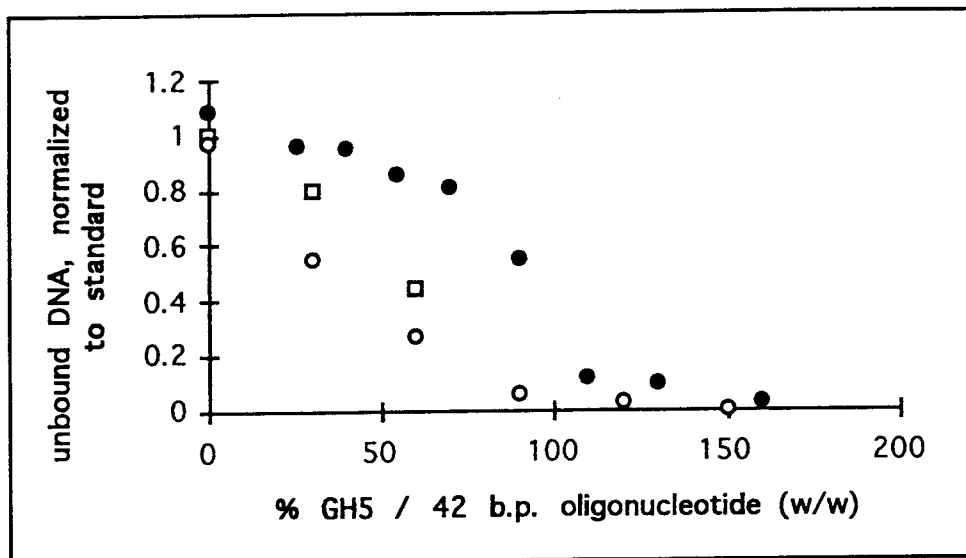
#### 4.3.1 The effect of glutaraldehyde crosslinking on histone-DNA interactions

In earlier chapters it has been demonstrated in several ways that the interaction of H5 and GH5 with linear DNA results in the formation of very large network structures

that cannot enter electrophoretic gels. At the same time, up to quite high histone/DNA ratios, free DNA is still observed, moving at the mobility expected for naked DNA. Does such a titration describe an equilibrium between free DNA molecules and those DNA molecules that are involved in the aggregate network? To investigate this possibility, DNA-binding by the globular domain of linker histone H5 was examined with and without glutaraldehyde treatment, which should irreversibly bind DNA into the network.

A 42 b.p. oligonucleotide (0.033 mg/ml) was titrated with increasing amounts of GH5. Samples were shaken at room temperature for 45 minutes in 10 mM sodium phosphate (pH 7.2), 0.2 mM EDTA then incubated in the presence and absence of 0.06% glutaraldehyde for 2 hours. Samples appeared to be effectively crosslinked as the UV illuminance of crosslinked DNA was considerably greater than that for uncrosslinked samples, and was likely either a result of increased binding by ethidium or DNA molecule fixation in the gel (data not shown). To examine the interactions of GH5 with the 42 b.p. oligonucleotide, the amount of unbound DNA for samples not treated with glutaraldehyde (as observed by native PAGE) was compared to the amount of DNA not crosslinked for glutaraldehyde-treated samples (as observed by SDS-PAGE) (Figure 4.2). Together, these results clearly show that glutaraldehyde crosslinking led to less free DNA at any given histone/DNA ratio. Thus, free DNA must have been in equilibrium with the gel network, and crosslinking shifted the composition by trapping DNA molecules into the aggregate, and therefore removing them from the equilibrium.

Figure 4.2. Effect of glutaraldehyde on GH5 binding to a 42 b.p. oligonucleotide. Comparing the DNA-binding curve of uncrosslinked GH5 to a curve representing DNA interacting with GH5 crosslinked in 0.06% glutaraldehyde. For the binding curve, GH5-DNA complexes were separated on a native 18% polyacrylamide:bisacrylamide (30:0.8) gel run in TBE, and stained with ethidium bromide (0.5  $\mu\text{g/ml}$ ). The amount of unbound 42 b.p. oligonucleotide was normalized to a lane consisting of only DNA (*solid circles*). For the curve representing uncrosslinked DNA, glutaraldehyde-crosslinked GH5-DNA complexes were first treated to 2 X SDS loading buffer to dissociate uncrosslinked GH5-DNA complexes, then samples were separated on an 18% SDS/polyacrylamide gel and stained with the diamine silver staining protocol. The amount of uncrosslinked 42 b.p. oligonucleotide was normalized to a lane consisting of only DNA (*open squares, open circles*). The two different symbols represents two separate experiments.



- GH5 bound to 42 b.p. oligonucleotide in 0.06% glutaraldehyde
- GH5 bound to 42 b.p. oligonucleotide in 0.06% glutaraldehyde
- GH5 bound to 42 b.p. oligonucleotide

Figure 4.2

#### 4.3.2 Elucidating linker histone-DNA intermediate structure in aggregate formation

SDS-PAGE coupled with protein-DNA crosslinking has previously been used to identify laser UV DNA-protein complexes (Hockensmith et al., 1991), and in analyzing the binding of sequence-specific proteins to nucleic acids (Hillel and Wu, 1978; Bourbonniere et al., 1997). In these techniques, proteins that had been bound to DNA were identified based on the covalent linkage of a short radiolabeled oligonucleotide that remained crosslinked following nuclease digestion. However, besides requiring the use of radioisotopes, such techniques are not informative concerning the stoichiometry of complexes. In the following report, use of SDS-PAGE in characterizing DNA-protein interactions was expanded to include a non-isotopic method for estimating the relative amounts of DNA and proteins in small nucleoprotein complexes. Samples were crosslinked in limiting concentrations of glutaraldehyde, separated by SDS-PAGE and silver stained using diamine and non-diamine silver staining protocols (Merril, 1990) in a process otherwise referred to as differential staining SDS-PAGE (DS-SDS-PAGE).

Avian erythrocyte-specific linker histone H5, and its trypsin resistant globular domain GH5, were utilized for this study. Because linker histones readily precipitate linear DNA (Chapter 3; Liao and Cole, 1981), characterization of linker histone-DNA complexes using standard native gel electrophoresis proved to be ineffective. In this study, DS-SDS-PAGE was applied, because SDS maintains non-aggregated GH5-DNA complexes in solution (Chapter 3). Furthermore, by using low concentrations of glutaraldehyde, stable substructure within the aggregate could be detected. Based on the composition of aggregate intermediate complexes identified with DS-SDS-PAGE, it is

clear that protein-protein interactions play an important part in GH5 assembly onto and precipitation of DNA

#### *4.3.2.1 Examining the effect SDS on DNA duplex stability and electrophoretic mobility*

Application of SDS-PAGE in the analysis of linker histone-DNA interactions requires that DNA behave predictably in the presence of SDS. DNA denaturation or anomalous electrophoretic mobility could make results difficult to interpret. SDS was used in both the sample loading buffer at 2% SDS, and in the separating polyacrylamide gel at 0.1% SDS following (Laemmli, 1970). To examine whether DNA denatured under the condition involved in SDS-PAGE, Hha I cut pPol208-12 was heat denatured in SDS loading buffer (2% SDS) (Figure 4.3, lane 3), and compared to a sample that had been treated similarly but without heat denaturation (Figure 4.3, lanes 2). Experiments conducted at room temperature suggest that DNA at least 40 b.p. in size did not denature in 2% SDS. Upon heat denaturation, smaller fragments were observed to re-associate more readily than large fragments, as expected.

As a general observation, small oligonucleotides were observed to migrate to the same position independent of the presence of SDS as gauged by the comparative migration of bromophenol blue in both native and SDS/polyacrylamide gels (data not shown). Additionally, the use of DNA markers for estimating nucleic acid molecular weights was evaluated. The twelve DNA fragments from Hha I-cut pPol208-12 (excluding the 2600 b.p. "208-12" insert) were separated on an 18% Laemmli gel, along with a 123 b.p. ladder (Pharmacia). The DNA size for each fragment was then determined

**Figure 4.3.** Sensitivity of DNA imaging by silver staining, and stability of DNA duplex in SDS. 18% SDS/polyacrylamide gel of DNA (about 0.3  $\mu\text{g}$ ) stained with the diamine silver-staining protocol (Methods and Materials). Lane 1, 123 b.p. DNA ladder, lane 2, Hha I-cut pPol208-12 DNA; and lane 3, Hha I cut pPol208-12 DNA denatured for 15 minutes at 90 °C in SDS loading buffer (2% SDS) before loading into the gel (containing 0.1% SDS).

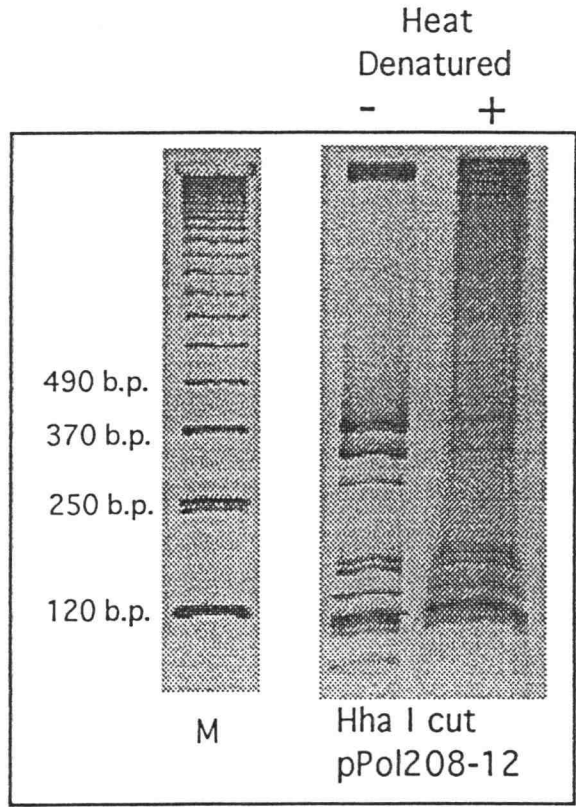


Figure 4.3

based on the 123 b.p ladder using standard procedures (Figure 4.4), and compared to that expected for Hha I-cut pUC19. Despite some variability in the alignment of individual fragments, overall, the fragments appeared to align well with predicted values (Table 4.1). Poor alignment between a few of the fragments may have been caused by a number of factors including: (a) inefficient restriction digestion leading to more fragments than expected, and (b) DNA secondary structure that altered electrophoretic mobility. Similar, minor discrepancies were observed in restriction-digested pUC19 with 1% agarose gel electrophoresis by Yaneva et al. (1995).

Finally, the electrophoretic migration of DNA fragments were compared with dithiobis (succinimidyl propionate) (DSP) and glutaraldehyde crosslinked GH5 homopolymers. Both DNA and protein fibers can be separated by size on SDS gels. A comparison of long DNA and polymers of GH5 crosslinked free in solution reveal important differences in the two macromolecules that affect their relative electrophoretic mobility as observed with SDS-PAGE. As evident from (Figure 4.4), DNA exhibited a significantly greater electrophoretic mobility than did a crosslinked GH5 complex of the same molecular weight. At the same time, the slope (electrophoretic mobility versus logarithm of the molecular weight) of DNA is considerably steeper than that for GH5. The linear relationship between the logarithm of the polymer molecular weight and electrophoretic mobility is indicative of Ferguson-type migration, thus allowing predictable estimates of DNA sizes and the number of protein molecules in self-crosslinked complexes.

**Figure 4.4.** Comparison of the electrophoretic mobility of chemically-crosslinked GH5 homopolymer complexes, a 42 b.p. oligonucleotide and marker DNA (pBSSK+ cut with XBA I, HIND III and Hinf I producing fragments of: 65 b.p., 75 b.p., 296 b.p., 396 b.p., 456 b.p., 517 b.p., and 1074 b.p.) (*open squares*). DNA molecular weights were estimated by multiplying the number of base pairs by 660 daltons / b.p. Crosslinked histone samples include: GH5 crosslinked in 0.1% glutaraldehyde (*solid squares*), and GH5 crosslinked in 0.1 mg/ml dithiobis (succinimidyl propionate) as described in Chapter 2 (*solid circles*). Protein molecular weights were calculated as multiples of the known weight of GH5. All distances were measured from the stacking gel-separating gel interface of an 18% SDS/polyacrylamide gel (30:0.8 polyacrylamide:bisacrylamide).

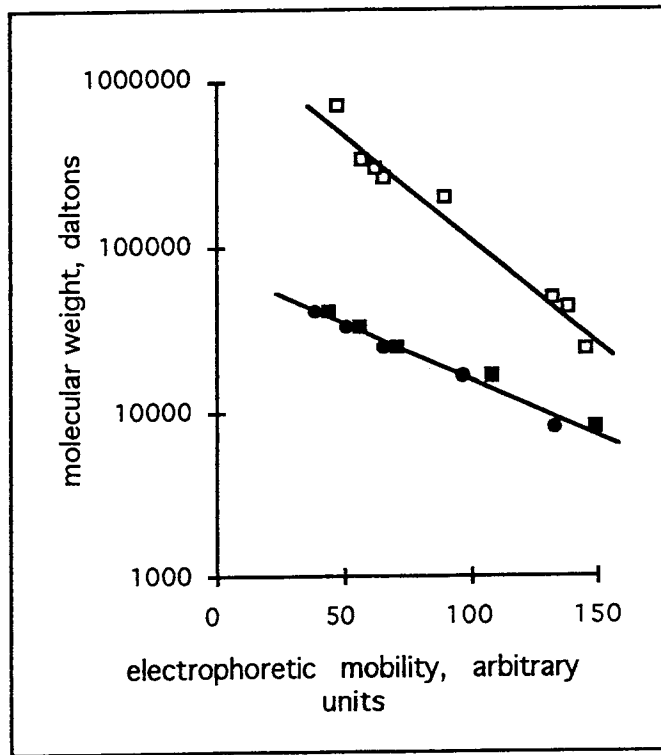


Figure 4.4

**Table 4.1.** A comparison of the theoretic and experimental values of pPol208-12 cut with Hha I as measured with an SDS polyacrylamide gel (18% polyacrylamide).

| Theoretical Values |                 | Preferentially bound by H1 <sup>1</sup> | Experimental Values |                  |
|--------------------|-----------------|---|---------------------|------------------|
| Location           | DNA size (b.p.) |   | Fragment number     | DNA size (b.p.)* |
| 1437-1829          | 392             | YES                                     | 12                  | 368 +/- 22       |
| 1923-2259          | 336             |   | 11                  | 361 +/- 15       |
| 2260-2591          | 331             |   | 10                  | 308 +/- 15       |
|                    |                 |   | 9                   | 306 +/- 15       |
| 717-986            | 269             |   | 8                   | 258 +/- 13       |
| 1154-1327          | 173             |   | 7                   | 162 +/- 13       |
|                    |                 |   | 6                   | 150 +/- 7        |
| 109-238            | 129             |   | 5                   | 129 +/- 9        |
|                    |                 |   | 4                   | 116 +/- 7        |
| 1328-1436          | 108             |   | 3                   | 108 +/- 8        |
| 6-108              | 102             |   | 2                   | 103 +/- 5        |
| 1054-1153          | 99              |   |                     |                  |
| 2592-5             | 99              |   |                     |                  |
| 1830-1922          | 92              |   |                     |                  |
| 987-1053           | 66              |   |                     |                  |
|                    |                 |   | 1                   | 86 +/- 5         |

<sup>1</sup> Based on H1 binding studies conducted by (Yaneva et al., 1996)

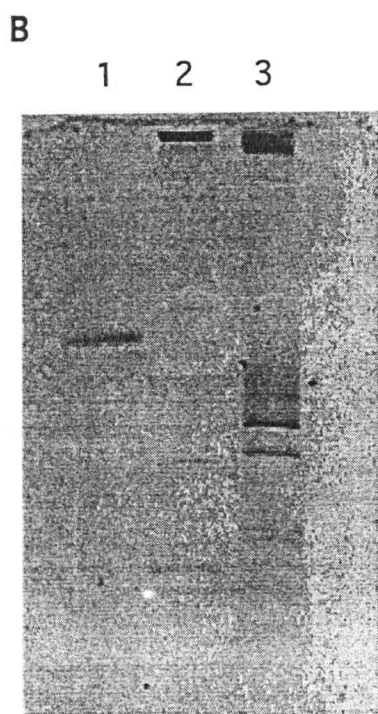
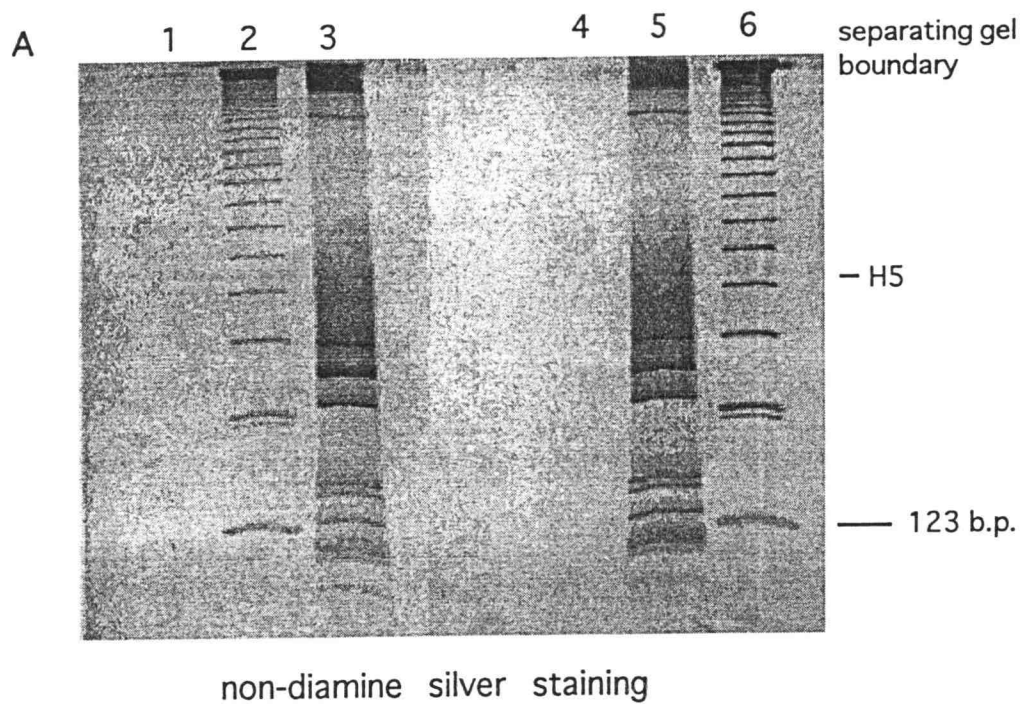
\* Calculated from the 123 b.p. ladder (Pharacia) as a reference, and by plotting log molecular weight vs distance migrated on the gel using standard procedures (average b.p. molecular weight = 660 daltons). Values based on three separate trials.

#### 4.3.2.2 Silver-staining protocols

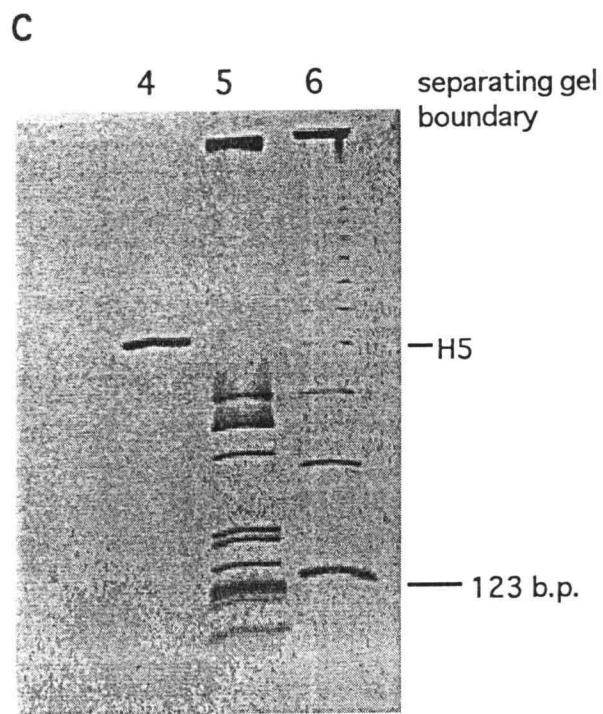
Silver staining was used to detect DNA separated with SDS-PAGE. This was required since ethidium nonspecifically bound SDS/polyacrylamide gels. After staining in 0.5  $\mu\text{g/ml}$  ethidium bromide, the entire gel fluoresced upon exposure to UV light, and identifying DNA was impossible. Ethidium, which has a positive charge, appears to have bound to SDS in the gels, and soaking the gel in water overnight did not appear to reduce the nonspecific effect (data not shown). Therefore, both proteins and DNA were imaged by silver staining gels, using two protocols that preferentially stained either proteins or DNA. One protocol, based on diamine reduction of silver nitrate (Sasse and Gallagher, 1991), stained linker histone H5 and its globular domain preferentially to DNA; the other protocol, based on non-diamine reduction of silver nitrate, preferentially stained DNA. In the first protocol ammonium hydroxide was used to complex silver ions with subsequent reduction by formaldehyde in citric acid solution (Merril, 1990), and the second protocol employed a gel prewash in nitric acid with silver reduction in formaldehyde.

Figure 4.5 illustrates the specificity of the two silver-staining protocols for either proteins or DNA. In this Figure, 0.5  $\mu\text{g}$  each of H5 (Figure 4.5, lanes 1 and 4), 123 b.p. DNA ladder (Pharmacia) (Figure 4.5, lanes 2 and 6), and Hha I-cut pPol208-12 (Figure 4.5, lanes 3 and 5) were loaded, and run, in separate lanes of an 18% SDS/polyacrylamide gel. The gel was stained using the non-diamine silver staining protocol (Methods and Materials), with the DNA clearly becoming visible (Figure 4.5A, lanes 2, 3, 5 and 6). In the same gel, H5 remained undetected (Figure 4.5A, lanes 1 and 4); the position where H5 should appear is marked accordingly. After washing the gels in water for a day with

**Figure 4.5.** Demonstrating the efficiency of specific staining of H5 and DNA using diamine silver staining and non-diamine silver staining protocols. (A) 0.5  $\mu$ g each of H5 (lanes 1 and 4), 123 b.p. DNA ladder (lanes 2 and 6), and Hha I cut pPol208-12 DNA (lanes 3 and 5) were separated on an 18% Laemmli gel. The gel was first stained using the non-diamine silver staining protocol (Methods and Materials). After extensively washing, the gel was divided in two parts with one side (B) stained in coomassie G-250 (Methods and Materials), and the other side (C) stained with the diamine silver staining protocol. DNA bands in (B) and (C) were due to residual staining from the non-diamine silver staining step.



coomassie staining



diamine silver staining

Figure 4.5

several changes of distilled water, the gel was physically cut in half, and restained with either: (a) coomassie (Figure 4.5B), or (b) the diamine protein-preferential silver staining protocol (Method and Materials) (Figure 4.5C); H5 dramatically appeared in both cases (Figure 4.5B, lane 1; Figure 4.5C, lane 4).

#### *4.4.2.3 Elucidating linker histone-DNA aggregate substructure using differential staining SDS-PAGE*

We have shown that both DNA and proteins migrate in SDS/polyacrylamide gels in a predictable manner based on their molecular weights (Figure 4.4). Furthermore, DNA does not denature upon exposure to 2% SDS (Figure 4.5A, lanes 2, 3, 5 and 6; Carter, 1997), and either linker histones or DNA can be preferentially stained depending on the appropriate silver-staining protocol (Figure 4.5). These results were combined in order to develop a means for detecting and estimating the relative composition of proteins and DNA in nucleoprotein complexes separated by SDS-PAGE. To demonstrate this technique, GH5 was bound to short oligonucleotides. With native PAGE, band shifting cannot be observed upon binding to linear DNA, so little information on GH5-DNA assembly can be ascertained (Chapter 3). The absence of any detectable band shift is likely the result of cooperativity in GH5 binding as well as GH5-DNA oligomerization and aggregation (Chapter 3). DS-SDS-PAGE was developed as way to better understand the aggregagete assembly process.

DS-SDS-PAGE was used to reduce glutaraldehyde-fixed GH5-DNA aggregates into a collection of soluble yet stably crosslinked nucleoprotein intermediate complexes that could be separated, and characterized. Optimal conditions for the production of

soluble intermediate complexes were identified by titrating GH5 with the respective oligonucleotide in 0.0039% to 0.25% glutaraldehyde. Crosslinking was characterized as either *complete*, in which case all the protein and nearly all of the DNA was crosslinked into aggregates too large to enter the SDS/polyacrylamide gel, or as *partial*, in which case intermediate complexes ranging from free DNA and protein to large complexes were observed (Figure 4.6). From 0.063% to 0.25% glutaraldehyde crosslinking was complete, while from 0.0039% to 0.031% glutaraldehyde crosslinking was partial. Based on the relative distribution of material between complex sizes, intermediate complex prevalence appeared to be a consequence of the simple chance that a crosslinking event occurred; monomer-size complexes dominated with progressively smaller amounts of dimer-and-trimer-sized complexes. Particularly noteworthy, neither free DNA nor GH5 (in the absence of DNA), appreciably crosslinked in glutaraldehyde under similar conditions, indicating that crosslinking was principally a result of DNA-GH5 interactions (data not shown).

The composition of individual bands (corresponding to GH5-DNA complexes) was estimated by comparing the two "differentially-stained" gels. For example, bands corresponding to free 42 b.p. oligonucleotide and free GH5 (which ran closely together as a "doublet") were stained differently depending on the silver-staining protocol. The band with the lower electrophoretic mobility was preferentially stained with the diamine silver reductive protocol, and therefore corresponds to free GH5 (Figure 4.6A); the band with higher electrophoretic mobility was preferentially stained with the non-diamine silver reduction protocol, indicating that this band corresponds to the 42 b.p. oligonucleotide

**Figure 4.6.** Differential staining SDS-PAGE (DS-SDS-PAGE) analysis of GH5-DNA complexes. GH5 at 0.04 mg/ml was incubated with DNA at 0.04 mg/ml in T.E. (pH 7.2), for 45 minutes then titrated with glutaraldehyde and incubated at room temperature for 2 hours. Samples were separated on an 18% Laemmli gels with immediate fixation in 10% glutaraldehyde. (A) GH5 was bound to a 42 b.p. oligonucleotide, and titrated with glutaraldehyde. The gel was silver stained with the non-diamine silver staining protocol. Crosslinked GH5-DNA "intermediate complexes" had an electrophoretic mobility at or near the electrophoretic mobility of crosslinked GH5 monomers, dimers, trimers, and larger multimers. For the monomer, and dimer bands, two closely migrating bands were observed, and corresponded to free DNA and monomeric GH5, and a crosslinked GH5 dimer and GH5-DNA crosslinked complex, respectively. (B) Identical to (A) except the gel was stained with the diamine silver staining protocol. Abbreviations: *L*, GH5 ladder created by crosslinking GH5 free in solution with 0.1 mg/ml DSP (Chapter 2); and *M*, pBSSK+ cut with XBA I, Hind III, and Hinf I.

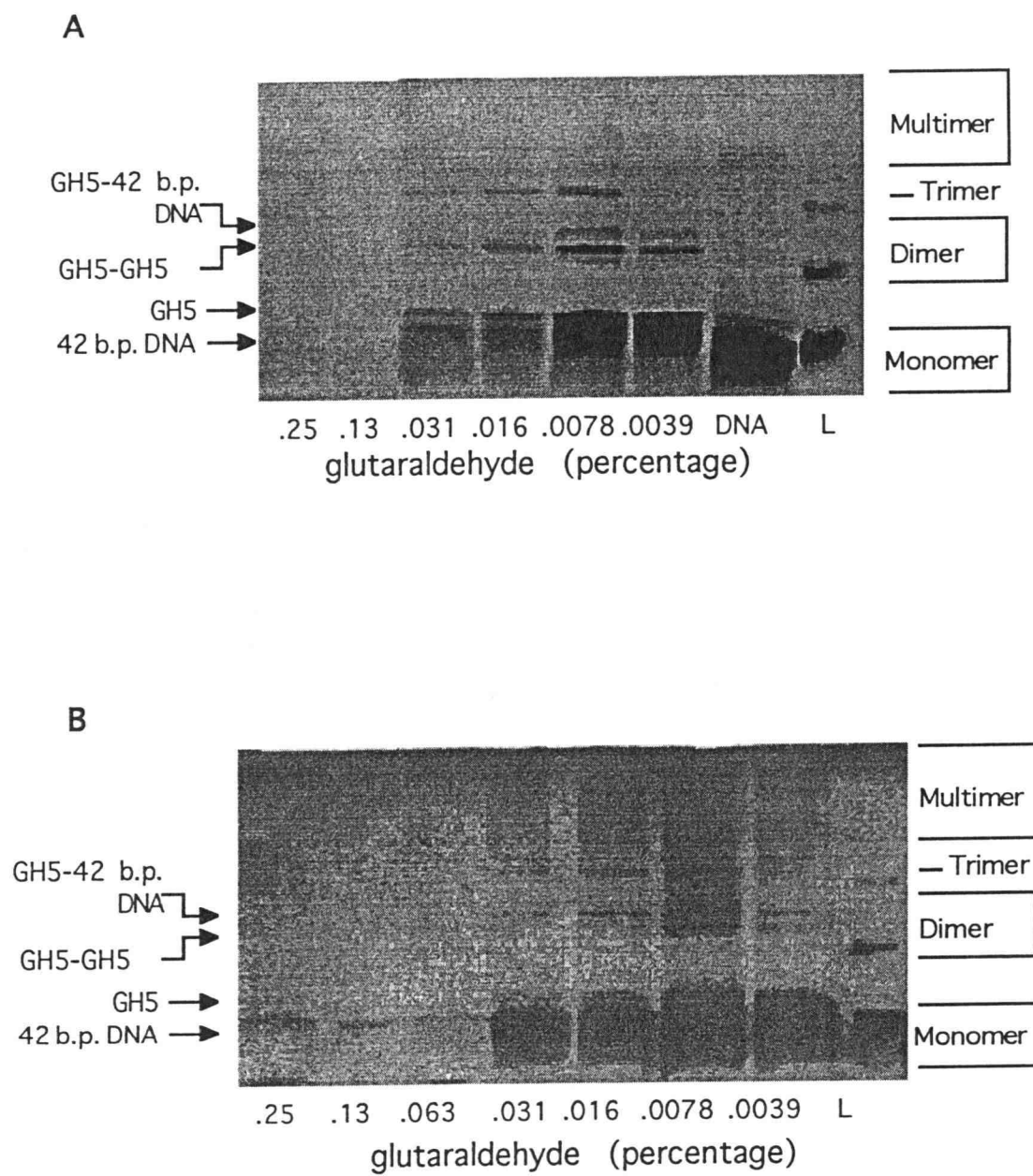


Figure 4.6

DNA (Figure 4.6B). The finding that free GH5 and the 42 b.p. oligonucleotide migrated with nearly-equivalent electrophoretic mobilities is as predicted by Figure 4.4. Similarly, DS-SDS-PAGE was used to characterize the "doublet bands" of the dimer-sized complex (so called because the electrophoretic mobility was roughly that of a crosslinked GH5 dimer). The band with the greater electrophoretic mobility corresponds to two glutaraldehyde-crosslinked GH5 molecules, and the band with the lower electrophoretic mobility corresponds to a GH5 molecule crosslinked to a 42 b.p. oligonucleotide. This was also apparent in other experiments in which GH5 was glutaraldehyde-crosslinked, separately, to a 22 b.p. oligonucleotide and a 42 b.p. One band, corresponding to the GH5 dimer, was independent of oligonucleotide size, and the other band, corresponding to a GH5-DNA complex, was dependent on the oligonucleotide size (data not shown).

The technique described above can be used to estimate the stoichiometric compositions of DNA-protein complexes. As an example, we show how relative stoichiometries of larger complexes of GH5 and DNA were estimated based on a calculation in which, separately, free GH5 and the nucleoprotein complex comprised of one GH5 and one 42 b.p. DNA served as absolute standards. Specifically, we determine whether the "trimeric-sized" complex has the composition of  $(GH5)_2DNA$  or  $GH5(DNA)_2$ . Free DNA was not used as an absolute standard due to uncertainty as to the effect of bound GH5 on nucleoprotein complex staining.

Based on calculations by Dr. Kensal van Holde, the equation describing the relative amount of molecule B in a nucleoprotein complex comprised of molecules A and B is:

$$F_B = \frac{R-R_0}{(R_1-R_0)-(R_1-R)(r_n-1)} \quad (4.1)$$

Here,  $F_B$  is the mass fraction of component B in the nucleoprotein complex comprised of components A and B, which also serve as the absolute standards. In addition,

$$R_0 = (f_A^d/f_A^n), \quad (4.2)$$

$$R_1 = (f_B^d/f_B^n), \quad (4.3)$$

and

$$r_n = \frac{f_B^n}{f_A^n}. \quad (4.4)$$

The symbol  $f$  refers to "staining factors" directly related to silver staining efficiency with superscripts  $n$  and  $d$  referring to non-diamine- and diamine-stained gels, respectively. The subscripts A and B refer to endpoint components A or B.  $R_0$  is equal to the staining intensity of component A in diamine gels relative to the staining intensity of the same quantity of component A stained in non-diamine gels;  $R_1$  is equal to the staining intensity of component B in diamine gels relative to the staining intensity of the same quantity of component B stained in non-diamine gels. Similarly,  $r_n$  is equal to the relative silver staining efficiency of component B and A in the non-diamine gel.

In this case, for reasons described above, B = GH5 and A = GH5-DNA (1:1 complex) were used as absolute standards in determining the composition of the trimer-sized complex (Figure 4.6). Estimating  $r_n \cong 0.4$ , based on a comparison of roughly equal amounts of GH5 and GH5-DNA on the non-diamine silver-stain gel, we obtained  $F_B \cong 0.3$  for the trimer band. That is, the trimer acts as a complex composed of 70% GH5-DNA plus 30% GH5. This essentially corresponds to a complex of about 2 molecules of GH5, and one molecule of 42 b.p. DNA. Even though the stoichiometric ratios may not be exact, the method allows a clear choice between  $(\text{GH5})_2\text{DNA}$  and  $\text{GH5}(\text{DNA})_2$ .

In applying DS-SDS-PAGE, a number of limitations were encountered. First, it was not possible to determine exact DNA-protein stoichiometries due to uncertainty as to the effect of protein binding to DNA and how this might affected silver reduction around the entire molecule. But for small complexes, the possible combinations of GH5 and oligonucleotides are limited so reasonable choices could easily be made. More accurate estimates are theoretically possible if  $r_n$  is precisely determined. As an additional consideration, increasing concentrations of glutaraldehyde may have altered silver reduction around both GH5 and the DNA in such a way that samples were less efficiently stained at higher concentrations. Thus, all analysis was done separately at each glutaraldehyde concentration, including the establishment of GH5 and GH5-DNA standard endpoints.

DS-SDS-PAGE offers a simple, safe non-isotopic alternative to radiolabeling that under certain conditions can be used to estimate protein-DNA ratios in nucleoprotein

complexes separated by gel electrophoresis. Furthermore, the technique allows for the analysis of insoluble aggregates by maintaining solubility in SDS. In applying DS-SDS-PAGE to GH5-DNA aggregate complexes it was observed that two GH5 molecules preferentially self-crosslinked onto a 42 b.p. DNA oligonucleotide complex. This finding suggests that protein-protein contacts are a fundamental part of GH5 assembly onto DNA, and may indicate an important role for protein-protein contacts in linker histone cooperativity. It is anticipated that other protein-DNA complexes can be similarly characterized, based on the differential ability for diamine and non-diamine silver staining protocols to stain proteins and DNA. Conceivably other stains may also be employed but silver staining offers unparalleled sensitivity in detection and fulfills the necessity of being able to stain both proteins and DNA (unlike coomassie).

#### 4.4.3 Characterizing linker histone DNA-binding motifs based on salt-dependent inhibition of glutaraldehyde crosslinking

Either GH5 or H5 was bound to DNA in the presence of salt, then crosslinked with glutaraldehyde. H5 at 175 % H5:DNA (w/w) and GH5 at 300% GH5:DNA (w/w) were incubated, separately, with Hha I cut pPol208-12 at 0.04 mg/ml in 10 mM sodium phosphate (pH 7.2), 0.2 mM EDTA over a range of NaCl concentrations. (Hha I cutting of pPol208-12 produces a collection of DNA fragments including a 2600 b.p. DNA, and a number of fragments smaller than 400 b.p.). The samples were then brought to 0.06% glutaraldehyde, and crosslinked (with shaking) at room temperature for several hours. Samples separated by SDS-PAGE were silver stained as a means of identifying uncrosslinked DNA and proteins on the same gel. SDS is a strong protein

**Figure 4.7.** GH5 and H5 crosslinking to Hha I cut pPol208-12 as a function of NaCl concentration. GH5 and H5 were crosslinked over a range of NaCl concentrations at room temperature in glutaraldehyde (added from 10X stock). Samples were then separated on an 18% Laemmli gel, and silver stained, revealing free DNA but no free protein. (A) A representative 18% Laemmli gel of GH5 crosslinking to Hha I cut pPol208-12. (B) A representative 18% Laemmli gel of H5 crosslinking to Hha I cut pPol208-12. (C) A plot of individual H5-uncrosslinked Hha I cut pPol208-12 DNA fragments (normalized to the amount of DNA released at 800 mM NaCl). The solid symbols indicate larger fragments, while open symbols represent smaller fragments. Fragment sizes are as follows: 12-208 5s DNA, 2600 b.p. (*solid squares*); fragment 12, 370 b.p. (*solid circle*); fragment 11, 360 b.p. (*solid triangles*); fragment 10, 310 b.p. (*solid diamonds*); fragment 9, 310 b.p. (*solid diamonds*); fragment 8, 260 b.p.; fragment 7, 160 b.p. (*dash*); fragment 6, 150 b.p.; fragment 5, 130 b.p. (*open squares*); fragment 4, 120 b.p. (*open diamonds*); fragment 3, 110 b.p. (*open triangles*); and fragment 2, 100 b.p. (*open circles*). Refer to [Table 4.1](#) for fragment identification. Fragment 3 data points are connected by a *small-dashed line*, and 208-12 DNA data points are connected by a *long-dashed line*. The plot of GH5-uncrosslinked Hha I-cut pPol208-12 DNA as illustrated in [Figure 4.7A](#) is represented by a *solid line*. Gels were stained with the diamine silver-staining protocol.

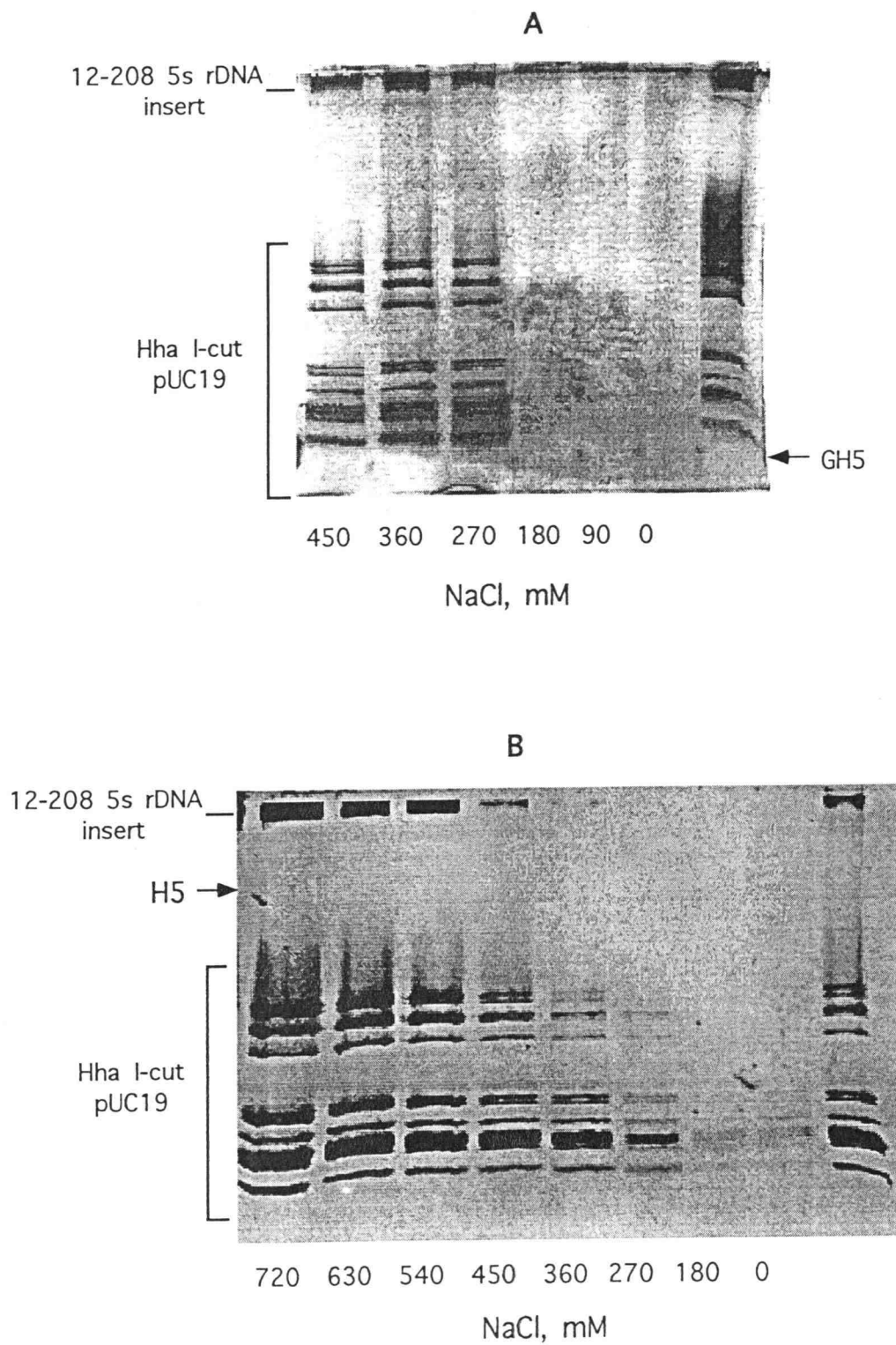


Figure 4.7

C

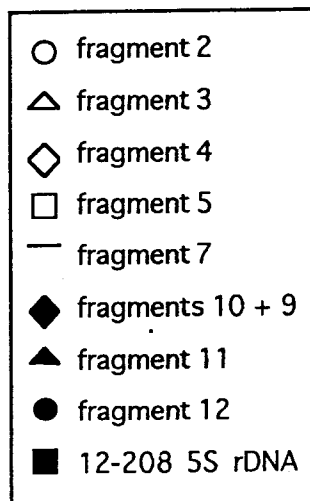
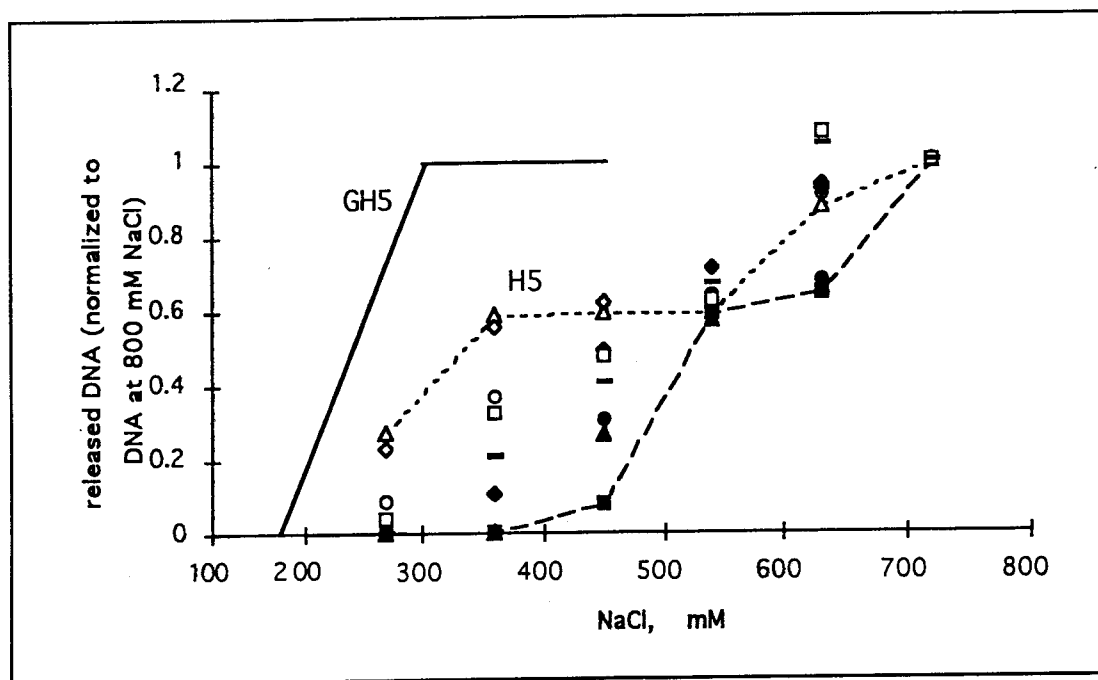


Figure 4.7 (continued)

denaturant, and was expected to disrupt protein binding, leaving only crosslinked samples. One noteworthy caveat: H5 bound in aggregates resists dissociation in response to denaturants like urea and SDS (Chapter 3). However, elevated salt concentrations appeared to prevent H5 binding, so H5-induced aggregation of DNA was not considered to be a serious problem in the experiment.

For GH5, DNA binding and consequent crosslinking to DNA abruptly ended between 180 mM and 270 mM NaCl, with all the DNA being released by the 270 mM NaCl concentration point (Figure 4.7A). In contrast, H5 binding and crosslinking to Hha I cut pPol208-12 was disrupted over a wide salt range, and required a considerably higher salt concentration to prevent DNA-protein crosslinking as compared to GH5. For H5, a considerable increase in uncrosslinked DNA occurred at 270 mM NaCl (Figure 4.7B). By plotting the amount uncrosslinked DNA (for each individual DNA fragment generated by Hha I-cut pPol208-12) as a function of the salt concentration (Figure 4.7C), it appears H5 crosslinking to large fragments was less affected by salt than for smaller fragments, though at 540 mM NaCl, all fragments were affected about equally. Clearly, NaCl prevented H5 binding and crosslinking to DNA in a manner that was not directly proportional to the salt concentration with a dependency on the DNA size.

## **4.4 Discussion**

### 4.4.1 The effect of glutaraldehyde crosslinking on histone-DNA interactions

Glutaraldehyde may be the most popular crosslinker applied in chromatin research. This is in large part due to its solubility in aqueous solution, as well as its ease in

application, and proven ability to fix histone proteins to DNA. Glutaraldehyde crosslinking complicates linker histone-DNA interactions. While  $k_{on}$  may be reduced by glutaraldehyde crosslinking, the average  $k_{off}$  decreases markedly since glutaraldehyde covalently attaches molecules together, and prevents dissociation ( $k_{on}$  is the kinetic binding rate constant and  $k_{off}$  is the kinetic dissociation rate constant). The net effect was for more DNA to be bound to GH5 (with less free DNA), as compared to samples not crosslinked as illustrated in [Figure 4.2](#). The results are consistent with the idea that in the absence of crosslinking, free, uncomplexed DNA molecules are in equilibrium with DNA molecules bound in the aggregate network.

GH5, and H5, crosslinking to DNA was examined in the presence of increasing salt concentrations. Results suggest that crosslinking did not dramatically interfere with the protein-DNA interactions. For both proteins, the salt concentration which prevented linker histone-DNA binding under crosslinking condition was close to that observed to prevent binding of the non-crosslinked protein to DNA and chromatin. For example, GH5 has been reported not to bind to DNA and chromatin at above about 200 mM NaCl (Segers et al., 1991; Thoma et al., 1983); as reported here, GH5 was unable to crosslink to DNA between 180 mM and 270 mM NaCl. Results for H5 may be more difficult to interpret since H5 continued to bind and crosslink to DNA even above 600 mM NaCl--which has been reported to be sufficient to dissociate H5 from DNA (Segers et al., 1991; Kumar and Walker, 1980; Losa et al., 1983). However, linker histones may be capable of weakly interacting with DNA above 800 mM NaCl as reported by (Glotov et al., 1978b; Hill et al., 1991). Such weak contacts appear to be "fixed" by glutaraldehyde

crosslinking. Why proteins and DNAs, modified with glutaraldehyde, interact in a salt-dependent manner very much like samples not crosslinked remains speculative, but may be a consequence of counterion theory (Lohman, 1992). According to counterion theory, binding is primarily an entropy-driven process involving the release of salt ions from the nucleoprotein complex upon protein binding, and enthalpy-related DNA-protein contacts contribute negligibly to the overall binding free energy.

#### 4.4.2 Elucidating linker histone-DNA intermediate structure in aggregate formation

It was of particular interest to determine whether gel electrophoresis could be used to obtain evidence supporting GH5-DNA "tramlines". The "tramline" model proposes that two DNA-binding sites on GH5 allow the protein to interact with two DNA fragments simultaneously. EM micrographs purportedly shows two, almost-parallel DNA molecules sandwiching GH5 molecules (Draves et al., 1992; Thomas et al., 1992), suggesting that this is a rather stable structure. As a means to identify "tramline" complexes, small oligonucleotides were incubated GH5, crosslinked with glutaraldehyde and analyzed with SDS-PAGE. Complex detection was achieved by using two silver-staining protocols, with the entire separation and detection process referred to as differential staining SDS-PAGE (DS-SDS-PAGE).

By following a straight-forward protocol, the otherwise aggregated GH5-DNA complex, was reduced to a collection of GH5-DNA intermediate complexes whose relative abundance was likely a product of their relative stability. Of special interest was a complex with three bio-molecules (as observed on an 18% SDS/polyacrylamide gel) that

was relatively abundant, possibly indicating stability. We reasoned that by determining the relative number of GH5 molecules and 42 b.p. oligonucleotides in the complex, information about GH5-DNA assembly kinetics and possible "tramline" formation could be ascertained. Based on DS-SDS-PAGE, the trimer-sized band was estimated to contain two GH5 molecules per 42 b.p. oligonucleotide. These results do not appear to support the existence of tramline structures as stable intermediates in aggregate formation, since a tramline would be expected to have one GH5 molecule per two 42 b.p. oligonucleotides. Instead, the results suggest that protein-protein contacts play an important part in GH5-DNA interactions. Admittedly, the relatively-high GH5:DNA (w/w) ratio used in the study or inefficient DNA-protein crosslinking (versus protein-protein crosslinking) may have also led to a 2:1 (GH5:DNA) ratio, so that "tramline" structures may have been undetected due to the experimental conditions.

#### 4.4.3 Characterizing linker histone DNA-binding motifs based on salt-dependent dissociation

Linker histones binding to DNA is complicated by the presence of two (Goytisolo et al., 1996) or three (Cerf et al., 1994) DNA-binding sites on the globular domain, multiple SPKK-motif sequences found in the terminal tail domains that have been linked to narrow minor groove binding (Churchill and Suzuki, 1989), and other poorly characterized  $\alpha$ -helical DNA-binding domains that are found in the C-terminal tail domain (Hill et al., 1988). Characterization of these domains has largely relied on the use of recombinant techniques in generating isolated domains, like the globular domain

(Goytisolo et al., 1996; Buckle et al., 1992) and peptides with the amino acid sequence SPKK (Churchill and Suzuki, 1989). While indispensable, this approach generally requires the availability of atomic resolution structural data, and a considerable investment of resources. A more general approach in identifying and characterizing DNA-binding domains was developed, and is based on the ability for H5 to crosslink to DNA at increasing concentrations of NaCl.

For H5-DNA, a salt-dependence in crosslinking was characterized according to the amount of DNA that was uncrosslinked at a given salt concentration. The first detectable disruption in H5 crosslinking to DNA occurred between 180 mM and 270 mM NaCl, and appears to have corresponded to the inability of DNA binding motifs in the globular domain to bind to DNA as GH5 also stopped crosslinking to DNA over this range of salt concentrations. From 270 mM to 540 mM NaCl, H5 crosslinking showed a clear preference for larger DNA fragments as small DNA fragments became uncrosslinked at lower salt concentrations than larger fragments. Based on studies by (Yaneva et al., 1994), this preference for large DNA is indicative of nonspecific binding, a recognized property of linker histones (reviewed in Zlatanova and Yaneva (1992)). It is almost a certainty that the motifs affected from 270 mM to 540 mM NaCl reside in the terminal tail domains since the globular domain was no longer able to bind and crosslink to DNA by 270 mM NaCl. The SPKK motif is a likely candidate to have been involved because: (a) it is present in the terminal tail domains (Appendix A1), and (b) the motif has been shown to be important for DNA binding (Hill et al., 1991). DNA crosslinking became

increasingly disrupted from 540 mM to 720 mM, again with smaller fragments, in general, being more susceptible to the effects of salt than larger fragments.

Performing parallel crosslinking studies on H5 and GH5 provided a means for partially elucidating the reason for the nonlinear, salt-dependent release of DNA from crosslinked H5-DNA complexes. 270 mM NaCl prevented GH5 from binding and crosslinking to DNA, and led to a considerable reduction in the amount of DNA bound and crosslinked by H5. This result identified the globular domain as an important element in overall H5 binding and crosslinking. This result also suggests that the plot of uncrosslinked DNA (as a function of salt concentration) was related to the composite of DNA-binding with each DNA-binding domain being additive towards the total binding affinity of the entire protein. In the simplest model, each binding domain acts independently, and thus each binding domain can be disrupted at a distinct salt concentration proportional to its DNA-binding affinity (Figure 4.8). In this way, DNA-binding motifs can be separately identified, and assigned a relative DNA-binding affinity. Of course, binding motifs may also show a dependence on one another resulting in cooperative effects and alterations in binding affinity. This would complicate any simple interpretation of salt-dependent binding and crosslinking.

The salt-dependent dependence of GH5 and H5 crosslinking clearly represents contrasting mechanisms of interactions with DNA. Results are consistent with low-salt dissociation of GH5 via a single, homogeneous, DNA-binding motif, or two motifs of nearly equal salt-dependent affinity (see below). High-salt dissociation of H5 is thus accounted for by a heterogeneous collection of non-uniform SPKK-type motifs, and other

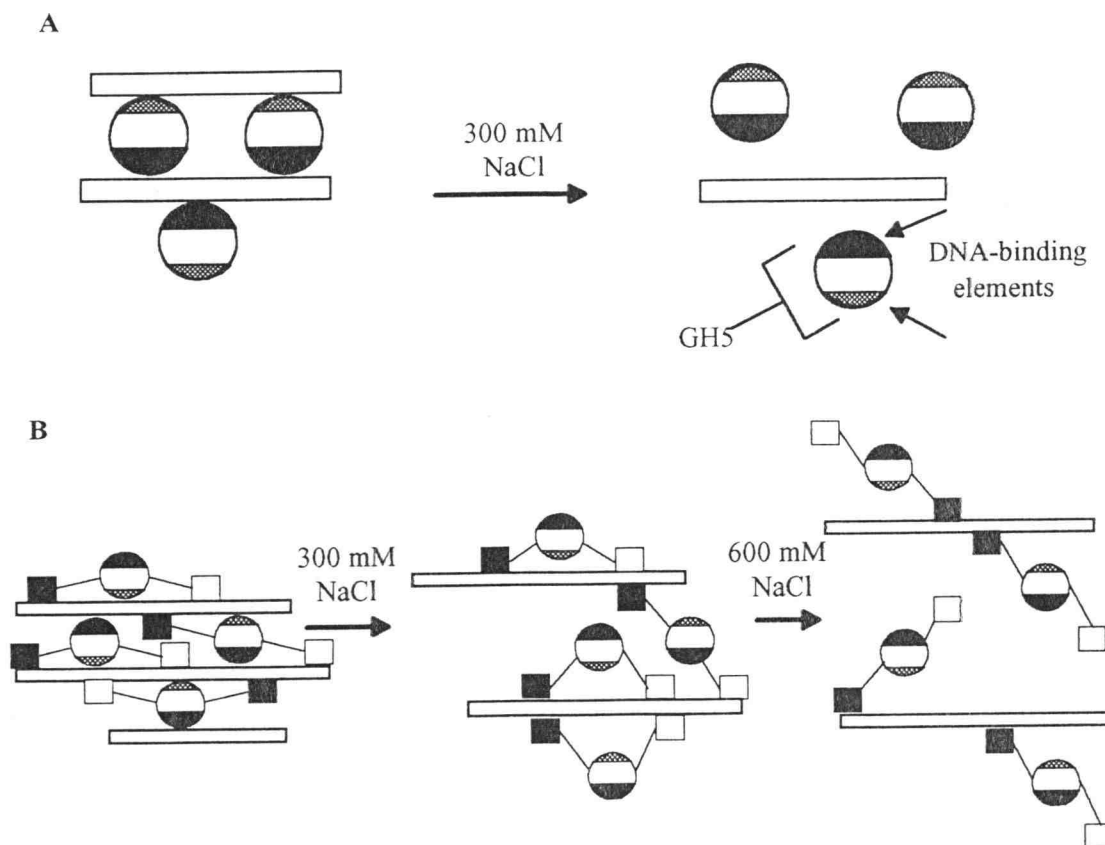


Figure 4.8. GH5 and H5 binding to DNA as a function of NaCl concentration in terms of an isolated binding motif model. (A) GH5 binding/crosslinking to DNA was uniform, becoming disrupted by 300 mM NaCl. This suggests that the globular domain bound DNA via a single binding element or similarly disrupted multiple motifs as represented by the various patterned spheres—with each pattern representing a separate binding domain. (B) H5 binding to DNA was considerably more heterogeneous than GH5, and appeared to occur in at least three distinct stages. This suggests that binding may have been facilitated by three separate DNA-binding motifs (or binding-related elements) with the salt concentration required for dissociation increasing with the motif's affinity for DNA. The terminal tail domains are represented by lines and boxes: the *solid box* represents hypothetical binding elements in the C-terminal tail domain, and the *open box* represents hypothetical binding elements in the N-terminal tail domain. As drawn, the C-terminal tail DNA binding element is less effected by salt than the N-terminal tail DNA binding element.

high-affinity binding structures in the tail domains. One apparent inconsistency between crosslinking results, and previous discussion should be noted. The disruption of GH5-DNA contacts occurred in a single step despite the presence of multiple binding elements in the globular domain (Goytisolo et al., 1996). However, this inconsistency may be easily explained if the salt dependence of the two putative binding motifs of GH5 are similar. This appears to be case; data from (Goytisolo et al., 1996) indicate that the binding motifs of the globular domains have nearly identical binding affinity (see their Figure 4).

Use of NaCl to prevent linker histone-DNA crosslinking originates with (Clark and Thomas, 1988), but improvements and important observations, reported here, have increased the potential applicability of this technique. First, instead of using the appearance (or disappearance) of the DNA-binding protein component to gauge crosslinking, in this study various-sized DNA fragments were tracked. This approach provided a means of determining: (a) whether binding and crosslinking was specific for any single fragment, (b) the general number of DNA-binding motifs, and (c) the relative binding affinities of the motifs. We found that the relative amount of uncrosslinked protein to be a poor marker for DNA crosslinking, as no free H5 or GH5 was ever observed, regardless of the salt concentration (Figure 4.7A, 4.7B), possibly indicating self-association. Second, it was recognized that by plotting the release of the DNA over a broad salt titration, the effect of individual motifs on DNA binding and crosslinking could be identified. This is based on a comparison between H5 and its globular domain, as well as the general disruption of H5 crosslinking to DNA and what is known about binding

motifs in the terminal tail domains. Considering these enhancements and results, it is expected that other DNA-binding proteins behave similarly to H5; binding can be reduced to a composite of isolated DNA-binding domains and motifs.

## CHAPTER 5

### Conclusion

#### 5.0 Summary

Linker histone binding to chromatin is complicated by a myriad of associated factors. These include (a) cooperativity, (b) binding to DNA via multiple binding domains with each displaying varying specificity and affinity, (c) formation of massive nucleoprotein aggregates, (d) differences in binding depending on DNA morphology, (e) effects of nucleosomes on binding, and (f) chromatin compaction as a result of binding to chromatin fibers. While much has been written on this subject, there is surprising little that is universally agreed upon. To better illustrate this predicament, the following discussion is divided into sections, which roughly mimics the introduction chapter. For each section, a brief background is presented to describe the current state of research, then the results of the thesis are placed within the context of this other work.

#### 5.1 Molecular aspects of linker histone binding

Linker histones are known to bind to DNA via multiple DNA-binding elements that are found both within the globular and terminal tail domains. For the globular domain, it has been speculated that two or three regions of clustered basic residues may act as DNA binding elements. These include residues near the recognition helix (or

$\alpha$ -helix 3) and residues on-or near the loop between  $\alpha$ -helix 1 and  $\alpha$ -helix 2 (Cerf et al., 1994). For the terminal tail domains, binding elements include the SPK(R)K(R) motif as well as other domains that are primarily comprised of  $\alpha$ -helices (Clark et al., 1988). Based on the resistance of the entire linker histone to salt dissociation from DNA and chromatin (compared to the globular domain) (Segers et al., 1991; Thoma et al., 1983; Glotov et al., 1978b), it has been inferred that the terminal tail motifs display a higher affinity for DNA.

In this thesis, two studies were conducted to specifically elucidate how the globular and terminal tail domains of linker histones participate in DNA binding. In the first study, a protease protection assay was used to locate the position of Phe 93 in the linker histone-DNA binding complex. From the X-ray diffraction data of the crystal of the HNF-3 $\gamma$ -DNA complex, Phe 93 would be expected to become solvent-inaccessible upon DNA binding. Contradictory to this prediction, results presented here demonstrate that H5 binding to DNA increased the exposure of Phe 93 to proteolysis. One likely explanation is that the globular domain of intact H5 interacts with DNA primarily via the loop between  $\alpha$ -helix 1 and  $\alpha$ -helix 2. This interpretation may be supported by Goyotisoló (1996) showing that this loop is capable of binding to DNA, and provides serious doubts as to the use of HNF-3 $\gamma$  as the only model for GH5 binding to DNA.

In a second, related study, H5 and GH5 were glutaraldehyde-crosslinked to DNA at increasing salt concentrations as a way to compare relative binding affinities. As previous results indicate, the binding elements in the tail displayed a higher binding affinity than those in the globular domain. Indeed, using this method, the contribution of the

globular domain to general H5 binding was identified only a minor contribution to overall binding. Additionally, binding by the globular domain was sensitive to salt over a narrow salt range indicating that binding involves a single element or elements with near equal affinity; in contrast, H5 binding involves heterogeneous elements that are nonspecific (for the DNA fragments used), and have wide variations in binding affinity. These results are in accordance with what is known about linker histone binding, and may justify the use of this approach in characterizing other DNA-binding proteins.

## **5.2 Model DNA and solution studies**

Model studies offer an important investigative tool that avoids the complications inherent in analyzing chromatin. These studies allow examination of properties related to linker histone binding and association that have been shown to have direct parallels to DNA-binding in chromatin. Such model studies have offered an important view of the mechanism by which linker histones interact with DNA (see above) that must have physiological significance. In this thesis, model studies were used to obtain evidence for linker histone self-interactions or DNA-protein interaction that may have relevance to linker histone interactions found in the chromatin fiber.

In the first series of experiments, evidence for GH5 and H5 self-association was used as a corollary to specific linker histone protein-protein interaction found in the chromatin fiber. Turbidity measurements were used to investigate, nonspecific assembly of proteins into large complexes; chemical crosslinking was used to analyze the

importance of transient, weak contacts involved in the assembly process; and equilibrium analytical ultracentrifugation was used to identify more stable interactive forces between protein molecules. The results indicate that while GH5 does show evidence for specific interaction, these interactions are decidedly weak, and potentially reliant on conditions in which charge-related repulsion are minimized. Additionally, H5 appears to show a stronger interacting affinity based upon equilibrium ultracentrifugation results, though the extent of this interaction was not quantitated due to nonidealities created by salt-dependent effects. Certainly, the results suggest that specific protein-protein contacts are possible in the chromatin fiber under concentrated conditions where charge repulsion is minimized.

The second series of experiments employed DNA models to better understand possible physiologically-relevant interactions of linker histones. As described for the solution study, this analysis relied heavily upon DSP crosslinking as a measure of contact frequency. Results indicate that DNA increased the ability for protein-protein contacts, and in support of the above solution studies, GH5 assembly on DNA occurred specifically. Perhaps relevant to nucleosome binding, GH5 was found to assemble on supercoiled DNA in small clusters of up to three in size, which is reminiscent of binding to four-way junctions. Indirectly, this may suggest that the dyad axis, which at least superficially resembles DNA crossovers and four-way junctions, acts as the point of binding for linker histones (see below for a parallel chromatin-related study). The process of aggregation was also analyzed in greater detail with clear evidence that supercoiled DNA remains resistant to the effects of aggregation, while linear DNA (regardless of size) undergoes

rapid oligomerization and precipitation. The process appears to be largely driven by DNA-protein contacts, and has previously been described as "crosslinking" through bridging of separate DNAs by the terminal tail domains (Glotov et al., 1978a). GH5 also produces aggregate networks, albeit not as efficiently as H5. However, GH5-dependent aggregation appeared to be less reliant on protein-DNA contacts and more dependent on protein-protein contacts for stabilization. Mechanisms related to aggregation may also contribute in maintaining high order chromatin structure. Conceivably, linker histones may "crosslink" distal parts of the chromatin fiber via the long tail domains and use protein-protein contacts via the globular domain (and terminal domains) for "close-range" stabilizing interactions.

### **5.3 Chromatin-related analysis**

Issues related to linker histone interaction with chromatin are paramount to understanding such topics as transcription, replication, and mitotic hypercondensation. It is generally agreed that linker histones help stabilize chromatin structure, though the process by which this is achieved remains unelucidated (reviewed in van Holde and Zlatanova, 1996a). This matter is further complicated by the finding that salts also facilitate the compaction process (Schwartz and Hansen, 1994; Hansen, 1989). An equally elusive question is where linker histones bind to the chromatin fiber, with most studies supporting binding to nucleosomes. As a complement to the DNA-binding studies, H5 was incubated with chromatin fibers that were reconstituted from purified components.

Results supports the premise that H5 indeed compacts reconstituted chromatin to a physiologically-relevant extent, but only in the presence of 30 mM NaCl. Like DNA, H5 aggregated chromatin fibers either in salt concentrations above 60 mM NaCl or by over-saturating the fiber with linker histones. Finally, an attempt to identify the location of linker histone binding on the nucleosome was conducted as an extension of the DNA-binding studies. Results of a restriction endonuclease protection assay suggests that linker histone binding covers a site 13 b.p. upstream of the dyad axis. Similar, results for a site 7 b.p. upstream from the dyad axis (Meersseman et al., 1991) suggest that linker histones bind asymmetrically to the nucleosome, though binding at the dyad axis still cannot be dismissed.

#### **5.4 Concluding remarks**

By using DNA models, and a purified chromatin fiber model, important topics related to the interaction of linker histones with chromatin were examined. The combination of the two approaches was particularly effective in developing a global model of linker histone binding to chromatin. The model DNA systems were well suited to characterizing linker histone assembly, and protein-protein interaction. Conducting such experiments in the presence of the histone octamer proteins would have undoubtedly complicated interpretations tremendously. Application of chromatin reconstitutions became necessary however in obtaining information related to fiber compaction, and nucleosome binding. In particular, results of H5 binding to and compaction of the

reconstituted 208-12 DNA demonstrates that this "artificial" system is ideal for examining the effects of chromosomal proteins on chromatin structure. Certainly such a model would be ideal for examining such related topics such as the interaction of linker histones in chromatin, the effect of nonhistone proteins on chromatin compaction, and a host of other important and relevant questions.

**BIBLIOGRAPHY**

- Albig, W., Kardalidou, E., Drabent, B., Zimmer, A., and Doenecke, D. (1980) Isolation and Characterization of Two Human H1 Histone Gene within Clusters of Core Histone Genes, *Genomics*, **10**, 940-948.
- Ali, Z. and Singh, N. (1987) Binding of Linker Histones to the Core Nucleosome, *J. Biol. Chem.*, **262**, 12989-12993.
- Allan, J., Hartman, P. G., Crane-Robinson, C., and Aviles, F. X. (1980) The Structure of H1 and Its Location in Chromatin, *Nature*, **288**, 675-679.
- Allan, J., Mitchell, T., Harborne, N., Bohm, L., and Crane-Robinson, C. (1986) Roles of H1 Domains in Determining High Order Chromatin Structure and H1 Location, *J. Mol. Biol.*, **187**, 591-601.
- Arents, G., Burlingame, R. W., Wang, B., Love, W. E., and Moudrianakis, E. N. (1991) The Nucleosomal Core Histone Octamer at 3.1 Å Resolution: A Tripartite Protein Assembly and a Left-Handed Superhelix, *Proc. Natl. Acad. Sci. USA*, **88**, 10148-10152.
- Aviles, F. J., Chapman, G. E., Kneale, G. G., Crane-Robinson, C., and Bradbury, E. M. (1978) The Conformation of Histone H5, *Eur. J. Biochem.*, **88**, 363-371.
- Bailly, F., Bailly, C., Colson, P., Houssier, C., and Henichart, J. (1993) A Tandem Repeat of the SPKK Peptide Motif Induces  $\Psi$ -Type DNA Structures at Alternative AT Sequences, *FEBS Lett.*, **2**, 181-184.
- Bates, L. D. and Thomas, J. O. (1981) Histone H1 and H5: One or Two Molecules Per Nucleosome?, *Nucleic Acids Res.*, **9**, 5883-5894.
- Bloomfield, V., Dalton, W. O., and van Holde, K. E. (1967) Frictional Coefficients of Multisubunit Structures. II Application to Proteins and Viruses, *Biopolymers*, **5**, 135-148.
- Bohm, L. and Creemers, P. C. (1993) Folding of Terminal Histone-H1 Peptides in the Presence of the Oligonucleotide 5'-(AT)<sub>6</sub>-3', *Biochim. Biophys. Acta*, **1202**, 230-234.
- Bonner, W. M. and Pollard, H. B. (1975) The Presence of F3-F2a1 Dimers and F1 Oligomers in Chromatin, *Biochem Biophys Res. Commun.*, **64**, 282-288.
- Boulikas, T., Wiseman, J. M., and Garrard, W. T. (1980) Points of Contact Between Histone H1 and the Histone Octamer, *Proc. Natl. Acad. Sci. USA*, **77**, 127-131.

Bourbonniere, M., Shekarabi, M., and Nalbantoglu, J. (1997) Determination of Molecular Weights of Nucleic Acid-Binding Proteins by UV Photo-Crosslinking and SDS-PAGE, *Biotechniques*, **23**, 60-62.

Brennan, R. G. (1993) The Winged-Helix DNA-Binding Motif: Another Helix-Turn-Helix Takeoff, *Cell*, **74**, 773-776.

Buckle, R. S., Maman, J. D., and Allan, J. (1992) Site-Directed Mutagenesis Studies on the Binding of the Globular Domain of Linker Histone H5 to the Nucleosome, *J. Mol. Biol.*, **223**, 651-659.

Butler, P. J. G., and Thomas, J. O. (1980) Changes in Chromatin Folding in Solution, *J. Mol. Biol.*, **140**, 505-529.

Castano, E. M., Ghiso, J., Prelli, F., Gorevic, P. D., Migheli, A., and Franglone, B. (1986) *In Vitro* Formation of Amyloid Fibrils from Two Synthetic Peptides of Different Lengths Homologous to Alzheimer's Disease Beta-Proteins, *Biochem. Biophys. Res. Commun.*, **141**, 782-789.

Cerf, C., Lippens, G., Muyldermans, S., Segers, A., Ramakrishnan, V., Wodak, S. J., Hallenga, K., and Wyns, L. (1993) Homo- and Heteronuclear Two-Dimensional NMR Studies of the Globular Domain of Histone H1: Sequential Assignment and Secondary Structure, *Biochemistry*, **32**, 11345-11351.

Cerf, C., Lippens, G., Ramakrishnan, V., Muyldermans, S., Segers, A., Wyns, L., Wodak, S. J., and Hallenga, K. (1994) Homo- and Heteronuclear Two-Dimensional NMR Studies of the Globular Domain for Histone H1: Full Assignment, Tertiary Structure, and Comparison with the Globular Domain of Histone H5, *Biochemistry*, **33**, 11079-11086.

Chalkley, R. and Hunter, C. (1975) Histone-Histone Proximity by Aldehyde Fixation of Chromatin, *Proc. Natl. Acad. Sci. USA*, **72**, 1304-1308.

Churchill, M. E. A. and Suzuki, M. (1989) 'SPKK' Motifs Prefer to Bind to DNA at A/T-Rich Sites, *EMBO J.*, **8**, 4189-4195.

Clark, J. and Thomas, J. O. (1986) Salt-dependent Co-operative Interaction of Histone H1 with Linear DNA, *J. Mol. Biol.*, **187**, 569-1.

Clark, D. J., Hill, C. S., Martin, S. R., and Thomas, J. O. (1988)  $\alpha$ -Helix in the Carboxy-terminal Domains of Histone H1 and H5, *EMBO J.*, **7**, 69-75.

Clark, D. J. and Thomas, J. O. (1988) Differences in the Binding H1 Variants to DNA, *Eur J. Biochem.*, **178**, 225-233.

Clark, K. L., Halay, E. D., Lai, E. and Burley, S. K. (1993) Co-crystal Structure of the HNF-3/Fork Head DNA-recognition Motif Resembles Histone H5, *Nature*, **364**, 412-420.

Clubb, R. T., Omichinski, J. G., Savilahti, H., Muizuuchi, K., Gronenborn, A. M., and Clore, G. M. (1994) A Novel Class of Winged Helix-Turn-Helix Protein: the DNA-Binding Domain of Mu Transposase, *Structure*, **2**, 1041-1048.

Creighton, T. E. (1993) in *Proteins* (W. H. Freeman and Company), 289.

Dashkevich, V. K., Nikolaev, L. G., Zlatanova, J. S., Glotov, B. O., and Severin, E. S. (1983) Chemical Crosslinking of Histone H1<sup>o</sup> to Histone Neighbours in Nuclei and Chromatin, *FEBS Lett.*, **158**, 276-280.

De Bernardine, W. , Losa, R. and Koller, T. (1986) Formation and Characterization of Soluble Complexes of Histone H1 with Supercoiled DNA, *J. Mol. Biol.*, **189**, 503-517.

Doenecke, D. and Tonjes, R. (1986) Differential Distribution of Lysine and Arginine Residues in the Closely Related Histones H1<sup>o</sup> and H5: Analysis of a Human H1<sup>o</sup> Gene, *J. Mol. Biol.*, **187**, 461-464.

Dong, F., Hansen, J. C., and van Holde, K. E. (1990) DNA and Protein Determinants of Nucleosome Positioning on Sea Urchin 5S rRNA Gene Sequences In Vitro, *Proc. Natl. Acad. Sci. USA*, **87**, 5724-5728.

Draves, P. H., Lowary, P. T. and Widom, J. (1992) Co-operative Binding of the Globular Domain of Histone H5 to DNA, *J. Mol. Biol.*, **225**, 1105-1121.

Dubochet, J. and Noll, M. (1978) Nucleosome Arcs and Helicies, *Science*, **202**, 280-286.

Edelhoch, H. (1967) Spectroscopic Determination of Tryptophan and Tyrosine in Proteins, *Biochemistry*, **6**, 1948-1954.

Finch, J. T. and Klug, A. (1976) Solenoidal Model for Superstructure in Chromatin, *Proc. Natl. Acad. Sci. USA*, **73**, 1897-1901.

Fletcher, T. M., Krishnan, U., Serwer, P., and Hansen, J. C. (1994a) Quantitative Agarose Gel Electrophoresis of Chromatin: Nucleosome-Dependent Changes in Charge, Shape and Deformability at Low Ionic Strength, *Biochemistry*, **33**, 2226-2233.

Fletcher, T. M., Serwer, P. and Hansen, J. C. (1994b) Quantitative Analysis of Macromolecular Conformation Changes Using Agarose Gel Electrophoresis: Application to Chromatin Folding, *Biochemistry*, **33**, 10859-10863.

Flory, P. J. (1953) *Principles of Polymer Chemistry* (Cornell Univ. Press, Ithaca), 319.

- Furrer, P., Bednar, J., Dubochet, J., Hamiche, A., and Prunell, A. (1995) DNA at the Entry -Exit of the Nucleosome Observed by Cryoelectron Microscopy, *J. Struct. Biol.*, **114**, 177-183.
- Garcia-Ramirez, M., Dong, F., and Ausio, J. (1992) Role of the Histone "Tails" in the Folding of Oligonucleosomes Depleted of Histone H1, *J. Biol. Chem.*, **267**, 19587-19595.
- Garcia-Ramirez, M. and Subirana, J. A. (1994) Condensation of DNA by Basic Proteins Does Not Depend on Protein Composition, *Biopolymers*, **34**, 85-292.
- Garcia-Ramirez, M., Leuba, S. H., and Ausio, J. (1990) One-Step Fractionation Method for Isolating H1 Histones from Chromatin under Nondenaturing Conditions, *Protein Expr. Purif.*, **1**, 40-44.
- Georgel, P., Demeler, B., Terpening, C., Paule, M. R., and van Holde, K. E. (1993) Binding of the RNA Polymerase I Transcription Complex to Its Promoter Can Modify Positioning of Downstream Nucleosomes Assembled *in Vitro*, *J. Biol. Chem.*, **268**, 1947-1954.
- Gerchman, S. E., Grazino, V., and Ramakrishnan, V. (1994) Expression of Chicken Linker Histones in *E. coli*: Sources of Problems and Methods for Overcoming Some of the Difficulties, *Protein Expr. Purif.*, **5**, 242-251.
- Gill, S. C. and von Hippel, P. H. (1989) Calculation of Protein Extinction Coefficients from Amino Acid Sequence Data, *Anal. Biochem.*, **182**, 319-326.
- Glotov, B. O., Itkes, A. V., Nikolaev, L. G., and Severin, E. S. (1978a) Evidence for the Close Proximity of Histones H1 and H3 in Chromatin of Intact Nuclei, *FEBS Lett.*, **91**, 149-152.
- Glotov, B. O., Nikolaev, L. G., Kurochkin, S. N., Trakht, I. N., and Severin, K. S. (1978b) Histone H1-DNA Interaction. Binding Properties of Some Individual Fragments of the Histone H1 Polypeptide Chain, *Studia Biophysica*, **69**, 145-156.
- Glotov, B. O., Nikolaev, L. G. and Severin, E. S. (1978c) Histone H1-DNA Interaction. On the Mechanism of DNA Strands Crosslinking by Histone H1, *Nucleic Acids Res.*, **7**, 2587-2605.
- Glotov, B. O., Nikolaev, L. G., Dashkevich, V. K., and Barbashov, S. F. (1985) Histone Crosslinking Patterns Indicate Dynamic Binding of Histone H1 in Chromatin, *Biochim. Biophys. Acta*, **824**, 185-193.
- Goytisolo, F. A., Gerchman, S., Yu, X., Rees, C., Graziano, V., Ramakrishnan, V., and Thomas, J. O. (1996) Identification of Two DNA-binding Sites on the Globular Domain of Histone H5, *EMBO J.*, **15**, 3421-3429.
- Grau, L. P., Azorin, F. and Subirana, J. A. (1982) Aggregation of Mono- and Dinucleosomes into Chromatin-like Fibers, *Chromosoma*, **87**, 437-445.

- Graziano, V., Gerchman, S. E., Schneider, D. K., Ramakrishnan, V. (1994) Histone H1 is Located in the Interior of the Chromatin 30-nm Filament, *Nature*, **368**, 351.
- Griess, G. A., Moreno, E. T., Easom, R. A., and Serwer, P. (1989) The Sieving of Spheres During Agarose Gel Electrophoresis: Quantitation and Modeling, *Biopolymers*, **28**, 1475-1484.
- Hamiche, A., Schultz, P., Ramakrishnan, V., Oudet, P., and Prunell, A. (1996) Linker Histone-Dependent DNA Structure in Linear Mononucleosomes, *J. Mol. Biol.*, **257**, 30-42.
- Hansen, J. C., Ausio, J., Stanik, V., and van Holde, K. E. (1989) Homogeneous Reconstituted Oligonucleosomes, Evidence for Salt-Dependent Folding in the Absence of Histone H1, *Biochemistry*, **28**, 9129-9136.
- Hansen, J. C., Kreider, J. I., Demeler, B., and Fletcher, T. M. (1997) Analytical Ultracentrifugation and Agarose Gel Electrophoresis as Tools for Studying Chromatin Folding in Solution, *Methods*, **12**, 62-72.
- Hansen, J. C. and Lohr, D. (1993) Assembly and Structural Properties of Subsaturated Chromatin Arrays, *J. Biol. Chem.*, **268**, 5840-5848.
- Hardison, R. C., Eichner, M. E., and Chalkley, R. (1975) An Approach to Histone Nearest Neighbours in Extended Chromatin, *Nucleic Acids Res.*, **2**, 1751-1770.
- Harrison, C. J., Bohm, A. A., and Nelson, H. C. M. (1994) Crystal Structure of the DNA Binding Domain of the Heat Shock Transcription Factor, *Science*, **263**, 224-227.
- Hayes, J. J. and Wolffe, A.P. (1993) Preferential and Assymmetric Interaction of Linker Histones with 5S DNA in the Nucleosome, *Proc. Natl. Acad. Sci. USA*, **90**, 6415-6419.
- Hermanson, G. T. (1996) *Bioconjugate Techniques* (Academic Press), 218-220.
- Heuser, J. and Griffith, J. (1989) Visualization of RecA Protein and its Complexes with DNA by Quick-freeze/Deep-etch Electron Microscopy, *J. Mol. Biol.*, **210**, 473-484.
- Hill, C. S., Martin, S. R., and Thomas, J. O. (1989) A Stable  $\alpha$ -Helical Element in the Carboxy-Terminal Domain of Free and Chromatin-Bound Histone H1 from Sea Urchin Sperm, *EMBO J.*, **8**, 2591-2599.
- Hill, C. S., Rimmer, J. M., Green, B. N., Finch, J. T., and Thomas, J. O. (1991) Histone-DNA Interactions and Their Modulation by Phosphorylation of -Ser-Pro-X-Lys/Arg- Motifs, *EMBO J.*, **10**, 1939-1948.
- Hillel, Z. and Wu, C. (1978) Photochemical Cross-Linking Studies on the Interaction of *Escherichia coli* RNA Polymerase with T7 DNA, *Biochemistry*, **17**, 2954-2961.

- Hockensmith, J. W., Kubasek, W. L., Vorachek, W. R., Evertsz, E. M., and von Hippel, P. H. (1991) Laser Crosslinking of Protein-Nucleic Acid Complexes, *Methods Enzymol.*, **208**, 211-236.
- Itkes, A. V., Glotov, B. O., Nikolaev, L. G., Preem, S. R. and Severin, E. S. (1980) Repeating Oligonucleosomal Units. A New Element of Chromatin Structure, *Nucleic Acids Res.*, **8**, 507-527.
- Ivanchenko, M., Hassan, A., van Holde, K., and Zlatanova, J. (1996) H1 Binding Unwinds DNA, *J. Biol. Chem.*, **271**, 1-6.
- Izaurrealde, E., Kas, E., and Laemmli, U. K. (1989) Highly Preferential Nucleation of Histone H1 Assembly on Scaffold-Associated Regions, *J. Mol. Biol.*, **210**, 573-585.
- Jin, Y. J. and Cole, R. D. (1986) H1 Histone Exchange Is Limited to Particular Regions of Chromatin That Differ in Aggregation Properties, *J. Biol. Chem.*, **261**, 3420-3427.
- Kas, E., Izaurrealde, E., and Laemmli, U. K. (1989) Specific Inhibition of DNA Binding to Nuclear Scaffolds and Histone H1 by Distamycin: The Role of Oligo(dA) Oligo(dT) Tracts, *J. Mol. Biol.*, **210**, 587-599.
- Klug, A. and Finch, J. T. (1976) Solenoidal Model for Superstructure in Chromatin, *PNAS*, **73**, 1897-1901.
- Klug, A., Rhodes, D., Smith, J., Finch, J. T., and Thomas, J. O. (1980) A Low Resolution Structure for the Histone Core of the Nucleosome, *Nature*, **287**, 509-516.
- Kowalczykowski, S. C., Paul, L. S., Lonberg, N., Newport, J. W., McSwiggen, J. A., and von Hippel, P. H. (1986) Cooperative and Noncooperative Binding of Protein Ligands to Nucleic Acid Lattices: Experimental Approaches to the Determination of Thermodynamic Parameters, *Biochemistry*, **25**, 1226-1240.
- Krylov D., Leuba, S., van Holde, K., and Zlatanova, J. (1993) Histone H1 and H5 Interact Preferentially with Crossovers of Double-Helical DNA, *Proc. Natl. Acad. Sci. USA*, **90**, 5052-5056.
- Kumar, N. M., and Walker, I. O. (1980) The Binding of Histone H1 and H5 to Chromatin in Chicken Erythrocyte Nuclei, *Nucleic Acids Res.*, **8**, 3535-3551.
- Kwon, H. J., Tirumalai, R., Landy, A., and Ellenberger, T. (1997) Flexibility in DNA Recombination: Structure of the Lambda Integrase Catalytic Core, *Science*, **276**, 126-131.
- Laemmli, U.K. (1970) Cleavage of Structural Proteins During the Assembly of the Head of Bacteriophage T4, *Nature*, **227**, 680-685.

- Lennard, A. C. and Thomas, J. O. (1985) The Arrangement of H5 Molecules in Extended and Condensed Chicken Erythrocyte Chromatin, *EMBO J*, **4**, 3455-3462.
- Leuba, S. H., Zlatanova, J., and van Holde, K. (1993) On the Location of Histone H1 and H5 in the Chromatin Fiber: Studies with Immobilized Trypsin and Chymotrypsin, *J. Mol. Biol.*, **229**, 917-929.
- Leuba, S. H., Zlatanova, J. and van Holde, K. (1994b) On the Location of DNA in the Chromatin Fiber: Studies with Immobilized and Soluble Micrococcal Nuclease, *J. Mol. Biol.*, **235**, 871-880.
- Leuba, S. H., Yang, G., Robert, C., Samori, B., van Holde, K., Zlatanova, J., and Bustamante, C. (1994a) Three-Dimensional Structure of Extended Chromatin Fibers as Revealed by Tapping-Mode Scanning Force Microscopy, *Proc. Natl. Acad. Sci. USA*, **91**, 11621-11625.
- Leuger, K., Mader, A. W., Richmond, R. K., Sargent, D. F., and Richmond, T. J. (1997) Crystal Structure of the Nucleosome Core Particle at 2.8 Å Resolution, *Nature*, **389**, 251-260.
- Liao, L. W. and Cole, R. D. (1981) Differences among Subfractions of H1 Histone in their Interactions with Linear and Superhelical DNA, *J. Biol. Chem.*, **256**, 11145-11150.
- Lohman, T. M. (1986) Kinetics of Protein-Nucleic Acid Interactions: Use of Salt Effects to Probe Mechanisms of Interaction, *CRC Crit. Rev. Biochem.*, **19**, 191-245.
- Lohman, T. M. and Mascotti, D. P. (1992) Thermodynamics of Ligand-Nucleic Acid Interactions, *Methods Enzymol.*, **212**, 400-458.
- Losa, R., Thoma, F., and Koller, T. (1984) Involvement of the Globular Domain of Histone H1 in the Higher Order Structures of Chromatin, *J. Mol. Biol.*, **175**, 529-551.
- Maman, J. D., Yager, T. D., and Allan, J. (1994) Self-Association of the Globular Domain of Histone H5, *Biochemistry*, **33**, 1300-1310.
- Maniatis, T., Fritsch, J. T., and Sambrook, J. (1982) *Molecular Cloning : A Laboratory Manual* (Cold Spring Harbor Lab., Plainview, NY).
- Matthews, H. R. and Bradbury, E. M. (1978) The Role of H1 Histone Phosphorylation in the Cell Cycle, *Exp. Cell Res.*, **111**, 343-351.
- McGhee, J. D. and von Hippel, P. H. (1974) Theoretical Aspects of DNA-Protein Interactions: Co-operative and Non-co-operative Binding of Large Ligands to a One-Dimensional Homogeneous Lattice, *J. Mol. Biol.*, **86**, 469-489.

- Merril, C. R. (1990) Silver Staining of Proteins and DNA, *Nature*, **343**, 779-780.
- Mirzabekov, A. D., Pruss, D. V., Ebralidse, K. K. (1989) Chromatin Superstructure-dependent Crosslinking with DNA of the Histone H5 Residues Thr1, His25, His62, *J. Mol. Biol.*, **211**, 479-491.
- Mitchell, L. G., Bodenteich, A., and Merrill, C. R. (1994) Use of Silver Staining in Detecting Nucleic Acids, *Methods Mol. Biol.*, **31**, 197-203.
- Moffat, B. A. and Studier, F. W. (1986) Use of Bacteriophage T7 RNA Polymerase to Direct Selective High-Level Expression of Cloned Genes, *J. Mol. Biol.*, **189**, 113-130.
- Nelson, P. P., Albright, S. C., Wiseman, J. M. and Garrard, W. T. (1979) Reassociation of Histone H1 with Nucleosomes, *J. Biol. Chem.*, **254**, 11751-11760
- Newman, M., Strzelecka, T., Dorner, L. F., Schildkraut, I., and Aggarwal, A. K. (1995) Structure of Bam HI Endonuclease Bound to DNA: Partial Folding and Unfolding on DNA Binding, *Science*, **269**, 656-663.
- Nikolaev, L. G., Glotov, B. O., Dashkevich, V. K., Barbashov, S. F., and Severin E. S. (1983a) Distribution of Histone H1 in Chromatin. Cross-Linkage of Central Globular Portions of the Molecule with a Bifunctional Reagent, *Mol. Biol. (Mosk)*, **17**, 1255-1261.
- Nikolaev, L. G., Glotov, B. O., Dashkevich, V. K., Barbashov, S. F., and Severin E. S. (1983b) Mutual Arrangement of Histone H1 Molecules in Extended Chromatin, *FEBS Lett.*, **163**, 66-68.
- Nikolaev, L. G., Glotov, B. O., Itkes, A. V., and Severin E. S. (1981) Mutual Arrangement of Histone H1 Molecules in Chromatin of Intact Nuclei, *FEBS Lett.*, **125**, 20-24.
- Noll, M. and Kornberg, R. D. (1977) Action of Micrococcal Nuclease on Chromatin and the Location of Histone H1, *J. Mol. Biol.*, **109**, 393-404.
- Olins, D. E., Olins, A. L., von Hippel, P. H. (1967) Model Nucleoprotein Complexes: Studies on the Interaction of Cationic Homopolypeptides with DNA, **24**, 157-176.
- Olins, A. L. and Olins, D. E. (1974) Spheroid Chromatin Units (v Bodies), *Science*, **183**, 330-332.
- Olins, D. E. and Wright, E. B. (1973) Glutaraldehyde Fixation of Isolated Eucaryotic Nuclei: Evidence of Histone-Histone Proximity, *J. Cell Biol.*, **59**, 304-317.
- O'Neill, R. R., Mitchell, L. G., Merrill, C. R., and Rasband, W. S. (1989) Use of Image Analysis to Quantitate Changes in Form of Mitochondrial DNA After X-Irradiation, *Appl. Theor. Electrophor.*, **1**, 163-167.

- Osipova, T. N., Triebel, H., Bar, H., Zalenskaya, I. A., and Hartmann, M. (1985) Interaction of Histone H1 from Sea Urchin Sperm with Superhelical and Relaxed DNA, *Molec. Biol. Rep.*, **10**, 153-158.
- Overdier, D. G., Porcella, A. and Costa, R. H. (1994) The DNA-Binding Specificity of the Hepatocyte Nuclear Factor 3/Forkhead Domain Is Influenced by Amino-Acid Residues Adjacent to the Recognition Helix, *Mol. Cell Biol.*, **14**, 2755-2766.
- Petersen, J. M., Skalicky, J. J., Donaldson, L. W., McIntosh, L. P., Alber, T., and Graves, B. J. (1995) Modulation of Transcription Factor Ets-1 DNA Binding: DNA-Induced Unfolding of an  $\alpha$  Helix, *Science*, **269**, 1866-1869.
- Pruss, D., Bartholomew, B., Persinger, J., Hayes, J., Arents, G., Moudrianakis, E. N., and Wolffe, A. P. (1996) An Asymmetric Model for the Nucleosome: A Binding Site for Linker Histones Inside the DNA Gyres, *Science*, **274**, 614-617.
- Ramakrishnan, V., Finch, J. T., Graziano, V., Lee, P. L., and Sweet, R. M. (1993) Crystal Structure of Globular Domain of Histone H5 and Its Implications for Nucleome Binding, *Nature* **362**, 219-223.
- Renz, M. and Day, L. A. (1976) Transition from Noncooperative to Cooperative and Selective Binding of Histone H1 to DNA, *Biochemistry*, **15**, 3220-3227.
- Riehm, M. R. and Harrington, R. E. (1989) Histone-Histone Interaction Mediates Chromatin Unfolding at Physiological Ionic Strength, *Biochemistry*, **28**, 5787-5793.
- Ring, D. and Cole, R. D. (1979) Chemical Cross-Linking of H1 Histone to the Nucleosomal Histones, *J. Biol. Chem.*, **254**, 11688-11695.
- Ring, D. and Cole, R. D. (1983) Close Contact between H1 Histone Molecules in Nuclei, *J. Biol. Chem.*, **258**, 15361-15364.
- Russo, E., Giancotti, V., Crane-Robinson, C., and Geraci, G. (1983) Histone H1 and Chromatin Higher Order Structure: Does Histone H1 Exhibit Specific Self-Association, *Eur. J. Biochem.*, **15**, 487-493.
- Sasse, J. and Gallagher, S. R. (1991) *Current Protocols in Molecular Biology*, 10.6.1-10.6.8.
- Schwarz, P. M. and Hansen, J. C. (1994) Formation and Stability of Higher Order Chromatin Structures, *J. Biol. Chem.*, **269**, 16284-16289.

Schultz C. S., Shields, G. C., and Steitz, T. A. (1991) Crystal Structure of a CAP-DNA Complex: The DNA Is Bent by 90°, *Science*, **253**, 1001-1007.

Segers, A., Muyldermans, S., and Wyns, L. (1991) The Interaction of Histone H5 and Its Globular Domain with Core Particles, Depleted Chromatosomes, Polynucleosomes, and a DNA Decamer, *J.Biol. Chem.*, **266**, 1502-1508.

Sevall, J. S. (1988) High-Resolution Analysis of a Histone H1 Binding Site in a Rat Albumin Gene, *Biochemistry*, **27**, 5038-5044.

Simon, R. H. and Felsenfeld, G. (1979) A New Procedure for Purifying Histone Pairs H2A + H2B and H3 + H4 from Chromatin Using Hydroxylapatite, *Nucleic Acids Res.*, **6**, 689-696.

Simpson, R. T., Thoma, F., and Brubaker, J. M. (1985) Chromatin Reconstituted from Tandemly Repeated Cloned DNA Fragments and Core Histones: A Model System for Study of Higher Order Structure, *Cell*, **42**, 799-808.

Singer, D. S. and Singer, M. F. (1976) Studies on the Interaction of H1 Histone with Superhelical DNA: Characterization of the Recognition and Binding Regions of H1 Histone, *Nucleic Acids Res.*, **3**, 2531-2547.

Singer, M. F. and Singer, D. S. (1978) Characterization of Complexes of Superhelical and Relaxed Closed Circular DNA with H1 and Phosphorylated H1 Histones, *Biochemistry* **17**, 2086-2095.

Smerdon, M.J. and Isenberg, I. (1976) Conformational Changes in Subfractions of Calf Thymus Histone H1, *Biochemistry*, **15**, 4233-4242.

Spolar, R. S. and Record, M. T. (1994) Coupling of Local Folding to Site-Specific Binding Proteins to DNA, *Science*, **263**, 777-784.

Stein, A. (1979) DNA Folding by Histones: the Kinetics of Chromatin Core Particle Reassembly, and the Interaction of Nucleosomes with Histones, *J. Mol. Biol.*, **130**, 103-134.

Stein, A. and Mitchell, M. (1988) Generation of Different Nucleosome Spacing Periodicities in Vitro: Possible Origin of Cell Type Specificity, *J. Mol. Biol.*, **203**, 1029-1043.

Story, R. M., Weber, I. T. and Steitz, T. A. (1992) The Structure of the *E. coli* RecA Protein Monomer and Polymer, *Nature*, **355**, 318-376.

Subirana, J. A. (1990) Analysis of the Charge Distribution in the C-Terminal Region of Histone H1 as Related to Its Interaction with DNA, *Biopolymers*, **29**, 1351-1357.

Takahashi, M. and Norden, B. (1994) Structure of RecA-DNA Complex and Mechanism of DNA Strand Exchange Reaction in Homologous Recombination, *Adv. Biophys.*, **30**, 1-35.

- Thoma, F., and Koller, T. (1977) Influence of H1 on Chromatin Structure, *Nature*, **12**, 101-107.
- Thoma, F., Koller, T., and Klug, A. (1979) Involvement of Histone H1 in the Organization of the Nucleosome and of the Salt-Dependent Superstructures of Chromatin, *J. Cell Biol.*, **83**, 403-427.
- Thoma, F., Losa, R., and Koller, T. (1983) Involvement of the Domains of Histone H1 and H5 in the Structure Organization of Soluble Chromatin, *J. Mol. Biol.*, **167**, 619-640.
- Thomas, J. O. (1989) Chemical Cross-Linkage of Histones, *Methods. Enzymol.*, **170**, 549-571.
- Thomas, J. O. and Khabaza, A. J. A. (1980) Crosslinking of Histone H1 in Chromatin, *Eur. J. Biochem.*, **112**, 501-511.
- Thomas, J. O. and Kornberg, R. D. (1975) Cleavable Cross-Links in the Analysis of Histone-Histone Associations, *FEBS Lett.*, **58**, 353-358.
- Thomas, J. O., Rees, C., and Finch, J. T. (1992) Cooperative Binding of the Globular Domains of Histones H1 and H5 to DNA, *Nucleic Acids Res.*, **20**, 187-194.
- Thomas, J. O. and Wilson, C. M. (1986) Selective Radiolabelling and Identification of a Strong Nucleosome Binding Site on the Globular Domain of Histone H5, *EMBO J.*, **5**, 3531-3537.
- Tuerk, C. and Gold, L. (1990) Systematic Evolution of Ligands by Exponential Enrichment: RNA Ligands to Bacteriophage T4 DNA Polymerase, *Science*, **249**, 505-510.
- Turnell, W. G., Satchwell, S. C., and Travers, A. A. (1988) A Decapeptide Motif for Binding to the Minor Groove of DNA, *FEBS Lett.*, **232**, 263-268.
- van Holde, K. E. (1985) *Physical Biochemistry*, 2nd Ed. (Prentice-Hall, Inc., Englewood Cliffs, N.J.), 117.
- van Holde, K. E. (1989) *Chromatin* (Springer Verlag, New York).
- van Holde, K. E. and Zlatanova, J. (1996a) What Determines the Folding of the Chromatin Fiber?, *Proc. Natl. Acad. Sci.*, **93**, 10548-10555.
- van Holde, K. E. and Zlatanova, J. (1996b) Chromatin architectural proteins and transcription factors: a structural connection, *Bioessays*, **18**, 697.
- Varga-Weisz, P., van Holde, K. E., Zlatanova, J. (1993) Preferential Binding of Histone H1 to Four-way Helical Junction DNA. *J. Biol. Chem.*, **268**, 1-2.

- Varga-Weisz, P., Zlatanova, J., Leuba, S. H., Schroth, G. P., and van Holde, K. (1994) Binding of H1 and H5 and Their Globular Domains to Four-Way Junction DNA, *Proc. Natl. Acad. Sci. USA*, **91**, 3525-3529.
- Vogel, T., and Singer, M. (1974) The Interaction of Histones with Simian Virus 40 Supercoiled Circular Deoxyribonucleic Acid *in Vitro*, *J. Biol. Chem.*, **250**, 796-798.
- Wallace, R. B. and Miyada, C. G. (1987) Oligonucleotide Probes for the Screening of Recombinant DNA Libraries, *In Methods Enzymol.*, **152**, 432-442.
- Watanabe, F. (1985) Cooperative Interaction of Histone H1 with DNA, *Nucleic Acids Res.*, **14**, 3573-3585.
- Welch, S. L. and Cole, R. D. (1979) Differences between Subfractions of H1 Histone in Their Interactions with DNA, *J. Biol. Chem.*, **254**, 662-665.
- Werner, M. H., Clore, G. M., Fisher, C. L., Fisher, R. J., Trinh, L., Shiloach, J., and Gronenborn, A. M. (1995) The Solution Structure of the Human ETS1-DNA Complex Reveals a Novel Mode of Binding and True Side Chain Intercalation, *Cell*, **83**, 761-771.
- Widom, J. (1989) Toward a Unified Model of Chromatin Folding, *Annu Rev Biophys Biophys Chem*, **18**, 365-395.
- Woodcock, C. L. F. (1973) Ultrastructure of Inactive Chromatin, *J. Cell Biol.*, **59**, 368.
- Yager, T. D., McMurray, C. T., and van Holde, K. E. (1989) Salt-Induced Release of DNA from Nucleosome Core Particles, *Biochemistry*, **28**, 2271-2281.
- Yaneva, J. N., Paneva, E. G., Banchev, T. B., and Zlatanova, J. S. (1991) The Structure of H1/DNA Complexes Differs with Ionic Strength in a Process Independent of Cooperativity, *Biologie*, **44**, 131-134.
- Yaneva, J., Schroth, G. P., van Holde, K. E., and Zlatanova, J. (1995) High-Affinity Binding Sites for Histone H1 in Plasmid DNA, *Proc. Natl. Acad. Sci. USA*, **92**, 7060-7064.
- Yaneva, J. and Zlatanova, J. (1992) Histone H1 Interacts Specifically with Certain Regions of the Mouse  $\alpha$ -Globin Gene, *DNA Cell Biol.*, **11**, 91-99.
- Yao, J., Lowary, P. T., and Widom, J. (1991) Linker DNA Bending Induced by the Core Histones of Chromatin, *Biochemistry*, **30**, 8408-8414.
- Zlatanova, J. and Doenecke, D. (1994) Histone H1<sup>o</sup>: A Major Player in Cell Differentiation, *FASEB J.*, **8**, 1260-1268.

Zlatanova, J. and van Holde, K. E. (1995) Chromatin Higher Order Structure: Chasing a Mirage?, *J. Biol. Chem.*, **270**, 8373-8376.

Zlatanova, J. and van Holde, K. E. (1996) The Linker Histones and Chromatin Structure: New Twists, *Prog. Nucleic Acid Res. Mol. Biol.*, **52**, 217-259.

Zlatanova, J. and Yaneva, J (1991) Histone H1-DNA Interactions and Their Relation to Chromatin Structure and Function, *DNA Cell Biol.*, **10**, 239-248.

**APPENDICES**

## APPENDIX A1

### Sequences of Relevant DNA and Proteins

#### A1.1 Sequence of recombinant GH5 expressed from expression vector GH5pLK

ATG TCG CAC CCC ACC TAC TCG GAG ATG ATC GCG GCG GCC ATC CGT  
     s h p t y s e m i a a a i r  
 GCG GAA AAG AGC CGC GGC GGC TCC TCG CGG CAG TCC ATC CAG AAG  
     a e k s r g g s s r q s i q k  
 TAC ATC AAG AGC CAC TAC AAG GTG GGC CAC AAC GCC GAT CTG CAG  
     y i k s h y k v g h n a d l q  
 ATC AAG CTC TCC ATC CGA CGT CTC CTG GCT GCC GGC GTC CTC AAG  
     i k l s i r r l l a a g v l k  
 CAG ACC AAA GGG GTC GGG GCC TCC GGC TCC TTC CGC TTG GCC AAG  
     q t k g v g a s g s f r l a k  
 TAA

Gerchman, S. E., Grazino, V., and Ramakrishnn, V. (1994) Expression of Chicken Linker Histones in *E. coli*: Sources of Problems and Methods for Overcoming Some of the Difficulties, *Protein Expr Purif*, 5, 242-251.

**A1.2 Sequence of recombinant GH1° expressed from expression vector  
pet15b-GH1°t**

ATG GGG TAT TCA GAC ATG ATC GTG GCT GCC ATC CAG GCC GAG AAG  
m g y s d m i v a a i q a e k  
AAC CGC GCT GGC TCC TCG CGC CAG TCC ATT CAG AAG TAT ATC AAG  
n r a g s s r q s i n k y i k  
AGC CAC TAC AAG GTG GGT GAG AAC GCT GAC TCG CAG ATC AAG TTG  
s h y k v l e n a d s q i k l  
TCC ATC AAG CGC CTG GTC ACC ACC GGT GTC CTC AAG CAG ACC AAA  
s i k r l v t t g v l k q t k  
GGG GTG GGG GCC TCG GGG TCC TTC CGG CTA GCC AAG TGA  
g v g a s g s f r l a k

Doenecke, D. and Tonjes, R. (1986) Differential Distribution of Lysine and Arginine Residues in the Closely Related Histones H1° and H5, *J. Mol. Biol.*, 187, 461-464.

**A1.3 Sequence of recombinant GH1.3 (without "read-through" peptides) expressed from expression vector pet15b-GH1.3**

ATG GGA CCC CCA GTA TCT GAG CTT ATC ACC AAG GCA GTG GCA GCT  
 m g p p v s e l i t k a v a a  
 TCT AAG GAG CGC AGC GGC GTT TCT CTG GCC GCG CTT AAG AAA GCG  
 s k e r s g v s l a a l k k a  
 CTT GCG GCT GCT GGC TAC GAT GTA GAA AAA AAC AAC AGC CGT ATC  
 l a a a g y e v e k n n s r i  
 AAG CTT GGC CTC AAG AGC TTG GTG AGC AAA GGT ACT CTG GTG CAG  
 k l g l k s l v s k g t l v q  
 ACC AAA GGT ACC GGT GCT TCT GGC TCC TTC AAA CTC AAC AAG TGA  
 t k g t g a s g s f k l n k  
 TGA TGA

Albig, W., Kardalidou, E., Drabent, B., Zimmer, A., and Doenecke, D. (1991) Isolation and Characterization of Two Human H1 Histone Genes with Clusters of Core Histone Genes, *Genomics*, 10, 940-948.

#### A1.4 Amino acid sequence of avian erythrocyte-specific linker histone H5

t e s l v l s p a p a k p k r v k a s r r s a s h p t y s e  
 m i a a a i r a e k s r g g s s r q s i q k y i k s h y k  
 v g h n a d l q i k l s i r r l l a a g v l k q t k g v g  
 a s g s f r l a k s d k a k r s p g k k k k a v r r s t s p  
 k k a a r p r k a r s p a k k p k a t a r k a r k k s r a s  
 p k k a k k p k t v k a k s r k a s k a k k v k r s k p r  
 a k s g a r k s p k k k

Bold type indicates the trypsin-resistant globular domain (Aviles et al., 1978).

Aviles, F. J., Chapman, G. E., Kneale, G. G., Crane-Robinson, C., and Bradbury, E. M. (1978) The Conformation of Histone H5, *Eur. J. Biochem.*, 88, 363-371.

Briand, G., Kmiecik, D., Sautiere, P., Wouters, D., Borie-Loy, O., Biserte, G., Mazen, A., and Champagne, M. Sequence of the Carboxy-terminated Half of the Molecule (96 Residues) and Complete Sequence (1980) *FEBS letters*, 112, 147-151.

**A1.5 Nucleic acid sequence of the 208 .b.p. 5S rRNA gene DNA from *Lytechinus variegatus*.**

Bold type represents the EcoR I restriction site and ♦ indicates the bond cleaved by EcoR I digestion; underlined b.p. represent the section protected by primary octamer positioning (Dong et al., 1990). Note that the sequence was originally referenced as having 207 b.p. (Simpson and Stafford, 1983). However re-sequencing of the fragment indicates that an additional G base was located at the very 5' end (Georgel et al., 1993; personal communications with Dr. Borris Demler).

**G♦AATTCCAACGAATAACTTCCAGGGATTTATAAGCCGATGCGTCATAACAT**  
**CCTGACCCTTTAAATAGCTTAACTTTCATCAAGCAAGAGCCTACGACCATAACC**  
**ATGCTGAATATACCGGTTCTCGTCCGATCACCGAAGTCAAGCAGCATAGGGCT**  
**CGGTTAGTACTTGGATGGGAGACCGCCTGGGAATACG♦AATTC~~CC~~CGAGG**

Dong, F., Hansen, J. C., and van Holde, K. E. (1990) DNA and Protein Determinants of Nucleosome Positioning on Sea Urchin 5S rRNA Gene Sequences In Vitro, Proc. Natl. Acad. Sci. USA, 87, 5724-5728.

Georgel, P., Demeler, B., Terpening, C., Paule, M. R., and van Holde, K. E. (1993) Binding of the RNA Polymerase I Transcription Complex to Its Promoter Can Modify Positioning fo Downstream Nucleosomes Assembled in Vitro, J. Biol. Chem., 268, 1947-1954.

Simpson, R. T. and Stafford, D. W. (1983) Structural Features of a Phased Nucleosome Core Particle, Proc. Natl. Acad. Sci. USA, 80, 51-55

## APPENDIX A2

**Using the Sedimentation Coefficient to Estimate the Number of Octamers Bound to the "208-12" DNA Fragment**

The number of octamers bound to the 2600 b.p. fragment, referred to as the 208-12 DNA, was estimated using a technique based on Hansen and Lohr (1993). The 208-12 DNA is twelve tandem copies of a 5S rDNA nucleosome positioning sequence (208 b.p.) from *Lytechinus variegatus*. The fragment has been cloned into a number of cloning vectors including most recently pUC19 to yield pPol208-12 (Georgel et al., 1993). The number of octamers bound to the 208-12 DNA ( $n$ ) was estimated from the nucleoprotein complex sedimentation coefficient  $s_{20,w}$ . By re-plotting the combined data from Figure 3 and Figure 8 of Hansen and Lohr (1993),  $n$  could be determined for both super-saturated and sub-saturated reconstituted fibers (Figure A2.1). The sedimentation coefficients for reconstitutes above 29.0 S remains speculative; the fibers may contain more than 12 octamers ( or additional subunits), or the fibers may experience localized compaction. However, the linear semi-logarithmic relationship between sub-saturated and "super-saturated" suggests that more than 12 octamers can deposit on the 208-12 DNA (Hansen and Lohr, 1993).

Hansen, J. C. and Lohr, D. (1993) Assembly and Structural Properties of Subsaturated Chromatin Arrays, *J. Biol. Chem.*, 268, 5840-5848.

Figure A2.1. Relationship between reconstituted 208-12 DNA and the nucleoprotein complex sedimentation coefficient. The  $s_{20,w}$  of reconstituted 208-12 DNA was determined for various  $n$  as determined by velocity analytical ultracentrifugation in 10 mM Tris-HCl (pH 7.8), 0.2 mM EDTA. The plot combines data both Figure 3 (*open triangles*) and Figure 8 (*solid circles*) from Hansen and Lohr (1993). The solid line represents a linear regression of the data points (Microsoft Excel 4.0).

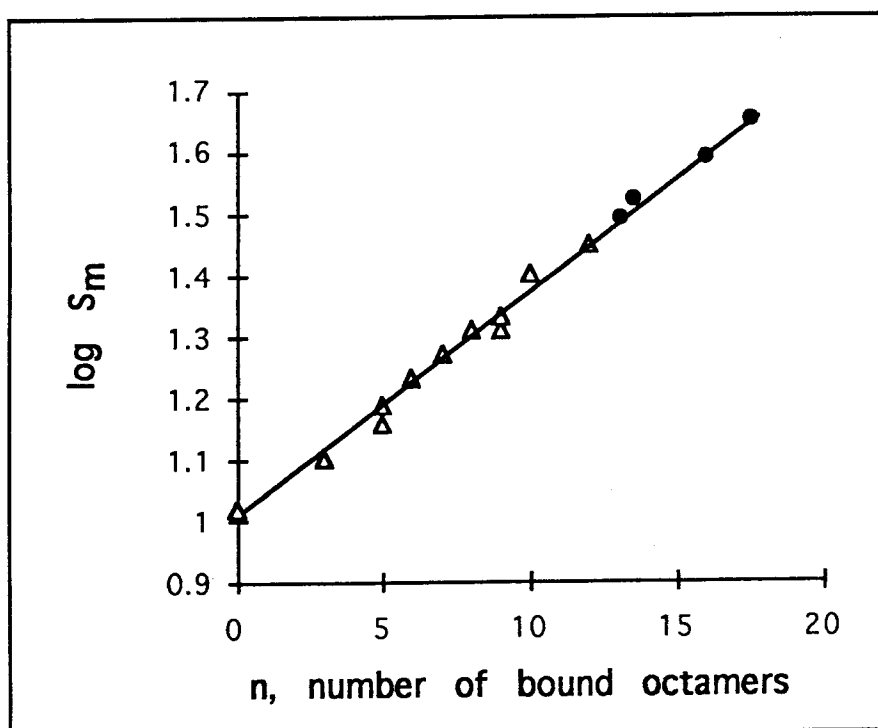


Figure A2.1

## APPENDIX A3

### Alternative Methods for Determining the Number of Octamer Histones Bound to the "208-12" DNA

#### Summary A3.0

A simple strategy was developed to estimate the number of octamers bound ( $n$ ) to a DNA containing twelve tandem 208 b.p. octamer histone positioning sequences from the 5S rDNA gene from *Lytechinus variegatus*. The procedures included 1% and 0.3% agarose gel electrophoresis and, in a separate assay, cleavage of the fibers with EcoR I restriction enzyme. Estimates of  $n$  made with these techniques were corroborated with measurements made by analytical ultracentrifugation. In the first procedure, the relative electrophoretic mobility (relative to free, unreconstituted DNA) was empirically related to the sedimentation coefficient of the same reconstituted DNA. For the latter, EcoR I was used to digest the reconstituted "208-12" DNA into individual 208 b.p. fragments that were either occupied or unoccupied by an octamer. A relationship to  $n$  (both experimentally-observed and theoretical-derived) was developed by comparing the amount of DNA associated with nucleosomes to free DNA fragments. Additionally, EcoR I digestion conditions were optimized by considering both the influence of salt and temperature. It was found that digestion at 37 °C and inclusion of 50 mM NaCl caused instability of the nucleosome complex, and could produce inaccuracies in the restriction digestion assay. In summary, the two procedures for determining  $n$  were found to be a reliable alternative to the potentially cumbersome task of estimating the number of

octamers bound to the 208-12 DNA using hydrodynamic methods, or imaging techniques like SFM, or EM.

### A3.1 Introduction

In recent years, artificially reconstituted chromatin has been used to examine such varied topics as chromatin morphology (Hansen et al., 1989; Schwartz and Hansen, 1994; Fletcher et al., 1994a; Fletcher et al., 1994b; Hansen and Lohr 1993), transcription (Li et al., 1994; Georgel et al., 1993; Hansen and Wolffe, 1992), and integration (Pruss et al., 1994). Artificially reconstituted chromatin combines purified DNA, octamer histones, as well as auxiliary proteins, in building small fibers that mimic actual native chromatin (Garcia-Ramirez et al, 1992). Artificially reconstituted chromatin has advantages over native chromatin, since the amount and/or modification of each protein component reconstituted onto the fiber can be carefully controlled. The most popular system utilizes a template of twelve tandem repeats of the 5S rDNA gene fragment from *Lytechinus variegatus*, often referred to as the "208-12 DNA". This construct was originally described by gel electrophoresis and endonuclease assays (Simpson et al., 1985), and more recently characterized by more elaborate biophysical techniques (reviewed in Hansen et al., 1997). Additionally, the importance of determining the number of octamers bound to template DNA has led to a considerable effort in developing a reliable method for this purpose. The number of octamer histones bound to the 208-12 DNA ( $n$ ) has previously been estimated from either the sedimentation coefficient (Appendix A2), or from  $\mu_o$ , the electrophoretic mobility in free solution (Fletcher et al., 1994a).

One drawback to the current methodologies is that determining the number of octamers bound to the 208-12 DNA requires either a sedimentation coefficient or  $\mu_s$ , with both values obtained using rather sophisticated analytical techniques. To circumvent this potential obstacle, two alternative assays were devised for relatively rapid, and simple, determination of  $n$ . The first technique is based on changes in electrophoretic mobility for samples run in 0.3% and 1% agarose gels, as originally noted by Simpson et al. (1985). This is due to both a decrease in the surface charge density of the nucleoprotein complex from the addition of basic octamer histones, and a decrease in the effective radius of the complex (relative to naked, linear DNA), because DNA is wrapped about 1.75 times around each octamer histone (Luger et al., 1997). EcoR I digestion of the reconstituted 208-12 provided another rapid method for counting the number of octamers. Digesting the reconstituted 208-12 DNA with EcoR I resulted in the release of a free 195 b.p. DNA fragment and nucleosomes. The value  $n$  was then estimated by comparing the relative amount of DNA associated with nucleosomes to that associated with free DNA. Results of both techniques were related to precise measurements of  $n$  determined from analytical ultracentrifugation, and/or previously reported data.

## **A3.2 Methods and materials**

### A3.2.1 Chromatin reconstitution

Chromatin was reconstituted from histone octamers and DNA using the "salt dialysis" technique as described in Hansen et al. (1989). Briefly, purified histone octamers

(see Chapter 3) were combined with a linear DNA composed of twelve tandem repeats of a 208 b.p. fragment of the 5S rDNA gene from *Lytechinus variegatus* (208-12 DNA) that was cloned into pUC19 (Georgel et al., 1993). The insert was separated from the parent cloning vector pUC19 as described in Hansen et al. (1989). Core histones at various concentrations were combined with the 208-12 DNA, typically at 0.05 mg/ml at 2 M NaCl, 10 mM Tris-HCl, 0.2 mM EDTA, and as described in Chapter 3, "stepped down" by dialysis to 1 M NaCl, T.E., 0.75 M NaCl, T.E., and T.E. Samples were stored on ice until use.

#### A3.2.2 Endonuclease digestion of reconstituted 208-12 DNA with EcoR I

In determining the number of octamer histones bound to the 208-12 DNA fragment by this method, chromatin reconstituted with histone octamers was digested at room temperature for 3-5 hours with EcoR I (New England Biolabs) at 0.65 units/ $\mu$ l in 3.5 mM MgCl<sub>2</sub>, 30 mM Tris-HCl (pH 7.8), 1 mM dithiothreitol based on conditions outlined by Hansen and Lohr (1993). The amount of chromatin (in terms of DNA mass) for the reactions was typically about 0.045 mg/ml. After digestion, samples were analyzed by PAGE (see below). Reconstituted 208-12 DNA that was used in the temperature- and salt-dependent stability experiments were treated at either room temperature or 37 °C with EcoR I at 1.33 units/ $\mu$ l under the same conditions as described above. Reactions were stopped by bringing the reaction to 5 mM EDTA.

### A3.2.3 Gel electrophoresis

For the analysis of octamer histone reconstituted 208-12 DNA, typically, 0.5 mg of samples (as DNA) were applied to each lane of either a 0.3% or 1% agarose gel (electroendosmosis < 0.01) and run in TAE buffer at 3.5 volts/cm at room temperature. The 0.3% agarose gel had little viscous consistency and required particular care in transport. Typically, the agarose was solidified in a casting tray over a glass plate at 4 °C. The glass plate was used as a structural support in ethidium bromide staining and UV illumination. Reconstituted 208-12 DNA that was digestion with EcoR I was applied to 6% polyacrylamide:bisacrylamide gels (29:1) run in TAE buffer at around 12.5 volts/cm. Estimates of DNA were determined from photographs of gels stained in ethidium bromide (0.5 µg/ml) that were processed with NIH IMAGE 1.57 (O'Neill et al., 1989).

### A3.2.4 Estimating number of octamers bound to the 208-12 DNA by velocity analytical ultracentrifugation

A Beckman XLA was used to analyze reconstituted 208-12 DNA in T.E.. Typically, 400 µl samples (along with buffer control) were analyzed at 260 nm at 20 minute time points over a period of several hours. Reconstitutes were run in T.E. at 21 °C with rotor speeds were set at about 20,000 rpm. Data was plotted as the natural log of the distance of the boundary half-way point as a function of time (seconds). The sedimentation coefficient was determined from,  $s \times \omega^2 = \Delta \ln r / \Delta t$ , where  $s$  is the sedimentation coefficient,  $\omega$  is the rotor speed (rads/second),  $t$  is time (seconds), and  $r$

is the midpoint of the boundary traveled at time  $t$ . Sedimentation coefficients taken at 21°C values were converted to  $s_{20,w}$  based on standard equations, then from a technique described in Hansen and Lohr (1993),  $s_{20,w}$  was used to estimate the number of octamers bound to the 208-12 DNA (see [Figure A2.1](#)).

### A3.3 Results

#### A3.3.1 Estimating the number of octamers bound to the 208-12 DNA by gel electrophoresis

As described in Chapter 3, movement of polymers under the influence of an electric field through a gel matrix is described by the empirically-derived equation

$$(A3.1) \quad \frac{\mu}{\mu_o} = \left(1 - \frac{R}{P_e}\right)^2,$$

where  $\mu$  is the relative electrophoretic mobility (usually referenced to a viral capsid standard),  $\mu_o$  is the mobility in free solution,  $P_e$  is the effect pore radius, and  $R$  is the "effective" radius of the molecule (Griess et al., 1989). Equation (A3.1) depends upon the probability that a sphere will make contact with the matrix when passing through an array of circular pores. In general, two useful parameters describe a macromolecule that moves under the influence of an electric field in an agarose gel including: (a) surface charge density that is related to  $\mu_o$ , and (b) the effective radius of a macromolecule,  $R$ . A calculation of these parameters for octamers histones reconstituted onto the 208-12 DNA at various saturation has been performed by Fletcher et al. (1994a) and Fletcher et al.

(1994b) using quantitative gel electrophoresis, a form of Ferguson-type analysis.

Additionally, the term reptation is given to polymers that can move through pores that are considerably smaller than the radius of gyration of the polymer, and is defined as the point where  $R$  changes with  $P_c$ . In the first assay, reconstitutes were analyzed with both 1% and 0.3% agarose gel electrophoresis. At 0.3% agarose, where  $\mu$  is closer to  $\mu_0$ , samples migrate largely dependent on surface charge density, and are affected to a lesser extent by  $R$ . Since actual values for  $\mu_0$  and  $R$  were not determined in this study, the relationship between electrophoretic mobility and  $n$  (at the respective agarose concentration) required an empirical approach.

The 208-12 DNA was reconstituted with various ratios of octamer to DNA, as described in methods and materials, and analyzed on agarose gels run in TAE and stained with ethidium bromide. For 0.3% agarose gel electrophoresis, naked 208-12 DNA had a greater electrophoretic mobility than did 208-12 DNA reconstituted with any number of octamers (Figure A3.1A, A3.1C). The electrophoretic mobility of the reconstitutes relative to naked 208-12 DNA ( $\mu_{DNA}$ ) decreased with increasing number of octamer histones, or with increasing sedimentation coefficients of the reconstituted samples. For 1% agarose gel electrophoresis, naked 208-12 DNA had a lower electrophoretic mobility than did reconstituted 208-12 DNA (Figure A3.1B, A3.1C). From these two observations it is clear that: (a) the net negative charge of the nucleoprotein decreased as more octamers became bound (relative to DNA) based on the 0.3% agarose gels, and (b) the effective size of octamer-DNA complex decreased (relative to free 208-12 DNA) based on the 1% agarose gel. Interestingly, for samples run on the 1% agarose gel, reconstitutes with  $n > 10$  were observed to show a decrease

Figure A3.1. Analyzing reconstituted 208-12 DNA chromatin fibers using agarose gel electrophoresis. (A) An ethidium bromide (0.5  $\mu\text{g/ml}$ ) stained 0.3% agarose gel of reconstituted 208-12 DNA with 0, 3, 5, 7, and 9.5 octamers bound per DNA fragment. 5  $\mu\text{l}$  of reconstituted samples at 0.05 mg/ml DNA were applied to each lane. M, 1 kb ladder marker. The number of octamers bound to the 208-12 DNA ( $n$ ) was estimated by the sedimentation coefficient ( $s_{20,w}$ ) that was obtained from velocity analytical centrifugation of samples in 10 mM Tris-HCl (pH 7.8), 0.2 mM EDTA. Conversion of  $s_{20,w}$  to  $n$  is based on Hansen and Lohr (1993, Table I) (see also Appendix A2). (B) An ethidium bromide stained 1% agarose gel of reconstituted 208-12 DNA with 0, 3, 5, 7, and 9.5 octamers bound per DNA fragment. 5  $\mu\text{l}$  of reconstituted samples at 0.05 mg/ml DNA were applied to each lane. Arrow indicates position of the 208-12 DNA. (C) Plot of the electrophoretic mobility of reconstitutes relative to free 208-12 DNA ( $\mu_{\text{DNA}}$ ) as a function of the sedimentation coefficient. The plot includes the experimental relative electrophoretic mobility of samples separated on a 1% agarose gel (*open squares*), and a 0.3 % agarose gel (*solid squares*). Calculations based on equation (A3.1) at 0.3% agarose are from data previously presented in Fletcher et al. (1994a) (*solid circles*), and (Fletcher et al., 1994b) (*open circles*) (see text for more a in-depth explanation). In the same way,  $\mu'_{\text{DNA}}$  was also calculated for 0.2% and 0.4% agarose concentrations (*dashed lines*). The sedimentation coefficient ( $s_{20,w}$ ) was obtain as described in (A) .

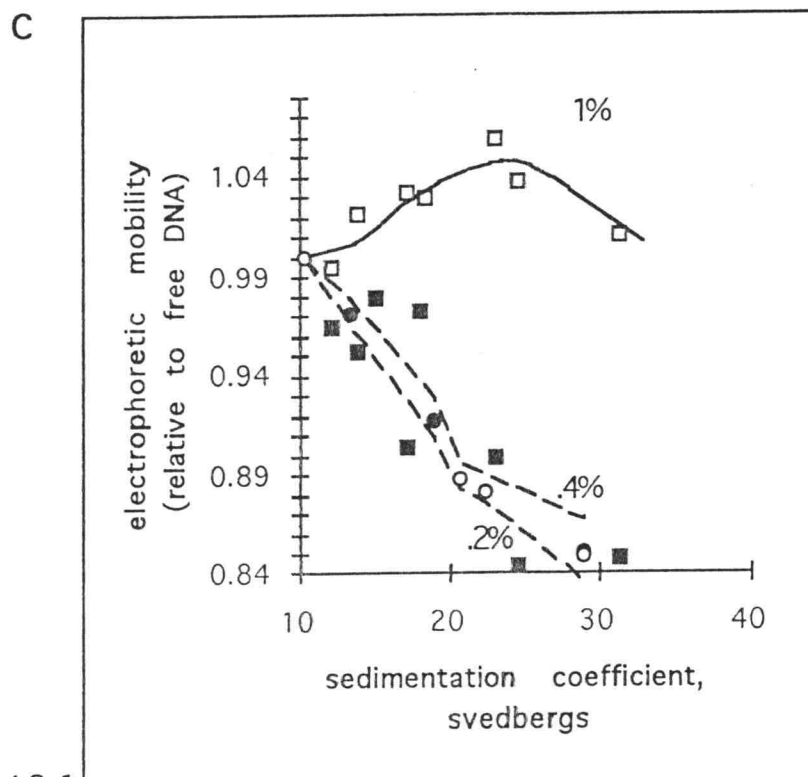
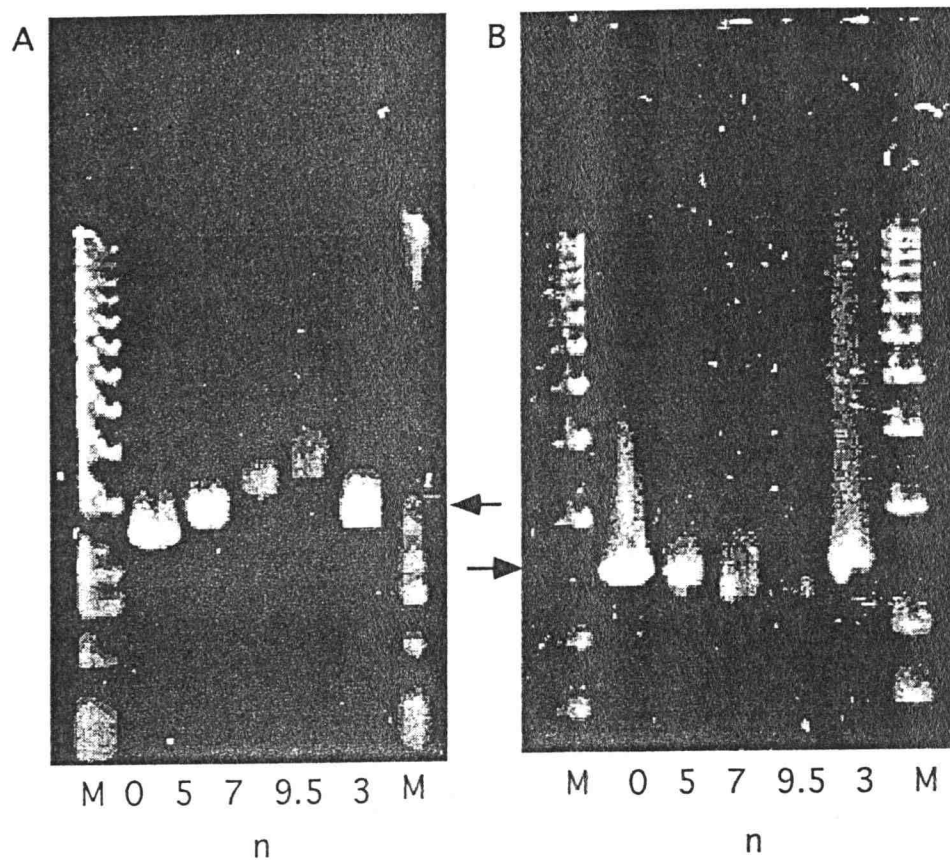


Figure A3.1

in relative electrophoretic mobility with increased octamer input concentrations (Figure A3.1C), and suggests that the effective  $R$  changed relatively little in this  $n$ -range, although the net charge continued to decrease.

Values of relative electrophoretic mobility determined by 0.3% agarose gel electrophoresis showed considerable dispersion that was not observed for samples examined using 1% agarose gel electrophoresis (Figure A3.1C). As a means of providing more confidence in experimentally-derived  $\mu_{\text{DNA}}$  at 0.3% agarose,  $\mu_{\text{DNA}}$  for reconstituted 208-12 DNA was also calculated from equation (A3.1) based on previously published values of  $\mu_0$  (Fletcher et al., 1994a, Figure 5), and effective  $R$  (Fletcher et al., 1994a, Figure 6; Fletcher et al., 1994b, Figure 4A) (see Table A3.1). In order to estimate the expected electrophoretic mobility of reconstitutes in 0.3% agarose,  $P_e$  was approximated at 380 nm<sup>1</sup>. The calculations correspond well with the experimental results reported here, thereby corroborating the validity of this experimental technique. Similarly,  $\mu_{\text{DNA}}$  calculated for 0.2% and 0.4% agarose concentrations<sup>1</sup> (Figure A3.1C, dotted lines) suggest that in this range of agarose concentrations, the expected electrophoretic mobility varies only slightly with agarose concentration. Experimental results reported in this study assumed that the effects of electroendosmosis were small, and therefore could be neglected.

---

<sup>1</sup> Personal communications from Isabelle Kreider and Dr. Jeffrey Hansen.  $P_e$  for 0.2% and 0.4% agarose were approximated at 500 nm and 280 nm, respectively.

Table A3.1. Electrophoretic and structural parameters of octamer-subsaturated 208-12 DNA reconstitutes.

| Paper*                  | <i>n</i> | s20, w** | $\mu_o$ , cm <sup>2</sup> /V s 10 <sup>-4</sup> | R <sub>e</sub> , nm |
|-------------------------|----------|----------|---|---------------------|
| Fletcher et al. (1994a) | 0        | 10.5     | 2.42  | 36.8                |
|                         | 8        | 20.7     | 2.1   | 33                  |
|                         | 9        | 22.5     | 2.08  | 32.6                |
|                         | 12       | 29       | 1.94  | 27                  |
| Fletcher et al. (1994b) | 3        | 13.5     | 2.3   | 33.2                |
|                         | 7        | 19       | 2.15  | 31.4                |
|                         | 12       | 12       | 1.94  | 26.6                |

\* Samples from Fletcher et al. (1994a) were run in TAE at room temperature (with buffer circulation), and samples from Fletcher et al. (1994b) (with buffer circulation) were run in "E buffer" (40 mM Tris-HCl (pH 7.8), 0.25 mM Na<sub>2</sub>EDTA pH 7.8).

\*\* Values estimated based on Fletcher et al. (1994a), Figure 5.

### A3.3.2 EcoR I digestion of the octamer histone-reconstituted 208-12 DNA

As described above, the 208-12 DNA is comprised of twelve tandem repeats of a 208 b.p. fragment from the 5S rDNA gene from *Lytechinus variegatus* (sea urchin). The DNA contains an octamer positioning sequence in which DNA is protected from micrococcal nuclease digestion, and includes base pairs between 2 - 147 (Figure A3.2A) (Dong et al., 1990). The rest of the DNA is considered to be unprotected from micrococcal nuclease, and is referred to as linker DNA. Also, within the 208 b.p. 5s rDNA gene fragment exists a collection of restriction endonuclease sites. EcoR I, for example, cleaves 3' of base pair 2 and 3' of base pair 197 (Figure A3.2A), resulting in a 195 b.p. fragment. Major octamer histone positioning results in the protection of the site at base pair 2, but leaves exposed the site at base pair 195. In Chapter 3 it was shown

that binding by H5 to reconstituted 208-12 DNA dramatically reduced access to both sites (Chapter 3). Furthermore, the use of restriction enzymes in buffers containing higher concentrations of  $\text{MgCl}_2$  ( $> 3.5 \text{ mM}$ ) has previously been used to analyze reconstituted 208-12 DNA with a minimal fiber aggregation (Simpson et al., 1985; Hansen and Lohr, 1993).

*A4.3.2.1 Estimating the number of octamers bound to the 208-12 DNA by comparing the relative amount of ethidium bromide-stained nucleosomes to free 195 b.p. 5s rDNA fragments released from reconstitutes digested with EcoR I*

As part of a second assay to determine the number of reconstituted octamers bound to the 208-12 DNA, EcoR I was used to digest octamer histone-reconstituted fibers into mononucleosomes and free 195 b.p. DNA. EcoR I at 0.60 units/ $\mu\text{l}$  was added to reconstituted 208-12 DNA (50  $\mu\text{g/ml}$  final DNA concentration) with the entire reaction mixture brought to 30 mM Tris-HCl (pH 7.8), 3.5 mM  $\text{MgCl}_2$ , 1 mM DTT, and digested at room temperature for up to 5 hours. Under these conditions, the reconstituted 208-12 DNA was largely digested into free 195 b.p. DNA, and mononucleosomes, though some large molecular weight complexes were also observed (Figure A3.3, A3.4).

A comparison of the products from EcoR I-digested 208-12 DNA reconstitutes was used to determine  $n$ . The basis for the analysis assumed that the EcoR I-digested reconstituted 208-12 either produces 195 b.p. 5s rDNA gene fragments that originally began as a 208 b.p. repeat free of a histone octamer, or mononucleosomes that were originally a 208 b.p. repeat occupied by a histone octamer. The UV illuminance of the nucleosome complex divided by the UV illuminance of the free 195 b.p. DNA, as

measured from ethidium bromide-stained 6% polyacrylamide gels, is referred to as  $r$ . Practically,  $r$  represents the relative amount of DNA associated with octamers as compared to free DNA in the reconstituted 208-12 DNA "chromatin fiber". If both nucleosomes and free DNA bound ethidium with equal efficiency,

$$(A3.2) \quad r = \frac{n}{N-n},$$

where  $N$  is the total number of sites available for octamer histone binding. However, nucleosomes and free DNA do not bind ethidium with equal affinity; in order to correct for this, a factor  $k_r$  must be introduced,

$$(A3.3) \quad r = \frac{k_r \times n}{N-n}.$$

Here,  $k_r$  is the relative ethidium intercalation coefficient, which describes the efficiency at which ethidium bromide intercalates into naked DNA compared to the efficiency of ethidium bromide intercalation into DNA bound by an octamer. Rearranging the equation and setting  $N=12$  for the 208-12 reconstitutes, we obtain,

$$(A3.4) \quad \frac{1}{r} = \frac{12}{k_r \times n} - \frac{1}{k_r}.$$

Thus, a linear relationship is obtained by plotting  $12/n$  versus  $1/r$ : the slope of the line is  $1/k_r$ , the x-axis intercept is 1, and the y axis intercept is  $-1/k_r$ .

To determine the merits of using a standardized curve to estimate  $n$  from the products of EcoR I digestion, the 208-12 DNA was reconstituted with a wide range of

octamer-DNA input ratios. After reconstituting octamers onto the DNA, the sedimentation coefficients for the samples were determined by velocity analytical ultracentrifugation (Hansen and Lohr, 1993; see Appendix A2). While the input values for  $n = 3$  and  $n = 5$  produced predicted reconstitutes with  $n = 3$  and  $n = 5$ , fibers with input octamer input values of  $n = 8$  and  $n = 12$ , actually produced reconstitutes with  $n = 7$  and  $n = 9.5$ , respectively (Figure 3.2B). This suggests that for  $n < 6$  virtually all input octamer protein bound to the 208-12, but for  $n > 6$  octamer deposition became increasing inefficient, possibly because of increased positioning-site occupation by octamers. Furthermore, the line based on the linear regression of EcoR I-digested reconstitutes was  $1/r = 1.34 (12/n) - 1.33$ , indicating that the slope and y-axis intercept were  $k_r$ , as predicted. It is noteworthy, that  $k_r = 1.34$ , and suggests that for the nucleosome, 36% fewer ethidium bromide molecules intercalate into DNA complexed with the octamer as compared to naked DNA<sup>2</sup> consistent with Baxter et al. (1989).

From these results, it appears that by comparing the number of octamer-bound 208 repeats to free 195 b.p. DNA from EcoR I-digested, octamer-reconstituted 208-12 DNA reasonable estimates of  $n$  were obtained, based on S-values from Hansen and Lohr (1993). It has been previously reported that secondary positions for octamer histone positioning on the 208 b.p. 5S rDNA fragment (Dong et al., 1990; Hansen et al., 1989) also exist-that could prevent EcoR I endonuclease digestion at 197. However, it does not appear that secondary site positioning posed a serious problem in obtaining meaningful results. Whether this was due the relatively low number of octamer histones positioned over base pair 197, or whether EcoR I was able to "push" octamer histones from the

---

<sup>2</sup> Calculations based on the assumption of 195 b.p. of DNA associated with the nucleosome, and an estimated binding-site size for the octamer of 145 b.p.

Figure A3.2. EcoR I endonuclease digestion of reconstituted 208-12 chromatin fibers. (A) Schematic representation a 208 b.p. DNA fragment from the 5S rDNA gene of *Lytechinus variegatus*. Octamers are reported to position from 2-147 b.p. leading to nuclease protection of this section of DNA. Bracketed numbers (and arrows) indicate EcoR I cleavage sites. (B) Plotting the products of EcoR I digested fibers (0.05 mg/ml with respect to DNA) in 3.5 mM MgCl<sub>2</sub>, 30 mM Tris-HCl, 1 mM DTT. Data was obtained from 6% polyacrylamide gels run in TAE, and stained in ethidium bromide.  $n$ , number of octamers bound to the 208-12 DNA, was plotted as a function of input protein ratios (solid squares), and as values (open circles) estimated by the sedimentation coefficient (Hansen and Lohr, 1993). Note that for  $n = 3$ , and  $n = 5$  the input values were identical to the values based on the sedimentation coefficient. The equation describing the "best fit" of points ( $1/r = 1.34 (12/n) - 1.33$ ) was determined by linear regression (Microsoft Excel 5.0). As described in the text,  $r$  is the ratio of DNA associated with octamer to free DNA produced by reconstituted 208-12 DNA, and the slope of 1.34 represents the relative efficiency of ethidium bromide intercalation into naked DNA as compared to DNA containing an octamer.

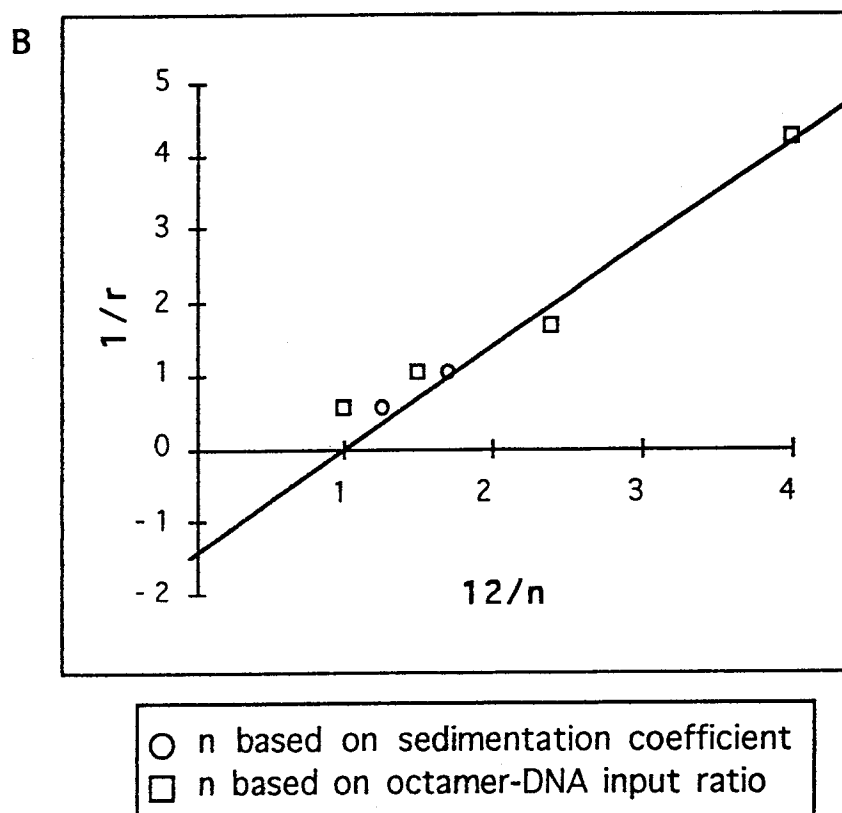
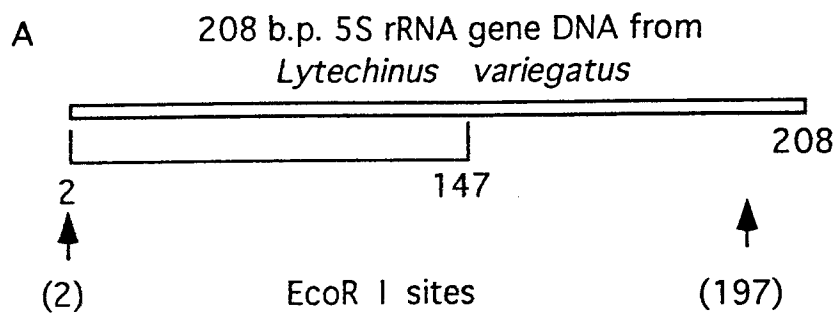


Figure A3.2

recognition site, is unclear. For the technique to provide reasonable values, it was important to completely digest the chromatin fiber, though lengthy digestion appeared to lead to some nucleosome dissociation. Alternatively, use of radiolabeled DNA would provide a simple measure of the relative amounts of DNA associated with free DNA and that associated with the mononucleosome. None-the-less, when radiolabeled DNA is not desired, a calibration curve is necessary since ethidium bromide poorly intercalates into the octamer-bound DNA, and thus underestimates this component. For this reason, free DNA and DNA associated with octamers cannot be directly compared.

#### *A4.3.2.2 Effect of NaCl concentration, temperature and time on the digestion of reconstituted 208-12 DNA*

The effects of NaCl and temperature on the EcoR I digestion rate of octamer-reconstituted 208-12 DNA, and on nucleosome stability were examined in detail. This was considered to be a necessary step, since conditions required that both nucleosome stability and EcoR I cutting efficiency be optimized. Instability of nucleosomes generated from the digestion of reconstituted 208-12 DNA is a potentially serious problem - octamer histone dissociation would lead to an artificially-high apparent abundance of free DNA. The effect of increased NaCl concentration on stability was of particular interest since it has previously been reported that salt promotes octamer sliding on DNA.

Results indicate that inclusion of 50 mM NaCl in the reaction buffer increased the digestion rate of reconstituted 208-12 DNA as compared to reaction solution without 50 mM NaCl (in 3.5 mM MgCl<sub>2</sub>, 30 mM Tris-HCl (pH 7.8)). This was true for both  $n = 4$

Figure A3.3. Effect of temperature, and 50 mM NaCl on EcoR I endonuclease digestion of octamer histone subsaturated 208-12 DNA chromatin fibers in 3.5 mM Mg Cl<sub>2</sub> and Tris-HCl (pH 7.8). (A) Fibers with an input n=4. (B) Fiber with an input n=8. Samples were analyzed with PAGE (6% polyacrylamide). At this polyacrylamide concentration, nucleosomes migrate between the 390 b.p. and 590 b.p. fragments as a diffuse band. Each lane contains about 0.5 μg of DNA.

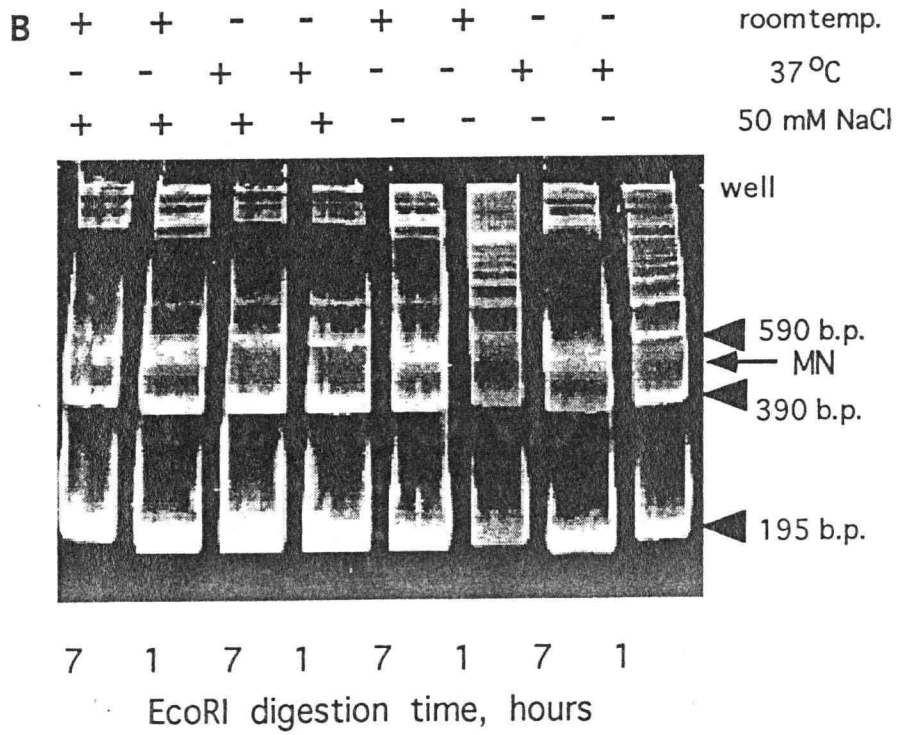
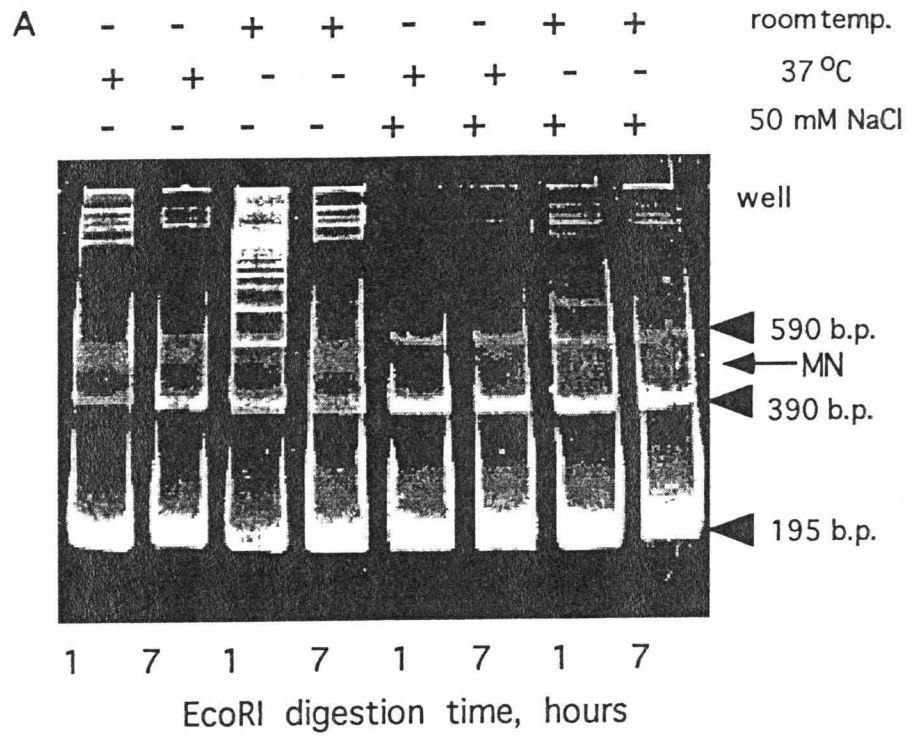


Figure A3.3

(Figure A3.3A, lane 1 versus lane 7) and  $n = 8$  (Figure A3.3B, lanes 2 and 4 versus lanes 6 and 8). In addition, EcoR I digestion conducted at 37 °C proceeded at a faster rate than for digestion conducted at room temperature (Figure A3.3A, lane 1 versus lane 3; Figure A3.3B, lanes 2 and 4 versus lanes 6 and 8). The difference in digestion rates appeared to be less dramatic for the fibers with  $n = 8$  suggesting that either fiber stability or simple octamer loading may play a role in limiting EcoR I digestion. These possibilities were further supported by the finding that fibers with  $n = 4$  digested more rapidly than the fiber where  $n = 8$  (Figure A3.3A, lanes 1 and 3 versus Figure A3.3B, lanes 6 and 8). Finally, octamers were more readily dissociated from 195 b.p. DNA with the inclusion of 50 mM NaCl (Figure A3.3A, lanes 1-4 versus lanes 5-8) and dissociation seems to have been enhanced at 37 °C (Figure A3.3B, lanes 1-2 versus lanes 3-4). Together these observations suggests that NaCl affects the EcoR I digestion rate by a possible combination of factors including: (a) increased EcoR I activity in 50 mM NaCl, and (b) increased exposure of linker DNA in 50 mM NaCl due to fiber restructuring or, more likely, nucleosomal sliding. The last factor appears particularly important especially considering the noticeable instability of nucleosomes in 50 mM NaCl (as described above), and suggests that EcoR I digestions be conducted without NaCl. The observed low stability of nucleosomes in either 50 mM NaCl or at 37 °C confer with Meerseman et al. (1992) and Pennings et al. (1991).

In a second study, stability of EcoR I products of digestion were evaluated over several hours. In this study, 208-12 DNA reconstituted with  $n=9.5$  octamer histones, as determined by the sedimentation coefficient, was digested with 0.47 units/ $\mu$ l in 3.5 mM

Figure A3.4. Effect of digestion time on the stability of mononucleosomes produced by digesting reconstituted 208-12 DNA with EcoR I. (A) 6% polyacrylamide:bisacrylamide (29:1) gel run in TAE and stained in ethidium bromide with 0.5  $\mu\text{g}$  of sample applied to each lane. (B) Change of  $r$  with time, where  $r$  is the intensity of UV illumination of the monomer complex divided by the intensity of UV lumination of the free, 195 b.p. DNA. Reaction conditions included 3.5 mM  $\text{MgCl}_2$ , 30 mM Tris-HCl (pH 7.6), 0.01% Triton X-100, 1 mM DTT with 0.43 unit/ $\mu\text{l}$  of EcoR I.

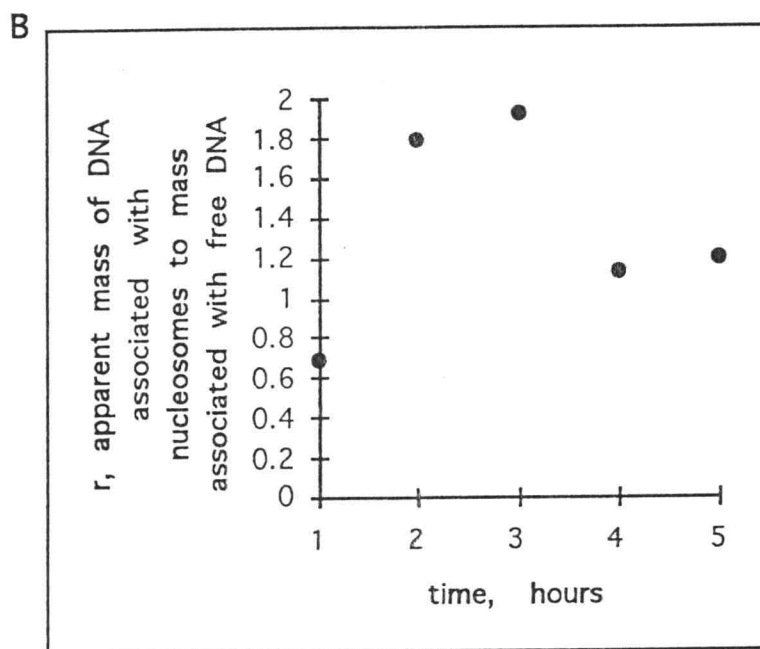
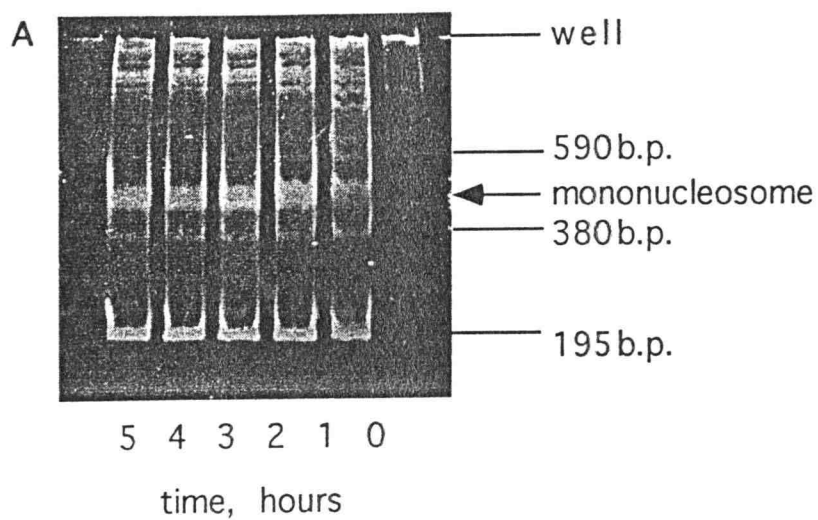


Figure A3.4

MgCl<sub>2</sub>, 30 mM Tris-HCl (pH 7.6), 0.01% Triton X-100, 1 mM DTT at room temperature. Results suggest that some nucleosome destabilization occurred for longer time points, and at 1 hour the fiber was not completely digested as indicated by the considerably lower values of  $r$  in both these cases ([Figure A3.4A, A3.4B](#)). It appears that under these specific reaction conditions the most accurate " $r$ -values" were obtained after 2 to 3 hours of digestion, and suggests that, in general, the most accurate values may be the highest values. For example, " $r$ -values" obtained from the 2 and 3 hour points yielded  $n = 8.6$  based on an average of  $r = 1.85$  and [Figure A3.2B](#), as compared to about  $n = 9.5$  based on the sedimentation coefficient; at 5 hours  $r$  dropped to 1.2 which translates to  $n = 7.4$ .

### A3.4 Discussion

Artificially reconstituted chromatin models offer a means for combining purified, chromatin-related proteins in a controlled system that closely mimics native chromatin (Garcia-Ramirez et al., 1992). Currently the most popular system is comprised of twelve tandem copies of a 208 b.p. fragment of the 5S rDNA gene of *Lytechinus variegatus*, and is commonly referred to as the 208-12 DNA (Simpson et al., 1985). Advantages of the system includes the presence of an octamer positioning sequence in each 208 b.p. repeat, which makes octamer histone reconstitutions highly reproducible, and the reconstituted DNA has been extensively characterized in both functional and biophysical studies (Fletcher and Hansen, 1996). However, one potential impediment in using the "208-12 DNA" system stems from difficulties in reliably measuring the success of the reconstitution. Quantitative gel electrophoresis and analytical centrifugation have been

used previously to determine the number of bound octamers; while highly precise, these techniques are potentially cumbersome, and may not be within the means of many laboratories. For this reason, two alternative techniques were developed, and include agarose gel electrophoresis and endonuclease digestion of the reconstituted fiber.

The first technique exploits differences in the relative electrophoretic mobility of octamer histone reconstituted 208-12 DNA as analyzed by 0.3% and 1% agarose gel electrophoresis. Fiber mobility in the 0.3% agarose gel is largely determined by surface charge density, while mobility in the 1% agarose gel electrophoresis is influenced by both surface charge density, as well as shape-related factors. Thus, the fibers migrate differently with respect to naked 208-12 DNA at the two agarose concentrations. For both agarose concentrations, the electrophoretic mobility was empirically related to the sedimentation coefficient of the respective sample as determined by analytical ultracentrifugation. The second technique involves digesting the octamer histone-reconstituted 208-12 DNA with EcoR I, and generating 5S rDNA repeats that are either bound as nucleosomes or unbound as free 195 b.p. DNA. A parameter referred to as  $r$  (ratio of ethidium stained nucleosomes to ethidium stained free DNA) was shown to be mathematically and experimentally related to  $n$ . These techniques may be somewhat restricted to analysis of reconstituted 208-12 DNA, though the use of electrophoretic mobilities may also be applied to other template DNAs of about 2600 b.p., and the methodology outline for the restriction endonuclease assay may be readily applied to any system featuring tandem repeating DNA "elements".

Both techniques outlined in this appendix offer simple, cost-effective alternatives to analytical ultracentrifugation and Ferguson plots. However, the techniques do have

caveats that may limit accuracy. For example, as shown above, one may get reasonable  $\mu_{\text{DNA}}$  values, on average, with 0.3% agarose gel electrophoresis, and theoretically, minor errors in agarose concentration should have a minimal effect on  $\mu_{\text{DNA}}$  at 0.3% agarose concentration (see [Figure A3.1](#)). None-the-less, we did observe a considerable dispersion of data points, suggesting that a number of trials need to be conducted to produce reasonably accurate results. As a second example, the results of the restriction endonuclease digestion assay, and calculation of  $r$ , showed a clear relationship to the time of digestion; values at early time points reflected incompletely digested fibers, and values at later time points reflected dissociated nucleosome complexes. Therefore, it is advised that a digestion time-course be conducted, with the maximum value of  $r$  corresponding to the most accurate measure of site occupancy.

**Appendix A3 References**

- Baxter, G. D., Smith, P. J., and Lavin, M. F. (1989) Molecular Changes Associated with Induction of Cell Death in a Human T-Cell Leukaemia Line: Putative Nucleases Identified as Histones, *Biochem. Biophys., Res. Commun.*, **162**, 30-32.
- Dong, F., Hansen, J. C., and van Holde, K. E. (1990) DNA and Protein Determinants of Nucleosome Positioning on Sea Urchin 5S rRNA Gene Sequences *In Vitro*, *Proc. Natl. Acad. Sci. USA*, **87**, 5724-5728.
- Fletcher, T. M. and Hansen, J. C. (1996) The Nucleosomal Array: Structure/Function Relationships, *Crit. Rev. Eukaryot. Gene Expr.*, **6**, 149-188.
- Fletcher, T. M., Krishnan, U., Serwer, P., and Hansen, J. C. (1994a) Quantitative Agarose Gel Electrophoresis of Chromatin: Nucleosome-Dependent Changes in Charge, Shape and Deformability at Low Ionic Strength, *Biochemistry*, **33**, 2226-2233.
- Fletcher, T. M., Serwer, P. and Hansen, J. C. (1994b) Quantitative Analysis of Macromolecular Conformation Changes Using Agarose Gel Electrophoresis: Application to Chromatin Folding, *Biochemistry*, **33**, 10859-10863.
- Garcia-Ramirez, M., Dong, F., and Ausio, J. (1992) Role of the Histone Tails in the Folding of Oligonucleosomes Depleted of Histone H1, *J. Biol. Chem.*, **267**, 19587-19595.
- Georgel, P., Demeler, B., Terpening, C., Paule, M. R., and van Holde, K. E. (1993) Binding of the RNA Polymerase I Transcription Complex to Its Promoter Can Modify Positioning of Downstream Nucleosomes Assembled *in Vitro*, *J. Biol. Chem.*, **268**, 1947-1954.
- Griess, G. A., Moreno, E. T., Easom, R. A., and Serwer, P. (1989) The Sieving of Spheres During Agarose Gel Electrophoresis: Quantitation and Modeling, *Biopolymers*, **28**, 1475-1484.
- Hansen, J. C., Ausio, J., Stanik, V. H., and van Holde, K. E. (1989) Homogeneous Reconstituted Oligonucleosomes, Evidence for Salt-Dependent Folding in the Absence of Histone H1, *Biochemistry*, **28**, 9129-9136.
- Hansen, J. C., Kreider, J. I., Demeler, B., and Fletcher, T. M. (1997) Analytical Ultracentrifugation and Agarose Gel Electrophoresis as Tools for Studying Chromatin Folding in Solution, *Methods*, **12**, 62-72.
- Hansen, J. C. and Lohr, D. (1993) Assembly and Structural Properties of Subsaturated Chromatin Arrays, *J. Biol. Chem.*, **268**, 5840-5848.

Hansen, J. C. and Wolffe, A. P. (1992) Influence of Chromatin Folding on Transcription Initiation and Elongation by RNA Polymerase III, *Biochemistry*, **31**, 7977-7988.

Li, B., Adams, C. C., and Workman, J. L. (1994) Nucleosome Binding by the Constitutive Transcription Factor Sp1, *J. Biol. Chem.*, **269**, 7756-7763.

Meerssemn, G., Pennings, S., and Bradbury, E. M. (1992) Mobile Nucleosomes- A General Behavior, *EMBO J.*, **11**, 2951-2959.

O'Neill, R. R., Mitchell, L. G., Merrill, C. R., and Rasband, W. S. (1989) Use of Image Analysis to Quantitate Changes in Form of Mitochondrial DNA After X-Irradiation, *Appl. Theor. Electrophor.*, **1**, 163-167.

Pennings, S., Meersseman, G., and Bradbury, E. M. (1991) Mobility of Positioned Nucleosomes on 5 S rDNA, *J. Mol. Biol.*, **220**, 101-110.

Pruss, D., Reeves, R., Bushman, F. D., and Wolffe, A. P. (1994) The Influence of DNA and Nucleosome Structure on Integration Events Directed by HIV Integrase, *J. Biol. Chem.*, **269**, 25031-25041.

Schwartz, P. M. and Hansen, J. C. (1994) Formation and Stability of Higher Order Chromatin Structures, *J. Biol. Chem.*, **269**, 16284-16289.

Simpson, R. T., Thoma, F., Brubaker, J. M. (1985) Chromatin Reconstitution from Tandemly Repeated Cloned DNA Fragments and Core Histones: A Model System for Study of Higher Order Structure, *Cell*, **42**, 799-808.